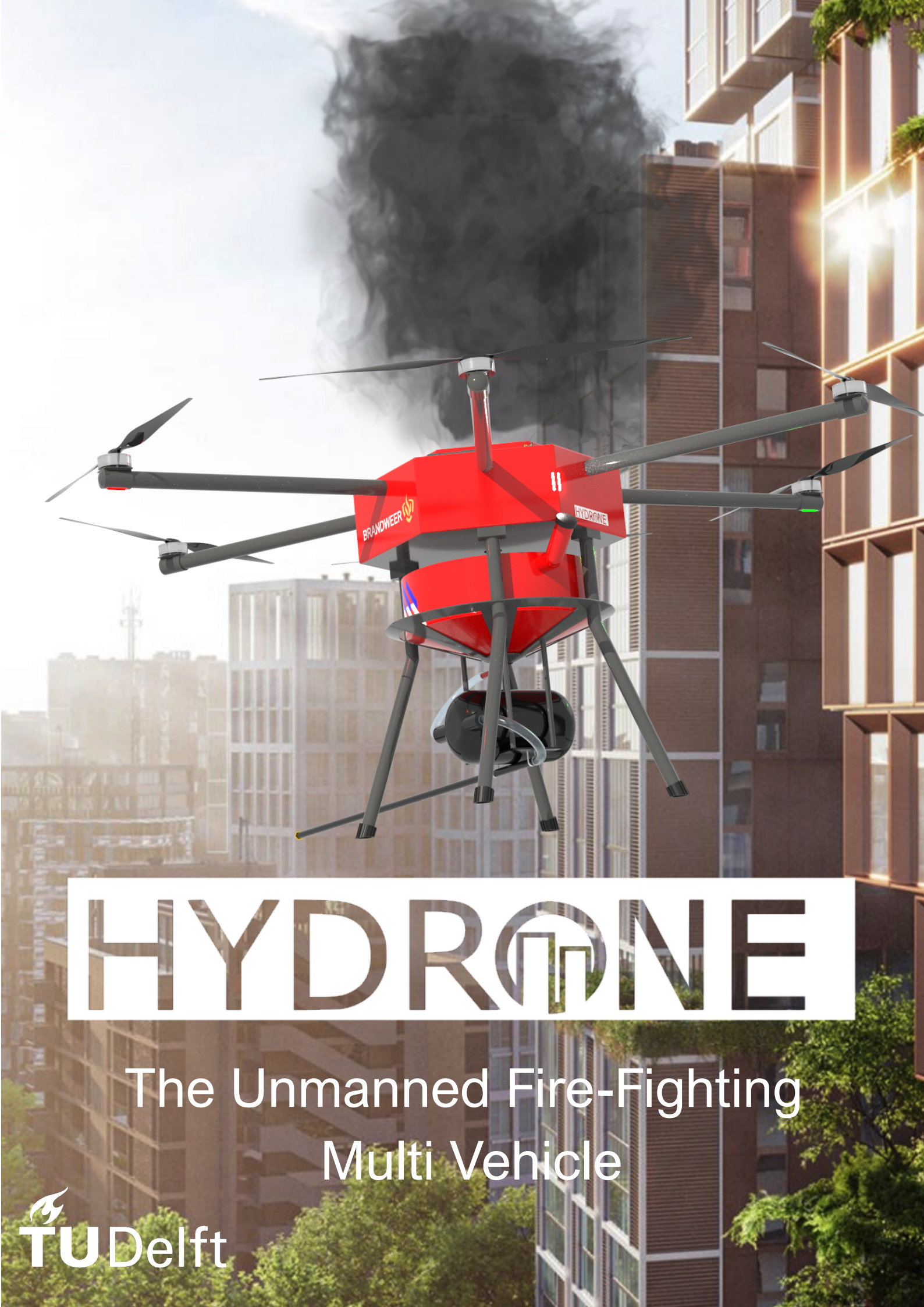

HYDRONE

The Unmanned Fire-Fighting Multi Vehicle

TU Delft

This page is intentionally left blank.

HYDRONE

The Unmanned Fire-Fighting Multi-Vehicle

by

DSE Group 29

Student Name	Student Number
Walid Amezguiou	5050995
Shivesh Damian Bhawan	5301602
Noud van Bohemen	5019087
Maxime Capelle	5261457
Tine Coutuer	5001196
Marianna Piperigou Grammatika	5236398
Laura Hoitingh	4869524
Yoari Karelsz	5087996
Annic Pattiwael	5101883
Syed Muneeb ur Rahman	5217482

to design a drone which can aid in saving lives in dangerous fire scenarios.

Project duration:	April 24, 2023 – June 29, 2023	
Under the Guidance of:	Dr. D. Ragni,	Tutor
	Babak Mohammadikalakoo	Coach
	Filip Surma	Coach

TU Delft Delft University of Technology

Executive Overview

Project Vision

As more and more high-rise buildings are being developed in the Netherlands, the Dutch Fire Brigade has warned about fire safety [118]. At the moment, the "*Zalmhaventoren*" in Rotterdam is the tallest building in the Netherlands, with a height of 215 meters [60]. In the future, the tower will most likely not be the only one of its kind as demand for housing is constantly increasing. Since firefighters can only reach up to 30 meters with their ramp, the heights of the tall buildings pose a big problem in case of emergencies [118]. To quickly get to higher levels from the inside of the buildings may be difficult and dangerous for the firefighters since equipment can be heavy and the inside routes to the upper floors may not be safe. Because of this, the developed mission need statement is:

"Supporting firefighters in combating fires in high-rise buildings"

The use of a drone may help save lives since they can reach the higher floors in little time. Once arrived at the desired altitude, the drone can start extinguishing the fire. The project objective statement is as follows:

"The UAV shall aid firefighters in combating fires in high-rise buildings by providing extinguishing capabilities for top-level floors"

Requirements

In order to design a drone that meets stakeholder expectations, clear requirements must be established and worked on. The requirements are received from the stakeholders and the user. The most important ones are the key and driving, shown in Table 1.

Table 1: *Key and driving requirements*

Key
The UAV shall be able to carry a minimum payload of 10 kg
The UAV shall have a horizontal hovering accuracy of ±0.1 m in nominal conditions
The UAV shall be able to achieve a flight altitude of 250 m
The UAV shall be able to operate in a 55°C environment for at least 120 seconds
The UAV shall be able to deliver the fire-combating payload from a horizontal distance of at least 4 m
Driving
The UAV shall be able to carry a minimum payload of 10 kg
The UAV shall have an average operational time of 20 min
The UAV shall be able to fit inside a fire brigade transport vehicle
The cost of the single unit shall not exceed EUR 25.000

Market Analysis

The performed market analysis concluded that the demand for firefighter drones will continue to increase in the upcoming years. Furthermore, it is expected that in the future the development of drones will be funded by several governments. For multi-rotor drones, there are two main categories: micro and macro drones. Macro drones are preferable in the Netherlands since they are able to deliver heavier payloads.

Looking at competitors, it can be concluded that there is a market for opportunities laying ahead. Since most of

the competitors originate from China, the unsaturated European market will give interesting opportunities for Western fire departments. The lower price compared to others may also be an attractive aspect.

Payload

For the drone to be able to extinguish a fire from a certain distance, a specific payload is designed. The final payload configuration was concluded on a tank filled with water, to which a pressure pump is attached. The tank is placed on the landing gear, which in its turn is connected to the bottom of the drone.

The water should be able to travel a horizontal distance of at least **6 m** at a relative height of approximately **2 m**. To achieve this, the exit velocity of the water has to be equal to **10 m/s** or higher. The ideal water tank is chosen to be custom-made. The tank has a conical design at the bottom to ensure the flow of the water into the pump, while the top part is flat to easily fit under the drone. The tank has a volume of **20 L**. The pump has a flow rate of **26.5 litres per minute** with a maximum pressure of **4.14 bar**. A nozzle is connected to the pump with a diameter of **4.8 mm**. In Figure 1, the payload configuration can be seen.

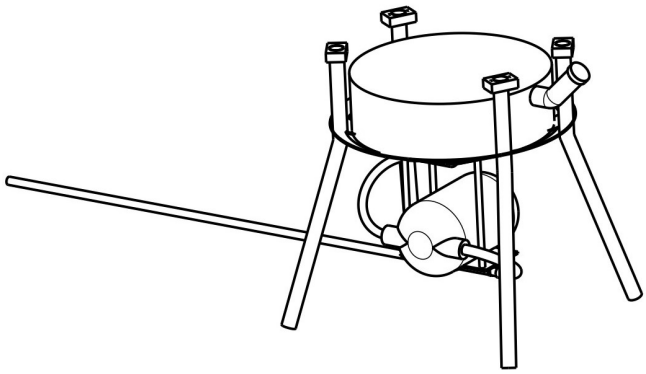

Figure 1: *The payload configuration*

Power & Propulsion

After the extensive trade-off and selection process performed earlier in the design process. The final configuration was chosen to be six **T-MOTOR MN1010 KV135** motors [159]. These are powerful, 12S motors that are each capable of a maximum thrust of **21.5 kg** at max power when using the matching propellers. This propeller is the Carbon Fibre plus Epoxy **G32*11 Prop** [157]. With this motor and propeller combination, the optimal battery was found to be two **LiPo 46000 12S2P 44.4v** batteries [17].

Electrical Components

To perform the mission as desired, the drone has several electrical components to help manoeuvre and analyse the situation. The components can be divided into four subsystems: Control, Communication, Sensors & Cameras, and Others.

Firstly, to control the UAV, a Flight controller (FC) is used. The FC can be seen as the motherboard of the drone. It ensures that the drone is always stable while performing flight manoeuvres and providing necessary flight data to the pilot. The FC used on the drone is chosen to be the *CubePilot Cube Orange*. Next, six Electronic Speed Controller (ESC)s are used to allow control of the electric motors by the flight controller. The chosen ESCs are from the same brand as the motors. The **T-MOTOR Flame 80A 12S** was chosen as ESC. Lastly, two Power Distribution Board (PDB)s are used. They are connected to the batteries and distribute the power from the sources to the rest of the system. The PDBs that are used are the **Sky-Drone SmartAP** PDB **400As**.

For communication, a transmitter and receiver are used. They will communicate with each other during the mission for effective control. The transmitter will help control the payload mechanism. It is important that the transmitter and receiver are compatible to ensure communication without any losses or sensitivity issues. Therefore, the **FrSky Taranis X9D** transmitter and **TBS Crossfire Nano RX** receiver are chosen. Furthermore, a data link between the FC and Ground Control Station (GCS) is added. The best option for the telemetry module was chosen to be the **Herelink Air Unit 1.1**.

The sensors and cameras are important to control the drone and to have an overview of the current situation in the building and surroundings. For altitude measurement, a LiDAR is placed on the bottom of the pump. The LiDAR should have a large range since the drone will fly at high altitudes. Because of this, the **Atollo Wasp 200** was chosen with a range of 315 meters. For frontal sensing, one LiDAR and two sonar sensors are placed on the front of the drone. The combination of both was chosen for redundancy, since smoke may interfere with the LiDAR which can give false results. The frontal LiDAR has a smaller range than the altitude LiDAR, the **Lightware SF20C** was chosen. The two sonars will both be the **MB1222 I2CXL-MaxSonar-EZ2**. A visual and thermal camera are also placed on the front of the drone. The **Hawkeye Firefly 4k Nakedcam** and the **FLIR Lepton 3.5** was chosen as visual and thermal camera, respectively. Although it is not intended for the drone to go out of sight of the controller, a GPS using Real Time Kinetic (RTK) is added to have knowledge of the drone's position with high accuracy. The **Here3 RTK GPS** was chosen.

One of the other electrical components is the **SmartAP PDB battery monitor**. This will sense when the battery of the drone becomes too low and will send a warning signal to the ground station. The second component is the **Grove - SPDT Relais (30A)**, which is a mechanical relay that will act as a switch for the payload pump. Lastly, the drone will be equipped with **LED lights**. This is done for safety and to comply with certain drone regulations when flying outside daylight periods.

Structure Design

After thorough analysis, the drone was chosen to have a six-rotor configuration, with 32-inch propellers. The rotors are positioned in an X-frame, driven by two lithium polymer batteries. The main airframe of the UAV body consists of three sandwich panels, stacked on each other and shaped as hexagons. Between the upper two panels, the ESCs, PDBs and arm tubes are attached. The batteries are placed between the lower and middle panels. Specific attachments are manufactured to attach the rods to the main body and the motors to the rods. Attachments to connect the three panels to each other are bought off-the-shelf. In Figure 2 the airframe structure is illustrated.

To safely land the drone after or during operation, a proper landing gear is designed. The landing gear consists of four legs, made of eight carbon fibre rods. The landing gear is integrated with the payload system as illustrated in Figure 1.

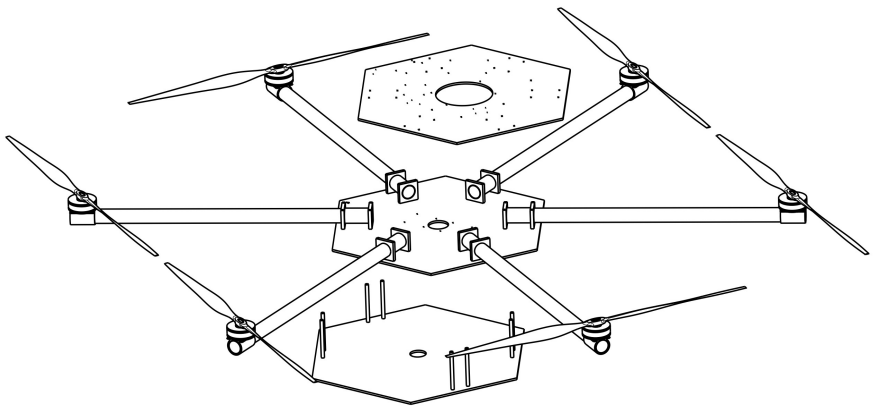

Figure 2: *Drawing of the air frame structure*

Control & Stability

Once the drone is fully designed, a thorough analysis was performed to ensure the drone is controllable with the configuration it has, observable with the sensors it is equipped with and stable with control software on board. The state space model constructed proved to be controllable and observable with the classic methods mentioned in "Introduction to Multicopter Design and Control" [129].

To perform a more in-depth analysis of the controllability, the advanced Available Control Authority Index method was adopted to establish which rotation direction configuration was optimal. This analysis is particular to multicopter drones and provides a valuable analysis of the drone's capabilities. Using this method, the

configuration in Figure 3 was chosen.

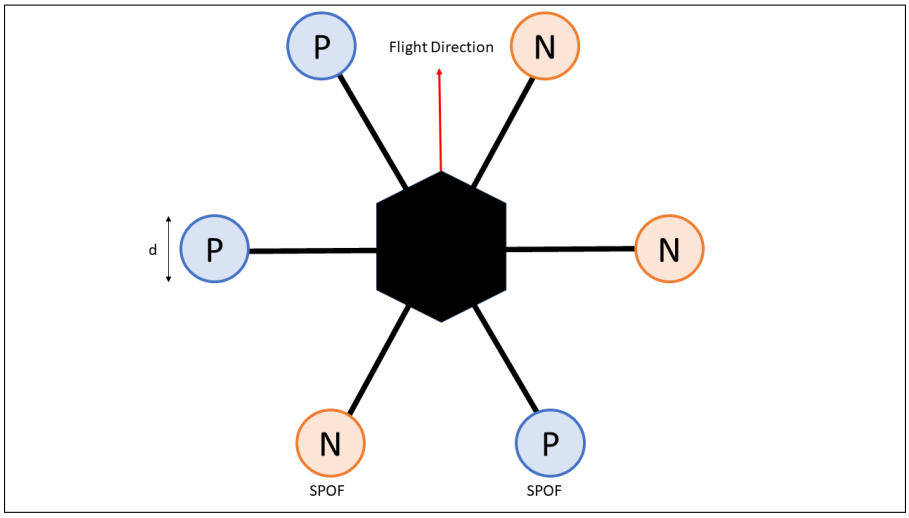

Figure 3: *Final rotor direction configuration (NNPNPP)*

In Figure 3, *P* denotes a clockwise rotation of the rotor, *N* denotes a counter-clockwise rotation. This final configuration was chosen as it had sufficient controllability when fully operational and due to its redundant properties with single rotor failures. Only the two rear rotors, with reference to the flight direction, can be considered single points of failure, hence they are placed furthest from the action.

Final Configuration

Since the drone is designed to extinguish the fires using water, the name **HYDRONE** was chosen. The name is a combination of the Greek word *hydro*, meaning water, and the word *drone*, emphasising the design being an Unmanned Aerial Vehicle (UAV).

A full CAD model of the final design was made. The final weight estimation resulted in a weight of **37.79 kg** without water. The UAV has a maximum take-off weight of 56.39 kg, assuming a minimum T/W of two is required. In Figure 4 the final design is shown.

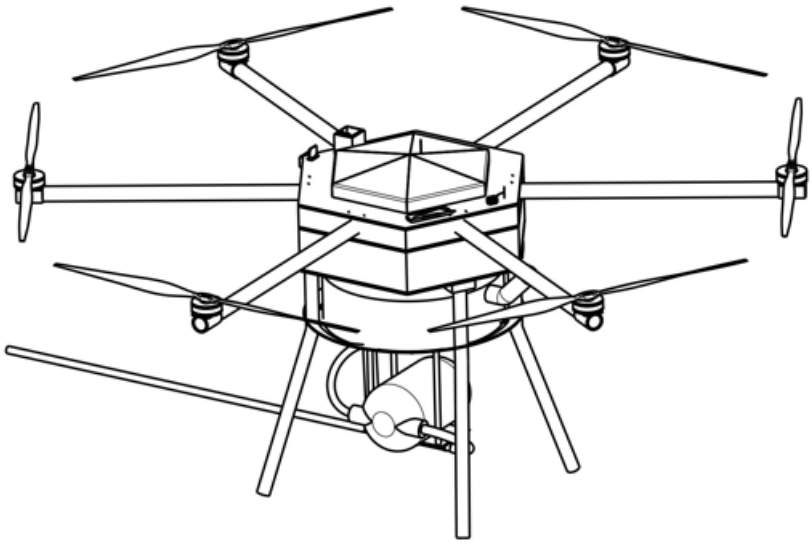

Figure 4: *Drawing of the final design*

Mission Profile

The mission and flight profiles are demonstrated in Figure 5a and Figure 5b, respectively. The mission is divided into the following six steps:

(a) Deployment
(b) Reach Altitude
(c) Approach Target
(d) Deliver Payload
(e) Disengage Target
(f) Descent/Re-target
(g) Turn Around

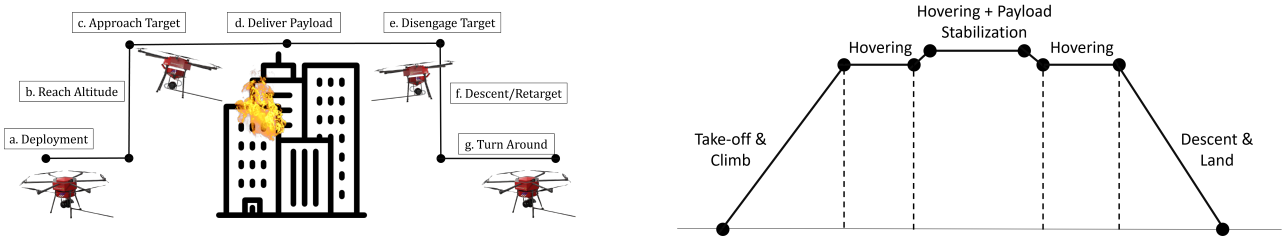

(a) *Illustration of the mission profile for the drone*

(b) *Illustration of the flight profile for the drone*

Figure 5: *Mission and flight profile diagrams of the drone*

It is important for the drone to have a quick take-off and climb to the floor in need. Next, the drone will hover at the desired position and deliver the extinguishing agent. Once empty, the drone will disengage and proceed to descend and land. After, the payload can be refilled and the batteries recharged or changed. The operational time of the entire mission depends on the payload and the height of the mission.

Payload Optimisation

To get a good estimate of the performance of the drone, simulations were run to find the optimum payload capacity. To find the optimum payload a new parameter, payload per minute (PPM), was introduced. After analysis, an optimum payload weight of **18.6 kg** was found with a final PPM of **2.07 kg/min** delivering a total payload of **130 kg** in **7 runs**. The total operational time of the drone for a complete battery usage comes to a final value of **23 min**.

Financial Analysis

In order to assess the economic feasibility of the drone a financial analysis is conducted. The costs of the drone consist of manufacturing costs, development costs and operating costs. The total cost of the components of the drone is equal to **€17,577**. To manufacture one drone the costs are around **€25,000**. During the development stage, other costs are also made, such as the wind tunnel costs and the building of the prototype. These account for €82,400. During the operation, some additional costs are also made such as the drone pilot training, having extra batteries at hand, maintenance costs and insurance.

The drone will be sold for **€35,000** per unit, which will lead to a profit margin of 40%. It is estimated that around 110 units will be sold in the Netherlands, with the goal to sell to other countries in the future. As in the Netherlands and the EU fire brigades do not use any drones with fire extinguishing capabilities the market share will be 100%.

With the sales value being equal to €3,85 Million and the cost of investment equal to €2,832 Million, the return on investment was found to be **36%**, which means that the project is predicted to be profitable. From a financial standpoint, the proposed drone is a feasible design.

Risk Analysis

Risk analysis consists of identifying risks that could occur during the design, manufacturing or the mission itself. After identifying, the severity of each risk is estimated based on an analysis of the impact and possibility

of occurrence. Next, mitigation actions have been established for the most severe risks. These are the ones with a risk score of ten or higher and can be considered to be catastrophic. The risks with the highest risk score are shown in Table 2. Since they have a major impact on mission outcomes, it is important to undertake mitigation actions. It is important to note that not all risks can be mitigated through design changes, these may be mitigated through implementing operational procedures for the users.

Table 2: *Risk analysis*

Risk	Likelihood	Impact	Risk score
The payload is not delivered at the desired spot	3	5	15
Pump malfunction or failure	3	5	15

Sustainable Development Strategy

The UAV aims to adhere to Sustainable Development Goals 3 and 13 of the United Nations [179]. To ensure that the UAV will adhere to these goals, certain requirements regarding sustainability are constructed. A sustainable development strategy is used to incorporate all the sustainability requirements in the design of the subsystems. Based on these, the main focus lies on the used extinguishing agents, the energy sources, and the End-of-Life (EOL) of the drone. Since the UAV will use water to extinguish the fires, the extinguishing agent is clearly non-toxic and biodegradable. To charge the batteries of the drone, clean energy sources can be used, such as wind and solar energy. Next, all the electronics and batteries can be easily accessed by removing just one of the panels. Therefore, it can be said that the drone is modular. This means that all components can be individually removed and reused if possible. The material used for most of the parts of the drone is carbon fibre. Due to the material being relatively lightweight, the fuel used may be decreased. Furthermore, carbon fibre is chemically stable which means that it will not corrode, or easily degrade. Lastly, since the drone will help rapidly extinguish fires, the spreading of the fire can be prevented which may lead to less property damage and environmental impact.

Contents

Acronyms

ACAI Available Control Authority Index. 44, 46, 47, 72, 73
AWG American Wire Gauge. 30

CAGR Compound Annual Growth Rate. 10
CASCO Casualty and Collision. 84
CFD Computational Fluid Dynamics. 17, 65
COGS Cost of Goods Sold. 84

DC Direct Current. 17
DEMO Dienst Elektronische en Mechanische Ontwikkeling. 76
DOD Depth of Discharge. 64
DOF Degree of Freedom. 45
DOT Design Option Tree. 20

EASA European Union Aviation Safety Agency. 84, 109, 115, 116
EKF Extended Kalman Filter. 52
EOL End-of-Life. vi, 9, 105, 106, 109, 112, 122
ESC Electronic Speed Controller. ii, iii, 23–25, 31, 37–39, 47, 51–53, 63, 68, 80, 89, 98, 102, 113
EU European Union. v, 7, 11, 74, 86

FC Flight controller. ii, 23, 24, 26, 31, 52, 89, 98, 109
FEM Finite Element Method. 73
FF Feed Forward. 50

GCS Ground Control Station. ii, 27, 29, 35
GPS Global Positioning System. iii, 23, 29–32, 44, 52, 91, 94, 96, 98, 99, 109, 113

ILT Human Environment and Transport Inspectorate. 84
IMU Inertial Measurement Unit. 52, 113

LED Light Emitting Diode. iii, 23, 30, 31
LG Landing Gear. 54
LiDAR Laser imaging, Detection, And Ranging. iii, 23, 27–29, 31, 32, 44, 76, 91, 94, 96, 102, 122
LPM Litres Per Minute. xii, 17, 18, 112, 122
LQR Linear Quadratic Regulator. 49

MTBF Mean Time Between Failure. 7, 74, 110, 113

OSO Operational safety objective. 116

PDB Power Distribution Board. ii, iii, 23–26, 30, 31, 37–39, 53, 63, 89, 90, 95, 98

PID Proportional, Integral, Derivative. 49, 50

PPM Payload Per Minute. v, 65

PVC Polyvinylchloride. 19, 79

PWM Pulse Width Modulation. 24, 51, 52

RAMS Reliability, Availability, Maintainability and Safety. 1, 101

ROC Rate of Climb. 64

ROI Return on Investment. 84, 86

RPAS Remotely Piloted Aircraft System. 84

RPM Rotations Per Minute. 25, 64, 119

RTK Real Time Kinetic. iii, 29, 30

SAIL Specific Assurance and Integrity Level. 116

SCL Serial Clock. 33

SDA Serial Data. 33

SDG Sustainable Development Goals. 105, 107, 122

SI International System of Units. 69

SPDT Single Pole Double Throw. iii, 30

SPOF Single Point of Failure. 48

SWOT Strengths, Weaknesses, Opportunities and Threats. 10, 12

T/W Thrust to Weight ratio. 7, 8, 11, 17, 20, 21, 25, 64, 65, 74, 109–114, 120, 121

TAT Turn Around Time. 7, 74, 102, 110, 113

TBD To Be Determined. 110, 112

TPD Total Payload Delivered. 65

UART Universal Asynchronous Receiver-Transmitter. 24

UAV Unmanned Aerial Vehicle. i–iv, vi, 1, 3, 6–11, 13, 15, 17, 18, 21, 23–28, 30, 33, 37, 39, 46, 52–55, 63–73, 76, 80, 84, 88, 105–113, 116, 118, 122

UN United Nations. 105, 106

UND Undetermined. 109

USD United States Dollar. xii, 10, 82

VRS Vortex Ring State. 120

List of symbols

Symbol	Definition	Unit
a	Acceleration	[m/s^2]
A	Area	[m^2]
C_d	Drag coefficient	[-]
C_M	Moment Coefficient	[-]
C_T	Thrust Coefficient	[-]
D	Drag	[N]
f	Frequency	[Hz]
F	Force	[N]
I	Area moment of inertia	[m^4]
I	Current	[A]
K	Head loss coefficient	[-]
l	Length of drone arm	[m]
L	Length	[m]
m	Mass	[kg]
M	Moment	[N/m]
$\dot{m}$	Mass flow	[kg/s]
n	number of states	[-]
N_{max}	Maximum rotations per minute	[deg/s]
N_{runs}	Number of runs	[-]
p	Pressure	[Pa]
q	Dynamic pressure	[Pa]
Q	Flow rate	[LPM]
r_i	Inner radius	[m]
r_o	Outer radius	[m]
s	Length of one side	[m]
S	Surface area	[m^2]
t	Time	[s]
T	Thrust	[N]
v_e	Exit velocity	[m/s]
V	Velocity	[m/s]
V	Voltage	[V]
V	Volume	[m^3]
W	Weight	[N]

Symbol	Definition	Unit
x	Distance in x-direction	[m]
$\dot{x}$	Velocity in x-direction	[m/s]
y	Distance in y-direction	[m]
$\dot{y}$	Velocity in y-direction	[m/s]
z	Distance in z-direction	[m]
$\dot{z}$	Velocity in z-direction	[m/s]
η_{prop}	Propeller efficiency	[%]
θ	Pitch angle	[degrees]
$\dot{\theta}$	Pitching velocity	[degrees/s]
ρ	Density	[kg/m^3]
σ	Bending stress	[Pa]
τ	Shear stress	[Pa]
ϕ	Roll angle	[degrees]
$\dot{\phi}$	Rolling velocity	[degrees/s]
ψ	Yaw angle	[degrees]
$\dot{\psi}$	Yawing velocity	[degrees/s]
€	Currency	[Euro]
$	Currency	[USD]

1 Introduction

In recent years, the number of high-rise buildings has been increasing in the Netherlands. Due to the current housing shortage, the amount of high-rise buildings will only continue to increase [118]. Unfortunately, this increase has raised concerns about fire safety in high-rise buildings as residents, especially on upper floors, tend to get trapped in case of fires. It has been noted that firefighters are only able to extinguish up to 30 meters from the outside of a building [141]. Firefighters face significant challenges when trying to reach the top floors, due to the heavy equipment they carry, the smoke, and extreme temperatures. However, the use of a drone offers a promising solution. With the use of a drone, these difficult-to-reach areas can be accessed. The drone can quickly fly to the top floors and start extinguishing from the outside. This means firefighting efforts can be enhanced, contributing to improved safety and effectiveness in combating high-rise building fires.

The aim of this report is to summarise the steps taken up to the final stage of the project and to provide a detailed description of how the design was developed. It covers the steps taken and explains the design choices that were made. In addition, other aspects of the project are presented such as analyses of the economic market, the risks, and sustainability in order to convey the feasibility of the project.

The report is structured as follows. First, in Chapter 2, the project vision will be presented and the mission will be described. The chapter will show the mission in the form of Functional Flow and Functional Breakdown Structure diagrams. In Chapter 3, all the requirements that were used to design the drone will be presented. The drone's market and competitors will be analysed in Chapter 4. Next, the payload mechanism will be chosen and further described in Chapter 5. Chapter 6 gives a brief summary of the method used earlier in the design process to determine the optimal motor, battery and propeller configuration. In Chapter 7, an overview of the electrical components of the drone will be given, as well as how they are connected to each other. The configuration of the UAV, the design of the main frame and the landing gear will be described in Chapter 8. The control and stability of the drone will be discussed in Chapter 9, while an overview of the final UAV configuration will be given in Chapter 10. In Chapter 11, the performance analysis will be presented. The verification and validation methods applied to the used models will be discussed in Chapter 12. After the drone's production, the manufacturing, assembly and integration plan will be given in Chapter 13. Furthermore, a financial analysis will be performed in Chapter 14. The different risks will be analysed in Chapter 15 as well as the plan to reduce them. In Chapter 16, the Reliability, Availability, Maintainability and Safety (RAMS) characteristics will be determined and discussed. The sustainability development strategy will be presented in Chapter 17. The feasibility of the drone design will be analysed in Chapter 18. Lastly, in Chapter 19, an overview and timeline of the activities after this project will be given.

2
Project Vision

In this chapter, the project vision will be described. Section 2.1 will explain the problem analysis, leading to the project objective in Section 2.2. In Section 2.3, a description of the mission will be given. Lastly, a functional analysis of the mission will be done in Section 2.4. Here, a Functional Flow Diagram and Functional Breakdown Structure for the mission can be found.

2.1. Problem Analysis

In 2008, the TU Delft Faculty of Architecture was hit by a large fire. The fire was initialised by a short circuit in a coffee machine on the seventh floor, caused by a broken water pipe on the floor above. The fire caused the building to collapse, despite the efforts of the Dutch fire brigade. This was mainly due to the firefighters only being able to extinguish fires up to 30 meters from the outside [118]. The Architecture Faculty, however, was 56 meters high, and thus the highest floors were unreachable from the outside. Figure 2.1 shows that the water, used to extinguish the fire, does indeed not reach the desired altitude.

Figure 2.1: *Fire at the TU Delft Faculty of Architecture on May 13, 2008 [97]*

A second example of a high-rise fire occurred in 2017 at the Grenfell Tower in London. Seventy-two people lost their lives in the fire. The building was 67 meters high, which led to a high number of victims being trapped in their apartments and unable to escape. Unfortunately, the fire spread rapidly and it engulfed the building. This made it even more difficult for the firefighters to reach the higher floors. The initial response capabilities of the

fire brigade were overwhelmed by the scale of the fire and the high number of residents in need of assistance [94].

In the Netherlands, every year more high-rise buildings are being realised, especially in the "Randstad". This is mainly due to the rising demand for housing. Currently, there are already approximately 50 buildings with a height of more than 100 meters, of which the Zalmhaventoren in Rotterdam is the tallest, with a height of 215 meters [60]. Not only in Rotterdam but in every large city, apartment buildings taller than 100 meters are in development [118]. High-rise buildings are associated with many risks in terms of fire safety, because the people on the higher floors tend to get trapped when fires occur on lower floors. As mentioned before, the lifting ramp the Dutch Fire Brigade uses can only reach up to 30 meters [141]. For this reason, the firefighters cannot reach the higher floors from the outside and carrying the heavy equipment up to the higher levels from the inside may be challenging due to the unsafe routes in the building.

2.2. Project Objective

As previously described in Section 2.1, firefighters may not always easily access the higher floors in high-rise buildings in case of a fire. The use of drones may help in these situations. Drones can quickly reach these heights from the outside and will not only help save buildings, but more importantly, they will help save lives.

The mission need statement has therefore been constructed as follows:

"Supporting firefighters in combating fires in high-rise buildings."

The project objective statement is as follows:

"The UAV shall aid firefighters in combating fires in high-rise buildings by providing quick extinguishing capabilities for top-level floors."

2.3. Mission Description

In case of an emergency on a higher floor, it may take between fifteen to twenty minutes for the fire department to reach the floor in need [132]. For a rescue mission, every second is crucial and these minutes can be life-determining. A drone may reach this floor within a matter of seconds. The design of the drone will be focused on being easily transportable by the fire brigade. Furthermore, the time it takes for the drone to be loaded with water and ready for take-off should be within a couple of minutes. Once ready, the drone can go up to the top floors. In case the window is already broken, due to the pressure and heat of the flames, the UAV will spray water through the broken window to start extinguishing the fire. If the window is still intact, the water will be sprayed to cool down the window and surroundings to prevent it from bursting or breaking. This is important since a broken window allows oxygen to fuel the fire. Once the water tank is empty, the drone will return to be quickly refilled. This way, the drone can keep operating until it is no longer necessary.

The name **HYDRONE** was chosen to reflect the drone's capabilities. HYDRONE combines the words *hydro* and *drone*. The word *hydro* was used in Ancient Greek, meaning water. This was chosen since the drone will use water to extinguish the fires and cool down the windows. Additionally, the name is a play, reflecting the drone's ability to fly and operate around high-rise buildings.

2.4. Functional Analysis

Functional analysis is necessary in the design process of the UAV. By understanding the functions, processes and interactions of a system, a problem-solving approach to the mission design can be taken. The independent functions the UAV must perform have been broken down into different components and every function has been broken down into sub-levels.

The Functional Flow Diagram and the Functional Breakdown Structure can be found on the next pages. The Functional Flow Diagram is a graphical representation of the step-by-step approach the system must follow to achieve a successful mission. It shows the logical flow of activities in the process, from beginning to end. The diagram uses arrows to indicate the connection between activities. The Functional Breakdown Structure is a hierarchical decomposition of the system showing the functions it should perform. It is presented in a tree-like structure, with the highest level function at the top, broken down into smaller supporting functions.

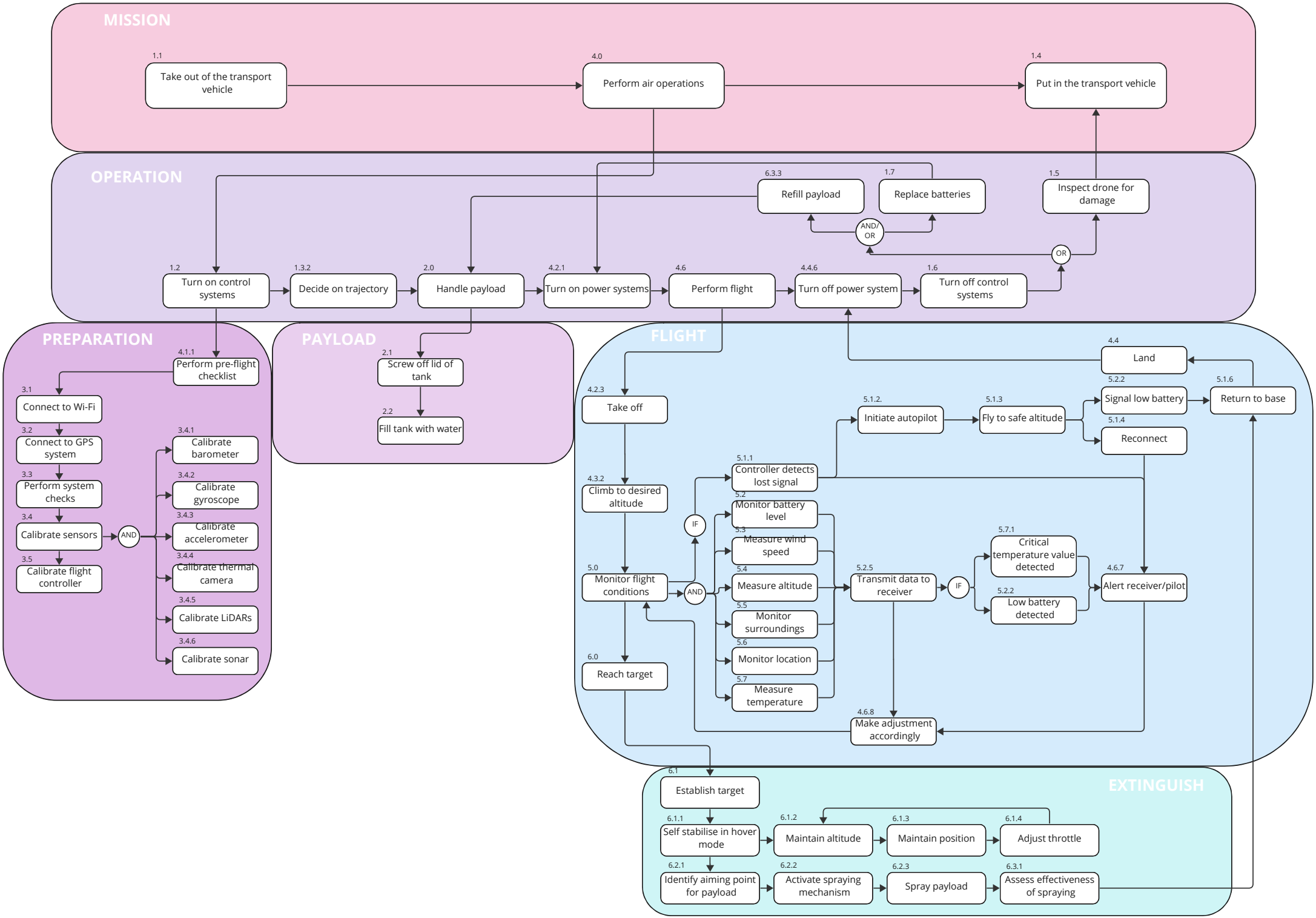
MISSION
1.1
Take out of the transport vehicle
4.0
Perform air operations
1.4
Put in the transport vehicle
OPERATION
6.3.3
Refill payload
1.7
Replace batteries
1.5
Inspect drone for damage
AND/ OR
OR
1.2
Turn on control systems
1.3.2
Decide on trajectory
2.0
Handle payload
4.2.1
Turn on power systems
4.6
Perform flight
4.4.6
Turn off power system
1.6
Turn off control systems
PREPARATION
4.1.1
Perform pre-flight checklist
3.1
Connect to Wi-Fi
3.2
Connect to GPS system
3.3
Perform system checks
3.4
Calibrate sensors
AND
3.5
Calibrate flight controller
3.4.1
Calibrate barometer
3.4.2
Calibrate gyroscope
3.4.3
Calibrate accelerometer
3.4.4
Calibrate thermal camera
3.4.5
Calibrate LiDARs
3.4.6
Calibrate sonar
PAYLOAD
2.1
Screw off lid of tank
2.2
Fill tank with water
FLIGHT
4.4
Land
4.2.3
Take off
5.1.2.
Initiate autopilot
5.1.3
Fly to safe altitude
5.2.2
Signal low battery
5.1.4
Reconnect
5.1.6
Return to base
4.3.2
Climb to desired altitude
5.1.1
Controller detects lost signal
IF
5.2
Monitor battery level
5.3
Measure wind speed
5.4
Measure altitude
5.5
Monitor surroundings
5.6
Monitor location
5.7
Measure temperature
5.0
Monitor flight conditions
AND
5.2.5
Transmit data to receiver
IF
5.7.1
Critical temperature value detected
5.2.2
Low battery detected
4.6.7
Alert receiver/pilot
6.0
Reach target
4.6.8
Make adjustment accordingly
EXTINGUISH
6.1
Establish target
6.1.1
Self stabilise in hover mode
6.1.2
Maintain altitude
6.1.3
Maintain position
6.1.4
Adjust throttle
6.2.1
Identify aiming point for payload
6.2.2
Activate spraying mechanism
6.2.3
Spray payload
6.3.1
Assess effectiveness of spraying

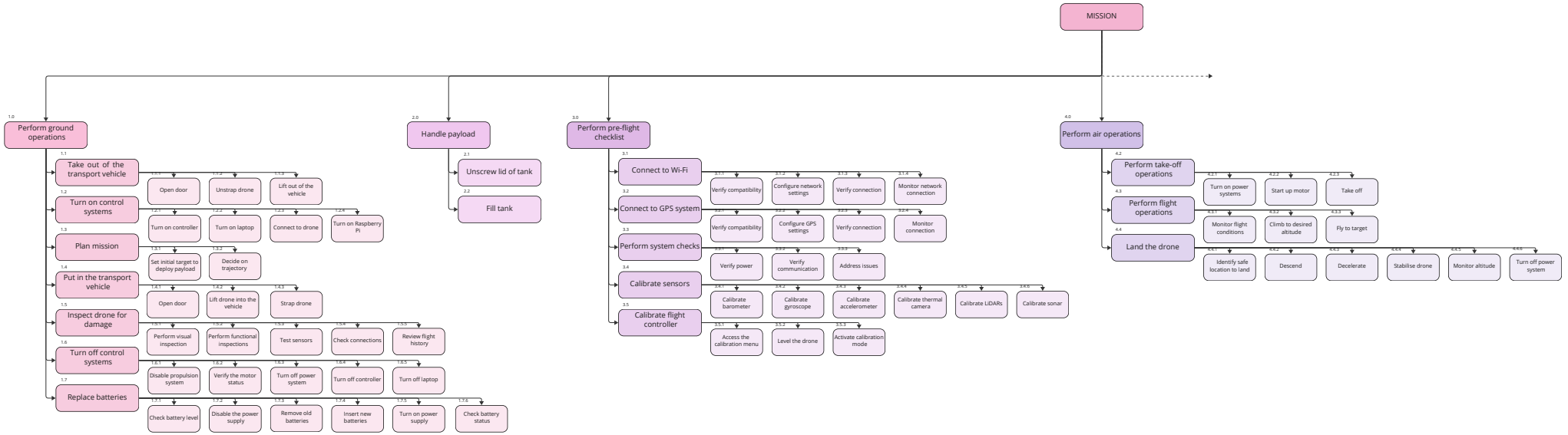
MISSION
1.0 Perform ground operations
1.1 Take out of the transport vehicle
1.1.1 Open door
1.1.2 Unstrap drone
1.1.3 Lift out of the vehicle
1.2 Turn on control systems
1.2.1 Turn on controller
1.2.2 Turn on laptop
1.2.3 Connect to drone
1.2.4 Turn on Raspberry Pi
1.3 Plan mission
1.3.1 Set initial target to deploy payload
1.3.2 Decide on trajectory
1.4 Put in the transport vehicle
1.4.1 Open door
1.4.2 Lift drone into the vehicle
1.4.3 Strap drone
1.5 Inspect drone for damage
1.5.1 Perform visual inspection
1.5.2 Perform functional inspections
1.5.3 Test sensors
1.5.4 Check connections
1.5.5 Review flight history
1.6 Turn off control systems
1.6.1 Disable propulsion system
1.6.2 Verify the motor status
1.6.3 Turn off power system
1.6.4 Turn off controller
1.6.5 Turn off laptop
1.7 Replace batteries
1.7.1 Check battery level
1.7.2 Disable the power supply
1.7.3 Remove old batteries
1.7.4 Insert new batteries
1.7.5 Turn on power supply
1.7.6 Check battery status
2.0 Handle payload
2.1 Unscrew lid of tank
2.2 Fill tank
3.0 Perform pre-flight checklist
3.1 Connect to Wi-Fi
3.1.1 Verify compatibility
3.1.2 Configure network settings
3.1.3 Verify connection
3.1.4 Monitor network connection
3.2 Connect to GPS system
3.2.1 Verify compatibility
3.2.2 Configure GPS settings
3.2.3 Verify connection
3.2.4 Monitor connection
3.3 Perform system checks
3.3.1 Verify power
3.3.2 Verify communication
3.3.3 Address issues
3.4 Calibrate sensors
3.4.1 Calibrate barometer
3.4.2 Calibrate gyroscope
3.4.3 Calibrate accelerometer
3.4.4 Calibrate thermal camera
3.4.5 Calibrate LiDARs
3.4.6 Calibrate sonar
3.5 Calibrate flight controller
3.5.1 Access the calibration menu
3.5.2 Level the drone
3.5.3 Activate calibration mode
4.0 Perform air operations
4.2 Perform take-off operations
4.2.1 Turn on power systems
4.2.2 Start up motor
4.2.3 Take off
4.3 Perform flight operations
4.3.1 Monitor flight conditions
4.3.2 Climb to desired altitude
4.3.3 Fly to target
4.4 Land the drone
4.4.1 Identify safe location to land
4.4.2 Descend
4.4.3 Decelerate
4.4.4 Stabilise drone
4.4.5 Monitor altitude
4.4.6 Turn off power system

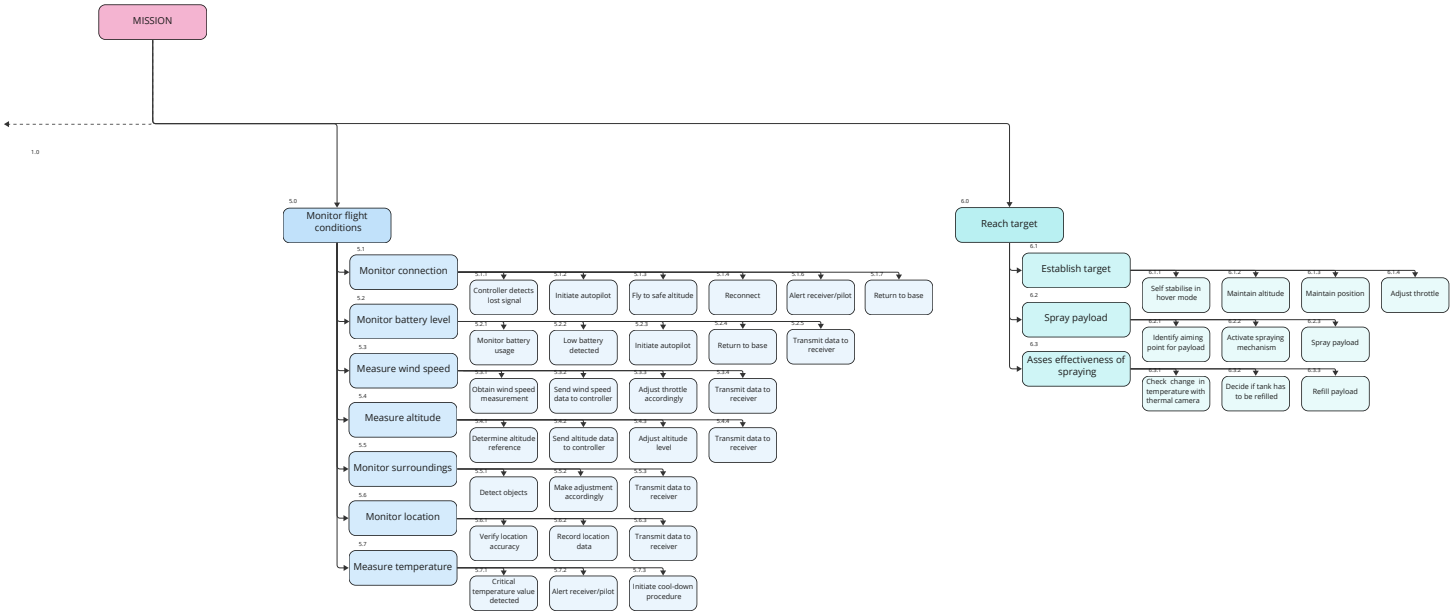
MISSION
1.0
5.0 Monitor flight conditions
5.1 Monitor connection
5.1.1 Controller detects lost signal
5.1.2 Initiate autopilot
5.1.3 Fly to safe altitude
5.1.4 Reconnect
5.1.5 Alert receiver/pilot
5.1.6 Return to base
5.2 Monitor battery level
5.2.1 Monitor battery usage
5.2.2 Low battery detected
5.2.3 Initiate autopilot
5.2.4 Return to base
5.2.5 Transmit data to receiver
5.3 Measure wind speed
5.3.1 Obtain wind speed measurement
5.3.2 Send wind speed data to controller
5.3.3 Adjust throttle accordingly
5.3.4 Transmit data to receiver
5.4 Measure altitude
5.4.1 Determine altitude reference
5.4.2 Send altitude data to controller
5.4.3 Adjust altitude level
5.4.4 Transmit data to receiver
5.5 Monitor surroundings
5.5.1 Detect objects
5.5.2 Make adjustment accordingly
5.5.3 Transmit data to receiver
5.6 Monitor location
5.6.1 Verify location accuracy
5.6.2 Record location data
5.6.3 Transmit data to receiver
5.7 Measure temperature
5.7.1 Critical temperature value detected
5.7.2 Alert receiver/pilot
5.7.3 Initiate cool-down procedure
6.0 Reach target
6.1 Establish target
6.1.1 Self stabilise in hover mode
6.1.2 Maintain altitude
6.1.3 Maintain position
6.1.4 Adjust throttle
6.2 Spray payload
6.2.1 Identify aiming point for payload
6.2.2 Activate spraying mechanism
6.2.3 Spray payload
6.3 Asses effectiveness of spraying
6.3.1 Check change in temperature with thermal camera
6.3.2 Decide if tank has to be refilled
6.3.3 Refill payload

3
Mission Requirements

For the designing of the drone, clear requirements had to be established. These requirements were received from the user and other stakeholders and will be discussed in Section 3.1 and Section 3.2, respectively. From these, system, subsystem and sustainability requirements were derived. These will be discussed in Section 3.3, Section 3.4 and Section 3.5. Lastly, the key and driving requirements are identified and will be discussed in Section 3.6.

3.1. User Requirements

User requirements are requirements that describe what the user expects from the drone. These requirements represent the needs and the wanted features from the perspective of the user. They are crucial as they ensure that the expectations of the user are met. The user for this mission is the Dutch Fire Brigade. The user requirements were determined after a discussion with Robbert Heinecke (Manager Operations & Training National Unmanned Flying Organization) from the fire department in combination with the given requirements. The user requirements are divided into performance, safety and cost and are presented in Table 3.1.

Table 3.1: *User requirements*

ID	Requirement
Performance	
REQ-USER-P-1	The UAV shall be able to carry a minimum payload of 10 kg
REQ-USER-P-2	The UAV shall have an average operational time of 20 min
REQ-USER-P-3	The UAV shall be able to fit inside a fire brigade transport vehicle
REQ-USER-P-4	The UAV shall be equipped with a thermal camera
REQ-USER-P-5	The UAV shall be equipped with a visual light camera
Safety	
REQ-USER-S-1	The UAV shall be controllable up to a minimum wind speed of 6 Bft
REQ-USER-S-2	The UAV shall be equipped with a visual warning system
REQ-USER-S-3	The UAV shall be able to safely land in case of loss of signal
Cost	
REQ-USER-C-1	The cost of the single unit shall not exceed €25,000
REQ-USER-C-2	The UAV shall have a modular payload
REQ-USER-C-3	The UAV shall consist of at least 20% recyclable components

3.2. Stakeholder Requirements

Stakeholder requirements are requirements that represent the needs and constraints of parties that have an interest or influence on the mission. The stakeholders are manufacturing companies, the fire brigade, insurance companies, the government, the users and the general public. The stakeholder requirements are shown below in Table 3.2

Table 3.2: *Stakeholder requirements*

ID	Requirement
Stakeholder	
REQ-STAKE-1	The UAV shall perform the mission without causing additional damage
REQ-STAKE-2	The UAV shall comply with EU regulations for unmanned vehicles
REQ-STAKE-3	The UAV shall have minimum operating costs in comparison to competitors
REQ-STAKE-4	The UAV shall be easily visible in unclear conditions
REQ-STAKE-5	The UAV shall be operable in unfavourable weather conditions
REQ-STAKE-6	The UAV shall not cause damage to the environment
REQ-STAKE-7	The UAV shall be recoverable upon failure of one of its sub-systems
REQ-STAKE-8	The UAV shall be easily deployable with minimum personnel
REQ-STAKE-9	The UAV shall be monitorable at any point during the mission

3.3. System Requirements

The system requirements describe the specifications and capabilities that the drone must meet. They describe the system in general technical terms at a high level. They focus on the technical aspects of the drone and are shown below in Table 3.3.

Table 3.3: *System requirements*

ID	Requirement
System	
REQ-SYS-1	The UAV shall have a minimum operational time of 20 min at an average T/W of 1.4
REQ-SYS-2	The UAV shall have a vertical hovering accuracy of ±0.1 m in nominal conditions
REQ-SYS-3	The UAV shall have a horizontal hovering accuracy of ±0.1 m in nominal conditions
REQ-SYS-4	The UAV shall be able to achieve a flight altitude of 250 m
REQ-SYS-5	The UAV shall achieve a climb rate of 7 m/s
REQ-SYS-6	The UAV shall have the option to be controlled remotely
REQ-SYS-7	The UAV shall be able to operate in a 55°C environment for at least 120 seconds
REQ-SYS-8	The UAV shall have a minimum MTBF of 100 operating hours
REQ-SYS-9	The UAV shall have a maximum deployment time of 120 seconds
REQ-SYS-10	The UAV shall have a maximum T/W ratio of at least 2
REQ-SYS-11	The UAV shall be able to yaw at a rate of 90 deg/s
REQ-SYS-12	The UAV shall have a turn around time (TAT) between flights of at most 300 seconds
REQ-SYS-13	The UAV shall be able to deliver the fire-combating payload from a horizontal distance of at least 4 m
REQ-SYS-14	The UAV and its payload shall be water-resistant
REQ-SYS-15	The UAV shall not exceed an empty mass of 50 kg

3.4. Subsystem Requirements

Subsystem requirements refer to the specific requirements for the individual subsystems within the larger system of the drone. The subsystems are propulsion, power, electronics, payload and structure subsystem. The

subsystem requirements are listed in Table 3.4

Table 3.4: *Subsystem requirements*

ID	Requirement
Propulsion	
REQ-SYS-PROP-1	The propulsion system at max throttle shall be able to achieve a T/W of 2
REQ-SYS-PROP-2	The propulsion system shall be fully compatible with the power system
Power	
REQ-SYS-POW-1	The power system shall be able to withstand temperatures up to 55°C for 120 seconds
REQ-SYS-POW-2	The power system shall be replaceable within 120 seconds
Electronics	
REQ-SYS-ELEC-1	The UAV shall have an on-board flight controller
REQ-SYS-ELEC-2	The UAV shall be operable from ground control stations
REQ-SYS-ELEC-3	The UAV shall have a recovery system in case of loss of connection
REQ-SYS-ELEC-4	The UAV shall have a communication range of at least 300 m
REQ-SYS-ELEC-5	The UAV electronics shall integrate all the sensors
Payload	
REQ-SYS-PAY-1	The thermal camera shall have a thermal sensitivity of at least 1°C
REQ-SYS-PAY-2	The light camera shall have a minimum frame rate of 30 FPS
REQ-SYS-PAY-3	The cameras shall have active stabilisation measures
REQ-SYS-PAY-4	The cameras shall be able to operate in an environment of 55°C for 120 seconds
REQ-SYS-PAY-5	The UAV shall be equipped with sensors for measuring altitude
Structure	
REQ-SYS-STR-1	The UAV structure shall be able to support a payload of at least 10 kg
REQ-SYS-STR-2	The UAV structure shall be able to withstand the ultimate load factor of 3
REQ-SYS-STR-3	The UAV structure shall be able to support all the other subsystems
REQ-SYS-STR-4	The UAV structure shall allow for disassembly

3.5. Sustainability Requirements

Sustainability is an aspect of the design process which must be taken into consideration. Certain constraints must be placed on the design to ensure it is as sustainable as possible. Requirements specific to sustainability are presented in the table below.

Table 3.5: *Sustainability requirements*

ID	Requirement
Sustainability	
REQ-SUS-1	The UAV shall use a clean energy source
REQ-SUS-2	The UAV shall only use non-toxic extinguishing agents
REQ-SUS-3	The UAV shall use biodegradable extinguishing agents

Continued on next page

Table 3.5 – continued from previous page

ID	Requirement
REQ-SUS-4	An EOL strategy shall be implemented to improve sustainability

3.6. Discussion

From these requirements, the key and driving requirements can be identified.

3.6.1. Key Requirements

The key requirements refer to the most important requirements that are essential for the mission. These types of requirements are often related to safety, reliability and performance, and failing to meet them results in project or mission failure. For this mission, the key requirements identified are:

- **REQ-USER-P-1**: *The UAV shall be able to carry a minimum payload of 10 kg*
- **REQ-SYS-3**: *The UAV shall have a horizontal hovering accuracy of ±0.1 m in nominal conditions*
- **REQ-SYS-4**: *The UAV shall be able to achieve a flight altitude of 250 m*
- **REQ-SYS-7**: *The UAV shall be able to operate in a 55°C environment for at least 120 seconds*
- **REQ-SYS-13**: *The UAV shall be able to deliver the fire-combating payload from a horizontal distance of at least 4 m*

3.6.2. Driving Requirements

The driving requirements are the requirements that have the strongest influence on the project. These requirements have a significant impact and can dictate the direction of the overall design. It is essential to identify these requirements early on in the design process. For this mission, the driving requirements are:

- **REQ-USER-P-1**: *The UAV shall be able to carry a minimum payload of 10 kg*
- **REQ-USER-P-2**: *The UAV shall have an average operational time of 20 min*
- **REQ-USER-P-3**: *The UAV shall be able to fit inside a fire brigade transport vehicle*

4
Market Analysis

This chapter will focus on the current market of drones used in firefighting. It will provide an overview of the current market for such drones and the key players in this market. The insights gained from this analysis will help understand the opportunities and risks in the market. First, in Section 4.1, the firefighting drone market will be explored. After this, the main competitors will be discussed in Section 4.2 and the value proposition of the drone will be determined, explaining what differentiates this design. The key partners will be briefly presented in Section 4.3. In addition, to investigate the position of the drone in the market, a SWOT analysis will be performed in Section 4.4.

4.1. Market Definition

In this section, the current market for firefighting drones is described. The current value of the market and the future trends of those markets are assessed.

4.1.1. Firefighting Drone Market Value

Since 2015, European fire brigades have been implementing UAVs to gain aerial intelligence and support in the difficult task of firefighting [15]. In the following years, the possibilities for drones have been further investigated and researched with significant funding. Before finalising the drone design, it is imperative to analyse the current state of the market and how it shall evolve in the coming years.

The global firefighting drone market size was valued at 1.31 billion USD in 2022 and is forecasted to be 2.76 billion USD by 2030 [135]. Firefighting drones accounted for nearly 12% share of the global drone market at the end of 2022. The United States and Europe each account for a third of the 2023 market and China adds an additional 11% [95]. However, it is expected that China will see rapid revenue growth, increasing its market share as they are heavily investing in new technologies to keep up with growing urbanisation. In this market, drones under 45 kg are predicted to account for a 61.9% share [69].

From this, it is clear that the demand for such drones will continue to rise within the following years. In addition, it is expected that the development of these drones will be backed by governments, which will lead to growth in the firefighting drone market. An example of this is the British Government which invested 43 million USD in 2020 to develop firefighting and COVID drones, which can help tackle global challenges [135].

4.1.2. Market Division

The market for firefighting drones is primarily divided based on type, size and application [41]. The two prominent groups within the market are fixed-wing and multi-rotor drones. Fixed-wing drones have significantly better endurance performance and range due to their gliding performance, however for the current mission, as described in Chapter 2, hovering capabilities are crucial for keeping constant coverage and access to the fire location. For this reason, only the multi-rotor market is investigated. The size of firefighting drones is typically separated into micro and macro drones. Due to *REQ-USER-P-1*, it is assumed that the Dutch fire brigade has a higher demand for macro drones that are capable of delivering higher payloads. The market trends support this idea because in 2021 the firefighting drone market was dominated by micro drones, however, between 2022 and 2031 macro drones are projected to have the highest Compound Annual Growth Rate (CAGR) of 11.2% [82]. The firefighting drone market has four types of applications: scene monitoring, search and rescue, post-fire assessment and firefighting. As the design and performance of the drone vary significantly with the application, it is most representative to solely compare drones that have firefighting/extinguishing capabilities.

4.2. Competitor Analysis

Currently, a large majority of firefighting drones on the market focus on scene monitoring [74]. Firefighting is an emerging application for UAVs as technology continues to improve. Chinese companies dominate the market for such drones and offer different types of drones that have extinguishing capabilities. An overview of the most relevant competitors is presented in Table 4.1.

Table 4.1: *Data of main competitors*

Company (Country)	Drone	Payload Type	Price	Payload	Endurance (min)
Walkera [178] (China)	WK-1900	Tethered hose	$138,000	60 kg	45
Walkera [172] (China)	Zhun 1800	Dry powder tank	-	20 kg	35
EHang [63] (China)	216F	Foam and extinguisher bombs	$336,000	100 L + 6 bombs	21
Digital Eagle [44] (China)	SK-XF07	Extinguisher bombs	$158,000	15 kg	20
Hercules [50] (China)	FDT100	Modular	$89,900	10 kg	45
FlyDragon [49] (China)	FDG100XH	Extinguisher bombs	$32,800	40 kg	20
BroUAV [31] (China)	FU-6	Extinguisher balls	$10,600	13 kg	50
Feilong Company [73] (China)	FD1600	Extinguishing balls	-	10 kg	40

Discussion

The most prominent competitors, in terms of drone type, size and application are collected in Table 4.1. Multiple aspects can be observed and shall be discussed below. It should be noted that the performance parameters such as endurance and payload capacity are usually stated with misleading ambiguity. Common examples include stating the maximum payload capacity without giving the corresponding endurance or providing an endurance, without stating at which payload or type of flight (hovering or a specific T/W).

Region:
After looking at competitors, it was concluded that most drones originate from China. This suggests that this design is one of the first of its kind in Europe. This claim is supported by Robbert Heinecke, from the Dutch Fire Brigade, who mentioned the struggle that comes with importing Chinese drones to the EU due to the difference in drone certifications and regulations. Hence why these drones are not used in Europe. Furthermore, the prices were usually found from resellers and were not available from their own sites. This again raises a question about their availability and accessibility in other regions, such as the EU. This shows the opportunity for this drone to enter the market and have a significant market share in the EU.

Payload:
In terms of payload, it can be seen that there is a variety of firefighting drones with extinguishing capabilities on the market. However, a large majority vary in mission type as they primarily deliver extinguishing balls/bombs. Only the *Walkera Zhun 1800*, *Hercules FDT100* and *EHang 216F* are similar as these drones make use of an onboard tank/spraying system. This is important to note when comparing the performance of the drones. As only three drones were found to have similar capabilities, this demonstrates another opportunity for this drone to have a significant market share.

Cost:
Furthermore, something noticeable is the prices of such commercially available drones. These types of drones can be expensive ranging from tens of thousands of dollars to hundreds of thousands of dollars. With *REQ-USER-C-1*, the newly designed drone will cost around €25,000, making it much more affordable than the drones of competitors.

From this, it can be concluded that, even though some drones may have been developed for this purpose, there are clear market opportunities. One is the competitive pricing of the drone, offering a fire extinguishing drone

for a much lower price. Second, being one of the only European drones on the market making it more accessible for Western fire departments.

4.3. Key Partners

In order to produce the drone, the partners that are involved must be clearly identified.

Dutch fire brigade: The Dutch fire brigade is the primary stakeholder for this drone. The user requirements are obtained and negotiated with them. They will be closely worked with to ensure that the drone is optimal for their applications.

Dutch government: The Dutch government is a key player in this drone design as they fund the fire brigade and implement laws and regulations on how the drones can be operated.

TU Delft: For this drone, a primary objective is to develop and manufacture the drone "in-house". This means that the production methods and manufacturing choices shall be tailored to match the capabilities and resources available at the TU Delft.

4.4. SWOT Analysis

From analysing the firefighting drone market and the existing competitors, a Strengths, Weaknesses, Opportunities and Threats (SWOT) analysis is conducted in order to gain a clear overview of the product in the market. It is presented in Figure 4.1. A SWOT analysis is a useful tool for identifying the strengths, weaknesses, opportunities, and threats of the design. By determining these factors, a better understanding of the drone's potential for success can be obtained by focusing on its strengths while minimising its weaknesses and threats.

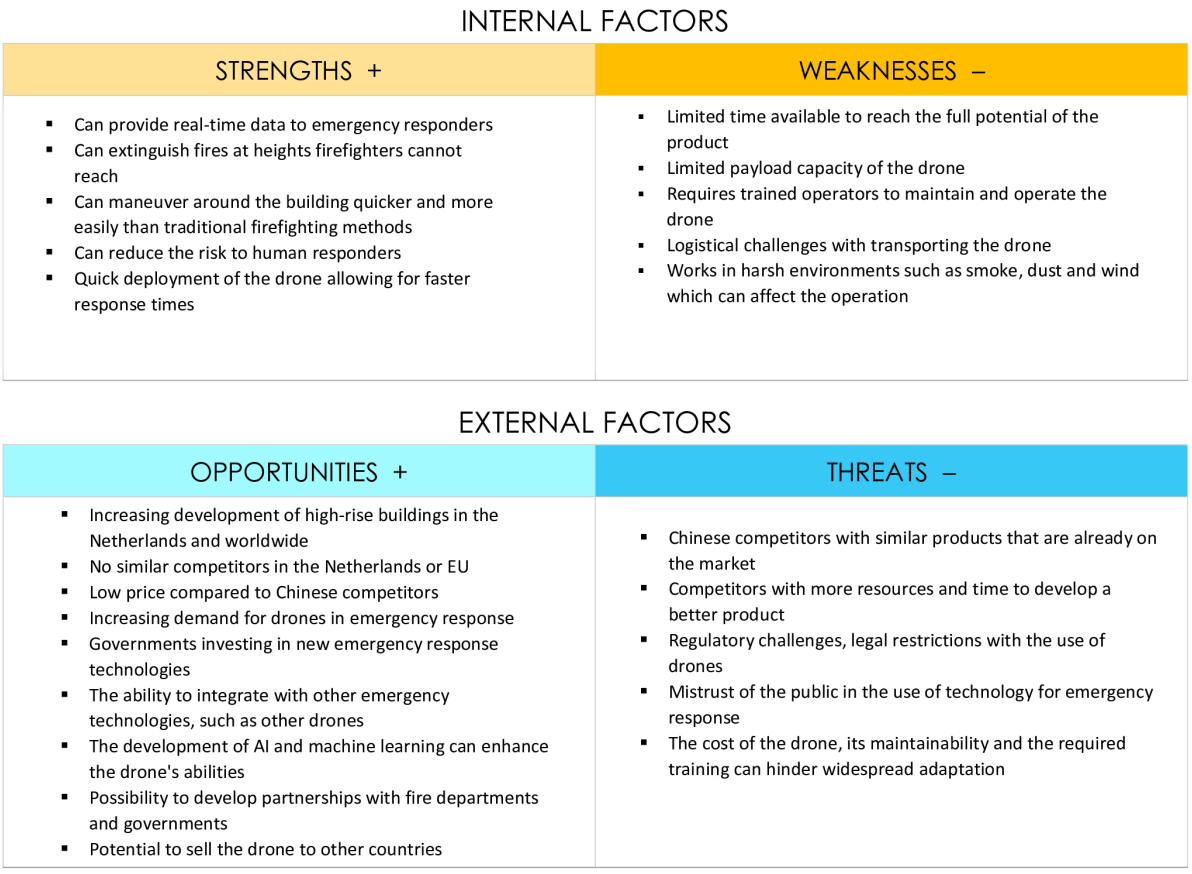

Figure 4.1: *SWOT analysis of the firefighting drone*

5
Payload

In this chapter, the final trade-off will be done for the payload mechanism and the final payload configuration will be determined. First, the final options will be revised in Section 5.1. Next, in Section 5.2, these options will be traded-off. In Section 5.3, the performance of the payload will be analysed. Lastly, based on the performance analysis, the final payload configuration will be finalised in Section 5.4.

5.1. Payload Mechanism Analysis

In the Midterm Report, the final options left for the payload mechanism were off-the-shelf fire extinguishers and a custom pressurised tank with a pump shooting out fire suppressant [56]. However, at that time, refill time, reliability and certification were not considered. Water pumps do not need certification, can be easily refilled and are highly reliable. They were previously removed from the trade-off for not being easily available off-the-shelf, but this is not as important as refillability for this mission. In this section, the previously removed option of a water pump will be reconsidered after the off-the-shelf fire extinguisher and custom pressurised tank are discussed.

5.1.1. Off-the-Shelf Fire Extinguisher

The selection of the off-the-shelf fire extinguishers has already been done in the Midterm Report [56]. Three types of tanks came out to be the best options: water, foam and dry powder. However, these were chosen according to the requirement that the total payload mass shall not exceed 10 kg. For this report, it has been decided that optimising the payload per minute delivered to the high-rise building is more important than maximising endurance by setting a limit of 10 kg on the payload. Further details on this topic can be found in Section 11.4.

A large variety of capacities are available for fire extinguishers, hence the weight of the initial selection can be decreased or increased easily. However, with a fire extinguisher tank weight greater than 15 kg, two or more tanks are necessary. This would add more complexity and weight to the design. The fire extinguishers would be implemented in the UAV as illustrated in Figure 5.1. It should be noted that the extinguisher is also mounted to a bracket, which has not been drawn. An advantage of this system is that it can use different suppression types, and the extinguishers are widely available. To activate the fire extinguisher, a linear servomechanism is used. The servomechanism and handles would be clamped in between two metal plates. The handles can also be removed completely to allow the servo to press the valve system of the extinguisher directly. This would improve reliability and weight but would require more preparation and careful handling of the extinguishers. Linear servos have enough force and speed to activate the fire extinguisher, but they have the disadvantage of being heavy. Linking the linear servos to the extinguisher valves adds complexity and risks. Furthermore, multiple extinguishers have to be brought to the mission location in order to be able to refill.

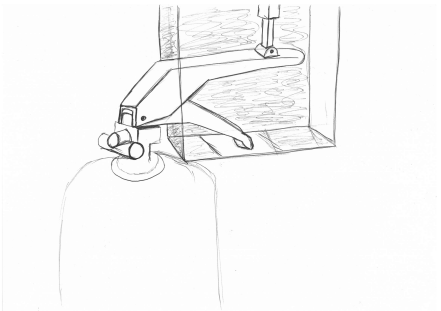

Figure 5.1: *Off-the-shelf fire extinguisher with activation mechanism*

5.1.2. Custom Pressure Tank

Designing a custom pressure tank has the main advantage that it can be designed to fit better underneath the UAV compared to an off-the-shelf tank. This may reduce the weight of the mechanism and opens up the possibility

to choose a specific tank capacity.

However, a custom pressure tank has a big disadvantage. When designing a custom tank there are strict regulations from the European Union [170]. The tank has to comply with all these regulations, which would cost a significant amount of time and money. Furthermore, getting a certification for the tank would introduce a significant extra cost [37].

5.1.3. Water Tank with Pressure Pump

This option was removed in the Midterm Report [56]. However, it is reconsidered since it appears to be more promising when taking reliability and refill time into account. With this configuration, a pressure pump is connected to a water tank. From the pressure pump, the water will flow through a tube. This tube is then connected to a nozzle, which can spray water. Depending on the pump and nozzle, this system can achieve even higher ranges than pressurised systems [181].

Another advantage is that the tank can be lightweight and custom-made without regulations, as it is not pressurised. The pressure pump can be chosen such that the pressure is enough to have a certain range that has been specified for a nozzle. The tank can also be easily refilled. However, only water can be used with this system due to the pressure pump.

5.2. Trade-Off

In this section, the trade-off for the payload mechanism will be done. The options will be analysed based on the criteria discussed in Subsection 5.2.1, whereafter a conclusion can be drawn in Subsection 5.2.2.

5.2.1. Trade-Off Criteria

Now that the three options are analysed, a trade-off can be done. This trade-off will be done based on the following parameters:

- Range
- Reliability & feasibility
- Refill time
- Capacity
- Suppression

Range

The range of the mechanism has a lot of influence on the mission performance. Hence this is also chosen as a criterion. **The range criterion has been given a weight of 30%.**

Reliability & Feasibility (R&F)

This parameter is a measure of how well the mechanism works, and how feasible the mechanism is to construct. **The feasibility criterion has been given a weight of 15%.**

Refill Time

For the mission, it is important that the turn-around time is as low as possible. To achieve this, the payload needs to be refilled quickly. **The refill time criterion has been given a weight of 20%.**

Capacity

The capacity is an important criterion since it gives an indication of the extinguishing capabilities of the system. **The capacity criterion has been given a weight of 25%.**

Suppression

Suppression capabilities were already analysed in the Midterm Report [56]. Water, foam and dry powder all came out to be the best option. Not all of the systems can use all of these options. All systems, however, can use water, which is already sufficient. **The suppression criterion has been given a weight of 5%.**

5.2.2. Trade-Off Results

In Table 5.1, the trade-off was done based on the criteria in Subsection 5.2.1, and information in Section 5.1. The **water tank with pressure pump** came out to be the best option.

The range has been given in metres. The range values for the custom pressure tank and off-the-shelf tank have been discussed in the Midterm Report [56]. The water tank can be found in Figure 5.4.1. For reliability, refill time and capacity, the systems were given a grade ranging from 1 to 4, with 4 being the best option and 1 the worst option. For suppression, a 1 was given if the system can be used for one type of suppressant, a 2 if it can be used for 2 types etc.

Table 5.1: *Payload trade-off table scoring*

Criteria	Range, 30.0%	R&F, 15.0%	Refill Time, 20.0%	Capacity, 25.0%	Suppression, 5.0%	Total
Design Concept	(6, 15) High Best, $\sigma = 3.682$	(1, 3) High Best, $\sigma = 0.816$	(1, 3) High Best, $\sigma = 0.816$	(3, 4) High Best, $\sigma = 0.471$	(1, 3) High Best, $\sigma = 0.943$	
Custom Pressure Tank	yellow 10	red 1	red 1	blue 4	blue 3	0.433
Off-the-Shelf Fire Extinguisher	red 6	green 2	green 2	red 3	blue 3	0.225
Water Tank with Pressure Pump	blue 15	blue 3	blue 3	blue 4	red 1	0.9

5.3. Payload Performance Analysis

In this section, the performance of the payload will be analysed with several methods. First, the range of the extinguisher will be analysed in Subsection 5.3.1, by using kinematic equations. Secondly, in Subsection 5.3.2, the flow in the pressure system will be analysed using the energy balance equation. Finally, the limitations of the analysis will be considered in Subsection 5.3.3.

5.3.1. Range Analysis

According to REQ-SYS-13, the payload shall be delivered from a horizontal distance of at least 4 m. For calculating the expected range from the extinguishing system, a simple model based on particle kinematics was constructed [166]. In this model, it is assumed that the UAV is firing at 100 m above the ground. The horizontal range is measured at the point where the particle reaches a height of 98 m. The UAV is allowed to spray 2 m downwards. The UAV will spray the water horizontally. The exit velocity from the nozzle is taken as input, and the range is the output. In Figure 5.2, trajectories for different exit velocities have been plotted. In Figure 5.2, the range for every exit velocity can be found. An exit velocity of 5 m/s, does not meet REQ-SYS-13, however from 10 m/s and onwards it will have sufficient range.

Table 5.2: *Water jet exit velocity with its respective range*

Exit Velocity [m/s]	Range [m]
5	3.19
10	6.39
15	9.57
20	12.78
25	15.95
30	19.14

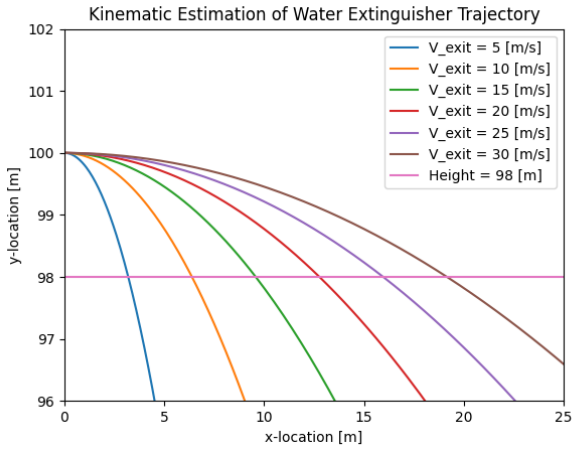

Figure 5.2: *Trajectory of the water jet for different exit velocities*

5.3.2. Pressure Pump Analysis

With the minimum exit velocities from Subsection 5.3.1, the required performance from the pressure pump can be analysed and a suitable nozzle can be found. This was done by assuming a constant flow rate and using the energy balance Equation 5.1 [77]. This equation is similar to Bernoulli's equation, however, three additional terms are included on the right-hand side of the equation.

The first new term is the Darcy-Weisbach equation. This equation incorporates the pressure loss due to the drag forces of the system, using the pipe length, diameter, dynamic pressure and friction coefficient. This friction coefficient can be estimated using the Moody diagram, which depends on the Reynolds number and roughness of the pipes.

The second additional term incorporates minor pressure losses due to valves and bends in the system. The term uses a dimensionless loss coefficient K and dynamic pressure. The flow in fittings and valves is complex hence this can merely be used for a conservative estimate [77].

The last term in Equation 5.1 adds the pressure gain due to the pump. Finally, it is important to note that both the friction and minor pressure loss terms do not depend on v_2 but on the velocity between points one and two.

$$p_1 + \frac{1}{2}v_1^2 + \rho g z_1 = p_2 + \frac{1}{2}v_2^2 + \rho g z_2 + f\frac{L}{d}\frac{1}{2}\rho v^2 + K\frac{1}{2}\rho v^2 - P_{pump} \tag{5.1}$$

The pressure system is shown in Figure 5.3 and will be analysed in two steps. First the flow from points one to two will be analysed in order to find the pressure at point two. Secondly, the flow from point two to point three will be analysed in order to find the exit velocity v_3.

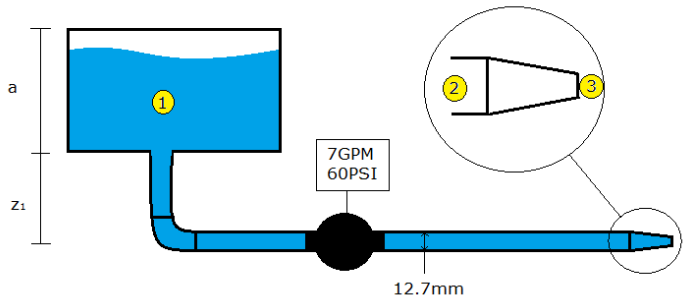

Figure 5.3: *Pressure system model*

When analysing the flow from point one to point two, the dynamic pressure term from point one and the potential pressure term from point two can be removed, since $v_1 = z_2 = 0$. Furthermore, p_1 can be calculated using Equation 5.2 and since the flow rate is assumed to be constant, v_2 can be found using Equation 5.3. Finally, since the pipe diameter between points one and two is also constant: $v = v_2$. This leaves Equation 5.4 and all the necessary values to calculate p_2, after f and K are estimated.

$$p_1 = p_0 + \rho g a \tag{5.2}$$

$$v = \frac{Q}{A} = \frac{Q}{\pi r^2} \tag{5.3}$$

$$p_1 + \rho g z_1 = p_2 + \frac{1}{2}v_2^2 + f\frac{L}{d}\frac{1}{2}\rho v_2^2 + K\frac{1}{2}\rho v_2^2 - P_{pump} \tag{5.4}$$

Now the flow from point two to point three needs to be analysed. First, using Equation 5.1, the potential pressure terms at both sides of the equation can be removed and the pump pressure may be left out since there is no height

difference and no pump. Furthermore, knowing that $p_3 = p_0$ and assuming $v = \frac{1}{2}v_3$, results in Equation 5.5. With the previously calculated p_2 and new estimations for f and K, v_3 can now be calculated. Furthermore, the nozzle diameter can be derived using Equation 5.3.

$$p_2 + \frac{1}{2}\rho v_2^2 = p_0 + \frac{1}{2}\rho v_3^2 \left(1 + \frac{K}{4} + f\frac{L}{4d}\right) \tag{5.5}$$

5.3.3. Analysis Limitations

Although the method described might seem accurate, it does come with some limitations. The main limitations are caused by the use of particle kinematics to calculate the expected range. This uses the assumption that there is no aerodynamic drag. At low velocities and short distances, aerodynamic drag can often be neglected. However, for water jets, this is not always the case. A solid water jet will break up into smaller droplets after a certain distance. This will substantially increase the aerodynamic drag [24]. The breakup distance and effect of aerodynamic drag on the stream after the breakup are difficult to model and would require extensive CFD modelling. Furthermore, the nozzle design would also have to be incorporated since this has a large influence on the shape of the water jet and droplet size [164]. Hence the calculations from Subsection 5.3.1 were only used in order to find a minimum exit velocity at the nozzle. The actual range of the spraying system will have to be experimentally tested and can be easily altered by changing nozzles due to the low price and high influence of nozzles.

As for the pressure pump analysis, the largest errors are caused by friction and minor pressure loss coefficients. However the pressure losses in the pipes are expected to be less than 0.5 bar, hence the errors will be small. The pressure losses in the nozzle are harder to estimate. However, data from existing nozzles can be used to estimate these losses and limit the errors.

5.4. Component Selection

The main components for the payload are the pressure pump, water tank, tubes and nozzle. In this section, the components will be selected based on the analysis methods from Section 5.3 and Section 11.4.

5.4.1. Pressure Pump

The pressure pump is the most important part of the payload system. The flow rate and maximum pressure will have a large influence on the range and discharge time, but also on the weight of the system. Due to the weight and DC low current requirements, it quickly became apparent that small membrane pumps for boats and RVs would be most suitable. These pumps are small, lightweight and require low voltages. Furthermore, they can be used for multiple purposes, one of them being used for wash downs which are closely related to the current purpose. Other pumps like bilge water pumps, or flexible impeller pumps were also considered. However, these would either not deliver enough pressure, become too heavy or require too much power.

The first suitable pump that was found was a membrane pump that had a flow rate of 18.9 LPM, a maximum pressure of 3.8 bar and a weight of only 1.85 kg and can be seen in Figure 5.4. However, performance analysis, from Section 11.4, showed that the discharge time of this pump would be the limiting factor instead of the total payload weight. Hence a new pump with a higher flow rate was needed. In Figure 5.5 the newly selected pump is shown. This pump has a flow rate of **26.5 LPM**, a maximum pressure of **4.14 bar** and a weight of **4.7 kg**. The pump requires 12 V and 20 A, meeting the low current requirements as well. Although this pump is substantially heavier, the increase in flow rate greatly reduced the hover time required for a mission. This increased the payload capacity and changed the limiting factor to the minimum T/W required for flight. This indicates that only the weight of the UAV can be further reduced for better performance.

Figure 5.4: *Membrane pump [26]*

Figure 5.5: *Washdown waterpump [173]*

Water Tank

According to the optimisation, discussed in Section 11.4, the ideal capacity of the water tank with the 26.5 LPM pump is **20 litres**. The water tank has to be accessible for refills whilst also leaving enough room for the pump and tubes. Furthermore, it is important that all the water in the tank can be used by the pump and that it can be properly mounted to the frame.

To meet all the requirements, a custom water tank is the best solution. In Figure 5.6a the custom water tank is shown. It has a conical design at the bottom to make sure that all the water flows into the pump. The top part is flat to make the tank easily fit under the airframe and has a small pipe protruding from the side for refills. However, a custom water tank would require a custom mould. These can cost between **€1000 and €5000** and are not suitable for one-time use [125]. Hence, only for **final production** would Figure 5.6a be feasible.

For **prototyping** an off-the-shelf water tank like Figure 5.6b could be used, even though it does not have the optimal capacity, shape or tube connections. The tank would still be able to provide water to the pump and allow for testing of the UAV. Furthermore, it is far more reasonably priced at only **€83.49**.

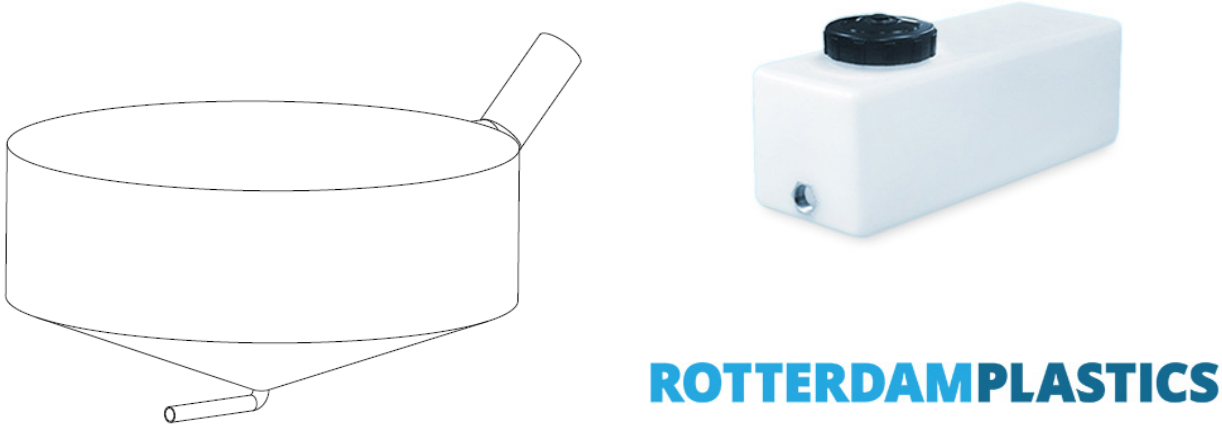

(a) *Custom 20 L water tank*

(b) *Off-the-shelf 12L water tank [124]*

Figure 5.6: *Water tank design options*

Nozzle

The nozzle that was chosen, is shown in Figure 5.7. The method described in Subsection 5.3.2 was used to find the nozzle diameter. With the pressure and flow rate data from different nozzles, the f and K coefficients for this type of nozzle were estimated. When combined with the rest of the pump system, this resulted in a nozzle diameter of 4.6 mm at 26.5 LPM and 4 bar.

However, a nozzle with an exact diameter of 4.6 mm is not available. Hence a large nozzle with a **diameter of 4.8 mm** was chosen instead. This will allow for higher flow rates, which were established to be an important parameter in Subsection 5.4.1. Furthermore, the pressure needed for these flow rates will also drop since the friction and minor loss pressures are quadratically related to the velocity, which in turn is inversely related to the nozzle diameter, as explained in Subsection 5.3.2. The maximum pressure of the pump is only 4.13 bar, hence a lower required pressure will leave more room for possible calculation errors. The range is expected to drop due to the higher diameter, however, data from the "Wildkamp" webshop and calculations from Subsection 5.3.1 result in **ranges of over 16 m** [181]. This means that even with a decrease in range, due to a larger diameter and aerodynamic forces, REQ-SYS-13 can still be easily met.

Figure 5.7: *4.8 mm diameter nozzle [181]*

As mentioned earlier in Subsection 5.3.3 the actual performance of the nozzle with the chosen pump has to be experimentally tested. The nozzle can easily be replaced if the performance is not acceptable or if different kinds of water jets are needed, like a straight stream instead of a solid stream [71].

Tubes and Pipes

The final part of the payload mechanism is to connect the pump, tank and nozzle. The connections can be made with **PVC tubes** and connectors as illustrated in Figure 5.8 and Figure 5.9. The inner diameter of the tube and connectors are **1/2 inch** due to the diameter of the pump connections. The PVC tubing in Figure 5.8 is able to withstand the temperature, and pressure requirements [6], other tubes can be used as long as these requirements are still met.

Figure 5.8: *1/2 inch PVC tube [6]*

Figure 5.9: *Tube connector [126]*

Apart from tubes, a pipeline is also needed. The nozzle has to be positioned beyond the propellers to ensure that the downwash will not affect the water stream. A carbon tube with an inner diameter of **1/2 inch** is used for this. The inside of a carbon tube is smooth to keep friction forces low whilst also being strong enough to not bend under the weight of water or aerodynamic forces.

6
Power and Propulsion

In the Midterm Report, an extensive and systematic approach was utilised to select the optimal motor, battery and rotor configuration. In this chapter, a summary of the entire process will be described. The full description of the method is documented in the Midterm Report [56].

6.1. Configuration Selection

After constructing a Design Option Tree (DOT) and excluding the unfeasible options, it was decided that the suitable options for the mission were multi-copters. To investigate whether the quad-, hexa- or octa-copter is most optimal for this mission, the best motor, battery and propeller combinations for each had to be found and discussed. To do this, the following steps were performed.

Weight Estimation

First, assigning preliminary values for each component of the drone, a preliminary weight estimation was performed to get an estimate of the mass of the drone.

Select T/W

Following the weight estimation, the desired maximum T/W is chosen. At that stage of the design process, the desired T/W was chosen to be 3 due to the large amounts of uncertainty in the design. *REQ-SYS-10* states that the drone should at least be able to achieve a T/W of 2 for sufficient controllability, however, integrating this margin ensures that the propulsion system shall still be feasible later on in the design process. Knowing this, the thrust required per motor to achieve this T/W ratio was calculated, and motors which could reach this value or higher were chosen for the motor selection.

Motor Selection

For the motor selection, several variables were taken into account. After choosing the best compatible propellers for each motor in order to produce the highest thrust, the data sheets, which are provided by the manufacturers, stating the current draw and thrust generation at the different throttle settings, were collected. Using this data, curves mapping the thrust of the motor and the current draw were created using interpolation. These mappings were used to establish the T/W and endurance capabilities of the motor. To perform a valid comparison between all the motors, they were evaluated using the same “baseline” battery. Based on the trade-off criteria, the highest-performing combination for each rotor configuration was selected.

In Table 6.1, the motors selected are presented and numbered from one to seven.

Table 6.1: *The seven Chosen Motor Options*

Motor	Name	Mass [g]	Cost [$]	Max Thrust [g]	Compatible propeller
1	KDE 10218XF-105 (12S) [45]	1075	985	19660	30.5” x 9.7 DUAL-EDN (KDE)
2	U12II KV120 [161]	778	370	20400	G30 · 10.5”
3	MN1010 KV135 [159]	645	340	21561	G32 · 11
4	MN805-S KV150 [160]	625	270	16028	G28 · 9.2
5	KDE 10218XF-105 (8S) [45]	1075	985	14721	35.5” x 12.1 DUAL-EDN (KDE)
6	KDE 10218XF-105 (10S) [45]	1075	985	16430	30.5” x 9.7 TRIPLE-EDN (KDE)
7	AntiG MN8017 KV120 [158]	453	290	16841	G30 · 10.5

Battery Selection

Once the best motor options have been chosen, the next step is to iterate them over different battery options, to find the best motor-battery combination. The seven battery options chosen can be seen in Table 6.2.

Table 6.2: *The seven Chosen Battery Options*

Battery 12S	Name	Mass [g]	Cost [$]	Capacity [Ah]	Max Discharge Rate [A]
a	62Ah 12S Lipo [18]	13312	3601	62	387.5
b	46Ah 12S Lipo [17]	9564	3120	46	287.5
c	34Ah 12S Lipo [19]	7577	2400	34	127.5
d	22Ah 12S Lipo [20]	5050	1680	22	220
e	16Ah 12S Lipo [21]	1874	690	16	240
f	11Ah 12S Lipo [22]	2530	840	11	110

The correct number of batteries is not immediately clear. Not only is each sub-configuration iterated over each battery, but also iterated over the number of batteries. This method of analysis leads to a plot of each sub-configuration with several different viable options for motor-battery-amount of battery combinations [56]. Only one example of these graphs will be shown: the six-rotor configuration and one type of motor. The in-detail analysis of each combination can be found in the Mid-term report [56].

6.2. Demonstration Configuration Selection

An example of what the battery selection looked like is shown in Figure 6.1. This means that for the six-rotor configuration with motor 3 [159], which ended up being the final motor choice for the UAV, different types of batteries and amounts of batteries were compared. The T/W ratio is shown on the x-axis and endurance in minutes is shown on the y-axis. Taking into account high performance in both, but also the cost and complexity of the entire system, the optimal battery is chosen for motor 3. “For this motor, many battery combinations greatly exceed the T/W requirements. Furthermore, all prices are within an acceptable range. C6.3.f.4, C6.3.e.4 and C6.3.d.3 are discarded, as a T/W ratio above 3 is over-designed and the corresponding endurance values are relatively low. These configurations also use 4, 4 and 3 batteries corresponding in order which creates more complexity which is not desirable. This leaves **C6.3.b.2** as the obvious choice as it outperforms the remaining options. Furthermore, it only has two batteries, reducing its complexity.”

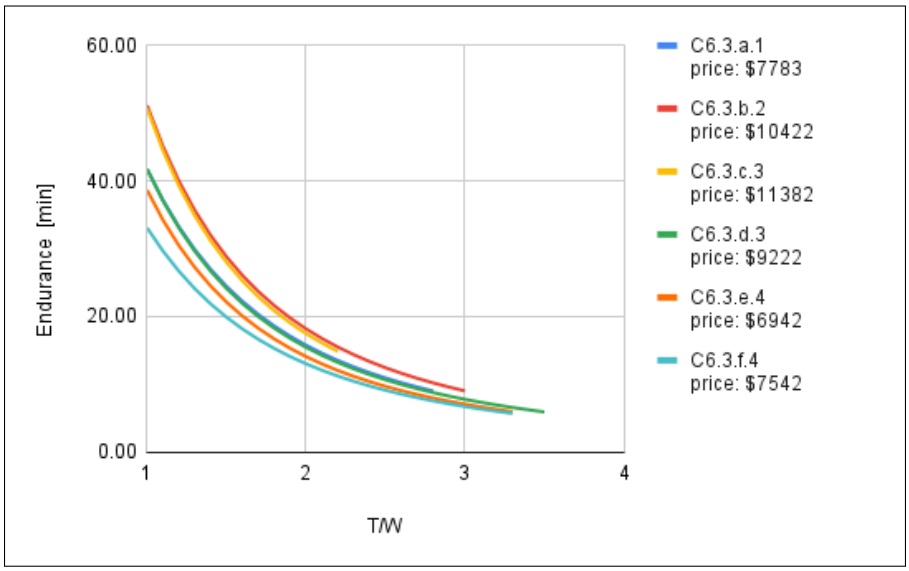

Figure 6.1: *C6.3 Battery Selection*

6.3. Trade-off Criteria

Once the selection above has been done for every single motor and rotor configuration, the final trade-off with only the most optimal combinations can be performed, For the trade-off of the final configurations, the criteria and their corresponding weights are displayed in Table 6.3. Each configuration was given a rating until the optimal motor-battery-propeller and rotor configuration was chosen.

Table 6.3: *Trade-Off Weight Factors*

Criteria	Weight Factor
Endurance	25
Max T/W	30
Complexity	10
Cost	20
Transportability	15

6.4. Results

This entire method resulted in six **T-MOTOR MN1010 KV135** motors [159]. These are powerful, 12S motors that are each capable of a maximum thrust of **21.5 kg** at max power when using the matching propellers. This propeller is the Carbon Fibre plus Epoxy **G32 · 11 Prop** [157]. With this motor and propeller combination, the optimal battery was found to be two **LiPo 46000 12S2P 44.4v** batteries [17].

7
Electrical Components

After finalising the trade-off of the structure, material and payload mechanism, the electrical components of the UAV were investigated. All the required components must be identified and off-the-shelf components must be chosen with regard to performance and compatibility. This process will be presented and explained below.

In Section 7.1, an overview of all the components in the drone will be presented. In Section 7.2, a discussion on each component comparing three different options will be made, and a final choice for every component will be decided. In Section 7.3, the insulation of the components will be discussed. The electronic block diagram denoting the entire electrical system in the drone, complete with all components including voltage and current specifications, will be given Section 7.4. Finally, the Input-Output relationship N2 chart of the system will be shown in Section 7.5 and the communication flow diagram will be presented in Section 7.6.

7.1. Overview Components

To analyse and create the electrical system of the drone, it is important to list all the required components needed for a complete system. To have a fully functional drone it is crucial that the different subsystems are correctly integrated. An overview of all the components is presented in Table 7.1.

Table 7.1: *Overview of components*

Subsystem	**Components**
Control	Flight Computer (FC)
	Electronic Speed Controller (ESC)
	Power Distribution Board (PDB)
Communication	Transmitter
	Receiver
	Hawkeye MicroController
	Raspberry Pi
	Telemetry
Cameras & Sensors	LiDAR
	Sonar
	GPS
	Camera
	Thermal Camera
Other	Battery Monitor
	Wiring
	LEDs

In Table 7.1, the components were divided into four main groups: Control, Communication, Camera & Sensors

and Other. For each of these components, multiple commercially available options are possible. In the following section, the most suitable options will be selected and explained.

7.2. Component Selection

In this section, the components shown in Table 7.1 shall be compared and selected. Note that for each component, research on existing products was done to obtain up to three suitable options.

7.2.1. Control

Components that will be used for the main control of the UAV are described as shown in Table 7.1.

Flight controller (FC)

The FC is the motherboard of the UAV. It controls the inputs, outputs, and the entire communication of the drone system. It ensures that the drone is always stable, performs precise flight manoeuvres and provides flight data to the pilot [105]. The FC consists of a circuit board that is equipped with sensors that can detect the drone's motions and user commands. In this way, the FC can control the speed of the motors to move in a certain direction. Some of the common sensors that are included in a FC are an accelerometer, gyroscope, barometric pressure sensor and compasses. Furthermore, the FC serves as the hub for connecting the ESCs, servos, PDBs, receiver, cameras, etc. FCs come in different firmware and processors. Depending on the use-case of the drone and the type of connections needed for the components, a proper FC has to be chosen that satisfies the requirements of the mission. Table 7.2 shows the considered FCs.

Table 7.2: *Overview of the FC options*

Option	FC model	Current rating [A]	Voltage rating [V]	Temperature rating [°C]	Price [$]	Mass [g]
1	CubePilot Cube Orange [127]	2.5	4.1 – 5.7	-10 – 55	350	73
2	CUA5 Plus [12]	-	4.3 – 5.4	-20 – 80	500	90
3	mRo Pixhawk [128]	-	7	-10 – 60	300	38
4	Holybro Pixhawk 6X [91]	1.5	4.75 – 5.25	-40 – 85	330	85

The criteria used to assess which FC is the most suitable for the mission are listed below.

- Simplicity
- Open source access to ample documentation
- Sufficient ports and interface capability
- Sensors
- UART connections
- Low price
- Low weight
- Market availability

The above flight controller options have all the necessary functions that are required for the drone. They have sufficient PWM and UART connection ports for connecting the various electronic components that are needed. There could be some differences in the way the flight controllers are programmed and how the software architecture of the components inside the flight computer is structured. Due to ample documentation on the Cube Orange and prior experience with this particular flight controller, this option is selected. In spite of it being a bit more expensive than the Pixhawk and Holybro, the price difference is worth it. The operating temperature range would not pose much of an issue as the mission profile is mostly outside the fire. Furthermore, the components are insulated and covered properly to ensure that they are protected against smoke and dirt and other environmental factors that might affect the FC.

After considering the different options and criteria, the FC that will be used for the drone is the **CubePilot Cube Orange**.

Electronic Speed Controller (ESC)

The ESC is needed to allow for the control of the electric motors by the flight computer. For guaranteed optimal compatibility between the motors and the ESCs, the ESC was chosen to be the same brand as that of the motors.

For the UAV, a *T-MOTOR MN1010 KV135* [159] was chosen, thus the two options available are presented in Table 7.3.

Table 7.3: *Overview of matching T-MOTOR ESCs*

Option	ESC model	Max continuous current [A]	Burst Current [A]	Price [$]	Mass [g]
1	T-MOTOR Alpha 12S [155]	80	100	130	110
2	T-MOTOR Alpha 12S [154]	100	120	170	360
3	T-MOTOR Flame 12S [156]	80	120	120	109

Assuming that all the current provided by the batteries is allocated to the motors, 96A can be used to generate thrust. This will limit the maximum throttle setting since the motor draws 104 A at 100% [159]. In order to choose the optimal ESC, a performance analysis must be done.

For options 1 and 3, the ESCs are much lighter, both totalling to a mass of around 660 g as one ESC is needed per motor. However, the current draw of the motor is limited to 80 A. The performance of the drone is calculated with respect to requirements *REQ-SYS-1* and *REQ-SYS-10*. With a payload of 10 kg, this resulted in a maximum T/W ratio of 2.36 and an endurance of 21.46 minutes at T/W of 1.4.

For option 2, the ESCs shall allow for the maximum current draw from the batteries of 96 A, however the total mass of the ESCs increases significantly to around 2.2 kg. With these changes, the performance with regards to *REQ-SYS-1* and *REQ-SYS-10* are calculated again. With a payload of 10 kg, this resulted in a maximum T/W ratio of 2.29 and an endurance of 20.43 minutes at T/W of 1.4.

When comparing the options, it can be seen that the different options result in small changes in T/W and endurance. Options 1 and 3 clearly result in increased performance. Using options 1 and 3, causes a 5% increase in endurance and a 3% increase in T/W. From this, the 80 A ESCs, options 1 and 3 prove to be preferable. Furthermore, operating at 80 A also means that the motor is operating at a lower RPM and thus a higher efficiency making it beneficial for sustainability purposes. Between the 80 A options, the main difference is the Burst Current. Using option 3 will limit the motors and battery less when operating within their burst state with the same mass. For these reasons, the final ESC selection is option 3, **T-MOTOR Flame 80 A 12S**.

Power Distribution Board (PDB)

The PDB is a crucial component of the electrical system that is needed for the distribution of power from the power sources to the rest of the system. With the two *LiPo 46000 12S2P 44.4 V Battery Packs*, a maximum continuous current of 287.5 A per battery can be discharged [17]. This is a crucial parameter to consider for full functionality of the drone and to prevent damage. After performing a review of commercially available PDBs, it was noticed that PDBs with maximum currents larger than 500 A significantly increased the mass of the single component compared to those below 500 A. Due to this, the option of using two separate PDBs was considered. This requires each PDB to attach to a battery and three motors. The remaining components are equally split over the two PDBs. The three most suitable commercially available power distribution boards are presented in Table 7.4.

Table 7.4: *Overview of most suitable PDB options*

Option	PDB model	Max current [A]	Price [$]	Mass [g]	No. of branches
1	APD 14S [2]	500	79	50	4
2	Sky-Drones SmartAP PDB [147]	400	90	16	6
3	Mauch PDB [110]	2x200	353	115	9

The three options presented in Table 7.4 are each high current, low weight PDBs. As none of them independently meet the maximum current requirement, a combination of two PDBs is considered. When comparing the cost of the different components, option 3 (*MAUCH 2x200 A)* clearly stands out as it is around four times more expensive than the alternatives for similar performance. Then when comparing options 1 and 2, their weights and number of branches were investigated. For this, option 2 (*Sky-Drones SmartAP*) appears to be most suitable for all categories. With option 1, despite being the cheaper option with a higher current rating, it is too high above the required value of 287.5 A needed per PDB. Furthermore, with a total of eight branches of which six are used for the motors, problems may arise when integrating all the other components on the remaining two branches. For this reason, the final PDB configuration was chosen to be **two Sky-Drones SmartAP PDB 400 A**.

Note that as the input voltage to the PDB is higher than 35 V, an aluminium electrolytic capacitor will need to be attached to the power input pads with an input rating of at least 100 V, as recommended by Sky-Drones [47].

An overview of how much current all components draw is shown in Table 7.2.3. It should be noted that not all components mentioned in the table are directly connected to the PDB, as can be seen in the Electrical Block Diagram.

7.2.2. Communication

In this subsection, all the components related to communication shall be selected and discussed.

Transmitter & Receiver

The transmitter and receiver are the controllers of the UAV. The receiver is the module that is attached to the FC which will effectively communicate with the transmitter for effective control of the UAV. The payload mechanism will be controlled with the help of the transmitter, motor speed, et cetera [28]. A correct combination of transmitter and receiver should be chosen to ensure that the UAV can communicate effectively without connection losses and sensitivity issues. For this reason, three combinations of transmitter and receiver have been looked into which work for this drone. Various factors were considered when choosing such a combination, namely:

- Compatibility
- Price
- Mass
- Performance

Based on these criteria, the second combination has been selected.

Table 7.5: *Overview of transmitter and corresponding receivers*

Option	Transmitter	Channels	Receiver	Frequency band [GHz]	Mass [g]	Price [$]
1	Spektrum DX8 [151]	8	AR8010T RX [150]	2.4	1800	330
2	FrSky Taranis X9D [78]	24	TBS Crossfire Nano RX [27]	2.4	700	250
3	Radiolink AT10II [131]	12	R12DS RX [7]	2.4	900	160

The Spektrum and FrSky transmitters are both reliable and compatible transmitters. The advantage of using the FrSky is the wide variety of customisation options available due to the OpenTX software. Furthermore, the combination of the transmitter and receiver in this scenario provides a much more robust link necessary for the drone mission with a sufficient range capability [76].

The cost is comparable for all three options and all of them utilise the 2.4 GHz frequency band. Furthermore,

the transmitters are required to have gimbals for ease of control. The FrSky Taranis utilises hall sensor gimbals which are more reliable in comparison to potentiometer gimbals [153].

After careful consideration and analysing of the functionalities of the transmitter and receiver, the **FrSky Taranis X9D** was selected along with the **TBS Crossfire Nano RX** receiver. This has been selected mainly due to its robustness and compatibility. The price is reasonable and since it is lightweight, ensures effortless handling for long periods of time.

Telemetry

The data link between the flight computer on board and the Ground Control Station (GCS) is responsible for communicating all the outputted data collected by the onboard components during the flight to the GCS. It needs to be highly reliable and have the right range for the mission. Three viable options for data links have been looked at, all of which have an acceptable range (REQ-SYS-4) and the overview information on cost, mass, range and radio frequency can be found in Table 7.6.

Table 7.6: *Overview of most suitable telemetry options*

Option	Data Link	Range [km]	Cost [$]	Mass (air module) [g]	Radio frequency [GHz]
1	Herelink Air Unit 1.1 [80]	20	500	98	2.4
2	SiK Telemetry Radio [13]	0.3	89.95	4	0.915
3	Sky-Drones SmartLink [148]	20	3990	139	1.2

The Herelink Air Unit 1.1 and the Sky-Drones SmartLink both have video transmission, while the SiK Telemetry Radio does not. Even though it is cheap, light and easy to use [13], it is not a good option for this mission, as live video feed is important. The SmartLink is eight times more expensive than the Herelink and has a less reliable radio frequency [168]. Therefore, the best option for the telemetry module of the drone is the **Herelink Air Unit 1.1**. It is used to send all the information coming from the flight computer to the GCS, which is a laptop.

Laser imaging, Detection, And Ranging (LiDAR)

For the drone, two LiDARs are used. A long-range LiDAR, is used for altitude measurement and another for frontal sensing. Different LiDARs are chosen for the two applications due to the different range requirements.

Altitude LiDAR:

On the UAV, a LiDAR is used to measure the altitude of the drone. This is needed for the operator and enables the flight computer to autonomously hover at a specified altitude or land safely in case of loss of signal. A large variety of LiDARs for altitude measurements exist. However, only two options stand out, these are presented in Table 7.7.

Table 7.7: *Overview of best performing LiDARs*

Option	LiDAR	Range [m]	Cost [$]	Mass [g]	Accuracy [cm]	Reflectivity
1	Atollo Wasp 200 [65]	315	530	26	<10	175 m at 18 % reflectivity & 300 m at 80 % reflectivity
2	Blickfeld Cube Range 1 [103]	250	3500	385	<1	> 30 m at 10 % reflectivity

When comparing the two options displayed in Table 7.7, the most prominent difference is in the price, accuracy and mass. They both meet the altitude requirement of 250 m as stated in *REQ-SYS-4*. As this mission is primarily remote-controlled by the firefighter, high accuracy in altitude is not required. The drawback of mass and cost that come with option two, is not worth the additional accuracy for this mission. For this reason, **Atollo Wasp 200** was chosen. If more accuracy is required for the altitude, an additional LiDAR could be considered to obtain a more accurate average measurement. An additional advantage of this specific LiDAR is its reflectivity. Even at less than 20 % reflective surface, can it detect objects at ranges of about 175 m. This is an important criteria as a surfaces can become difficult to detect during fire conditions. With this, a good estimate of the altitude can be made even in difficult visibility conditions.

Frontal Sensing LiDAR:

For the frontal LiDAR, the operational range can be less. Hence, a cheaper LiDAR is desired. From *Lightware*, three suitable options were found.

Table 7.8: *Overview of most suitable frontal sensing LiDARs*

Option	LiDAR	Range [m]	Cost [$]	Mass [g]	Accuracy [cm]	Reflectivity
1	SF000/B [107]	50	261	9.7	± 10	50 m with white wall in daylight
2	SF20/C [106]	100	261	10	± 10	100 m with white wall in daylight
3	SF30/C [108]	100	280	35	± 0.7	100 m with natural surface and 175 m with reflective surfaces

In Table 7.8, three valid options are presented. For compatibility with the other components, the LiDAR will need to be capable of an I2C connection with the flight computer. This excludes the *SF30/C*, however, it can be reconsidered if increased performance is required for minimal increases in price and weight. For the *SF000/B* and *SF20C*, both have identical specifications except for the weight and range of the component. For this reason, for the improved range with negligible increase in weight, the **Lightware SF20C** is chosen. Looking at the reflectivity of the LiDAR, the specific relation between the three options cannot be compared. However, since all of them are from the same company, it can be estimated that they behave in the same way with less reflective surfaces. Henceforth, Option 2 comes out to be as the best option.

Sonar

The UAV shall require sensors for frontal distance measurements. LiDARs are known to be effective for this type of application, however, as the drone shall operate in harsh, smoky environments this must be re-evaluated. LiDARs have shown to frequently fail in smoke when the lack of visibility is too great [138]. The alternative option is sonar, which despite having a lower resolution is not affected by the smoke.

The sonar sensor used in the drone is the **MB1222 I2CXL-MaxSonar-EZ2** [111]. It reports the range to the closest target and can detect targets up to 7.65 m away. It is also affordable, at $115 per piece, and lightweight, at 50 g.

Camera

For the camera, three options were considered. These are enlisted below:

1. GoPro HERO11 Black Mini [84]
2. Hawkeye Firefly 4K Nakedcam [52]
3. DJI Osmo Action 3 [46]

Among these three options, they were compared with their telemetry capability, camera quality, price, weight and communication protocol. The first and last options can communicate through Bluetooth, although they are

heavy and more expensive in comparison to the second option. The second option (Hawkeye Firefly) can be connected to the herelink telemetry channel. This can be transmitted to the telemetry channel for viewing on the laptop or Herelink ground station for a live camera view of the drone. Furthermore, all the cameras have 4K capability so the quality is similar. Another benefit of the Hawkeye camera is its small size which allows it to be fitted at difficult-to-reach locations on the drone. As the Hawkeye Firefly has no built-in stabilisation, a **Copterlab gimbal** is used [40]. Even though this leads to an increase in weight, size, and cost, the **Hawkeye Firefly 4k Nakedcam** still is advantageous over the other options and is therefore selected.

Figure 7.1: *Hawkeye Camera with the micro controller board*

Figure 7.1 shows the camera with the micro controller board attached to it. This camera in combination with a gimbal is integrated on the drone for high-quality video transmission with camera manoeuvring for increasing the field of view while payload delivery.

Hawkeye Micro Controller

The **Hawkeye micro controller** board is a small circuit board that pulls telemetry data from the light camera and provides it to the Herelink Air Unit to provide live video of the drone view. This component comes up with the selected camera choice, namely Hawkeye Firefly 4K [87]. This micro-controller board can be connected with an HDMI cable to the Herelink Air Unit that is used for high-quality video transmission. Figure 7.1 shows the image of the micro controller board attached to the camera.

Thermal Camera

For thermal imaging, the **FLIR Lepton 3.5** is used. The micro thermal camera module has a mass of only 0.9 grams and can be easily connected through the FLIR Lepton Breakout Board V2.0 to a Raspberry Pi 4 Model B. The Raspberry Pi is connected to the Herelink, which is responsible for transmitting the live thermal video to the GCS. As the camera is radiometric, it is able to measure and display the temperature with an accuracy of 5 °C. The Lepton 3.5 is chosen over the Lepton 2.5, as it offers twice the resolution and does not differ much in price [149]. Other thermal cameras are available but were deemed not feasible as their price is in the order of thousands of dollars. In order to provide stabilisation for the thermal camera, the FLIR Lepton is mounted on the gimbal of the visual camera.

Global Positioning System (GPS)

For improved accuracy compared to standard, real-time kinetic data (RTK), GPS modules for the drone were researched. The two best options are shown in Table 7.9. The Holybro GPS is more than double the price of the Here3, for better navigation update rate and horizontal accuracy at a similar weight. The accuracy and update rate of the Here3 GPS is sufficient for the mission, since the drone is not intended to leave the direct line of sight of the pilot, and the LiDAR and Sonar sensors on board also aid in situational awareness. For these reasons, and most of all a lower price, the **Here3 RTK GPS** was chosen.

Table 7.9: *Overview of most suitable GPS options*

Option	GPS model	Cost [$]	Mass [g]	Nav. update rate [Hz]	Horizontal accuracy
1	Holybro RTK F9P Helical [90]	440	58	20	1.5 m / RTK: 0.01 m
2	Here3 RTK GPS [81]	176	48.8	8	2.5m / RTK 0.025m

7.2.3. Other

Battery Monitor

The **SmartAP PDB** discussed in Subsection 7.2.1 has integrated voltage and current sensors and can therefore be used as a battery monitor. It can be configured such that a failsafe will trigger when the voltage or remaining capacity drops below a set value [11]. The electromagnetic sounder (a buzzer) of the PDB will go off and the ground station will receive a warning. The UAV can be set up to automatically land or return to base when a failsafe is triggered.

Wiring

Selecting the correct wiring is crucial for the functionality of the entire system. If the current drawn through the wire exceeds the designed value, the wire can generate large amounts of heat introducing additional risks which may lead to total failure of the system. If the component is provided with recommended cables, they should be used to ensure suitability. If not, the required American Wire Gauge (AWG) can be checked using AWG charts, however, these are estimates which can be further optimised.

Mechanical Relay

The mechanical relay will act as the switch which will control the pump that shoots out the payload. The pump chosen has a nominal voltage of 12 V, a peak current of 20 A and a power consumption of 240 W [173]. It is important to choose a relay that will allow the 20 A of current to pass through it without getting damaged. Furthermore, the relay must have a switching voltage of 5 V, as that is what the flight computer can provide.

For this reason, the relay chosen is the **Grove - SPDT Relais (30A)** [180]. It is rated for up to 30 A, it has a switching voltage of 5 V and has an operating temperature of up to 70 °C.

LEDs

For safety and to comply with drone regulations when flying outside daylight periods, the drone is equipped with LED lights [96]. To adhere to safety regulations set by Inspectie Leefomgeving en Transport for flying outside of daylight periods, **four VIFLY strobe lights** are mounted on the drone [174]. A red LED solid light has to be placed on the left side of the drone and a green LED solid light on the right side. A white strobe light is mounted on the back of the drone. To allow a person on the ground to distinguish the UAV from a manned aircraft, a green flashing light is placed at the bottom. The lights have visibility of over 4.5 km and can be mounted on the drone using a 3M dual lock. As the lights have their own built-in batteries, which provide a run-time of up to 4 hours, they will not have to be connected to the drone's power system [174].

Table 7.10: *Overview of component voltage and current requirements*

Component	Voltage [V]	Current [A]
FC [127]	5.7	2.5
Battery [17]	44.4	287.5
ESC [156]	44.4	80
Motor [159]	44.4	104
PDB [147]	60	400
Altitude LiDAR [65]	5	0.075
Frontal LiDAR [106]	5.5	0.1
Sonar [111]	5.5	0.0034
GPS [81]	5	-
Light Camera [72]	12	0.3
Thermal Camera [149]	3.1	0.048
Gimbal [40]	12	-
Mechanical Relay [180]	5	0.185
Raspberry Pi (Model 4B) [134]	5	3
Light Camera Micro Controller [87]	12	1
Telemetry link [80]	12	0.3
Transmitter [78]	-	-

7.3. Component Insulation

When deploying drones in a variety of environments, it is critical to consider the sensitivity of the sensors to high temperatures. Compared to typical drone operating conditions, the temperatures close to a burning building are higher. Since not all electrical components are designed to operate in these circumstances, the drone must have thermal protection to ensure optimal performance is possible. Without protection through thermally isolated shieldings, effective performance would not be achievable. Table 7.11 shows the maximum operational temperatures of the main electrical components. This section will first discuss the characteristics of the sensors, followed by a discussion of insulation material.

Table 7.11: *Maximum operational temperature of electrical components*

Component	Maximum operational temperature [°C]
Sonar [111]	65
LiDAR 1 [65]	60
LiDAR 2 [106]	50
Thermal camera [149]	80
GPS [81]	85
Relay [180]	70
LEDs [174]	85
Camera [75, 53]	45
Transmitter [78]	60
Receiver [27]	40
Telemetry [88]	70

A sonar operates by emitting a soundwave and analysing the reflected echoes. Therefore, choosing thermal insulation materials while preserving their acoustic functions, is critical in ensuring good performance.

GPS receivers require a higher level of insulation as they need a material that can withstand drastic temperature changes, ensuring the consistent operation of the sensitive electronics inside and minimising the possibility of physical damage such as collision with small particles or smoke. The ideal materials should have appropriate insulation properties along with a low thermal conductivity level necessary for sustenance under different environmental conditions.

When working with sensors that have a reflective sensor one must be cautious regarding the selection of optimal insulation materials. As a result of the potential for intense reflections from surfaces like glass or mirrors, distortions may occur and the sensor can get overloaded, thereby affecting its acoustic qualities.

Thermal insulation materials for cameras, sonar, GPS, and LiDAR sensors are usually chosen based on their ability to protect sensitive electronic components from high temperatures and temperature fluctuations to maintain optimal operating conditions. While there are various insulation options available, three commonly used are foam insulation, ceramic insulation and, aerogel. Their advantages and disadvantages are discussed below.

Foam Insulation

Foam insulation is a material commonly used to provide thermal and acoustic insulation in various applications. It is made from a cellular structure that traps air or other gases, offering excellent insulation properties. Foam insulation is lightweight, versatile, and easy to install, making it an effective solution for enhancing energy efficiency and reducing heat transfer in buildings and other systems.

Advantages:

- Good thermal insulation properties: Foam materials such as polyurethane or polystyrene offer a decent insulation performance, minimising heat transfer [176].
- Lightweight and easy to handle: Foam insulation is lightweight and can be easily shaped or moulded to fit different sensor configurations [176].
- Cost-effective: Foam insulation materials are generally affordable, making them a popular choice for many applications [176].

Disadvantages

- Limited temperature resistance: Foam insulation may have temperature limitations and can degrade or lose effectiveness at extremely high or low temperatures [176].
- May require additional protection: Foam insulation may need to be combined with other materials or coatings to provide sufficient protection against moisture, dust, or impacts [176].
- Lower insulating efficiency than other options: Compared to some advanced insulation materials, foam insulation may have lower insulation efficiency [176].

Ceramic Insulation

Ceramic insulation for sensors refers to the use of ceramic materials to provide thermal insulation and protection for sensors. Ceramic insulation helps in maintaining stable operating temperatures, shielding sensors from external heat sources, and improving their accuracy and longevity.

Advantages:

- Good thermal resistance: Ceramic insulation materials, such as alumina or silica-based ceramics, offer high-temperature resistance and excellent insulation properties.
- Chemical resistance: Ceramic materials are often resistant to corrosion, and chemical degradation [16].

Disadvantages:

- Brittle and fragile: Ceramics are brittle materials and can be broken easily under mechanical stress.

- Higher cost: Ceramic insulation can be more expensive compared to foam materials, making it less suitable for some budget-sensitive applications.

Silica Aerogel

Silica aerogel is a type of aerogel insulation material derived from silica (silicon dioxide). It is known for its extremely low density and exceptional thermal insulation properties. Silica aerogel is often referred to as *"frozen smoke"* or *"blue smoke"* due to its translucent appearance [1]. Silica aerogel has good acoustic performances, is transparent, light and good for thermal insulation [112].

Advantages:

- Exceptional thermal performance: Silica aerogel is one of the most effective insulating materials available, with extremely low thermal conductivity. It provides excellent insulation against heat transfer, making it suitable for applications where temperature control is critical.
- Lightweight: Silica aerogel has an extremely low density, making it lightweight and advantageous for applications where weight reduction is desired [112]. It can help minimise the overall weight of cameras, sensors, and other devices without sacrificing thermal insulation.
- Space-efficient: Silica aerogel is highly porous and has a unique nano-structured network [112]. This structure allows it to have a large surface area relative to its volume, enabling efficient use of space in sensor enclosures or camera housings.

Figure 7.2: *Sillico aerogel application [117]*

Disadvantages:

- Fragility: Silica aerogel is brittle and can be fragile. Care must be taken during handling and installation to prevent damage, which can reduce its insulating properties.
- Cost: Silica aerogel insulation can be relatively expensive compared to other insulation materials. The production process and specialised manufacturing techniques contribute to its higher cost.
- Moisture sensitivity: Silica aerogel has a high surface area, which makes it susceptible to adsorbing moisture from the surrounding environment. Moisture can degrade its insulation performance, so moisture protection measures or coatings may be required.

It is worth noting that the choice of insulation material depends on the specific requirements of the sensor, including operating temperature range, size and weight constraints, and budget considerations. As the maximum working temperature is 50°C, **polyurethane** is the best option [38]. It is easy to apply and the acoustic performance of the sensors is not influenced much. Only for the camera, **glass or silica aerogel** is used as the insulation material needs to be transparent. It is difficult to predict the exact amount of insulation needed for the sensors, hence a rough estimate of 500 g has been allocated to insulation and covering of sensors and electrical components.

7.4. Electrical Block Diagram

The electrical block diagram of the system is shown on the next page. Every hardware component and its wiring can be seen. In the legend, the different colours for each wire type show the protocol or type of signal each component uses. For example, an I2C connection is denoted by a red voltage and black ground wire, a yellow clock signal (SCL) wire, and a light blue data signal (SDA) wire.

Furthermore, the voltage and current requirements for each component can be found in Table 7.2.3. These are important as they indicate the thickness needed per wire in order to handle the amount of current passing through it, as well as the step-down voltage converter needed within the electrical system. It will also be useful when creating the power budget of the UAV that will be done in Section 11.3.

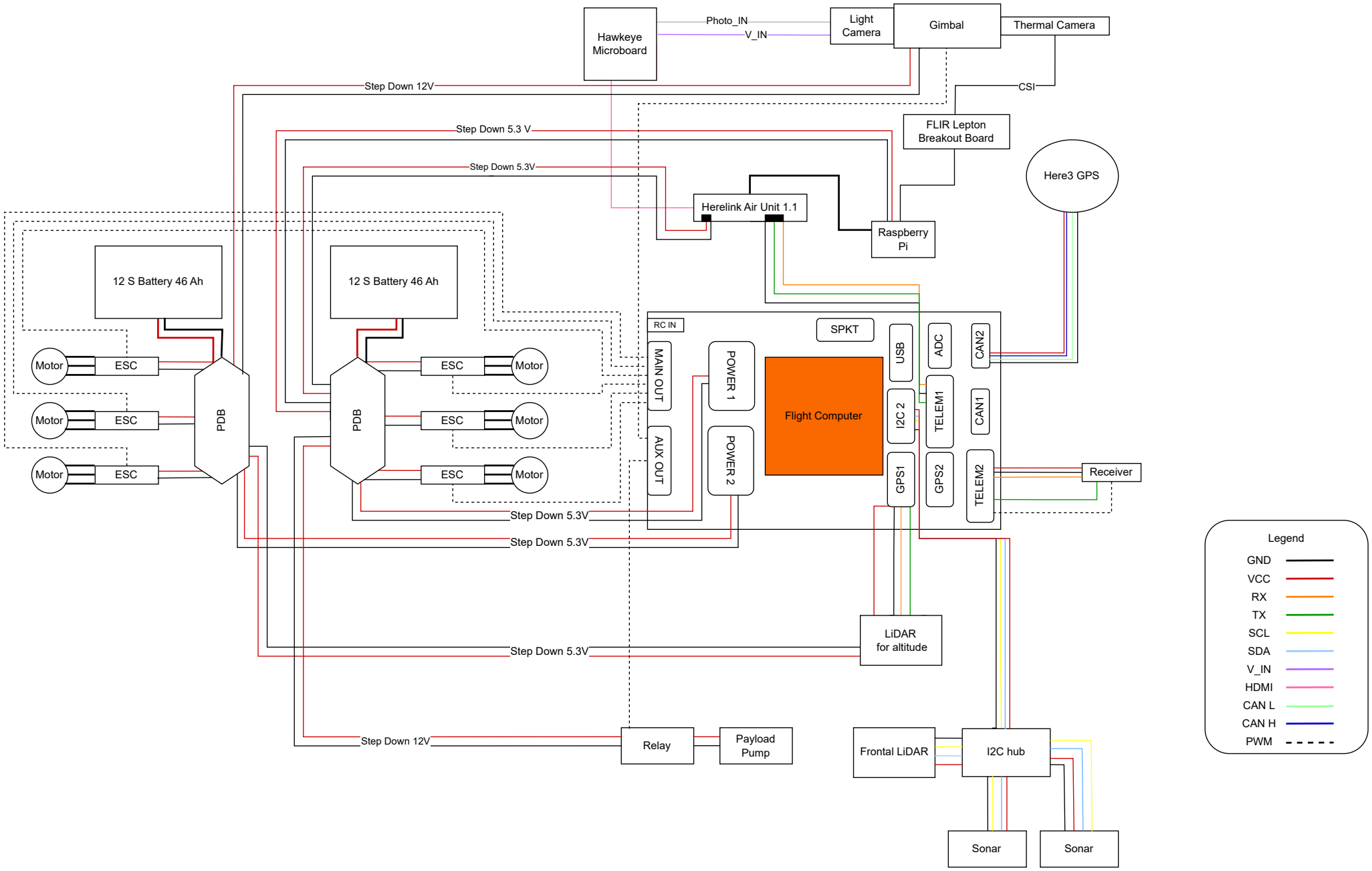
Hawkeye Microboard
Photo_IN
V_IN
Light Camera
Gimbal
Thermal Camera
Step Down 12V
CSI
Step Down 5.3 V
FLIR Lepton Breakout Board
Step Down 5.3V
Here3 GPS
Herelink Air Unit 1.1
Raspberry Pi
12 S Battery 46 Ah
12 S Battery 46 Ah
RC IN
SPKT
MAIN OUT
AUX OUT
POWER 1
POWER 2
Flight Computer
USB
I2C 2
GPS1
GPS2
ADC
TELEM1
TELEM2
CAN2
CAN1
Receiver
Motor
ESC
PDB
Step Down 5.3V
Step Down 5.3V
LiDAR for altitude
Step Down 5.3V
Step Down 12V
Relay
Payload Pump
Frontal LiDAR
I2C hub
Sonar
Sonar
Legend
GND
VCC
RX
TX
SCL
SDA
V_IN
HDMI
CAN L
CAN H
PWM

7.5. N2 Chart of System Architecture

The N2 Chart showcasing all the Input/Output relationships in the drone is presented in Figure 7.3. The main components and subsystems in the drone are shown in the coloured blocks. Inputs are vertical, and outputs are horizontal. This chart is used to denote all the interactions and inter-dependencies between subsystems in the drone and is also used as a guide for the communication flow diagram in the next section.

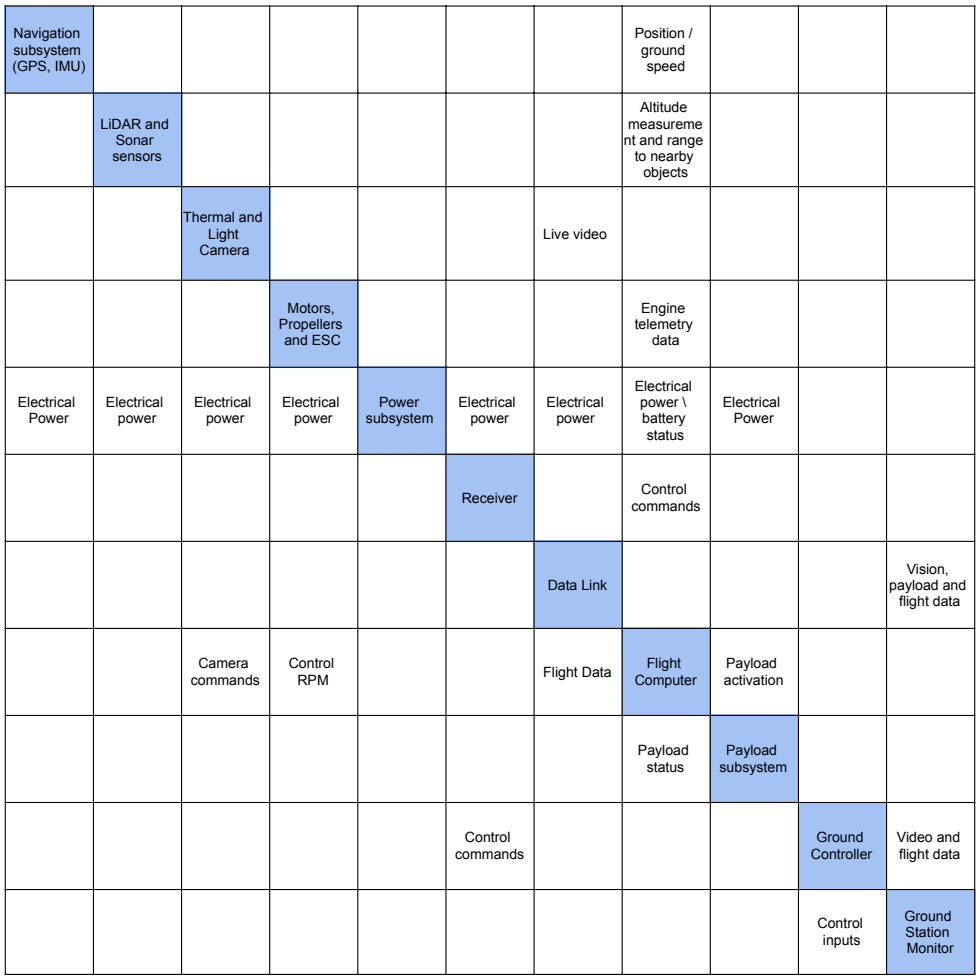

Figure 7.3: *N2 Chart of system architecture*

7.6. Communication Flow Diagram

Communication within the drone system is integral to the success of the mission. At any point, the pilot must have live video and frequent updates coming from all the cameras and components on board. The breakdown of all the links between components, the flight computer and the Herelink is presented in Figure 7.4, and shows which parts of the system need to communicate in detail. This diagram denotes the data outputted and refresh rate in Hz of each component in the drone, as well as the radio frequency used to communicate between the onboard system and the Ground Control Station (GCS). The onboard communication and components are inside the pink box, and the GCS components are in green. The type of information is written inside the communication lines, as well as the type of protocol and refresh rate of the data. Furthermore, the radio frequency used to transmit data to the GCS is shown, and it is 2.4 GHz.

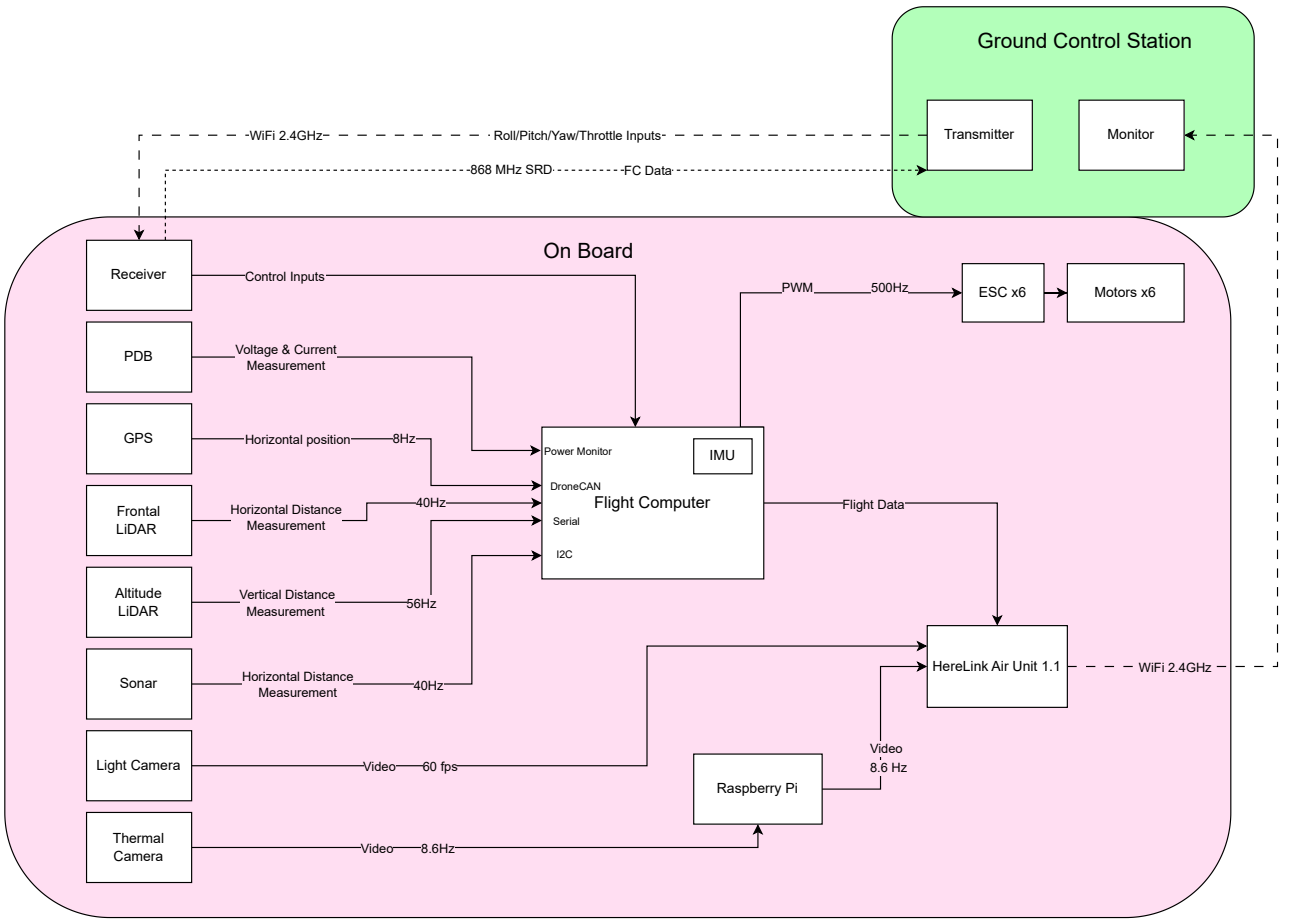

Figure 7.4: *Communication flow diagram of electronic system*

7.6.1. Link Budget

The link budget analyses the telemetry components with respect to their bandwidths and data transmission rates to see the compatibility with the selected transmitter. The following table lists all the telemetry components and checks with the FrSky transmitter specifications. If it meets it, the corresponding cell is coloured in green, else it is coloured in red.

Table 7.12: *Link Budget that analyses the data rates of the telemetry components and compares with the transmitter specifications*

Component	Bandwidth	Compatibility
Herelink AirUnit 1.1	2.4 GHz ISM	Yes, it complies with any monitor with a Wi-Fi communication capability with a band of 2.4 GHz which can then provide live video footage
TBS Crossfire RX	868 MHz SRD	Yes, it complies with the FrSky transmitter that has a frequency rating of 2.4 GHz

8
Structure Design

This chapter will first discuss the final configuration of the rotors in Section 8.1. Next, multiple options for the layout of the main airframe body will be discussed and analysed in Section 8.2 and a final decision will be made. In Section 8.3, the different attachments needed to connect everything will be discussed. Calculations are done to ensure a strong design, these will be discussed in Section 8.4. Lastly, the landing gear of the UAV will be described in Section 8.5.

8.1. Configuration

In order to find the right power source, multiple options were considered, such as chemical, electrochemical and electrical sources. After considering the different sources, it was decided that either lithium polymer or lithium-ion batteries are the best options. In the design, it was chosen to go with lithium-polymer batteries as they are widely available.

A single-rotor, four-rotor, six-rotor and eight-rotor configuration were considered. To determine the most optimal configuration, each rotor configuration was paired with a motor type, a battery type and the number of batteries, where every possible combination was created. These were then traded off using endurance, maximum thrust-to-weight, cost, transportability and complexity as the criteria. From the propulsion trade-off, a six-rotor configuration was chosen, also called a **hexacopter**. Completed with **two lithium-polymer 46Ah 12S batteries** and **32-inch propellers**.

With a six-rotor configuration, the different rotors can be arranged in different ways. The two that were considered are the X-frame and the Y-frame, where for the X-frame the rotors are arranged in a circle and for the Y-frame two rotors are stacked on each other resulting in three rotor 'groups'. It was chosen to go for the X-frame, as it is more efficient than the Y-frame. Furthermore, the controllability of the X-frame is preferred over the Y-frame. Lastly, choosing the Y-frame leads to an increased complexity, which made the **X-frame** a more beneficial option.

8.2. Main Airframe Body Layout

First, the different possibilities for the layout of the main body of the drone were looked into. For now, only the large electronic components are taken into account. These are the ESC, PDB and batteries. These components take up the most space and are most important when choosing a layout. This resulted in the following four different options:

1. Rectangular body with two layers,
2. Rectangular body with three layers,
3. Hexagon body with three layers, in an aligned design,
4. Hexagon body with three layers, in a compact design.

For all four designs, the cameras and sensors are placed on top of the upper panel. Here, they are less protected than when they would be inside the main body, however, some form of protective cover will be designed to go over/around the electronics to protect them from the environment. Besides this, the landing gear/payload mechanism is a separate part which does not vary much per design and is looked at after a design option for the main body is chosen.

Option 1: Rectangular Body with Two Layers

For option 1, the layout of the body consists of two rectangular carbon fibre sandwich panels, placed on top of each other. The two batteries and both the Electronic Speed Controllers (ESC) and Power Distribution Boards (PDB) are placed in between the two sheets. The ESCs and PDBs are placed on top of each other: for every pair, one is attached to the inside of the lower panel, and one to the inside of the upper panel. Furthermore, the tubes, on which the rotors are connected on the other side, are also connected within the two panels. Some benefits of this design are the spacious layout, meaning there is a lot of space to place all of the electronics. The batteries are easily accessible and replaceable from the side. However, the non-symmetric layout makes it harder for controllability and makes stress distribution through the body asymmetric. The main body of this design is larger pertaining to the second design option. This means that the arms become shorter which results in less stress in the carbon tubes, which is preferable. The layout of the design is shown in Figure 8.1.

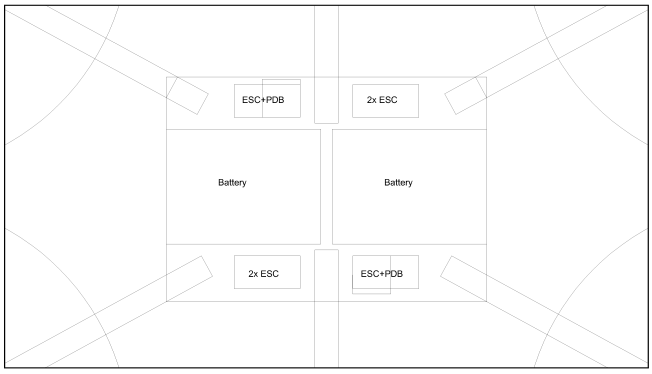

Figure 8.1: *Design option 1*

Option 2: Rectangular Body with Three Layers

Option 2, the "three-layer-rectangle" configuration, consists of two rectangular carbon fibre sandwich panels on both the upper and lower side. The third layer is placed between these sandwich panels and is a rectangular carbon fibre sheet. The two batteries are placed between the lower sandwich panel and the middle sheet. The ESCs and the PDBs are placed on the upper half, between the middle sheet and the upper sandwich panel. For this design option, the rods are also attached in the upper half. The main difference between options one and two is the area size of the main body. Since option two has moved the ESC and PDB one layer above the batteries, the entire main body can stay within the footprint of the batteries. This reduces the area of panels needed by about 33%, which saves a lot of weight. The design is, however, less spacious which would make it harder to wire all the electronics. Besides all of this, this layout is also not completely symmetric which makes it hard for controllability. The arms also get longer which leads to more stress within the tubes, which might lead to the need for thicker and heavier tubes. The design is shown in Figure 8.2.

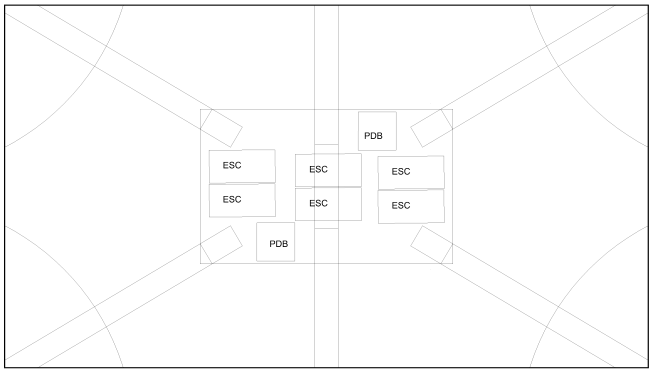

Figure 8.2: *Design option 2*

Option 3: Hexagon Three Layers, Aligned Design

Option 3 consists of three carbon fibre sandwich panels, cut as a hexagon. Like in design option 2, the batteries lie between the lower and the middle sheets, and the ESCs and PDBs are placed between the middle and the upper sheets. The rods are also attached to the main body in the upper half. This design is called 'aligned' since the ESCs are directly in line with the rods. This is done so the cables of the ESCs can go directly into the tubes, to the rotor. This design can be seen in Figure 8.3. Another benefit of this design is the fact that it is fully symmetric which is a great help with stability and controllability. Furthermore, there is a lot of redundant space which makes it easy to fit all of the electronics in the drone. However, this design is quite heavy since the main body consists of three large sandwich panels.

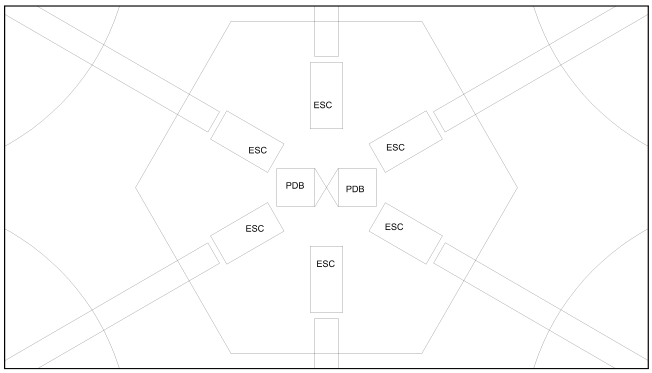

Figure 8.3: *Design option 3*

Option 4: Hexagon Three Layers, Compact Design

Option 4 is quite similar to the third design. The general layout is the same; three sandwich panels with the batteries in the lower half and the ESCs, PDBs and rods placed in the upper half. The difference between the more aligned configuration and the more compact one is the position and orientation of the ESCs. In this design, they are placed such that a lot of space is spared. This leads to a decrease in weight, which is preferable. Furthermore, another advantage is the possibility to slide the rods more to the middle if necessary which increases the overlap. This extra overlap gives a stronger bond between the panels and the rods. Although the design is more compact, there is still enough space for all the wires, while being lighter than design option 3. The design is shown in Figure 8.4.

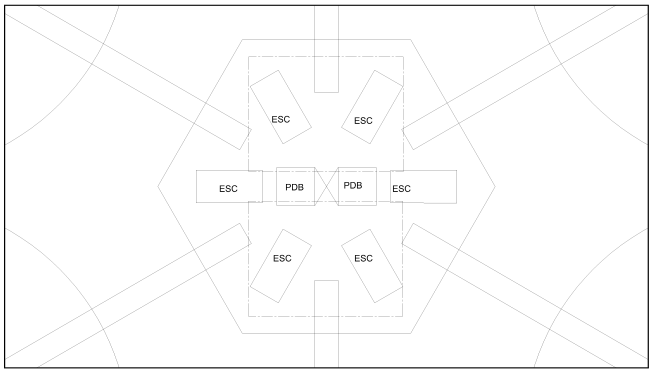

Figure 8.4: *Design option 4*

8.2.1. Final Choice

In the end, **option 4** was chosen. This decision was mainly based on weight calculations and controllability analysis. First, comparing the first and second designs; design 2 has an overall smaller area of the sheets since the ESCs and PDB are placed in approximately the same surface area as the batteries occupy. A smaller area results in a lower weight. Therefore, three layers are more desirable than two. Comparing options 3 and 4 is also based on certain weight calculations. As mentioned above, the area, and thus the weight, of design 4 is smaller than that of design 3 and thus design option 4 is preferable. Lastly, a decision was made between the second and the fourth option. The hexagon layout of design 4 is more symmetric than the rectangular one of option 3. A symmetric design is preferable since it will make the UAV more controllable. Therefore, the compact design with the hexagon form is chosen as the final design.

8.3. Attachments

To properly connect each separate part into a nice whole, different attachments need to be designed. This section looks into how the different layers are connected to each other, how all the rods are connected to the main body and how the motors are attached to the rods.

8.3.1. Layer Attachments

To connect the three layers, multiple **aluminium spacers** are used, which can be screwed in through the sheets. Between the lower and the middle sheet, sixteen connectors are placed: two spacers below every rod attachment in the upper half and four spacers between the two batteries in the middle. These spacers are indicated in Figure 8.5 with round holes. The indicated locations might be off by a few millimetres but are mainly used to give an impression of their approximate location. Between the middle and upper sheets, only four spacer rods are used, placed in the middle of the sheets. In this layer, the rod attachments will carry a great part of the load and will also function as a connection between the middle and upper layers.

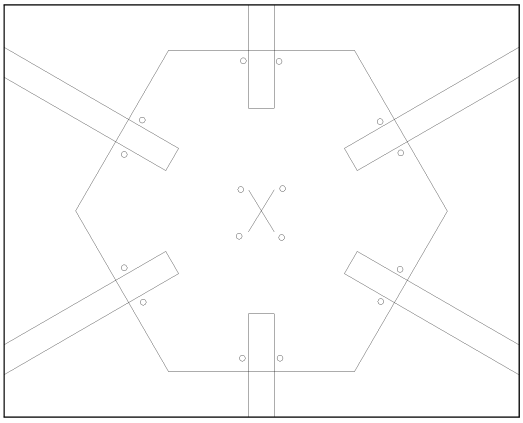

Figure 8.5: *Layer spacer holes*

8.3.2. Rod Attachments

Every rod has to be attached to the main body at a certain predetermined angle and distance from the centre. To safely attach the rods, they are glued to **an aluminium mounting**. This can be seen in Figure 8.6a. The rod is glued in the mounting since the clamping force required is too high for the rod to withstand. Carbon rods tend to break when clamped too hard which may cause critical failure, resulting in the breaking-off of an arm.

8.3.3. Motor Attachments

To attach the motors to the rods, the **aluminium clamp** shown in Figure 8.6b is slid around the rod at the end, on the side of the motor. This clamp will also be glued to the rod since also for this part the clamping force might compromise the strength of the rod.

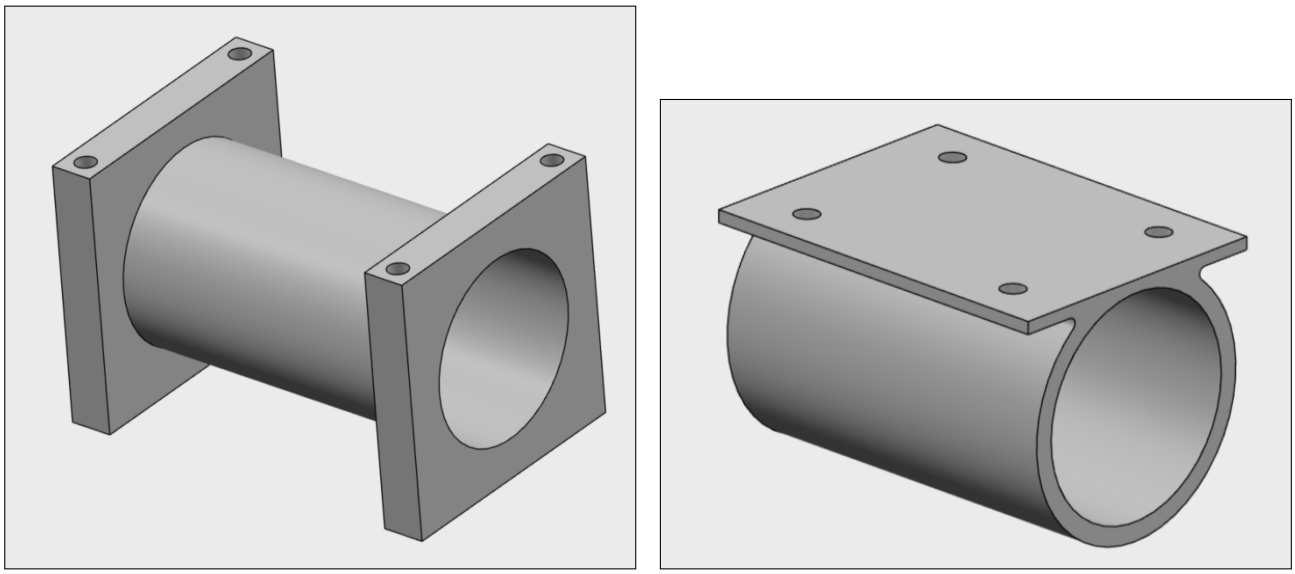

(a) *Rod attachment* **(b)** *Motor attachment*

Figure 8.6: *Rod mountings*

8.4. Calculations

After the layout of the body was chosen, calculations were performed to determine the forces and stresses in the rods, sheets and bolts. This was done to choose the proper thickness of the sandwich panels and the thickness of the rods and to make sure the final design is able to withstand the possible exerted forces. To ensure this process was correctly performed, Dr Calvin Rans was contacted. He looked over the proposed calculations and gave extra advice for possible solutions.

8.4.1. Rods

First, the force in the rod is calculated. The rod has a length of 733 mm with a maximum force of 190 N applied by the motor. This leads to a shear force of 190 N and a **maximum moment of $\approx$ 140 N/m**.

Shear in Rod

The shear force in the rod is calculated by Equation 8.1, where F is the force exerted on the rod and A is the cross-sectional area of the rod. The rods have an **inner diameter of 33 mm** and an **outer diameter of 35 mm** which leads to an area of $1.068 \cdot 10^{-4}$ m^2. This leads to a **shear stress of 1.778 MPa** in the rods. The carbon rods used have shear stress strength in the range of GPa [34]. Because of this, it can be concluded that the shear in the rod will not cause a problem.

$$\tau_{rod} = \frac{F_{rod}}{A_{rod}} \tag{8.1}$$

Bending in Rod

The bending stress, σ, in the rod is calculated using Equation 8.2.

$$\frac{\sigma}{y} = \frac{M}{I} \tag{8.2}$$

Where M is the moment, mentioned before, equal to approximately 140 N/m. y is the distance from the centre to the point where the stress is calculated, which is half of the diameter and thus equal to 17.5 mm. I is the area moment of inertia of the rod. Since the rod is a hollow tube, Equation 8.3 is used to calculate I.

$$I = \frac{\pi}{4}\left(r_o^4 - r_i^4\right) \tag{8.3}$$

Where r_o is the outer radius, and r_i is the inner radius, respectively equal to 35 and 33 mm. This gives an I equal to 15450 mm^4. This results in a **bending stress of 160 MPa**. From the given properties of the rod, it is known that the maximum allowable stress is 420 MPa. This means that with a safety factor of 2, resulting in a bending stress of 320 MPa, the design can still be considered safe [34].

8.4.2. Panels

Secondly, the forces in the panel are calculated in a number of worst-case scenarios. It is assumed that the mounting between the rod and panels is rigid and that the moment and shear forces in the rod are directly translated to the panels.

Bolt Shear

To determine the shear stress in the bolts, Equation 8.4 was used.

$$\tau_{bolt} = \frac{F}{A_{bolt}} \tag{8.4}$$

To determine F, the assumption is made that the top and bottom panels each carry half of the moment load. Because of this, the moment exerted by the motor may be divided by half of the rod attachment height. The moment equals 140 N and the height of the attachment is 50 mm. This equals a force of 2800 N on each panel. Since four bolts are used to attach each rod attachment to the panel, the force is divided by four and thus equal to 700 N. A is the area of the bolt in the panel. Using a bolt with a diameter of 5 mm, the area equals approximately 20 mm^2. This results in **shear stress of 35.6 N/mm^2**. The maximum allowed stress for the worst quality bolt is equal to 139 MPa, which means that the bolt is safe.

Panel Shear Tear Out

To determine the stress at which the failure due to panels shear tear out will occur, Equation 8.5 is used.

$$\tau_{tear} = \frac{F}{A_{tear}} \tag{8.5}$$

F is the same force as above and thus equals 2800 N which results in 700 N per hole. A refers to the area the bolt may shear through. Assuming a plate with a thickness of 5 mm, and the bolt 15 mm away from the side of the plate, the area equals 75 mm^2. This results in a **stress of 9.3 MPa**. The maximum allowable shear stress is in the range of $>$ 100 MPa [100] which is a factor 10 larger than the calculated stress, so the panel can be assumed to be safe.

Panel shear

The sandwich panels consist of 200 grams twill carbon, as both the top and bottom layers. In between these layers, a core of Airex C71.75 is used. The shear strength of the core is 1.35 N/mm^2. As mentioned above, a force of 2800 N is exerted on each panel. Since the main body is a hexagon with one side, s, equal to 289 mm. The area can be calculated using Equation 8.6.

$$A_{hexa} = 3 \cdot \sqrt{3} \cdot \frac{s^2}{2} \tag{8.6}$$

Using the determined values and the result of Equation 8.7 being 216507 mm^2, the shear stress equals **0.013 N/mm^2**. This means that the allowable stress is one hundred times greater than the occurring stress. The panels may be assumed to be safe.

$$\tau_{panel} = \frac{F_{panel}}{A_{panel}} \tag{8.7}$$

8.5. Landing Gear

To make sure the drone can land safely, a landing gear is designed. The landing gear is constructed out of **four 'legs'** made of carbon fibre. Each leg consists of two carbon fibre rods, connected to each other. In between the legs, the payload tank, described in Section 5.4, is attached. Underneath the tank, the pump is placed. Since the total height of the tank and the pump together equals approximately 360 mm, and an extra 220 mm is added for assembly and safety reasons, the total height of the landing gear results in approximately **580 mm**.

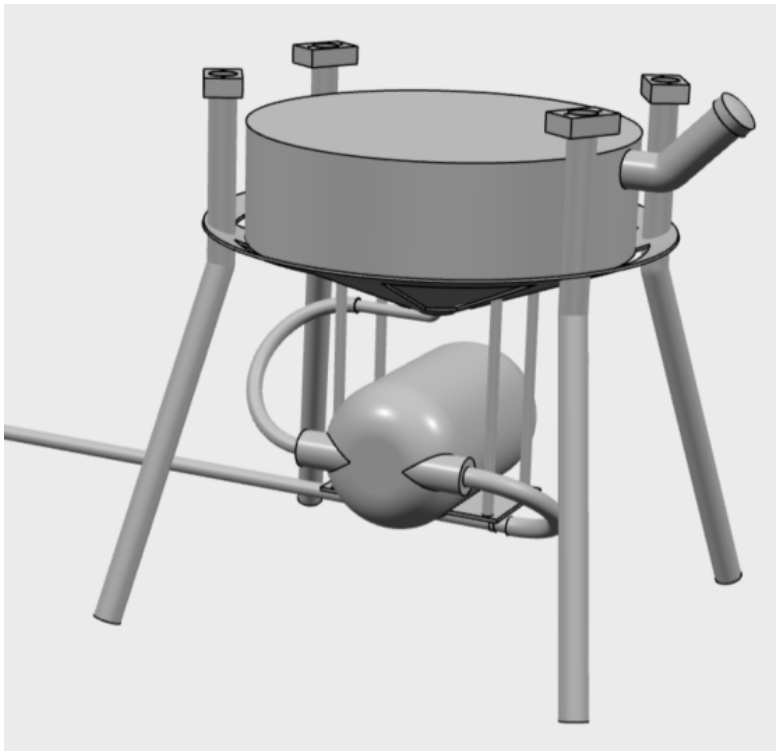

Figure 8.7: *Landing gear*

9
Control and Stability

The stability and controllability of the drone are crucial. As its main mission is aiding firefighters in saving lives, it must be robust and reliable. In this Chapter, the controllability, observability and stability will be analysed with the use of a state space model and subsequent matrix calculations. Through the guidance and consultation of coach from the Control & Simulation faculty Filip Surma, the analysis presented in this chapter has been made possible. In Section 9.1 the derived state space model will be presented. In Section 9.2 the controllability of the drone will be analysed, followed by the observability in Section 9.3. In addition, in Section 9.4, two different types of controllers will be investigated in order to ensure a sophisticated and successful control system for the drone. Furthermore, the stability will be analysed in Section 9.5. Lastly, in Section 9.6 the software block diagram is presented.

9.1. State Space Model

In order to analyse the control and stability of the drone, a state space model must be made and analysed. The state space model is a mathematical model of the physical drone relating the input, output and state variables. The model takes the form shown in Equation 9.1.

$$\begin{aligned} \dot{x} &= A\vec{x} + B\vec{u} \\ y &= C\vec{x} + D\vec{u} \end{aligned} \tag{9.1}$$

The state variables must be identified. There are 12 states in the system. These states denote the $\vec{x}$ vector, also called the state vector. The $\dot{x}$ vector is identical, but every entry is the derivative of the original variable. The states in $\vec{x}$ are listed below.

1. Position x
2. Position y
3. Position z
4. Roll angle ϕ
5. Pitch angle θ
6. Yaw angle ψ
7. Velocity $\dot{x}$
8. Velocity $\dot{y}$
9. Velocity $\dot{z}$
10. Rolling velocity $\dot{\phi}$
11. Pitching velocity $\dot{\theta}$
12. Yawing velocity $\dot{\psi}$

The input vector is given as $\vec{u}^T = \begin{bmatrix} U_1 & U_2 & U_3 & U_4 \end{bmatrix}$, and denotes the four forces and torques acting on the system. U_1 denotes the total upward thrust force coming from the motors (z-axis), U_2 the roll torque (x-axis rotation), U_3 the pitch torque (y-axis rotation) and U_4 the yaw torque (z-axis rotation) exerted on the drone.

The **A, B, C** and **D** matrices must be defined. The information needed to construct these matrices is explained in the paper "State Space System Modelling of a Quad Copter UAV" by Tahir et al. [162], and are adapted for a hexacopter. The equations used to create these matrices are already linearised. The **A** matrix is called the state matrix and is shown in Equation 9.2. It relates the derivatives of each state denoted in the $\vec{\dot{x}}$ vector to the state vector $\vec{x}$. The **B** matrix is called the input matrix and can be seen in Equation 9.3.

$$A = \begin{bmatrix} 0&0&0&0&0&0&1&0&0&0&0&0 \\ 0&0&0&0&0&0&0&1&0&0&0&0 \\ 0&0&0&0&0&0&0&0&1&0&0&0 \\ 0&0&0&0&0&0&0&0&0&1&0&0 \\ 0&0&0&0&0&0&0&0&0&0&1&0 \\ 0&0&0&0&0&0&0&0&0&0&0&1 \\ 0&0&0&0&-g&0&0&0&0&0&0&0 \\ 0&0&0&g&0&0&0&0&0&0&0&0 \\ 0&0&0&0&0&0&0&0&0&0&0&0 \\ 0&0&0&0&0&0&0&0&0&0&0&0 \\ 0&0&0&0&0&0&0&0&0&0&0&0 \\ 0&0&0&0&0&0&0&0&0&0&0&0 \end{bmatrix} \tag{9.2}$$

$$B = \begin{bmatrix} 0&0&0&0 \\ 0&0&0&0 \\ 0&0&0&0 \\ 0&0&0&0 \\ 0&0&0&0 \\ 0&0&0&0 \\ 0&0&0&0 \\ 1/m&0&0&0 \\ 0&1/J_{\mathrm{x}}&0&0 \\ 0&0&1/J_{\mathrm{y}}&0 \\ 0&0&0&1/J_{\mathrm{z}} \end{bmatrix} \tag{9.3}$$

The two remaining matrices are the **C** matrix, also known as the output matrix, and the **D** matrix, also known as the feed forward matrix. The **C** matrix represents the variables that can be known through measurements taken by the onboard sensors. This is shown in Equation 9.4. The first two rows represent the GPS measurements in the x and y direction. The next row is the altitude from the LiDAR, which measures distance in the z-direction. The roll and pitch angles are measured by the accelerometer in the next two rows, the yaw angle is measured by the magnetometer, and finally, all three angular rates are measured by the onboard gyroscope. In this case, the **D** matrix is all zeroes, as the outputs are not affected by the inputs of the system, as shown in Equation 9.5.

$$C = \begin{bmatrix} 1&0&0&0&0&0&0&0&0&0&0&0 \\ 0&1&0&0&0&0&0&0&0&0&0&0 \\ 0&0&1&0&0&0&0&0&0&0&0&0 \\ 0&0&0&1&0&0&0&0&0&0&0&0 \\ 0&0&0&0&1&0&0&0&0&0&0&0 \\ 0&0&0&0&0&1&0&0&0&0&0&0 \\ 0&0&0&0&0&0&0&0&0&1&0&0 \\ 0&0&0&0&0&0&0&0&0&0&1&0 \\ 0&0&0&0&0&0&0&0&0&0&0&1 \end{bmatrix} \tag{9.4}$$

$$D = \begin{bmatrix} 0&0&0&0 \\ 0&0&0&0 \\ 0&0&0&0 \\ 0&0&0&0 \\ 0&0&0&0 \\ 0&0&0&0 \\ 0&0&0&0 \\ 0&0&0&0 \\ 0&0&0&0 \end{bmatrix} \tag{9.5}$$

The output vector, $\vec{y}$ is the final output of the second equation in Equation 9.1. In this case, it is $\vec{y}^T = \begin{bmatrix} x & y & z & \phi & \theta & \psi & \dot{\phi} & \dot{\theta} & \dot{\psi} \end{bmatrix}$. The **A, B, C , D** matrices in combination with $\vec{x}$, $\dot{\vec{x}}$, $\vec{y}$ and $\vec{u}$ complete the state space model of this drone.

9.2. Controllability

For the controllability of the drone, two methods of analysis were performed. "Classical Controllability" and "Available Control Authority Index" (ACAI) were used and were obtained from "Introduction to Multicopter Design and Control" by Quan Quan [129]. For both methods, the three following motor rotation configurations shall be investigated: *PNPNPN*, *PPNNPN* and *PPPNNN*. The *P* denotes clockwise rotation, *N* denotes counter-clockwise. The position of the *P*'s and *N*'s within the name of the configurations represent the spin directions of the motors in those positions. In Figure 9.1, the enumeration of the motors is demonstrated.

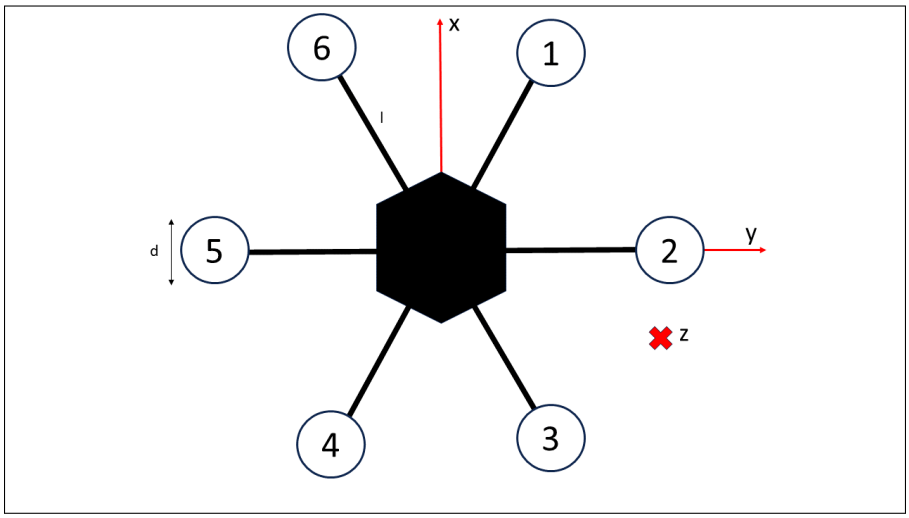

Figure 9.1: *Hexacopter "X" configuration*

Note that other configurations such as, *PPPPNN*, were not considered as it is nonsensical to design for more rotors rotating in one direction than the other for this application.

9.2.1. Classic Controllability

To ensure the controllability of the drone, an analysis must be performed. In "Classic Controllability", complete controllability represents the ability to control each degree of freedom (DOF) independently, using a single or combination of motor inputs. Note that complete controllability only states if a force can be generated in all directions, not whether the magnitudes of the forces are sufficient. Using the method for "Classical Controllability" described in "Introduction to Multicopter Design and Control" by Quan Quan [129], the aforementioned state space model can be simplified. Rather than using the full 12 states defined in Section 9.1, the controllability for hovering only requires eight states. States relating to the positions and velocities of x & y are omitted (states 1, 2, 7, 8). Doing these simplifications results in the following matrices.

$$A = \begin{bmatrix} 0_{4x4} & I_{4x4} \\ 0_{4x4} & 0_{4x4} \end{bmatrix} \qquad B = \begin{bmatrix} 0_{4x4} \\ J_f^{-1} \end{bmatrix} \tag{9.6}$$

Where 0_{4x4} is a zero matrix of dimensions "4x4", I_{4x4} is the identity matrix of dimension "4x4" and J_f is a diagonal matrix of the moment of inertia for the drone including the mass of drone as presented in Equation 9.7.

$$J_f = diag(-m, J_{xx}, J_{yy}, J_{zz}) \tag{9.7}$$

Where J represents the moment of inertia in an axis and m is the mass of the drone. Next, the control effectiveness matrix, B_f, must be derived. This matrix depends on the drone configuration and the direction of rotation of the individual motors. The parameters l and d represent the length of the arm and the diameter of the propeller, respectively. For the initial analysis, the motor rotation directions are intuitively arranged to be alternating between clockwise and counter-clockwise, with opposing motors spinning in opposite directions. This is the aforementioned *PNPNPN* configuration, where 1, 3 and 5 are *P*, and 2, 4 and 6 are *N*. With this, the control effectiveness is derived and shown in Equation 9.8.

$$B_f = \begin{bmatrix} k_1 & k_2 & k_3 & k_4 & k_5 & k_6 \\ \frac{-1}{2}l_1k_1 & -l_2k_2 & \frac{-1}{2}l_3k_3 & \frac{1}{2}l_4k_4 & l_5k_5 & \frac{1}{2}l_6k_6 \\ \frac{\sqrt{3}}{2}l_1k_1 & 0 & \frac{-\sqrt{3}}{2}l_3k_3 & \frac{-\sqrt{3}}{2}l_4k_4 & 0 & \frac{\sqrt{3}}{2}l_6k_6 \\ -k_1k_u & k_2k_u & -k_3k_u & k_4k_u & -k_5k_u & k_6k_u \end{bmatrix} \tag{9.8}$$

In Equation 9.8, k is the efficiency of the motor, l is the length of the arm and k_u is the ratio between the moment coefficient of the motors and the thrust coefficient of the motors. With the relation of thrust and moments specified by the manufacturers [159], the coefficients can be calculated using the relations presented in the paper [144]. After further deriving the state space model, the resultant input matrix, B', is calculated by matrix multiplying the input matrix, B, with the control effectiveness matrix, B_f. Finally, the controllability matrix, $\mathcal{C}$, is calculated as shown in Equation 9.9.

$$\mathcal{C}\left(\mathbf{A}, \mathbf{B'}\right) \triangleq \left[\mathbf{B'AB'} \dots \mathbf{A}^{n-1}\mathbf{B'}\right] \tag{9.9}$$

$$\text{rank}\, \mathcal{C}\left(\mathbf{A}, \mathbf{B}\right) = n \tag{9.10}$$

In Equation 9.10, if the rank of the controllability matrix is equal to the number of states, n, the configuration is deemed fully controllable. For the *PNPNPN* configuration, this method was performed with the parameters displayed in Table 9.1. After the analysis, configuration *PNPNPN* was deemed to be **fully controllable** as it had a rank of eight.

This analysis was repeated for the two other configurations. With the control effectiveness matrices adjusted accordingly, it was found that all configurations are deemed fully controllable.

Table 9.1: *Parameters of final configuration of UAV*

Parameter	Value
k	1 [-]
m	57 kg
d	32 inch
l	0.854 m
c_T	0.0736 [-]
c_M	0.00335 [-]

9.2.2. Available Control Authority Index

ACAI is a new, more specific method of evaluating the controllability of aerial vehicles introduced by Quan Quan [85]. Unlike classic controllability, using the parameter of control authority, ρ, enables the calculation to take into account the disturbance force and torques in the z-direction and around the x, y and z axes. This means that the magnitude of the forces relative to the disturbances, such as gravity, must be overcome to be labelled controllable. This introduces a more valuable indication of the controllability of the drone.

Method: The method involves analysing the maximum thrust and torques the drone can generate in all directions and defining it as a boundary for controllability, Ω in a four-dimensional plane. Next, depending on the defined disturbance translation vector, G, the point g shall either lie within or outside the boundary of Ω. The control authority parameter $\rho(g, \delta\Omega)$ is the radius of the biggest enclosed sphere within Ω which indicates how much "margin" the drone has to remain controllable. In order for the drone to be deemed controllable $\rho(g, \delta\Omega)$ must be larger than zero [129]. This concept is demonstrated in Figure 9.2.

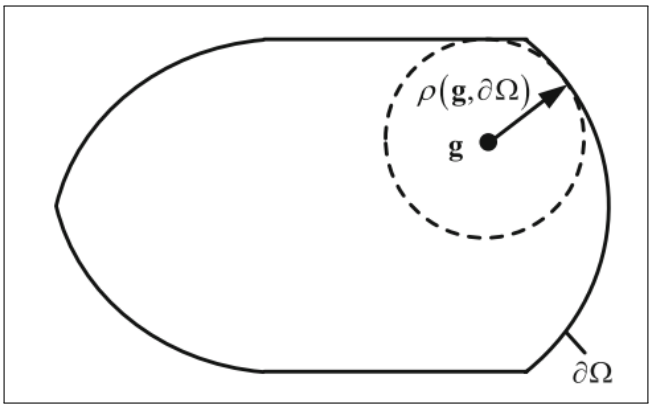

Figure 9.2: *Illustration of definition of control authority ρ [129]*

Calculation: After contacting Quan Quan by email for a link to the code made by the creators at *Rfly Open HA*, the functions to calculate the needed ACAI values were acquired [130]. This code was used to investigate the aforementioned configurations, in two different scenarios, fully operational and with propeller failures.

No Failures: With all motors fully functional and with an efficiency of 1, the different configurations were iterated over the available throttle settings to determine the boundary at which they can fly with full controllability. The results are displayed in Table 9.2, where the minimum thrust is the amount of thrust needed for controllability.

Table 9.2: *Controllability analysis with no rotor failures*

Configuration	**Minimum Thrust** [%]	**Max ACAI - 100%**
PNPNPN	52	23.7
PPNNPN	52	16.1
PPPNNN	52	7.2

In Table 9.2, it can be seen that in order to be controllable during flight, the minimum throttle must be 52%. In optimal conditions, *PNPNPN* can achieve the highest control authority at maximum throttle. Note, the throttle of the motors is limited to 85% due to the chosen ESCs in Section 7.2. The same analysis can be performed for the configurations with a single rotor failure.

Single Rotor Failures: During missions there is a realistic chance that a propeller/motor may fail. In these cases, it may be important to assess if the drone is capable of safely landing with full controllability. With the ACAI, one can simulate a rotor failure by setting the efficiency of a motor to zero. In Table 9.3, the minimum required throttle to maintain full controllability is shown.

Table 9.3: *Controllability analysis with single rotor failure, each rotor*

	Minimum Thrust [%]		
Motor Failure	PNPNPN	PPNNPN	PPPNNN
1	Uncontrollable	75	Uncontrollable
2	Uncontrollable	87	Uncontrollable
3	Uncontrollable	87	Uncontrollable
4	Uncontrollable	75	Uncontrollable
5	Uncontrollable	Uncontrollable	Uncontrollable
6	Uncontrollable	Uncontrollable	Uncontrollable

As can be seen in Table 9.3, only configuration *PPNNPN* has redundancy that can operate with a single rotor failure. This gives a degree of redundancy that could be crucial when operating in highly populated areas. Note that rotors 5 and 6 can not be recovered in case of failure.

Since the drone will be operating in close proximity to chaotic and unpredictable environments, there is a realistic chance that a piece of debris may hinder or prevent the operation of a rotor. Seeing as the drone is fully controllable with a sufficient margin with all three configurations, only *PPNNPN* has a form of redundancy for most of its rotors. The ***PPNNPN*** configuration is selected for the drone. Note that the *PPNNPN* configuration can be rotated such that the Single Point of Failure (SPOF) are positioned as far away from the building as possible to minimise the risk. This configuration has the same controllability and would be named *NNPNPP*. The final configuration is shown in Figure 9.3.

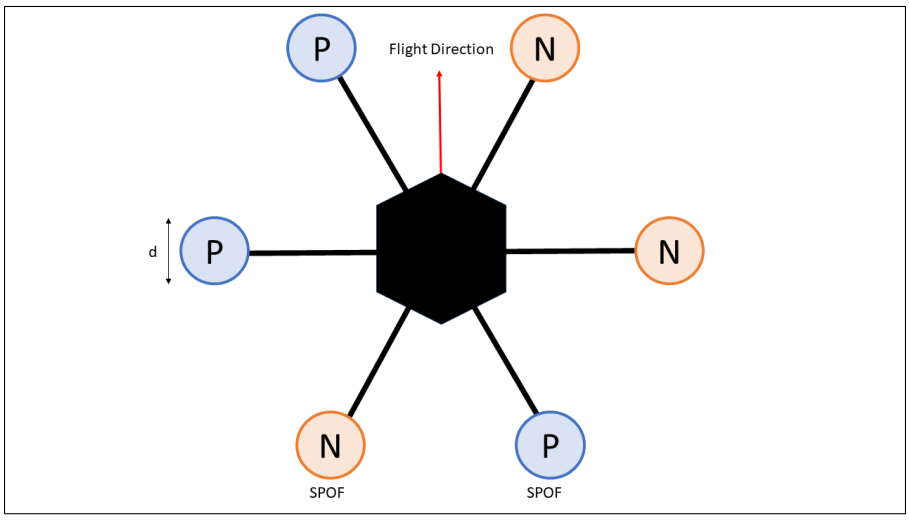

Figure 9.3: *Final rotor direction configuration (NNPNPP)*

9.3. Observability

The observability of a system represents the ability to measure or calculate all states of the system using the sensors on board. In matrix terms, it means that the rank of the observability matrix is full and equal to the number of states, n. This condition is demonstrated in Equation 9.3. This method is taken from "Introduction to Multicopter Design and Control" by Quan Quan [129]. Using the state matrix $\mathbf{A}$ and output matrix $\mathbf{C}$, the observability matrix can be constructed, as shown in Equation 9.3.

$$\mathcal{O}\left(\mathbf{A}, \mathbf{C}^{\mathrm{T}}\right) \triangleq \begin{bmatrix} \mathbf{C}^{\mathrm{T}} \\ \mathbf{C}^{\mathrm{T}}\mathbf{A} \\ \vdots \\ \mathbf{C}^{\mathrm{T}}\mathbf{A}^{n-1} \end{bmatrix}. \tag{9.11}$$

$$\operatorname{rank} \mathcal{O}\left(\mathbf{A}, \mathbf{C}^{\mathrm{T}}\right) = n \tag{9.12}$$

Using this method to calculate the rank, it was found that the system is **fully observable**. This means there are enough sensors on board to measure or calculate each state, which ensures the control system of the drone has the information it needs to control the drone continuously.

9.4. Controllers

Now that the controllability of the drone has been analysed in detail, the drone controller must be examined. A controller takes inputs from the pilot and the sensors and uses an algorithm to output motor commands to the drone. In this section, two different controllers, PID and LQR, will be presented and compared in order to find the optimal one for the control system of the drone.

9.4.1. PID

PID stands for Proportional, Integral, Derivative. It is a classical control algorithm which takes as input a target value for a certain parameter, calculates the error between the target value and the sensor-measured value of that parameter, and outputs a command to the system to correct this error. The Proportional controller is responsible for correcting the present error. The output value of this term is proportional to the error, so if the error is large, the gain will be large too. The Integral controller integrates the past values of error over time. This corrects for even the smallest errors such as the steady-state error, as the error is accumulated over time. The Derivative controller predicts the future error based on its current rate of change. If the error is minimising rapidly, the response output will become slower [64]. These three controllers can be tuned to create a functional PID controller that minimises the error and reaches the target value as effectively as desired.

9.4.2. LQR

Another controller which can be used is the Linear Quadratic Regulator (LQR) controller, which is an optimal control algorithm. The LQR controller aims to minimise the cost function, which describes the system's performance and is defined as the sum of the weighted quadratic error between the actual system state and the desired state. By adjusting the weights in the cost function, certain aspects of the control performance can be optimised, such as improving settling time or reducing overshoot [79]. This method of control must be compared to PID. While it involves more mathematical computations in order to calculate the feedback matrix which minimises the cost function, it is computationally efficient and possesses excellent inherent robustness, whereas PID is not equally robust to system uncertainties and disturbances. However, LQR is not as effective with the transient behaviour of a system, and PID is better as it can tune the gains for optimised transient behaviour [165].

9.4.3. Discussion of PID and LQR

Both types of controllers have advantages and disadvantages, but for this specific task, drone and mission, the most important criteria when choosing a control system are simplicity and availability. In the time frame that is given, the technical background, and the desire to deliver a complete and ready-to-use drone design, these criteria are imperative. As the drone is relatively large, any disturbance from wind gusts or otherwise will not cause the drone to rotate by a large margin, therefore a highly robust control system is not necessary. The disturbance angles are assumed small, and high manoeuvrability will not be required. For this reason, PID is a more appropriate choice. It is less complex and widely available, and will successfully aid the drone in performing its mission.

One of the benefits PID control can provide to the project is the ability to purchase flight computer firmware with PID control built-in off-the-shelf. This is available in the form of ArduPilot, an open-source flight computer system capable of controlling the drone reliably. It can be tuned through flight testing to optimise to what the mission requires. In the next section, a high-level stability analysis method of the ArduPilot software will be presented.

9.5. Stability

The control system determines the stability of the drone. To gain insight into the stability of the entire drone, extensive analysis and testing must be performed. However, the first step consists of ensuring that the individual controllers within the control system are stable. To do this for the selected ArduPilot control system [8], a simplified system has been created. From existing sources [146], it can be seen that typical PID systems are separated into three controllers: Attitude, Altitude and Velocity controllers. An illustration of this is demonstrated in Figure 9.4.

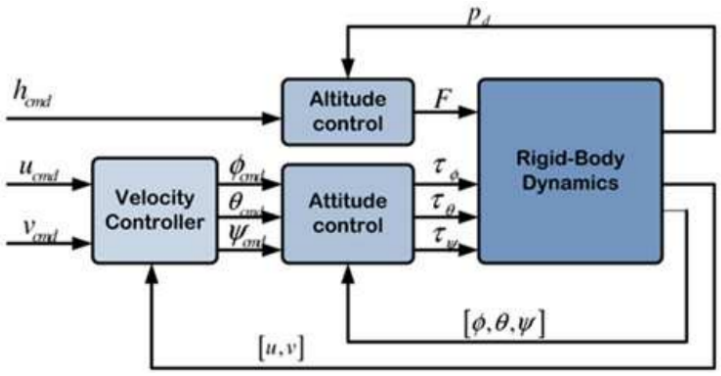

Figure 9.4: *Typical control system of a multi-copter drone [146]*

The attitude controller is further investigated to present the stability analysis method. The attitude controller is responsible for converting the angle error to a required rotation rate which the PID converts into correction motor commands. The control loop for one angle is presented in Figure 9.5. For the analysis performed in this report, a simplified control loop shall be utilised. The simplification includes removing the non-linearities, such as the acceleration limiter (Acc-limiter) which is present in the control loop to make it more robust to disturbances and the additional proportional controller is removed to limit the complexity of the system. The ArduPilot software also utilised a Feed Forward (FF) loop. The FF block corrects the error originating from the difference between the body frame and the world frame.

The simplified control loop is displayed in Figure 9.5.

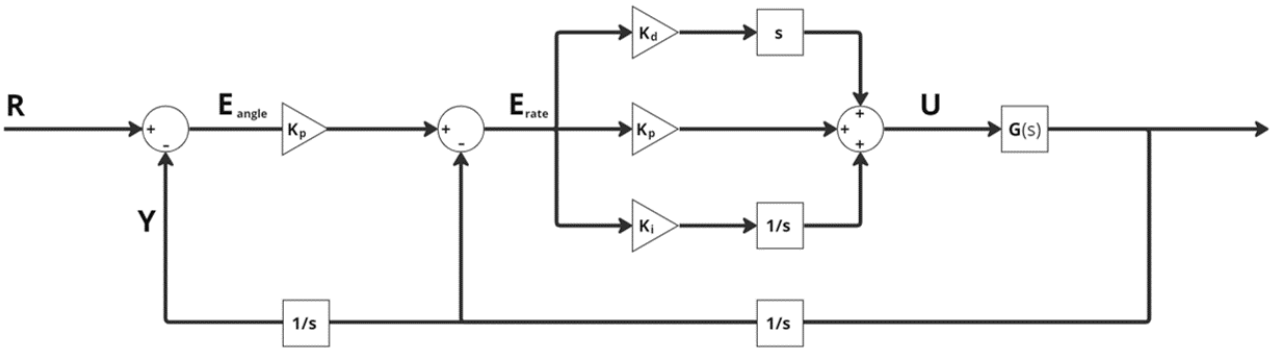

Figure 9.5: *Simplified control loop for stabilising an attitude angle (ArduPilot)*

To demonstrate the stability analysis method used in the control loop of Figure 9.5, an example is shown for stabilising the roll angle of the drone. This analysis of the stability of the drone shall only be detailed in theoretical terms, with no qualitative analysis, as this is only a preliminary design stage, and will not be valuable until a later design stage when tuning is being performed. In Figure 9.5, R is the reference input giving the desired roll angle ϕ_{des}, Y is the output giving the actual angle ϕ, E_{angle} and E_{rate} are the error between the reference input and the output for angle and angular rate, respectively. U is the control input obtained from the three controllers, and $G(s)$ is the plant of the control loop ($G(s) = \frac{1}{J_{xx}}$ for the roll angles). Furthermore, K_d, K_p and K_i are the derivative, proportional and integral gains, respectively. From this, the transfer function of the control loop must be derived. This results in:

$$\frac{\phi}{\phi_{des}} = \frac{K_{p1}(K_d s^2 + K_{p2} s + K_i)}{K_d J s^3 + (K_d K_{p1} + K_{p2}) s^2 + (K_{p1} K_{p2} + K_i) s + K_i} \tag{9.13}$$

With Equation 9.13, the Routh-Hurwitz criterion can be used to determine whether the system is stable. In other words, the poles in the 'S' plane must lie on the left side of the imaginary axis. This ensures that the real parts of the eigenvalues of the state space model are negative and thus allow for convergence. The Routh-Hurwitz

criterion takes the characteristic equation of the transfer function and divides by the leading coefficient obtain format as demonstrated in Equation 9.14 [92].

$$s^n + a_1 s^{n-1} + a_2 s^{n-2} + \ldots + a_{n-1} s + a_n = 0 \tag{9.14}$$

For third-order polynomials, $n = 3$ and the Routh-Hurwitz criterion state that in order for the system to be stable, the following two relations must hold [92].

$$a_1, a_2, a_3 > 0 \qquad\qquad a_1 a_2 > a_3 \tag{9.15}$$

If this holds, it ensures the single controller is stable however does not ensure the stability of the entire drone. This criterion can be used to tune the individual controllers and shall be valuable once the drone is constructed. A similar process can be done for the different attitude angles, altitude, and velocity relations. More elaborate analysis and testing must be performed to ensure the total stability of the drone. In the next section, the actual ArduPilot software that shall be purchased off-the-shelf shall be presented and briefly explained.

9.6. Software Block Diagram

The software architecture describes how the ArduPilot code structure works and gives a simple overview of how the flight controller communicates with each of the components, and how it works with the components in general. Figure 9.6 shows the software architecture of the code. The Software architecture follows a general flow structure where it starts with background information from the sensors which is fed into the software and finally converted to PWM signals to communicate with the ESCs for efficient control. The chosen **Cube Pilot Cube Orange** will fly on the Ardu Pilot Software.

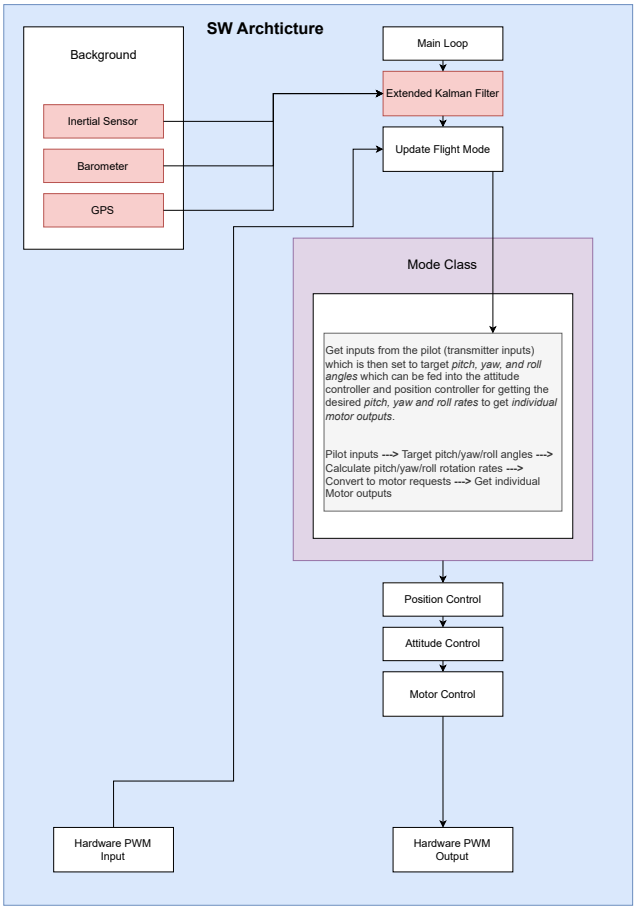

Figure 9.6: *Software architecture of ArduPilot Copter system [10]*

By looking at Figure 9.6, a brief description of how the software is structured will be given. The information from the sensors (Inertial, Barometer, GPS) is fed into the Extended Kalman Filter (EKF). The EKF is fed into a main loop which then updates the flight mode. A **Mode Class** is initialised and run with input from pilots that sets the target roll, pitch, and yaw angles. This is then used to calculate the target roll, pitch, and yaw rotation rates. This is converted to motor requests which can be used to get the individual motor outputs. Finally, these outputs are scaled and sent as PWM signals to the ESCs. In the following subsections, each part of the ArduPilot software architecture will be described in more detail.

Background
This is where the measurements and readings from the sensors (IMU, Barometer, and GPS) are fed into the EKF.

Extended Kalman Filter
An EKF algorithm is used to estimate vehicle position, velocity and angular orientation based on gyroscopes, compass, GPS, and barometric pressure measurements. An advantage of EKF over other algorithms is that it fuses all sensor measurements to reduce significant errors and faults that are more susceptible when using just one sensor. The EKF can also estimate offsets from the compass readings which is beneficial as it is less sensitive to compass calibration errors [9].

Update Flight Mode
This is where the flight mode keeps updating based on the pilot inputs which is continued from the Mode Class for converting the pilot inputs to actual PWM outputs.

Mode Class
The mode class is where most of the inputs are converted to target pitch, yaw and roll angles that are fed to the attitude and position controller.

Position, Attitude, and Motor Control
The target angles set from the Mode Class is used to calculate the target pitch, yaw and roll rotation rates which is further converted to motor requests. These motor requests are then used to get individual motor outputs.

Hardware PWM I/O
The hardware PWM inputs and outputs is where the PWM signals are received and sent from the corresponding components which run the software. In the UAV, these are namely the transmitter, receiver, telemetry unit and FC.

10
Final UAV Design

This chapter will discuss the outcomes of the final decisions made. In Section 10.3, a CAD model of the drone will be presented. Next, Section 10.1 will give an overview of the final weight estimation of every component. Lastly, the transportability of the UAV will be explained in Section 10.2.

10.1. Weight Estimation

With the UAV design now completed, a weight estimation will be performed. For this weight estimation, the payload mass was excluded as the payload optimisation must still be performed.

The estimated weights of the subsystems are displayed in Table 10.1. Note, most components have been selected and thus exact weights can be obtained from the manufacturers. For certain components such as "*wiring*" and "*bolts*", rough estimates have been given with an assumed margin, however, the true mass will only be obtained after manufacturing. This also includes the insulation/cover, which has been implemented to prevent the heating of the components and provide effective water resistance.

Table 10.1: *Finalised UAV weight estimation per subsystem*

Component	Quantity	Mass per unit [g]	Total Mass [g]
Propulsion			
Propeller [157]	6	107	642
Motor [159]	6	645	3870
ESC [154]	6	109	654
Total			5166
Power			
Battery [17]	2	9564	19128
PDB [147]	2	16	32
Total			19160
Communication & Control			
Receiver [27]	1	1	1
Data link [80]	1	98	98
Flight computer [127]	1	73	73
Total			172
Electronics & Sensors			
Altitude LiDAR [65]	1	26	26
Frontal LiDAR [108]	1	10	10
Sonar [111]	2	50	100

Continued on next page

Table 10.1 – continued from previous page

Component	Quantity	Mass per unit [g]	Total Mass [g]
GPS [81]	1	49	49
Camera [52]	1	27	27
Thermal camera [149]	1	1	1
Gimbal [40]	1	80	80
Raspberry Pi [134]	1	66	66
Wiring	unk.	unk.	1500
Relay [180]	1	20	20
LEDs [174]	4	6	24
Total			1903
Structures			
Arms	6	217	1302
Body	1	1390	1390
LG	1	2000	2000
Cover/Insulation	unk.	unk.	500
Bolts	unk.	unk.	500
Total			5692
Payload			
Pump [173]	1	4700	4700
Tank	1	1000	1000
Total			5700
OEW			37793

10.2. Design features

The HYDRONE is set apart from drones currently on the market by some unique features. Most noticeable is the custom payload system as can be seen in Figure 10.6. This payload system is optimised for effectively delivering the most payload. Furthermore, the HYDRONE has the capability to measure altitude and the distance from objects in the front to detect how close it is to buildings.

Controllability wise the drone is also set up differently than drones currently on the market. Instead of alternating the rotors in spin direction, the rotors are set up so that one of the front rotors can be lost due to debris or heat from the fire and still be controllable. In contrast to normal drones with alternating rotor rotations which will lose controllability once a rotor fails.

For *REQ-USER-P-3*, the drone must easily fit inside the fire brigade's transport vehicle. The following dimensional constraints were established based on the transport vehicle demonstrated in Figure 10.1b.

The vehicle demonstrated in Figure 10.1b has a transport capacity of 2607 x 1787 x 1599 mm. When rotating the propellers into the optimal configuration, the rotors are positioned as shown in Figure 10.1a. The outer dimensions of the UAV in transport configuration are **1833 x 1509 x 831 mm**.

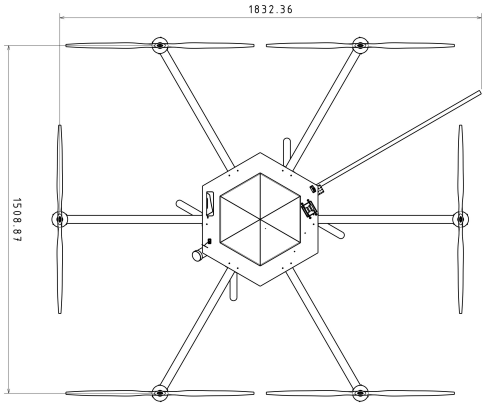

(a) *Dimensions at transport configuration*

(b) *Chosen Dutch fire brigade transport van [169]*

Figure 10.1: *Transportability*

10.3. Technical Drawings of UAV Design

A complete CAD model of the final design has been made. From this model multiple drawings are extracted to convey the design of the UAV. The drawings are divided into the complete UAV, payload/landing-gear and electronics. As illustrated in Figure 10.3 and Figure 10.6, the main components of the UAV can be disassembled. Furthermore, no wall thickness is indicated in Figure 10.5 since only the inside dimensions are needed for the volume. The thickness is dependent on the manufacturer and strength of the material used. For any difficulties faced with the rendering of the UAV CAD drawings, Eddy van den Bos was consulted.

UAV Overview

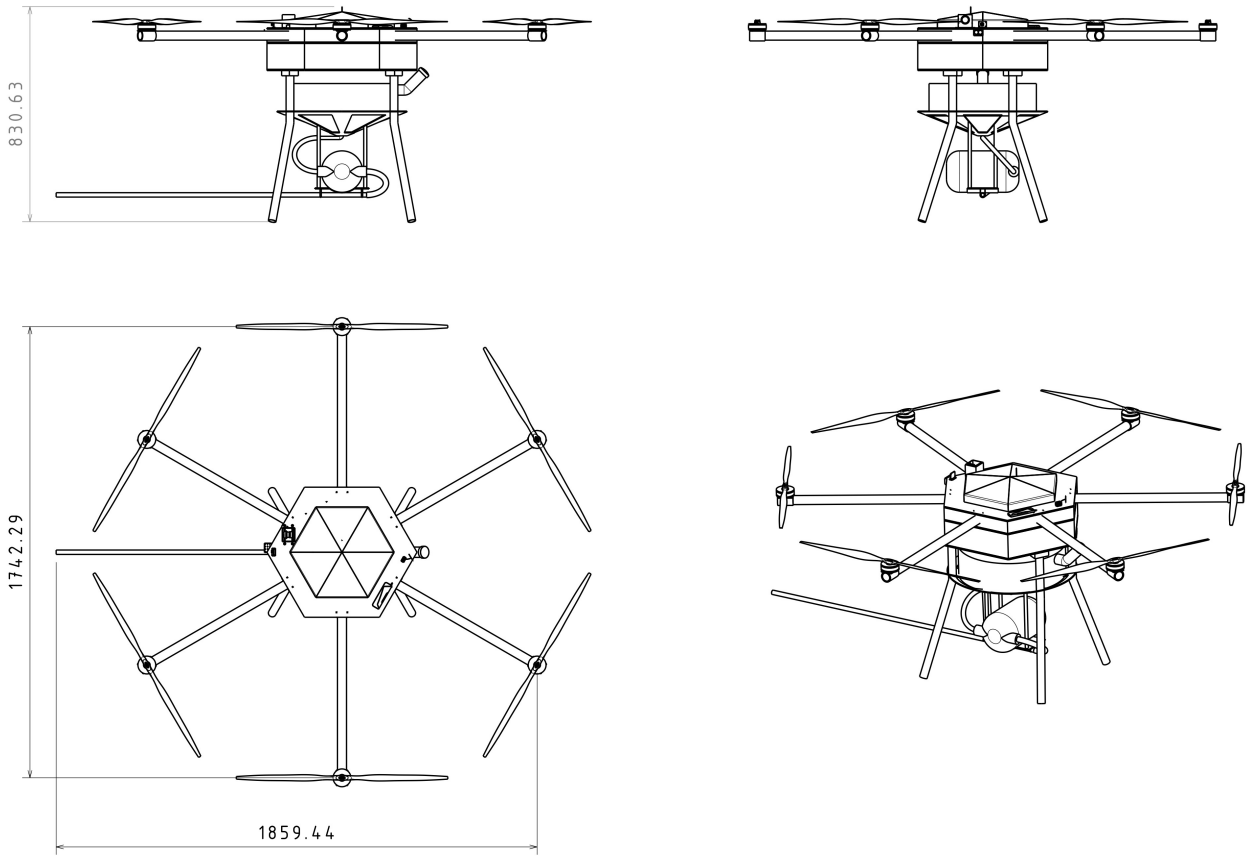

Figure 10.2: *Side views and top view of the UAV*

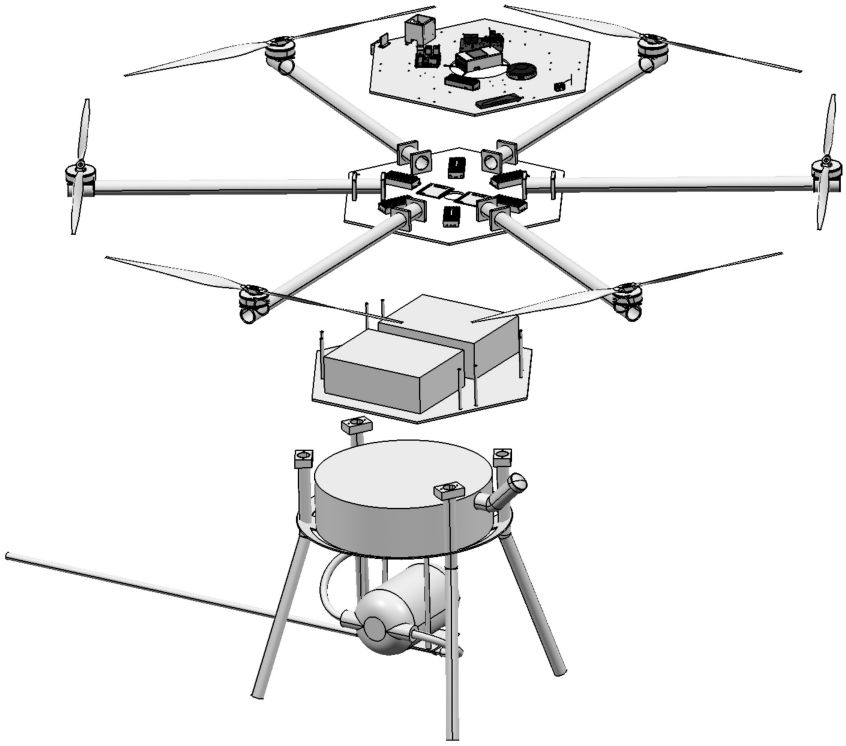

Figure 10.3: *Exploded view of the UAV without plastic covers*

Payload System

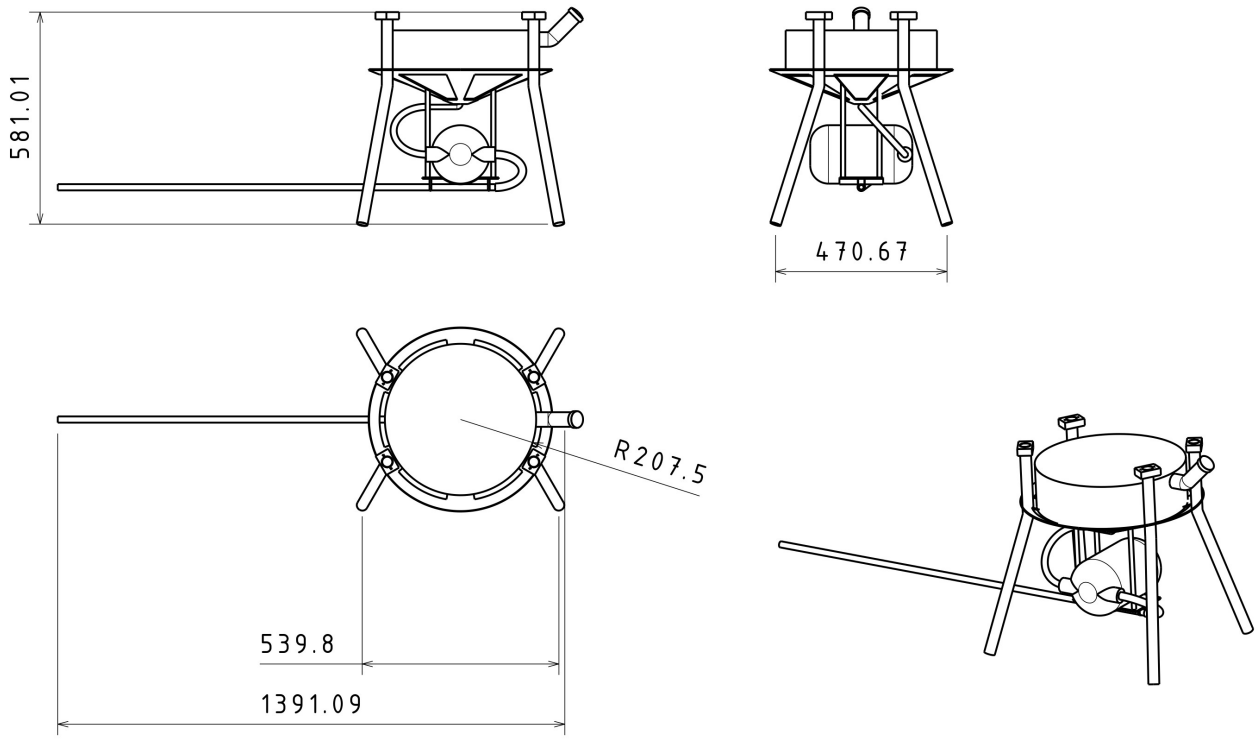

Figure 10.4: *Side views and top view of the payload system*

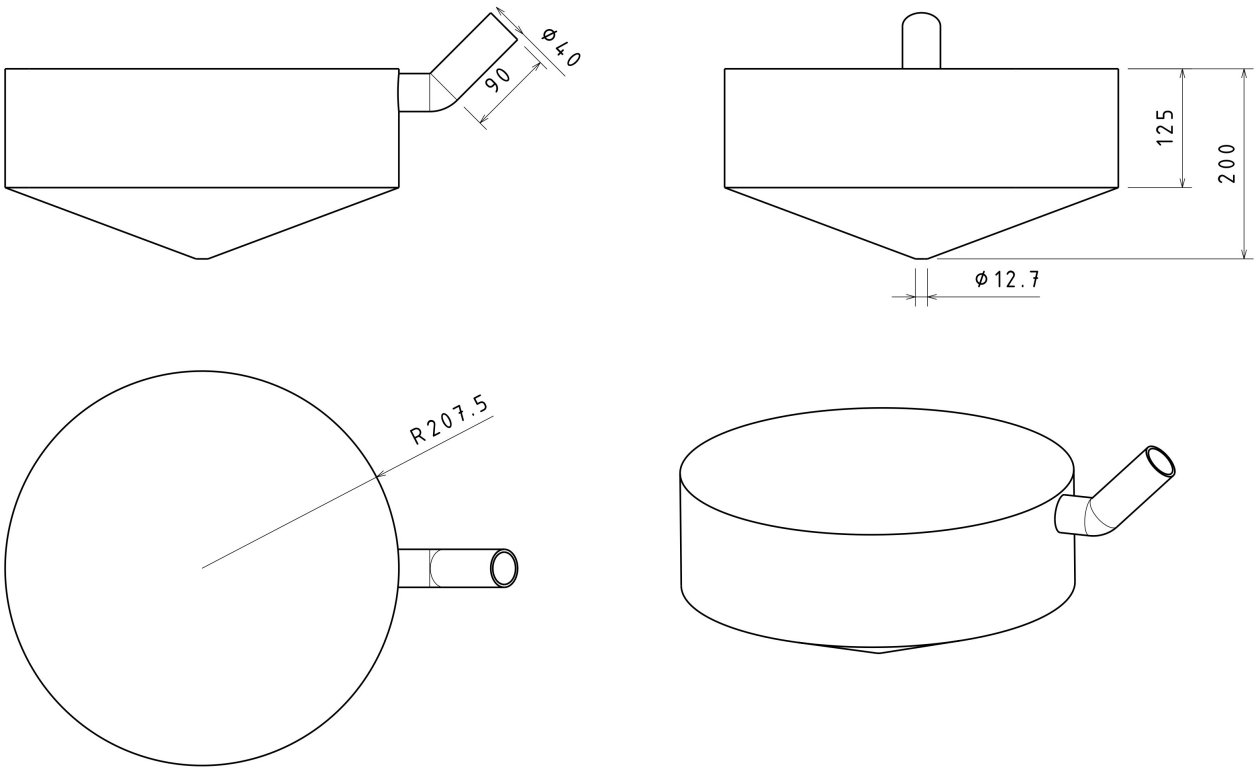

Figure 10.5: *Part drawing of the custom water tank*

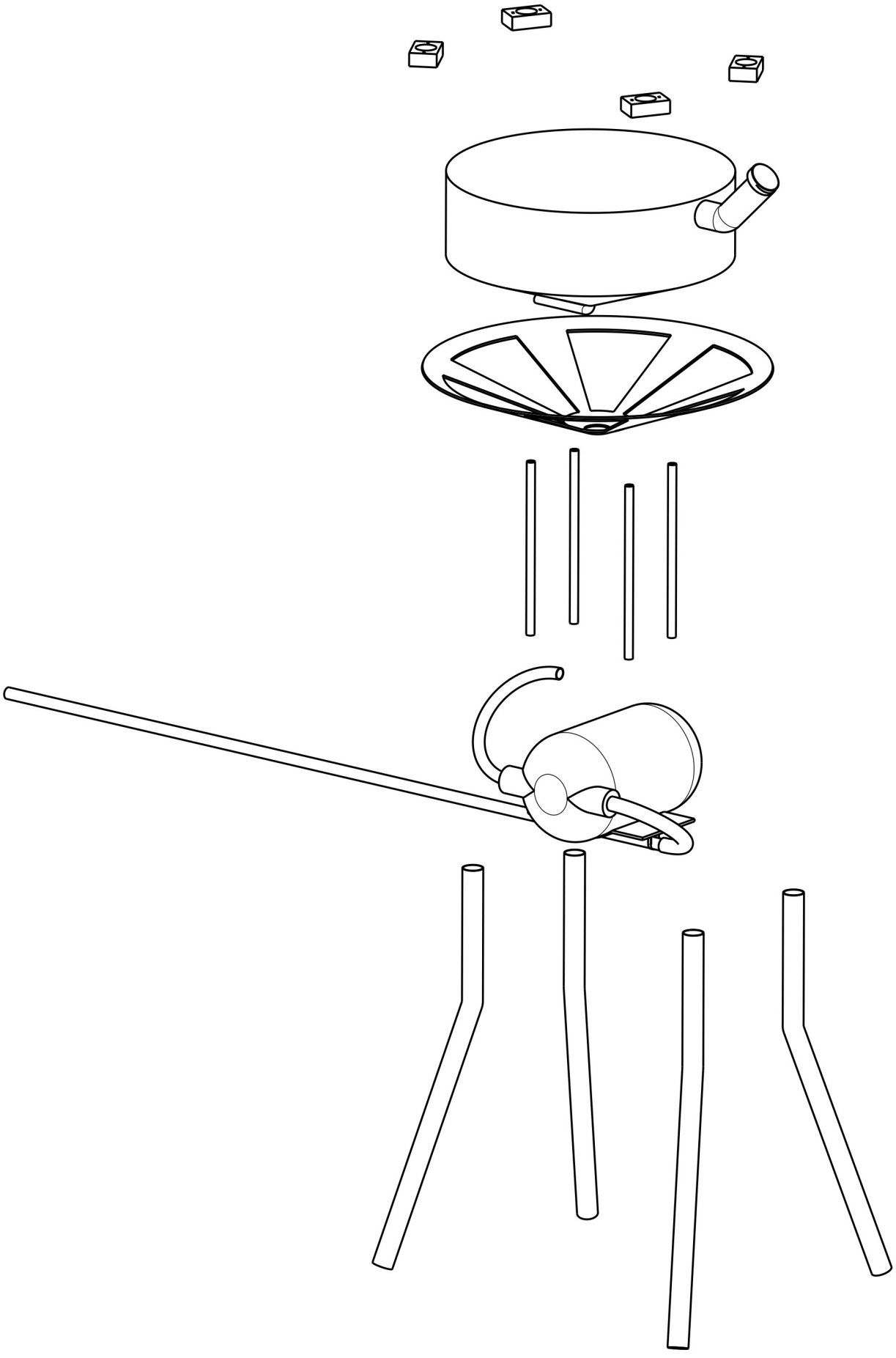

Figure 10.6: *Exploded view of the payload system*

Electronics

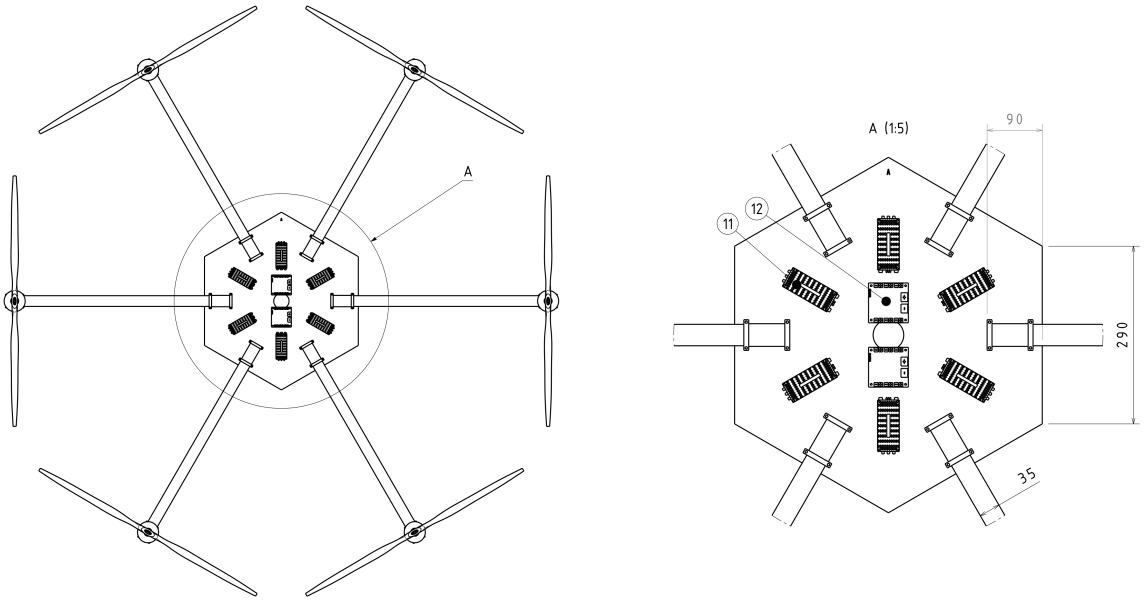

Figure 10.7: *Bottom electronics detailed view*

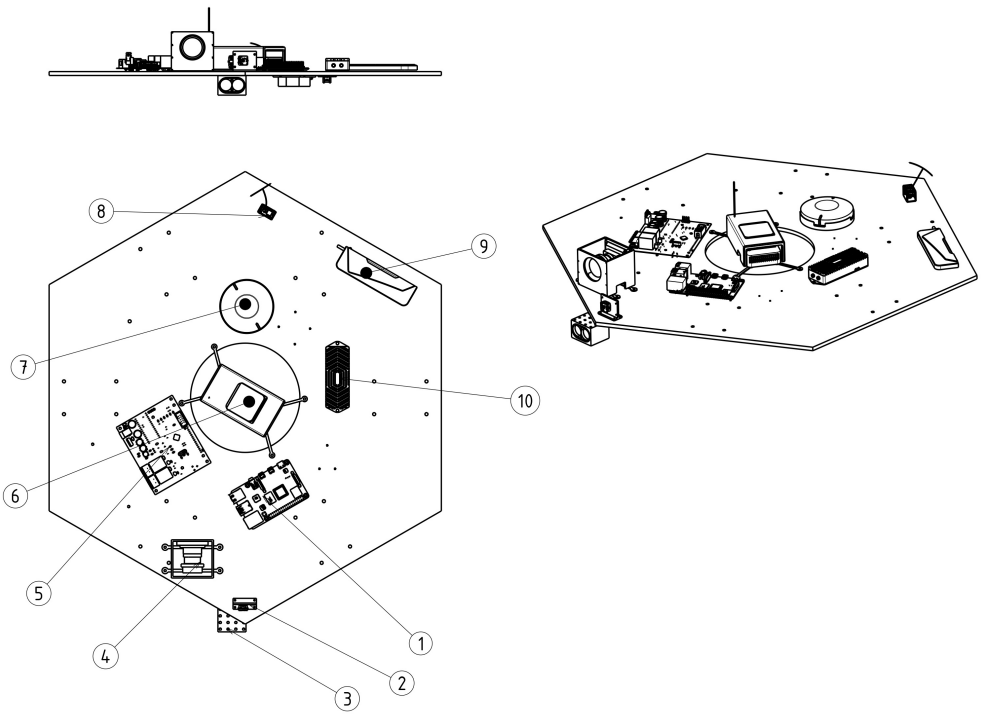

Figure 10.8: *Top electronics side views and top view*

Table 10.2: *Overview of electrical components*

No.	Component
1	Raspberry Pi 4 Model B
1	FLIR Lepton 3.5 - Thermal Imaging Module
3	Lidar SF20/C
4	Visual camera, Hawkeye Firefly 4k Nakedcam
5	Hawkeye Micro Controller
6	Flight Computer, CubePilot Cube Orange
7	Here3 RTK GPS
8	Antenna, TBS Crossfire Nano RX
9	Herelink Antenna
10	Telemetry, Herelink Air Unit 1.1
11	ESC, T-MOTOR Flame 80A 12S
12	PDB, Sky-Drones SmartAP PDB 400A

11
Performance Analysis

This chapter will first discuss the mission profile in Section 11.1, including all the steps taken during the mission. Secondly, an analysis of the climb rate with different payloads will be performed in Section 11.2. This will be followed by an optimisation of the payload in Section 11.4. Next, the mass and power needs of each component will be discussed in Section 11.3. In Section 11.5, an analysis will be performed to know what magnitude of wind gusts or other disturbances the drone can handle. After the design has been established, a logistics concept description will be given in Section 11.6. Lastly, an environmental impact analysis will be performed in Section 11.7.

11.1. Mission Profile

As the final design of the drone and its system architecture has been decided, the analysis of the mission profile must be performed. In Figure 11.1, the sequence of events which will take place during the flight is shown. In Figure 11.1a, the steps taken to complete the mission are shown, and separated into six sections.

(a) Deployment
(b) Reach Altitude
(c) Approach Target
(d) Deliver Payload
(e) Disengage Target
(f) Descent/Retarget
(g) Turn Around

The first step, *deployment*, involves calibrating and getting the drone ready so that it is fully functional. The second step is the drone's pure climbing motion to reach the desired altitude, which is known as the *reach altitude* step. *Approach target* refers to positioning the drone such that the payload can be delivered. This is followed by *delivering payload*, which consists of spraying the extinguishing agent on the target. The drone must then *disengage target* which involves moving out of the hot environment. During *descent/retarget*, the operator needs to decide whether to return to part b (*"reach altitude"*) or return to base. This depends on the amount of surplus extinguishing agent. The final phase, *turn around*, refers to landing, replacing the payload and/or batteries, and starting the mission over again until no longer necessary.

In Figure 11.1b, the required flight type for each section of the mission profile is demonstrated. The drone will need to take off and rapidly climb to the level where the fire is located. Then, it will hover, stabilise as it begins delivering the extinguishing agent, and once the situation is under control or the fire extinguisher has been completely emptied, the drone will descend and land. The entire operational time depends on the amount of payload and the height at which the fire is. This will be further analysed in Section 11.4.

The two most important flight types are stabilised hover and climb, as the whole operation is time constrained, and the drone must be able to perform these with optimal efficiency. The climb rate and stability of the drone will be analysed further in the next sections.

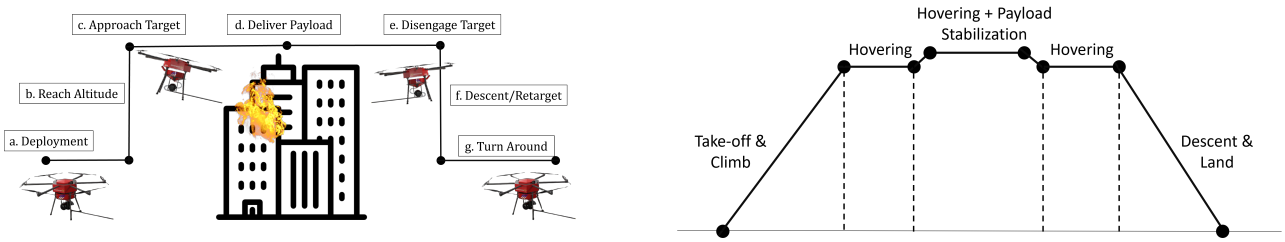

(a) *Illustration of the mission profile for the drone*

(b) *Illustration of the flight profile for the drone*

Figure 11.1: *Mission and flight profile diagrams of the drone*

11.2. Climb Rate

The climb rate is an important parameter for the mission. The MAVLAB (Micro Air Vehicle Laboratory) of TU Delft was consulted to discuss the approach used for the climb rate analysis in this section. In order to calculate the climb rate, the vertical forces on the drone have to be analysed when going straight up, since this will be the fastest way to climb. The vertical forces will be the thrust, weight and drag as shown in Equation 11.1. To analyse the climb rate, a Python script was written to compute the acceleration, the velocity and the height at small time steps. However, this required the drag coefficient and surface area which was unknown at this moment. Hence `flyeval.com` was used to get estimates on the drag. This program gives estimates of performance specs, including the drag coefficient in N/(m/s)^2 which also removes the unknown area variable as can be seen in Equation 11.2. To get these performance specs multiple inputs like: parts weights, discharge currents, battery capacity, propeller pitch, motor torque etc. are needed.

$$\sum F_y = T - W - D = ma_y \tag{11.1}$$

$$D = \frac{1}{2}\rho C_D V^2 S = C_d V^2 \tag{11.2}$$

The estimated C_d for the drone was taken to be 2. However, the climb speed for different drag coefficients was computed in order to see the effects of a wrong estimation. To obtain an accurate value for the drag coefficient, extensive wind tunnel testing must be performed with the manufactured prototype. Figure 11.2 shows the climb rate for different drag coefficients and payloads. As expected, an increase in drag will result in lower maximum velocity. Furthermore, a maximum climb velocity will be imposed for operational safety at **8 m/s**. In Figure 11.2, it can be seen that only for high payloads at large drag coefficients this maximum velocity cannot be reached.

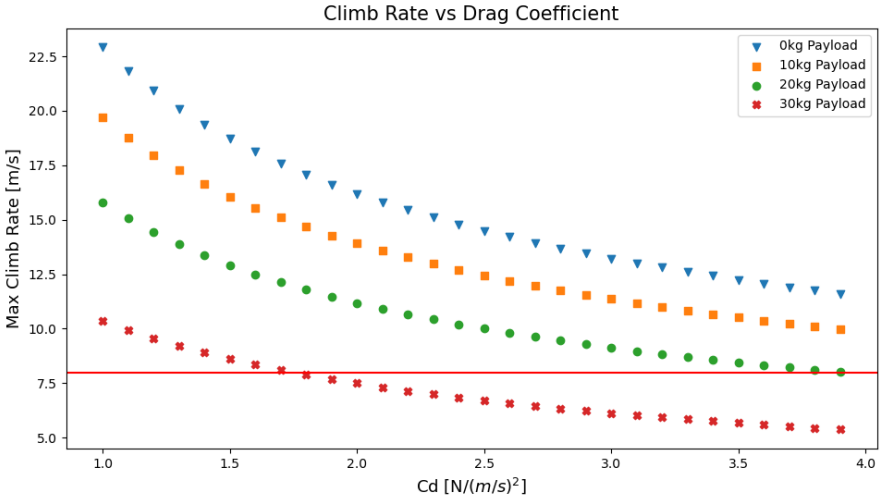

Figure 11.2: *Climb rate vs drag coefficients at different payloads with a 80% throttle setting*

11.3. Power Budget

When it comes to the performance analysis of the UAV in relation to the power requirements, figuring out the power that each component consumes will help to optimise the power distribution of the drone. Calculating the power usage will enable to efficiently distribute the power over all the components and maximise the performance of the UAV.

The total power consumption of the UAV is a combination of the motor power consumption and the power consumed by all the electrical components on the drone. The power consumed by each of the components is presented in Table 11.1. The motors are left out of the table since the power that the motors draw depends on the amount of thrust they have to deliver. As shown in Table 11.1, the total power consumption due to the electronic components, excluding the motors, equals **363.3 W**.

Table 11.1: *Power consumption by a single component and the corresponding total power consumed*

Component	Quantity	Power per unit [W]	Total Power [W]
Propulsion			
ESC [154]	6	3	18
Total			18
Power			
PDB [147]	2	25	50
Total			50
Communication & Control			
Receiver [27]	1	4	4
Data link [80]	1	4	4
Flight computer [127]	1	14	14
Total			22
Electronics & Sensors			
Altitude LiDAR [65]	1	1	1
Frontal LiDAR [108]	1	0.5	0.5
Sonar [111]	2	1	2
GPS [81]	1	0.15	0.15
Camera [52]	1	12	12
Thermal camera [149]	1	0.65	0.65
Gimbal [40]	1	2	2
Raspberry Pi [134]	1	15	15
Relay [180]	1	0.1	0.1
Total			57.4
Payload			
Pump [173]	1	240	240
Total			240
Net Power Consumption Electronics			387.4

The power that the motors draw is limited by the ESC as previously discussed in Section 7.1. Only the nominal state of the UAV will be considered, meaning that the burst state of the ESC and batteries are neglected. In Figure 11.3, the thrust delivered by a single motor at different amps is shown. Due to the ESC, a maximum of

80 A can be delivered to each engine. Combining this with the voltage of the motor and multiplying it by the number of motors results in a power drawn of 23621 W. The batteries can supply up to 25530 W, therefore there is enough power to supply all the electrical components simultaneously at max thrust. Furthermore, the curve from Figure 11.3 can be inverted to obtain Equation 11.3 from the trend line. In Equation 11.3, T is the total thrust in Newton and I is the current in amps. This equation can be used to calculate the amount of Ah used by the motors when multiplied by the amount of time the thrust is needed.

$$I = 5.35 \cdot 10^{-5} T^2 + 9.8 \cdot 10^{-3} T + 3.78 \tag{11.3}$$

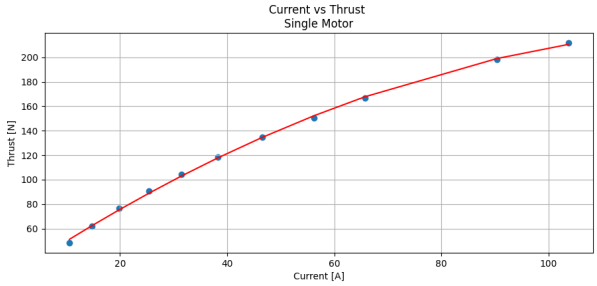

Figure 11.3: *Current vs Thrust curve*

11.4. Payload Optimisation

With the mission profile, the climb rate and the power analysed, the payload of the drone can be investigated. The purpose of this section is to optimise the payload of the UAV for the chosen mission profile in Section 11.1. For this, the following assumptions were made.

Clean Conditions For the optimisation of the drone payload, the mission is assumed to be in clean conditions. This assumes no disturbances such as wind during operation. This results in a T/W of 1 for hovering, 1.4 for manoeuvring and 0.8 for controlled descent. Note however, that at all times during the mission, the drone must be able to achieve a maximum T/W of 2 to ensure that the drone can still correct for significant disturbances.

Optimised Altitude To optimise the payload for the mission, an estimate was done for the typical mission altitudes for which the drone shall be applied in the Netherlands. As typically these drones are most beneficial for extinguishing fires in high-rise buildings, the payload was optimised for the average high-rise building in Europe. This gives a design **altitude of 130 m** [122]. With this optimised altitude the payload shall be selected.

Climb Throttle Setting For the climb, it is desired that a margin of throttle is remaining to allow for necessary stabilisation and correction against disturbances. Furthermore, climbing at 100% also leads to the motors operating in the less efficient RPM setting for endurance. The chosen **thrust setting is 80%** of total thrust, as this enables sufficient remaining thrust for high disturbance environments and allows for a fast Rate of Climb (ROC).

Approach/Manoeuvre Time As shown in Figure 11.1a, after the altitude has been reached, the subsequent step is to approach the target. This involves evaluating the scene and repositioning the drone for optimal payload delivery. Assuming the firefighters are trained professionals, it is estimated that this can be done in **under 30 seconds**. The same amount of time is allocated to disengaging from the target and evaluating whether to *"Retarget"* or *"Descend"*.

Battery Capacity For the operation of the batteries, additional margins must be implemented to ensure each battery operates as expected without getting damaged. For the Depth of Discharge (DOD), the general rule is to remain below 80% as the number of cycles and the cycle life drastically reduce if it is exceeded. An additional safety margin is implemented in case of mission failure to allow the drone to safely descend from the operational

altitude. Furthermore, 5 Ah is dedicated to the electronics and payload of the UAV during one battery life. The 2.3 Ah margin is calculated from the power needs demonstrated in Section 11.3. This is done assuming an average operational time of approximately 25 min (for additional margin with *REQ-USER-P-2*) and assuming payload spraying 50% of the time. **This reduces the battery capacity available for flying from 92 Ah to an estimated 71 Ah**.

After defining the set of mission profile parameters, payloads from 1 to 50 kg are analysed. The objective is to optimise the payload to obtain the best Payload Per Minute (PPM) delivered to the target. The PPM is used to assess the optimal payload mass. Objectives such as Total Payload Delivered (TPD) in one battery life do not account for how long it takes for the payload to be delivered and thus are not desirable. In firefighting emergencies, every second can be crucial, which is why improving the PPM is beneficial. The following equations were used to calculate the total time needed to deliver all the payload over one battery cycle life. First, the time taken to perform a singular "run" of delivering the payload, t_{run}, is calculated.

$$t_{run} = t_{climb} + t_{manoeuvre} + t_{deliver} + t_{manoeuvre} + t_{descent} \tag{11.4}$$

In Equation 11.4, the different t values represent the duration of the stages of the mission in a single run. As t_{run} represents all the parts of the mission where batteries are required, the required battery capacity can be calculated and added up for each stage of the mission. From there, the number of entire runs can be derived. Additional times must also be included for when the drone is turned off and the payload tank is being refilled and the battery is being replaced, indicated by t_{refill} t_{bat}, respectively. These were integrated as follows to obtain a total mission time, t_{total}.

$$t_{total} = N_{runs} \cdot (t_{run} + t_{refill}) + t_{bat} \tag{11.5}$$

In Equation 11.5, N_{runs} is the number of runs. The refill time of the payload was assumed to be constant, regardless of the tank size as the majority of the time is allocated to performing the safety checks and protocols for the tank use. **The refill time is set to 300 s**. The battery replacement occurs once after the calculated runs are done and can be done parallel to the refilling of the tank. However, due to the additional safety checks, **the battery replacement introduces an additional 180 s**.

From these values, the PPM is obtained by dividing the total payload delivered after the number of runs by t_{total}. Furthermore, this optimisation was performed with two primary constraints: the maximum T/W of the drone must be above two and the velocity of the drone shall not exceed 8 m/s during climb. To optimise the PPM, the endurance requirement (*REQ-SYS-1*) is no longer as driving as delivering more payload per minute is overall more valuable to the stakeholders. For this reason, the constraint of endurance was not applied.

After running the model multiple times, iterating weights each time, a final **optimal payload of 18.6 kg** was found. However, a **tank of 20 L** is chosen, since this will allow for possible deviations in weight estimates with only a marginal increase in tank weight. With this tank a **PPM of 2.07 kg/min** and **total delivery of 130 kg** is reached in **7 runs**. For one battery life, the operational time of the drone was calculated to be 23.2 min. This meets the requirement (*REQ-USER-P-2*).

11.5. Wind Gust and Disturbance Analysis

It is important for control- and manoeuvre-ability to know what magnitude of wind gusts or disturbances the drone can handle whilst flying. However, the effect of wind gusts is complex due to the shape and rotor downwash of the drone. Extensive CFD analysis would be required, which is beyond the scope of this report. Hence, only estimates are made by using a simplified analysis. The analysis assumes that wind gusts will only affect the airframe-, tank- and pump-areas as shown in Figure 11.4. The aerodynamic forces are modelled as a single point force acting through the centroid of the combined areas. Calculation showed that the centroid is situated about 45 mm below the centre of gravity. This distance is so small that the moment induced by a wind gust is negligible.

The force induced by the wind gust however is not negligible. To counter this force, the thrust has to be vectored sideways against the wind as illustrated in Figure 11.5. The force is calculated with Equation 11.2 as done

previously in Section 11.2, with V now being the wind gust velocity. By balancing the forces on the horizontal axis, a minimum flight angle of twelve degrees was found. This is within the boundaries of the small angle approximation [4], hence it can be concluded that the drone will be able to handle wind gusts up to 6 Bft in hover.

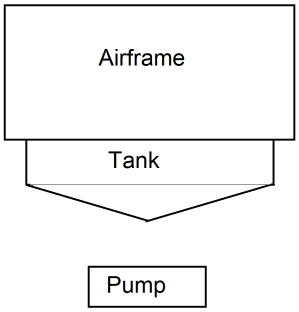

Figure 11.4: *Simplified analysis for wind gusts*

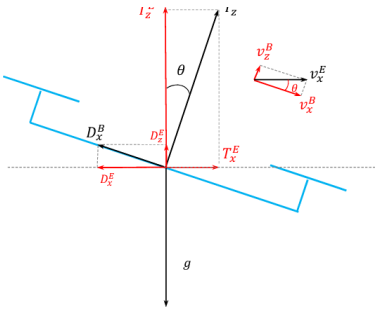

Figure 11.5: *Drone free body diagram [104]*

Apart from wind gusts there is another important disturbance that has to be analysed. The spraying of water will create a reaction force on the drone. Since the nozzle is located at an approximated distance of 1100 mm from the centre of gravity this has the potential to induce a large moment. However, when using Newton's second law, by rewriting it as shown in Equation 11.6, to calculate this force it is found that only a force of around 11 N will be created with the expected nozzle velocity. This is so small that it can be easily controlled by changing the thrust of opposite motors.

$$F = ma = \frac{\Delta p}{\Delta t} = \frac{\rho V v_e}{V/\dot{m}} = \dot{m}\rho v_e \tag{11.6}$$

11.6. Operations and Logistics Concept Description

Now the performance of the UAV has been established, the mission will be reviewed in more detail. It is important to define what a successful mission looks like and how this can be achieved. The mission will therefore be described in this section from beginning to end.

Planning a successful mission and flight for the drone involves a number of procedures. The logistics of getting to the scene and safely deploying the drone, as well as the operational procedure of the mission, must be carefully prepared once a call for help has been made to the fire brigade. The required procedure is shown in a flow diagram in Figure 11.6.

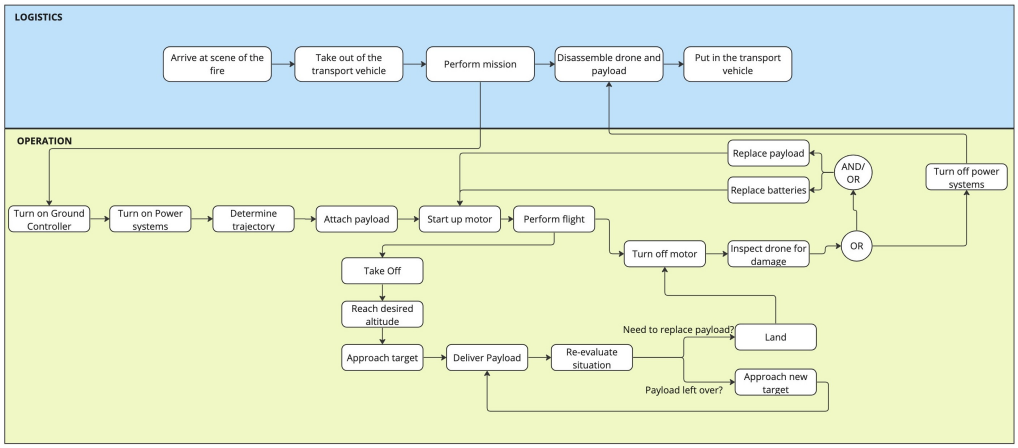

Figure 11.6: *Operation and logistics flow diagram*

The logistics are as follows: the fire brigade will arrive at the scene with the drone, which is securely stored inside a designated transport vehicle. Two people are necessary to lift the drone carefully out of the vehicle and

place it in the takeoff position. The drone will be deployed as swiftly as possible, in around two minutes, as per *REC-SYS-9*. The pilot, present at the scene, will switch on the controller and power systems of the UAV, and perform the mission.

It is important to bear in mind that the drone mission profile can alter based on the amount of water on board and the deployment scene. If all the water is delivered at once, the drone will need to land (*Descent* in Figure 11.1a), refill and, depending on the battery level, replace batteries before redeploying (*Turn Around* in Figure 11.1a). If during this stage of the mission, enough extinguisher agent is left and the situation at the current target is under control, the drone can fly to a different target (*Retarget* in Figure 11.1a). To ensure a successful operation, the situation must be regularly assessed. The drone's purpose is to help those in need more quickly as the fire brigade is ready to enter the structure or start extinguishing operations. During all times, the pilot is in charge of the drone and responsible for the drone's activity.

Inspection and Maintenance

An important and key aspect during the operation of the drone is to regularly inspect the drone for damages as a damaged drone can be life-threatening. The inspections have to be done mainly on the motors and electronics as these are the most critical parts of the drone and are susceptible to further points of failure pertaining to the high temperatures of the environment. Furthermore, the payload has to be inspected to see if the tank and pressure do not have leaks and do not create a situation of vacuum in the tank. Thus, the vacuum sensor has to be regularly checked for errors in measurements. Furthermore, the drone has to be regularly cleaned and all the components have to be regularly maintained with the insulation materials applied for protection. Doing this would ensure that the drone is always kept in good health and the components can be replaced when necessary.

11.7. Environmental Impact Analysis

To minimise the ecological footprint of the drone, the environmental impact will be examined, focusing on noise pollution, emissions and recyclability. The potential noise disturbances caused by the UAV will be assessed in Subsection 11.7.1, and then the emissions' contribution to climate change will be analysed in Subsection 11.7.2. Lastly, recycling options for sustainable disposal will be explored in Subsection 11.7.3.

11.7.1. Noise

Noise pollution caused by drones is a common annoyance of the general public. Nevertheless, no official regulations on drone noise levels exist. Guidelines have been set up by the European Union Aviation Safety Agency and a method is proposed for testing, however, these are only voluntary and recommended [3]. As the drone will solely be operating in emergency situations, its noise emission will not be analysed. Apart from it being an emergency situation, during these operations, a lot of noise will be produced by other sources, such as fire alarms and sirens, diminishing the noise effects of the drone.

11.7.2. Emissions

A huge positive of using batteries to power the drone is the lack of emissions during the firefighting mission. While there are no air emissions during the flight of the UAV, it is difficult to properly estimate how much CO_2 and other greenhouse gases are emitted during the process of manufacturing the UAV and its components. This highly depends on the materials used, how they are sourced and the energy sources used to manufacture them [86]. This is important since the environmental impact of the drone must be taken into account during the design stage.

The emission analysis will focus on the carbon fibre and aluminium structure production, and most importantly the battery production emissions. These are the two largest components within the drone. Components such as the hardware and sensors, or the motors themselves, are bought off-the-shelf and are considerably small. This means that the emissions created in their production are difficult to analyse. However, it is worth noting that several off-the-shelf components chosen are based outside of Europe. The environmental impact of importing products from China or any country far away from the Netherlands is not negligible in the long run.

Carbon Fibre

The use of carbon fibre has some environmental benefits. It is lightweight, which means the drone is highly energy efficient, as it needs less power for less weight. Furthermore, it has a long life span and does not need

to be replaced for many decades, if proper care is taken [33]. Since a firefighting drone is designed to enter harsh environments at high temperatures, carbon fibre is durable and heat-proof enough to withstand these unfavourable conditions for an extended time period. Less need to produce or replace carbon fibre means less negative environmental impact. This is because the extraction and production of carbon fibre parts is not emission-free. For every 1 tonne of carbon fibre produced, the production process emits 20 tonnes of carbon dioxide [145]. It is therefore highly important to minimise the amount of carbon fibre waste by taking proper care of the drone structure, and by not replacing many carbon fibre parts too soon.

Aluminium

Aluminium is used for the rod attachments, as it is much cheaper to create complex shapes out of aluminium rather than carbon fibre, which needs a custom mould and cannot be machined into complex shapes. The production of aluminium creates 16 tonnes of CO_2 per tonne of aluminium, mostly because of the need to perform electrolysis, a "hugely energy-intensive process" [25]. Fortunately, the use of aluminium on this drone is limited to just attachment points and small, complex parts.

Battery

The drone is powered by lithium polymer (LiPo) batteries. While there are no emissions during the flight due to the batteries, the production of lithium batteries requires lots of energy which often comes from CO_2 emitting fossil fuels [101]. The process of acquiring lithium is where most of the CO_2 is emitted into the atmosphere. Up to 15 tonnes of CO_2 can be released into the atmosphere during hard rock mining, which is the most common way to extract lithium [61]. Furthermore, the disposal of lithium batteries can pose environmental risks. If disposed of badly, they can cause fires in the landfills they end up in [102]. For this drone, the fire department must ensure the proper disposal of the batteries at their End-of-Life. Furthermore, the batteries themselves will be stored at the proper storage voltage of 3.8 V per cell [35]. This will ensure the batteries last as long as they possibly can, which will mean less lithium battery consumption in the long run, which will contribute to the reduction of the carbon footprint of this drone.

11.7.3. Recyclability

To minimise the carbon footprint of the UAV, it is critical to examine the recyclability of its components when they reach the end of their useful life and the materials used. Applying recyclable materials to the UAV reduces waste, as well as saving on production and energy expenses. Additionally, for proper End-of-Life disposal of components, disposal and recycling facilities need to be available.

The LiPo batteries of the UAV will be replaced when they become damaged or exhibit signs of depreciation. They should be taken to a recycling facility for proper disposal after being fully discharged to lower the risk of fire.

The electronics of the drone can be handed to a company that has the means and knowledge to refurbish (parts of) the components. Reusing already manufactured components reduces the need for additional mined metals (such as gold, silicon, and lithium) and plastics and thereby reduces the amount of water and air pollution [39].

The drone's T-MOTOR rotors are composed of carbon fibre epoxy and finished with a glossy treatment [157]. Additionally, the frame and the chassis are also made of carbon fibre epoxy. Due to cross-linked thermosets, epoxy-based composites are challenging to recycle [143]. When heated, these materials become rigid and cannot be remoulded. Pyrolysis is considered one of the most effective and viable processes for recycling carbon fibre epoxy since it not only recovers valuable materials but also produces fuel and chemicals [143, 115]. However, the pyrolysis process is still undergoing optimisation before commercialisation. These procedures aim to produce materials with sufficient mechanical properties and low energy consumption [115]. Additionally, mechanical recycling can be used to recover the carbon fibre from the components. The carbon fibre-reinforced plastic is reduced to microscopically-sized pieces and then separated on their content. The recycled carbon fibre pieces can be re-used to create new composites [58].

The remaining parts of the drone, such as the motor and ESC, can be handed in at a specialised facility, such as a disposal facility for electrical and electronic waste.

12

Model Verification and Validation

The UAV consists of many subsystems. A lot of these were designed with the help of models in Python or Excel. In Section 12.1, the verification methods will be explained. In Section 12.2, the validation methods will be explained. These verification and validation methods will be applied to the models used for the UAV. The used models will be explained in Section 12.3. Finally, Section 12.4 will describe the verification of the requirements.

12.1. Verification Methods

Models can contain coding mistakes that might cause errors in the output. Therefore, the code has to be verified, to mitigate the chances of the code output being wrong. The method to test the numerous codes made during the design phase are as follows: First, unit tests will be performed. These are tests that test small individual parts of the model. In addition, two system tests will also be performed, where the sensitivity of the code is analysed.

UT-1: Syntax Errors

Syntax errors are defined as human-made mistakes for missing or incorrect usage of programming syntax. These include small errors like missing commas or colons. Syntax errors prevent the code from running completely, which incites the need for fixing these errors. Luckily, the compilers can specify the type and location of the error. To ensure that all the syntax errors are removed, every section of the code will be run to ensure that the program gives an output. For Excel files specifically, syntax errors can easily be checked by checking every cell. No syntax errors may be present if the code is to be considered verified. The UT-1 test thus either passes or fails [171].

UT-2: Input/Output Format

With this unit test, the size and shapes of the data will be verified. This will ensure that the function converts inputs to outputs in the correct data format. However, this test is limited by the fact that a correct data format does not imply that the data itself is correct. No accuracy can be provided, as the code either passes or fails.

UT-3: Unit Format

This test will verify whether the calculated parameters are converted to SI units. For this test, all the input parameters need to be checked individually for their units. If conversions to SI units were done, these also need to be checked. The task to check this has been simplified by defining the input parameters and the conversions at the start of the functions they are used for. No accuracy can be provided, as the code either passes or fails.

UT-4: Equation Implementation

With this unit test the equations used in the models will be visually inspected, re-calculated by hand or compared to reference solutions to verify that the equations have been implemented correctly in the models. This test ensures that no human errors are present from mistyping equations. What limits this test is that having correctly implemented equations does not imply that the data and equations used are correct. Small discrepancies between model and hand calculation outputs are allowed as these can be attributed to rounding errors.

UT-5: Extreme Value

With this test, the inputs are changed into atypical and extreme values. With these new atypical inputs, an increased amount of errors is expected. This allows errors to be detected that may have been unnoticed for normal inputs. The code is expected to either pass or fail. The run time of the code can possibly increase by doing this test.

SYS-1: Sensitivity

The goal of the sensitivity system test is to verify whether or not the output changes accordingly to different inputs. This can be done by changing one input variable and looking at the change in output. For example, when increasing the initial velocity in the payload range model the range should also increase. If strange relations between input and output variables are found this indicates that parts of the model may not be integrated correctly.

SYS-2: Analytical Comparison

Analytical comparison can also be used to verify the model. UT-4 also uses hand calculations to verify parts of the model, however, this does not verify if the different parts of the code have been integrated correctly. Therefore, an analytical solution has to be compared to the model solution. As with UT-4, small errors between the two solutions are allowed.

12.2. Validation Methods

Validation is an important process in order to see if the models actually simulate reality. The UAV was constructed using multiple models. These models are summarised in Section 12.3. Validation methods will be different for each model since they all serve different purposes. However, due to the specific simulations of some models, validation for this report is not always possible. For the models where this is the case, optional validation methods for in the future will be discussed.

12.3. Models

During the design phase, multiple models have been constructed to help with making design decisions. These models have to be verified and validated according to the methods discussed in Section 12.1 and Section 12.2. In this section, all the different models that were used and the verification and validation methods for these models are described.

12.3.1. Payload Range Model

To calculate the range of the water stream a simple Python model was made in Subsection 5.3.1. This model computes the location, velocity and acceleration of a particle at different intervals. An initial exit velocity can be set which will result in different ranges. Aerodynamic forces are neglected for simplicity as discussed in Subsection 5.3.3.

Verification

Unit tests **UT-1, UT-2, UT-3, UT-4** and **UT-5** were all done and all **Passed**. By doing **SYS-1**, the gravity constant was changed to an extremely high value, which gave smaller ranges. By changing it to an extremely low value, the ranges increased as expected. The initial height was also changed and it did not have an effect on the range, which was expected. When increasing the exit velocity, the range increases, which is as expected. No other errors were found, thus **SYS-1** also **Passed**. **SYS-2** also **Passed**.

Validation

This range model does not take into account any sort of drag or forming of droplets of the water jet. The only possible way in which the code can be validated is to have data for similar payload systems. Payload systems designed for this UAV have not been designed yet or data is not widely available. For validating this model it is advised to test the payload range in specific environments in the future. Different environments are needed to not only find the actual range but also the influence of wind gusts on this range.

12.3.2. Pressure Pump Model

To find the required pump performance the calculations described in Subsection 5.3.2 were put into an Excel model. The system parameters, illustrated in Figure 5.3, like tube length, flow rate and diameters are used as inputs. Afterwards, the Reynolds numbers will be calculated to check if the flow is turbulent or laminar. Following this, the changes in pressures and velocities are calculated. Friction and minor pressure loss coefficients need to be estimated. Coefficients for the tube system can be found fairly easily from experimental data [77], however, nozzle coefficients are difficult to estimate. Hence, nozzle data [181] was used as input into the model. Coefficients were then varied until the model output closely matched the data. Afterwards, the coefficients corresponding to the diameters close to the expected diameter were used as input for the model. This resulted in an exit velocity, nozzle diameter and pressure difference needed.

Verification

Unit tests **UT-1, UT-3, UT-4** and **UT-5** were all done and all **Passed**. Unit test **UT-2** can not be done for this model as this model is in Excel. **SYS-1** indicated correct relations between the inputs and outputs, such as an increase in nozzle velocity when the pump pressure is increased. Furthermore, **SYS-2** showed only negligible errors between the analytical and model solution. Thus both tests **Passed**.

Validation

Validation for the pressure pump model is currently not possible. This is due to the fact that experimental data has already been used as input for the coefficients in this model. Hence, when validating separate parts of the system the model obviously will produce correct results. Validating the complete system would be interesting, however, this can only be done after the construction of a prototype since experimental data for this exact system does not exist yet. When experimental data can be obtained the effect of different nozzles, flow rates and operating pressures should be researched. This data can be used to validate the model and check if more optimal designs are possible.

12.3.3. Climb Performance Model

A climb performance model was made to estimate the maximum climb rate of the UAV. The model uses estimates for the drag coefficient and gives the climb rates for multiple different payload weights. This is done by computing the acceleration, velocity and distance at short time steps. The weight, thrust and drag coefficients are used as input and a maximum climb rate is given as output.

Verification

Unit tests **UT-1 UT-3, UT-4** and **UT-5** were all done and all **Passed**. **SYS-1** was performed by changing the thrust input, since all other inputs vary already. However, the output behaviour was checked to behave as expected for all inputs. Although the time steps method cannot be verified with **SYS-2**, an analytical solution for the maximum climb rate can be found by equating the thrust to the drag and solving for the velocity. Hence, **SYS-2** was also **Passed**.

Validation

To validate the climb rate model, a real drone was put into `flyeval.com`. The DJI Matrice 210 was chosen for this purpose since Flyeval already has data stored for this drone. With thrust and C_D data from Flyeval the difference between the real climb performance of 5 m/s [167] and the model performance can be calculated. As can be seen in Figure 12.1 the model output is 0.4 m/s higher than the actual climb rate. This can be attributed to a decline in thrust performance at higher velocities or errors in the C_D estimation. Therefore the climb rate model can be used for initial performance estimates. However, testing should be done to find the actual performance since the real drag and influence of velocity of thrust for the design is unknown.

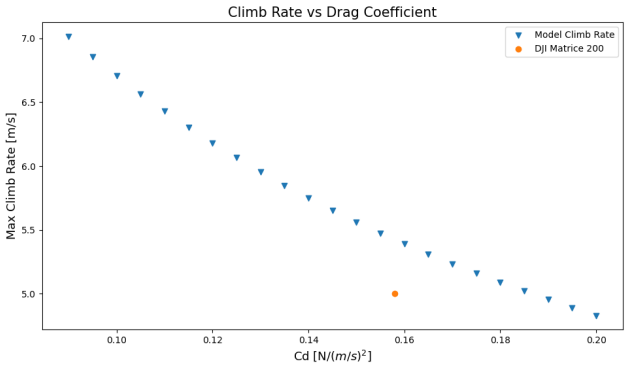

Figure 12.1: *Model climb rate and actual climb rate*

12.3.4. Payload Optimisation Model

In Section 11.4 an optimum payload capacity was analysed in order to deliver as much water as possible within a certain time frame. To do this a model was constructed which simulated a mission at different payload capacities. It is of utmost importance that no mistakes and errors are in the code, since the output drives the tank design of the UAV.

Verification

Unit tests **UT-1, UT-2, UT-3, UT-4** and **UT-5** were all done and **Passed**. **SYS-1** was difficult due to the complicated relations between the inputs and output of the model. However, systematic analysis of each input and the effect on all outputs enabled the test to be **Passed**. **SYS-2** was not possible since an analytical solution to this problem does not exist. Especially calculating the power used during climb and descent would require different methods in order to find an analytical solution. Any errors could then be the result of coding and rounding errors or due to these additional assumptions, making the test useless.

Validation

Validation of this model can only be done after a prototype has been constructed. With this prototype, the same mission simulated by the model can be performed. Power usage data or the maximum amount of runs during tests can then be used to validate if the output of the model for the corresponding payload capacity is similar.

12.3.5. Controllability Models

For the analyse of controllability, multiple models were created and used in Chapter 9. Controllability consisted of two parts, “Classic Controllability” and ACAI. Each method required different models to determine the controllability. Classic Controllability required the matrices defined in the state space model to construct the controllability matrix and then check its rank. ACAI utilised open source code made available from the creators of the ACAI parameter [85], which was then adapted to the specific use case.

Verification

Classic Controllability: As this model consisted primarily of matrix calculations the following unit tests were performed and **Passed**: **UT-1**, **UT-4**, **UT-5**. For **UT-4**, simpler examples [139] were run through the code to verify whether it was functioning as intended. Seeing as all such tests were passed. The classic controllability checks are considered verified with high confidence. Then to ensure that the code also makes sense, **SYS-1** was performed. This consisted of setting certain values in the matrices to zero to check whether the model reacts as expected. This test was also **Passed.**

ACAI: For this model, the core of the code was obtained from the Github of the creators of the method [130]. Unit tests: **UT-1**, **UT-2**, **UT-3** and **UT-4** were all performed and **Passed**. The two primary functions that were used were a function that creates the control effectiveness matrix and the ACAI calculator. For the control effectiveness matrices generated, **UT-4** was performed by hand deriving the matrices of the three different configurations and checking them accordingly. For the ACAI calculator function, this was not possible and thus, **SYS-2** was used to verify this. Calculation examples [129] and tutorials [136] are provided by the creators

and made available, thus after adapting the code to the needed use case, the examples were calculated once again to ensure that the code still ran correctly. This test was also **Passed**.

Validation

To perform validation for this model, real-life testing data would be required. To validate the ACAI calculator, flight data would be required from similar hexacopters with different configurations. The drones would have to be tested multiple times for controllability with different single rotors turned off each time. However, due to the short time frame, it was not possible to obtain flight data.

12.3.6. Observability Model

The observability model was structured and performed calculations similar to those for "Classic Controllability" with slight adaptations. Observability also required the matrices defined in the state space model to construct the observability matrix and then to check its rank.

Verification

For the observability calculations, **UT-1**, **UT-2** and **UT-4** were done and **Passed**. For the observability, the most prominent source of error is the output matrix, C, and the calculation of the observability matrix, $\mathcal{O}$. For **UT-4**, reference solutions [140] were used to verify that the implemented code also produces known solutions with specified inputs.

Validation

For observability, validation requires the drone to be built with all the sensors. To ensure the drone is fully observable, all states of the drone must be able to be measured/calculated with the equipped sensors. The results can then be compared to the results obtained in the model.

12.3.7. Structures Model

An analysis of the whole structure of the UAV has been made in an Excel file. In Section 8.4, all the steps are explained in detail. For the rods, the thrust force from the motor is the largest force working on it. The inputs for the rods are the material, dimensions, weight, density and E-modulus. The program outputs the shear force, bending stress and moment of inertia of the rod. For the panels, a simplified model has been made to give an estimate of what forces will work on the panels. A shear and shear tear-out analysis was then carried out.

Verification

Unit tests **UT-1, UT-3, UT-4** and **UT-5** were all done and all **Passed**. Unit test **UT-2** can not be done for this model as this model is in Excel. **SYS-1** has been done for different calculations. For calculating the force on a rod from the motor thrust, the moment force was increased. The force over the length of the beam increased everywhere, as expected. With decreasing the moment, the force decreased everywhere, which was expected. For the panel calculations, a simplified model was made, which has forces at the clamps of the panels. When increasing the thrust force all of the forces at the clamps increase, and when decreasing the force all the forces at the clamps decrease, as expected. **SYS-1** has thus **Passed**. For **SYS-2**, all the calculations in the Excel file were verified by hand. **SYS-2** also **Passed**.

Validation

The free body diagram that is used for the structure calculations can be validated by literature, where similar examples can be found [32]. For a more accurate analysis, it is advised to do FEM analysis. The best analysis that can be done, however, is to build the UAV and measure the components against which stresses they are resistant.

12.4. Product Verification

To ensure the design process was correctly executed, confirmation of the product meeting the requirements is required. This is the process of product verification. The following four methods are used for conducting product verification:

- Inspection
- Analysis

- Demonstration
- Test

Table 12.1 indicates which verification method is applicable for each requirement. A short description of the requirement is given, the full requirements can be found in Chapter 3. Further details of the methods are provided in the next subsections.

Table 12.1: *Verification methods for the requirements*

Inspection		
REQ-USER-P-3: *Fit inside fire brigade vehicle*	REQ-USER-P-4: *Have thermal camera*	REQ-USER-P-5: *Have visual light camera*
REQ-USER-S-2: *Have visual warning system*	REQ-USER-S-3: *Safely land in case of loss of signal*	REQ-USER-C-2: *Have modular payload*
REQ-SYS-POW-1: *Power system able to withstand temperatures up to 55°C for 120 seconds*	REQ-SYS-ELEC-1: *have on-board flight controller*	REQ-SUS-3: *Use biodegradable extinguishing agents*
REQ-SYS-PAY-5: *Have sensors for measuring altitude*		
Analysis		
REQ-USER-C-1: *Shall not exceed €25,000*	REQ-USER-C-3: *Consist of at least 20% recyclable components*	REQ-STAKE-2: *Comply with EU regulations*
REQ-STAKE-3: *Minimum operating costs*	REQ-SYS-8: *Minimum MTBF of 100 operating hours*	REQ-SYS-PROP-1: *Able to achieve a T/W of 2*
REQ-SYS-STR-1: *Structure support payload of at least 10 kg*	REQ-SYS-STR-3: *Structure able to support other subsystems*	REQ-SUS-1: *Use clean energy source*
REQ-SUS-2: *Use non-toxic extinguishing agents*	REQ-SUS-4: *Strategy to improve sustainability*	
Demonstration		
REQ-USER-P-1: *Carry minimum payload of 10 kg*	REQ-USER-P-2: *Have average operational time of 20 min*	REQ-STAKE-8: *Easily deployable with minimum personnel*
REQ-SYS-1: *Minimum operational time of 20 min at average T/W 1.4*	REQ-SYS-2: *Vertical hovering accuracy of ±0.1 m*	REQ-SYS-3: *Horizontal hovering accuracy of ±0.1 m*
REQ-SYS-4: *Flight altitude of 250 m*	REQ-SYS-5: *Climb rate of 7 m/s*	REQ-SYS-6: *Option to be controlled remotely*
REQ-SYS-9: *Maximum deployment time of 120 seconds*	REQ-SYS-10: *Maximum T/W of at least 2*	REQ-SYS-11: *Yaw at a rate of 90 deg/s*
REQ-SYS-12: *Turn around time (TAT) of at most 300 seconds*	REQ-SYS-13: *Deliver payload from horizontal distance of at least 4 m*	REQ-SYS-15: *Not exceed an empty mass of 50 kg*
REQ-SYS-PAY-1: *Thermal camera sensitivity of at least 1°C*	REQ-SYS-PAY-2: *Light camera minimum frame rate of 30 FPS*	REQ-SYS-PAY-3: *Cameras have active stabilisation*
REQ-SYS-PROP-2: *Propulsion system compatible with power system*	REQ-SYS-ELEC-2: *Operable from ground control stations*	REQ-SYS-ELEC-4: *Communication range of at least 300 m*

Continued on next page

Table 12.1 – continued from previous page

REQ-SYS-ELEC-5: *Electronics integrate all the sensors*	REQ-SYS-STR-2: *Structure able to withstand ultimate load factor of 3*	
Testing		
REQ-USER-S-1: *Controllable up to minimum wind speed of 6 Bft*	REQ-SYS-STR-4: *Structure allow for disassembly*	REQ-STAKE-1: *Perform mission without causing additional damage*
REQ-STAKE-4: *Easily visible in unclear conditions*	REQ-STAKE-5: *Operable in unfavourable weather conditions*	REQ-STAKE-6: *Not cause damage to the environment*
REQ-STAKE-7: *Recoverable upon failure of one of sub-systems*	REQ-STAKE-9: *Monitorable at any point during mission*	REQ-SYS-7: *Operate in 55°C for at least 120 seconds*
REQ-SYS-14: *Payload shall be water-resistant*	REQ-SYS-ELEC-3: *Have recovery system in case of loss of connection*	REQ-SYS-PAY-4: *Cameras operate in 55°C for 120 seconds*
REQ-SYS-POW-2: *Power system replacable within 120 seconds*		

Inspection

During verification by inspection, the product is not destructed or damaged. It is done by using the human senses, such as sight, hearing and touching. The requirements containing information about the dimension of the system or subsystems can easily be done by measuring. The requirements for the presence of payloads and specific layers can be verified by inspecting if they are indeed present.

Analysis

The analysis method is carried out using existing methods and calculations. Analysis is used if the requirement concerns costs, if it can only be verified by certain models or if testing is not feasible due to equipment, time or budget. Cost requirements are verified by performing calculations about the costs of the different subsystems and payloads. Other requirements, including efficiency for example, are verified by using existing equations which are already verified on their own. The ones that are situational requirements should be analysed by taking real-life situations and experiences in mind.

Demonstration

During the demonstration, the system or subsystem is operated to verify the proper working. Requirements concerning the working properties of the cameras can be verified by operating them and checking if they match the required performance.

Test

Testing is used to verify if the system or subsystems work as intended under specific conditions. Unlike demonstration, the testing method is focused on gathering data about the product to verify its performance and to further analyse the model.

13 Manufacturing, Assembly, and Integration plan

Since the UAV consists of multiple individual parts, a proper manufacturing, assembly and integration plan is necessary to construct the drone and to ensure a working product as desired. In order to get an overview of what is possible in terms of manufacturing methods and their feasibility, a tour was done at the Dienst Elektronische en Mechanische Ontwikkeling (DEMO) facility on the TU campus before setting up the plan. Here, an extensive tour was given and the machines available were shown. Knowing this, a clear and correct manufacturing plan can be devised.
First, Section 13.1 will discuss the manufacturing of several individual parts of the drone. After manufacturing, it is necessary to assemble all the parts into a whole. This will be discussed in Section 13.2. Lastly, Section 13.3 will give an overview of the integration of all assemblies.

Figure 13.1 shows all production activities required in sequential order, presented in a flow diagram. Each phase is discussed in more detail in the following sections. LiDAR 1 and 2 in the integration phase refer to the altitude LiDAR and the front-facing LiDAR, respectively.

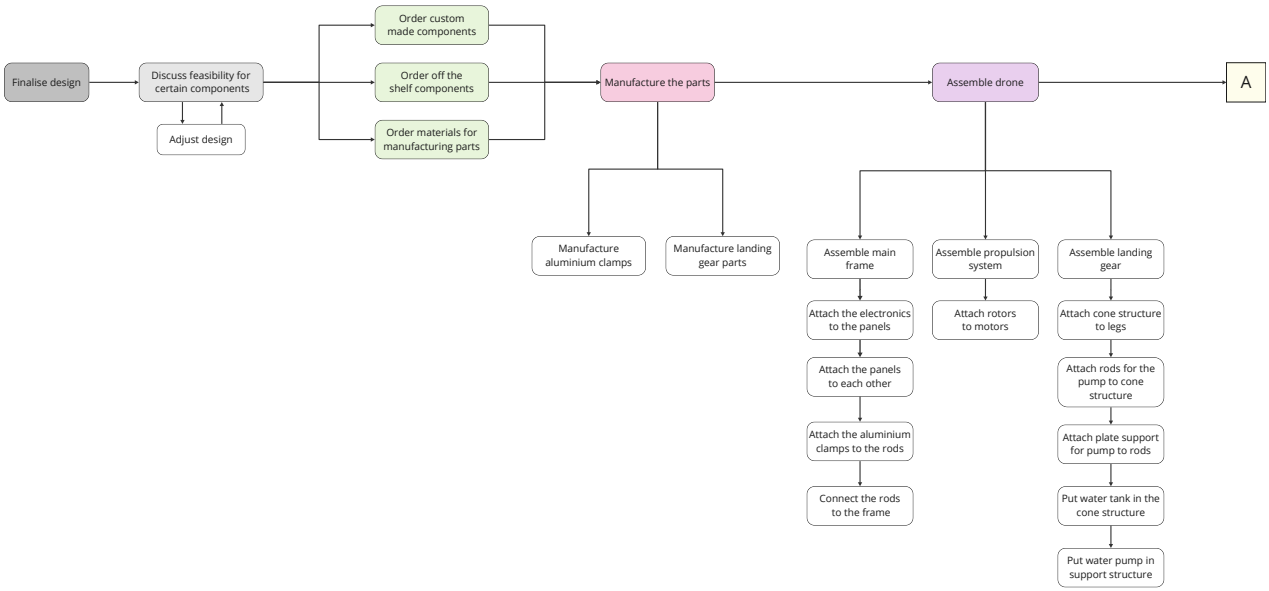

Figure 13.1: *Production flow diagram*

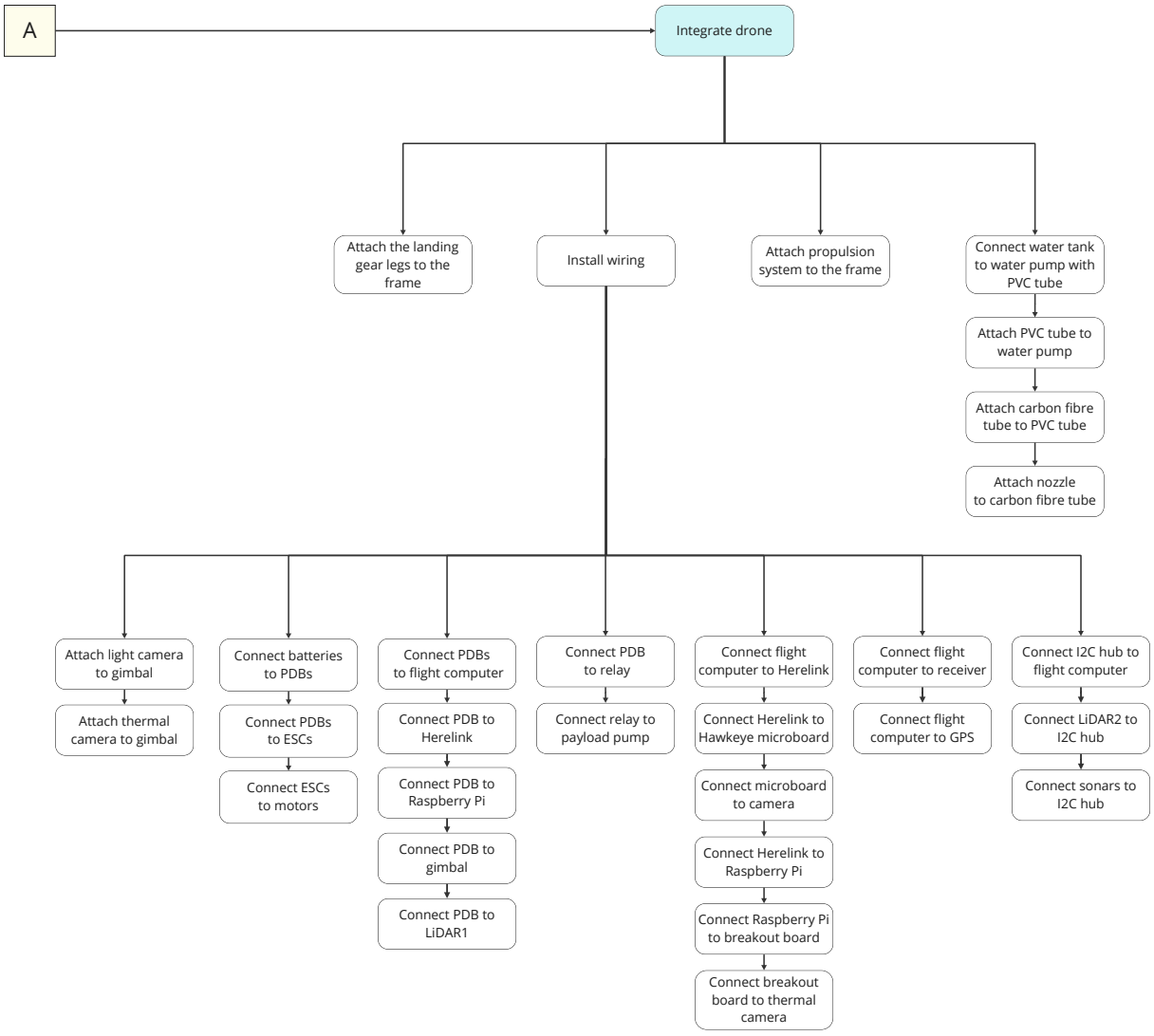

Figure 13.2: *Production flow diagram (contd.)*

13.1. Manufacturing

In this section, the manufacturing process of several parts of the drone will be discussed. The primary parts of the drone will be described, and after examining the component's structural and material characteristics, it will be addressed how it will be made. For a detailed look at all the components, CAD images of can be found in Section 10.3.

13.1.1. Main Body

As described in Chapter 8, the main body of the drone consists of three sandwich layers shaped as hexagons. The rods are connected to the body between the two upper layers, using specific attachment parts. The attachments are made from aluminium and are glued to the rods, so no or little clamping force is exerted on the rods. To provide a better understanding, Figure 13.3a shows one of the attachments. The upper and middle carbon fibre panels are attached on the upper and lower sides of the attachment. The third layer is situated underneath and is connected by aluminium spacers to the middle layer.

The rotors are attached to the rods with aluminium attachments, shown in Figure 13.3b.

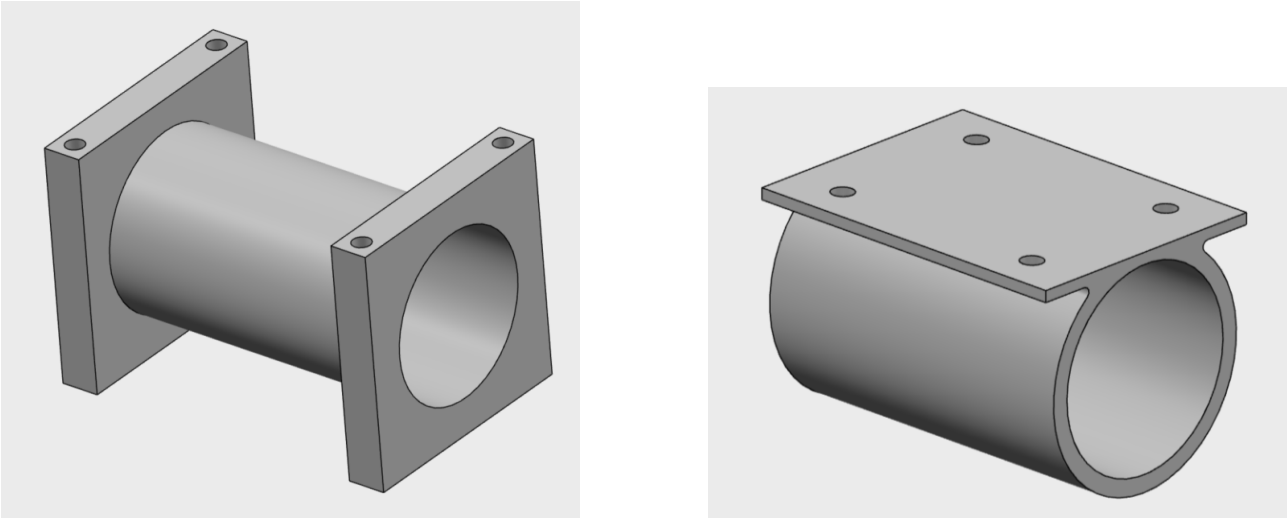

(a) *Rod attachment* **(b)** *Motor attachment*

Figure 13.3: *Rod and motor attachments*

Panels and Rods

The panels and rods are made of carbon fibre and can be ordered from CarbonWebshop [34]. The CarbonWebshop offers a service where the panels and rods can be cut and delivered in the desired shape and length. The second option is to cut them in-house. To save time, the cutting will be done by the CarbonWebshop as they are specialised, ensuring the cutting of the panels and rods is of high quality.

In addition, holes need to be made in the panels for the aluminium spacers. This is done by drilling as this is the fastest and easiest way to create clean holes. However, the process has to be carefully handled, to ensure no delamination occurs at the edges of the holes.

Aluminium Clamps

The aluminium clamps for both the rod and motor attachments need to be custom-made to fit the exact size of the rods. To manufacture the clamps, multiple techniques can be used. In this case, casting is used. A decision was made between sand casting and investment casting. Sand casting was chosen due to the low tooling cost. Additionally, the limitations of sand casting will not be an issue for the clamp, as its thickness is approximately 8 mm and a rough surface will not be a problem for the design [114, 119].

Aluminium Spacers

For the aluminium spacers, 16 spacers with a length of 100 mm are needed and four spacers with a length of 50 mm. The spacers do not have to be custom-made as they can be bought off the shelf at Farnell [70].

13.1.2. Landing Gear

The landing gear consists of four legs that are attached to the lower layer of the main frame as shown in Figure 13.4a. For each of the four legs, an aluminium block is screwed underneath the lower layer, to which the leg will then be attached. The four blocks can be cut from one long block of aluminium. The leg is straight for one part and then has a slight bend. To achieve this, it will consist of two individual parts which are connected to each other at a specific angle using a modular connector as shown in Figure 13.4b [48]. The rods for the legs will also be cut to size by the CarbonWebshop.

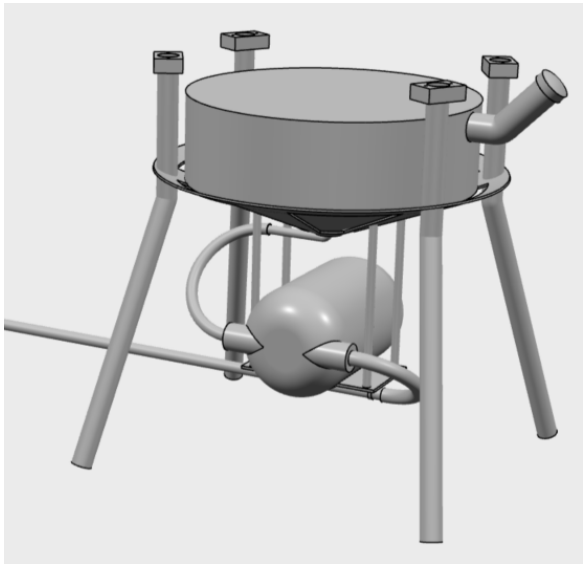

(a) *Landing gear subsystem*

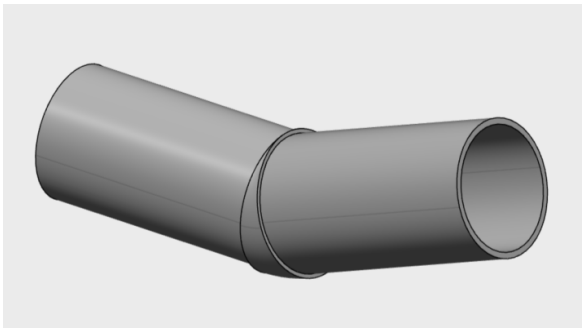

(b) *Modular connector for the landing gear legs*

Figure 13.4: *Landing gear subsystem and modular connector for the legs*

The payload is connected to the landing gear. The water tank lies in an aluminium cone-like structure that can be slid through and attached to the four legs. At the tank, there is a small tube that allows for filling the tank with water. This cone structure has to be custom-made. As it is a specific shape, casting will be used to produce the structure. Investment casting can be used, as it allows for making complex geometries, it produces parts with excellent surface finish and it is cost-efficient [163].

Furthermore, the water pump is supported by an aluminium plate that is carried by four carbon fibre rods, that are connected to the bottom of the cone structure. The plate and rods are bought off the shelf. The plate has to be punched after purchase to fit the size of the pump.

Lastly, a long carbon fibre tube is connected to a flexible PVC tube, that is connected to the pump for the shooting of the water. This will be bought and cut to size by the CarbonWebshop.

13.2. Assembly

After all the parts are manufactured, it is time for the assembly. During this stage, the unfinished (sub-)systems that were created during manufacturing will be put together to form a finished (sub-)assembly.

13.2.1. Main Body

Before the three layers are attached to each other, the electrical components are attached to the panels. Then, the three layers can be connected using the aluminium spacers. As mentioned in Subsection 8.3.1, sixteen spacers are placed between the lower and middle panels. Only four spacers are needed between the middle and upper panels.

The next step is to connect the rods to the two upper layers. The aluminium rod clamps are glued onto the rods in the right position. At the other end of the rods, the aluminium rotors attachments are glued for the mounting of the rotors. The glueing can be done with epoxy glue. There are multiple types, one of them is the 3M SCOTCH-WELD constructional glue type 1. Type 1 glue has a high thermal performance, and high strength properties at 80 ºC and is the hardest type [68]. Another option is cyanoacrylate, also known as super glue. However, the suitability depends on the type of plastic. The glues should be tested first on sample parts to test the compatibility and bond strength [121]. Now, the rods can be connected to the two layers. This is done by screwing the aluminium clamps to the layers.

To attach the rotors, the propellers can be attached through the installation method provided by T-MOTOR [157]. Threadlocker can be applied to increase reliability and prevent corrosion. Next, at the other end of the rods, the motors with the rotors are attached. This is again done by glueing with epoxy glue.

13.2.2. Landing Gear

After the legs are assembled, the cone structure for the water tank support can be slid through the four legs. To attach them, the cone is glued to the legs with epoxy. Next, the structure for carrying the water pump can be assembled. The four carbon fibre rods are used to connect the plate creating a basket-like structure. The rods are glued to the bottom of the cone structure, and to the plate.

13.3. Integration

The final step is integration, connecting all subsystems to each other and wiring the electronic components to get to a complete and operational drone. In order to ensure proper power distribution and signal transmission, accuracy is essential during the wiring procedure. To confirm the correct working, testing and quality control procedures will take place. The end result is a fully functioning drone, ready for flight.

13.3.1. Electronics

During integration, all loose assemblies and components are put together to create a single, complete UAV. Integration is essential as correct connections and wiring between all components are critical to mission success.

The flight computer must be connected to the ESC through the correct signal pins, and the ESC must connect to the motors. Connection and wiring between all of the electrical components are described in detail in Chapter 7, and more specifically in the electrical block diagram shown in Section 7.4. One of the most critical connections is the battery. Improper connection can lead to short-circuiting and an explosion of the LiPo batteries. The XT-90 batteries must be carefully connected and the batteries monitored during their connection time to ensure no accidents occur.

13.3.2. Payload

The next step is to attach the payload to the drone. The payload consists of the water tank, water pump, nozzle and tubes.

The water tank is connected to the water pump with a tube. The tank is then connected to another tube, which is in turn connected to a carbon fibre rod. Lastly, the nozzle is attached to the end of the carbon fibre rod.

The water tank is placed in the cone structure in the landing gear structure, and the water pump is placed on the plate underneath. The legs are glued onto the aluminium blocks, that are screwed onto the lower panel of the main frame. The glueing can be done with epoxy glue.

14
Financial Analysis

In this chapter, a financial analysis of the drone is done in order to gain a better understanding of its financial performance once produced. By investigating multiple financial aspects, it is determined if the production of the drone is a viable and profitable investment. In Section 14.1 an overview of the cost of all components will be given as well as an estimation of the manufacturing, development and operational costs. In addition, in Section 14.2 the market price will be determined, the market volume, value and share are discussed and the return on investment will be calculated.

14.1. Cost Budget

The cost of the drone consists of the manufacturing cost of the drone, i.e. the components the drone is made out of as well as the costs of building the drone, the development costs and the operational costs. Figure 14.1 presents the cost breakdown structure of the drone, which shows an overview of the different costs. In the following sections, these costs will be further broken down.

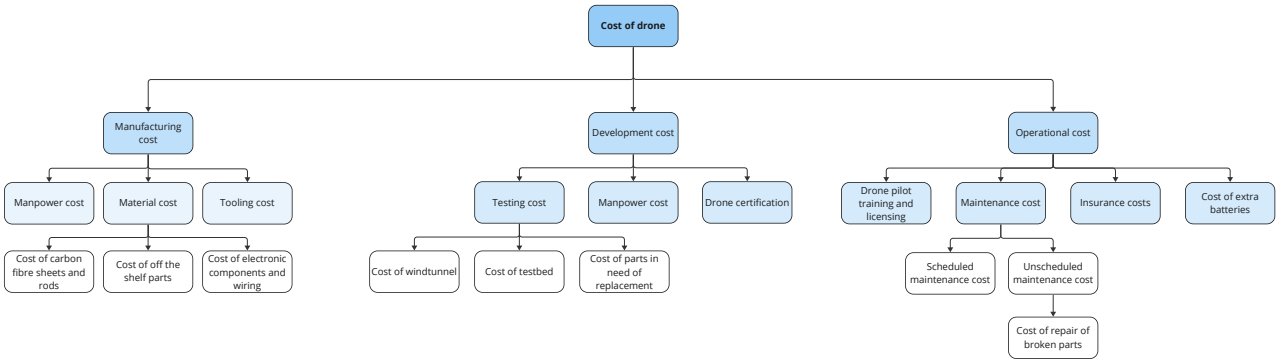

Figure 14.1: *Cost breakdown structure*

A summary of all the costs is provided in the table below. Further explanations will be elaborated on in the upcoming subsections.

Table 14.1: *Summary of all the costs*

Cost of Manufacturing	€ 25,000
Cost of components	€ 17,577
Manpower cost	€ 5,400
Manufacturing costs	€ 1,800
Cost of Development	€ 82,400
Wind tunnel testing cost	€ 18,400
Manpower cost	€ 64,000
Cost of Operation	€ 9,790
Cost of training	€ 4,000
Cost of battery replacement	€ 5,790

14.1.1. Cost of Manufacturing

The cost of manufacturing consists of manpower cost, material costs and tooling costs. In Table 14.2, an overview of all materials and components and their prices are given. The total cost of the components of the drone is € 17,577. When manufacturing, the actual total price might differ a bit as some prices were converted from USD, these prices are as of June 21st 2023.

Table 14.2: *Costs of all components of the drone*

Component	Type	No.	Total Price [€]
Propulsion			
Propeller	G32*11 Prop-2PCS/PAIR	6	1965.12
Motor	MN1010 KV90	6	1866.29
ESC	T-MOTOR Alpha 80A 12S	6	713.79
Power			
Battery	LiPo 46000 12S2P 44.4v Battery Pack	2	5710.33
PDB	Sky-Drones SmartAP PDB 400A	2	164.72
Communication & Control			
Receiver	TBS Crossfire Nano RX	1	22.88
Transmitter	FrSky Taranis X9D	1	228.78
Data link	Herelink Air Unit 1.1	1	457.56
Flight computer	CubePilot Cuve Orange	1	320.29
Electronics & Sensors			
Altitude LiDAR	Atollo Wasp 200	1	485.01
Frontal LiDAR	Lightware SF20C	1	255.32
Sonar	MB7040 I2CXL-MaxSonar-WR	2	210.37
GPS	HEX Here3 CAN GNSS GPS Module w/ iStand	1	161.05
Visual camera	Hawkeye Firefly 4K	1	98.00
Thermal camera	FLIR Lepton 3.5	1	150.08
Gimbal	Copterlab 2 Axis Hawkeye Firefly 4K Nano Gimbal	1	175.54
Raspberry Pi	Raspberry Pi (Model 4B)	1	159.99
Lights	VIFLY strobe light	1	49.41
Relay	Grove SPDT Relais (30A)	1	13.00
Airframe			
Sandwich panel	CarbonWebshop Carbon Sandwich Panel 600x600x5mm	3	617.10
Rods	CarbonWebshop High Performance Tube 35x33x2000mm	3	357.57
Aluminium blocks	Aluminiumopmaat.nl platstaf 40x20x240 mm	1	9.64
Landing gear legs	CarbonWebshop High Precision Tube 28x26x2000mm	1	89.43
Landing gear legs	CarbonWebshop High Precision Tube 28x26x1000mm	1	44.71
Pump support rods	CarbonWebshop High Performance Tube 12x10x2000mm	1	61.71
Pump support plate	Plaatopmaat.nl aluminium plate 220x120x4 mm	1	3.20
Payload			
Water tank	Rotterdam Plastics Custom Made Tank	1	2500.00
Pressure pump	VEVOR Washdown Dekpompset Waterpomp 12V	1	84.99
Tube	Amazon Clear Vinyl Tubing Flexible PVC Tubing 1/2 Inch ID, 10-Feet Length	1	11.88
Tube connector	Praxis Slangpilaar 1|2" x 19mm	1	5.99
Nozzle	Vyr nozzle voor sproeier, type 60, 70 en 33 AF, 4,8 mm	1	4.28
Carbon fibre tube	High Performance Tube 14x12x2000mm	1	81.07
Wires, screws, bolts etc.	-	-	500.00
Total			**17,577.63**

After all the parts are ordered, the drone needs to be assembled as described in Section 13.2. In the Netherlands, an assembly worker earns around € 15 an hour [133]. Three workers can build one drone in 15 working days. The manpower cost for one drone is therefore **€ 5,400**.

Some parts still need to be manufactured after the material is purchased. These parts are listed in Section 13.1 and will be manufactured by DEMO at TU Delft. At DEMO they charge around € 40 - 50 per hour. This includes the use of machines, equipment and tools. The use of materials costs extra, this holds for the aluminium parts. As aluminium is relatively inexpensive and it is hard to estimate the amount used, these costs are not taken into account for the estimation. It is estimated that all parts can be manufactured in five working days as only a small number of parts need to be made. This can be done by one DEMO worker. Taking an average of € 45 an hour, the manufacturing costs are therefore **€ 1,800**.

This means that the total cost of manufacturing one drone is around **€ 25,000**.

14.1.2. Cost of Development

During the development of the prototype of the drone, different costs are made. As seen from Figure 14.1, the development costs are made up of testing, manpower and certification costs. The testing costs include wind tunnel costs, testbed costs and the cost of parts that need to be replaced during testing. The latter is hard to predict, so for the analysis, these will not be taken into account. The same hold for the test bed cost, the test bed is a platform or piece of equipment used for testing. As a testbed is a broad term and can be made as expensive or inexpensive as desired, these costs are hard to estimate. Furthermore, relatively these costs will be negligible compared to the larger costs.

A wind tunnel will be used to investigate the aerodynamic properties of the drone and to improve the design. Renting a wind tunnel for an hour costs approximately € 2300 [42]. The wind tunnel will be used for a day, 8 hours. The wind tunnel testing will have a total cost of approximately **€ 18,400**.

In the Netherlands, a UAV test engineer earns on average € 40 an hour [62]. It is estimated that building the prototype will take around 8 weeks. Five full-time engineers will work on the prototype. This means that manpower accounts for **€ 64,000**.

Lastly, the certification costs need to be taken into account. In the Netherlands, drones used for government operations need to have a Remotely Piloted Aircraft System (RPAS) license. Furthermore, the drone must also comply with European regulations. The drone also requires a certificate of airworthiness, known as the S-Bvl, which needs approval from the Human Environment and Transport Inspectorate (ILT). The S-Bvl certificate needs to be renewed annually to ensure that the drone still meets the necessary safety requirements for flying [54, 55]. This should be further explored after the prototype of the drone is finished.

14.1.3. Cost of Operation

While the drone is being used by the fire brigade, some costs are also made. The operational costs consist of the pilot training, maintenance costs, insurance costs and the cost of extra batteries.

The drone must be operated by a certified pilot, this comes with costs for the training and the certification. However, as the drone does not fall into any existing training or certification category these costs cannot be estimated accurately. Training for the EASA specific category, which is for UAVs flying outside of standard scenarios, is approximately € 4,000 [59]. This is the closest training similar to what will probably be needed for the drone.

The maintenance costs are mainly the costs of components that are in need of replacement or the costs that are associated with repairing damaged parts of the drone.

In case the battery of the drone dies during the mission, the battery can easily be swapped for a full battery. Having extra batteries on hand will cost around € 5,790 per battery.

Liability insurance is mandatory for drones, this is in case the drone damages private property. In case of damage to the drone, it is wise to also have CASCO (Casualty and Collision) insurance for the drone which covers this [51]. The cost of insurance varies and can account for hundreds of euros per month.

14.2. Return on Investment

In this section the market price is chosen, this is the price the drone will be sold for. After this is established, the market volume, market value and market share are calculated. With these numbers, the return on investment (ROI) is determined to assess the profitability of the drone.

14.2.1. Market Price

First, the selling price of the drone is determined. As seen from Subsection 14.1.1 the cost of the drone is approximately € 25,000. To determine the market price of the drone, the profit margin is important to decide on. To get an idea, gross profit margins in the drone market were investigated. The gross profit margin percentage is the cost of goods sold (COGS) subtracted from the net sales, divided by the net sales [5]. Usual margins were found to be around 40% for enterprise solutions and customised drones, i.e. drones that are specifically designed for industrial or commercial applications. This is quite high compared to consumer drones, as the competition for those drones is high resulting in lower margins. However, from the market analysis done in

Chapter 4, one important aspect of the value proposition is that the drone will be on the market for a lower price than competitors. So, this should also be taken into account when deciding on a selling price. When taking a profit margin of 40% the selling price will be **€ 35,000**, which is still significantly lower than that of similar existing firefighting drones. This price allows for good profit margins, while still offering a lot lower price than the existing drones on the market.

14.2.2. Market Volume, Value and Share

In the first instance, the drone is built for the Dutch fire brigade. So for this analysis, it is assumed that the drones will for now only be used in the Netherlands, with the goal to sell to other countries in the future. Currently, there are around 1000 fire stations in the Netherlands [30]. Another aspect influencing the sales is the government and more specifically the budget the government has to invest in the drones. It is unlikely that every fire station will buy a drone, the percentage of fire stations that will buy a drone is also referred to as the penetration rate. The potential market volume is the number of fire stations multiplied by the penetration rate [109].

To get a first estimation, the two types of fire stations are investigated. There are 'beroeps' (professional) and 'vrijwillige' (voluntary) fire stations. At the 'beroeps' the firefighters are full-time workers, whereas at the 'vrijwillige' the firefighters work on call basis [30]. It can be seen that in larger cities, there are more 'beroeps' fire stations so this also shows the spread of the demand that is expected. This can be seen in Figure 14.2 This is important as in bigger cities, it is predicted that more drones will be bought. There are around 110 'beroeps' fire stations. In addition, at these fire stations, the firefighters can be qualified to fly the drone as they are working full-time. To start off, this is the number that will be used. This leads to a penetration percentage of 11% and thus a market volume of 110. This is relatively low, but it is expected that the percentage will increase as more high-rise buildings will also be built outside of the big cities.

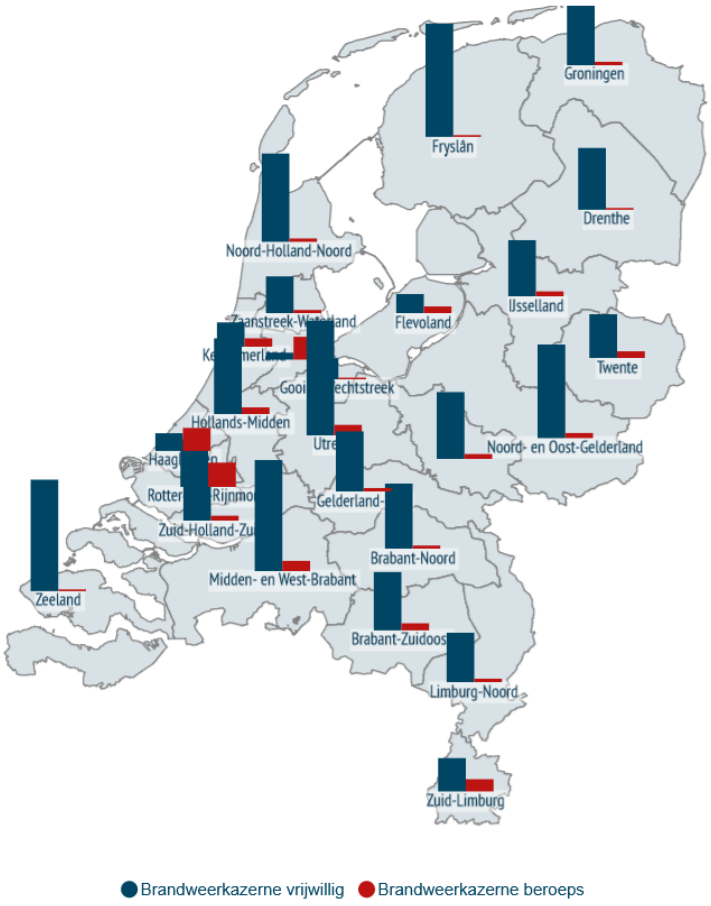

Figure 14.2: *'Beroeps' and 'vrijwillige' fire stations in the Netherlands [116]*

The market value is defined as the market volume multiplied by the selling price. With a retail price of **€ 35,000**

and 110 sold units, this means a revenue of **€ 3.85** Million will be realised. In the Netherlands and the EU, the market share will be 100% as European fire brigades do not use any drones with fire extinguishing capabilities.

14.2.3. Return on Investment

With the numbers obtained from the previous sections the return on investment (ROI) can be calculated, which is done as follows [14]:

$$\text{ROI} = \frac{\text{sales value - cost of investment}}{\text{cost of investment}} \text{x } 100 \tag{14.1}$$

The sales value refers to the total sales made and the cost of investment is the total cost of the development and manufacturing of the drone. For the drone to be profitable, the value of the ROI must be positive. The higher the ROI the more profit is made. The sales value is equal to € 3,85 Million. The cost of investment consists of the cost of the components of the drone, the manufacturing costs and development costs. The total cost of investment is around **€ 2.832 Million**. This means that the ROI is equal to **36%**. This means that the investment has generated a positive return. This demonstrates the profitability that is expected of the project. Meaning that from a financial standpoint, the proposed drone is a feasible design.

15
Risk Analysis

This chapter outlines the technical risk assessment and contingency management plan. The chapter is structured as follows. Firstly, the risks will be identified and evaluated, and their probability and impact will be examined in Section 15.1. Secondly, risk maps will be displayed to assist in visualising the severity of the potential risks in Section 15.2. Next, a mitigation strategy for the most severe risks will be devised, and new risk maps will be developed in Section 15.3 and Section 15.4, respectively. Lastly, a contingency plan will be composed in Section 15.5.

15.1. Risk Identification

In this section, the potential risks during the development and mission are identified and are shown in Table 15.1. Each risk is identified by its unique ID. A short description of each risk is given and the likelihood of occurrence and impact are assessed. The probability and impact of each risk are rated from one to five. For likelihood, a rating of one means that it is unlikely to happen. A rating of five means that the probability of occurrence is high. The rating for the impact is comparable. A rating of one means that the risk will not have a large effect. A five indicates that the risk may have a catastrophic impact.

To properly perform a risk assessment, the risks are divided into multiple categories. Firstly, general potential problems that may affect the design and operation of the firefighting drone are identified and analysed. Secondly, risks concerning the different components of the drone and its operational environment were analysed. Factors such as software or hardware malfunctions, signal interference, temperature issues, and safety concerns were considered. Next, the likelihood and impact of each risk were given on a scale from one to five.

To determine the likelihood, the reliability of the components, previous instances of similar risks, and preventive measures in place were considered. For impact, potential consequences like safety hazards, operational disruptions, damage, and harm to people were looked into. An example of a high likelihood of occurrence score is risk *RSK-RASP-06*. The higher number is due to the high demand for Raspberry Pi components, leading to an unfortunate scenario where this popular device is frequently out of stock. People searching for a Raspberry Pi board for personal projects often encounter frustrating messages proclaiming unavailability and extended delivery times. However, in the face of this challenge, there are alternative solutions and valuable options to consider.

Table 15.1: *Risk identification and analysis*

ID	Risk	Likelihood	Impact	Risk score
Technical Risk Management				
RSK-TRM-01	Misunderstanding the expectations of the customer	2	3	6
RSK-TRM-02	There are privacy concerns due to the cameras	2	3	6
RSK-TRM-03	There are problems with regulations and restrictions from the Government	2	3	6
RSK-TRM-04	Forgot to charge the battery of the drone	2	4	8

Continued on next page

Table 15.1 – continued from previous page

ID	Risk	Likelihood	Impact	Risk Score
RSK-TRM-05	Forgot to charge the battery of the controller	2	4	8
RSK-TRM-06	Carelessness of the person controlling the drone	1	4	4
RSK-TRM-07	Wrong input into the controller	2	4	8
RSK-TRM-09	War in the world causing materials to be less available	3	2	6
RSK-TRM-10	Pandemic outbreak	2	2	4
Materials				
RSK-MAT-01	Materials out of stock	2	4	8
RSK-MAT-02	Higher-than-expected material costs	3	2	6
RSK-MAT-03	Long delivery time (main frame material)	3	3	9
RSK-MAT-04	Material with poor properties (main frame)	2	4	8
RSK-MAT-05	Material not easily manufacturable (main frame)	2	4	8
RSK-MAT-06	Material prone to corrosion (main frame)	2	3	6
RSK-MAT-07	Material causing signal interference (main frame)	2	4	8
RSK-MAT-08	Long delivery time (rotor)	3	3	9
RSK-MAT-09	Material with poor properties (rotor)	2	4	8
RSK-MAT-10	Material not easily manufacturable (rotor)	2	3	6
RSK-MAT-11	Material prone to corrosion (rotor)	2	2	4
RSK-MAT-12	Material causing signal interference (rotor)	1	2	2
RSK-MAT-13	Long delivery time (insulation material)	2	3	6
RSK-MAT-14	Material with poor properties (insulation)	2	3	6
RSK-MAT-15	Material not easily manufacturable (insulation)	2	3	6
RSK-MAT-16	Material prone to corrosion (insulation)	1	2	2
RSK-MAT-17	Material causing signal interference (insulation)	1	5	5
Performance				
RSK-PER-01	Collision with another UAV	2	4	8
RSK-PER-02	Software stops working	2	5	10
RSK-PER-03	Collision with the building	2	5	10
RSK-PER-04	Hardware stops working	2	5	10
RSK-PER-05	Battery dies during flight	3	4	8
RSK-PER-06	Desired flight altitude is not reached	1	5	5
RSK-PER-07	The drone cannot take-off	1	5	5
RSK-PER-08	The payload is not delivered	2	5	10
RSK-PER-09	The payload is not delivered at the desired spot	3	5	15
RSK-PER-10	The drone cannot withstand the temperatures of the fire	2	4	8
RSK-PER-11	The drone returns to the wrong spot (in case of self-returning)	2	2	4

Continued on next page

Table 15.1 – continued from previous page

ID	Risk	Likelihood	Impact	Risk Score
RSK-PER-12	Cameras stop working	2	3	6
RSK-PER-13	Sensors stop working	2	3	6
RSK-PER-14	Smoke prevents the cameras from useful view	3	3	9
RSK-PER-15	Fog prevents the cameras from useful view	2	2	4
RSK-PER-16	Warning signal stops working	1	3	3
RSK-PER-17	Warning signal at the wrong time	1	3	3
RSK-PER-18	Propeller stops working	2	4	8
RSK-PER-19	The battery gets stuck so it is not replaceable during the mission	2	4	8
RSK-PER-20	The payload can not be refilled during the mission	2	4	8
RSK-PER-21	One of the propeller blades falls off	1	5	5
Flight Controller				
RSK-FC-01	FC software stops working	2	5	10
RSK-FC-02	FC hardware stops working	2	5	10
RSK-FC-03	FC not compatible with other components	2	4	8
RSK-FC-04	FC integration issues with other systems	2	4	8
RSK-FC-05	FC malfunctions or fails to function	2	5	10
RSK-FC-06	FC overheats or thermal issues	2	4	8
RSK-FC-07	FC communication failure with other components	2	4	8
RSK-FC-08	FC is not compatible with the software	2	3	6
RSK-FC-09	FC hardware incompatibility or connectivity issues	2	3	6
RSK-FC-10	FC power supply failure or instability	2	3	6
Electronic Speed Controller				
RSK-ESC-01	ESC hardware stops working	2	5	10
RSK-ESC-02	ESC is incompatible with flight controller	2	4	8
RSK-ESC-03	ESC overheats or thermal issues	3	4	12
RSK-ESC-04	ESC is not compatible with the FC software	2	3	6
RSK-ESC-05	ESC communication failure with other components	2	3	6
RSK-ESC-06	ESC power supply failure or instability	2	3	6
Power Distribution Board				
RSK-PDB-01	PDB malfunctions or fails to function	2	5	10
RSK-PDB-02	PDB inadequate power distribution	3	4	12
RSK-PDB-03	PDB poor quality or unreliable	2	4	8
RSK-PDB-04	PDB overheats or thermal issues	2	4	8
RSK-PDB-05	PDB wiring and connection issues	2	3	6
RSK-PDB-06	PDB power supply failure or instability	2	3	6

Continued on next page

Table 15.1 – continued from previous page

ID	Risk	Likelihood	Impact	Risk Score
RSK-PDB-07	PDB inaccurate battery level readings	2	3	6
RSK-PDB-08	PDB limited monitoring capabilities or insufficient data	2	3	6
RSK-PDB-09	PDB battery monitor system drains power from the battery	2	3	6
RSK-PDB-10	PDB difficulty in installation or integration	2	3	6
RSK-PDB-11	PDB battery monitor system malfunction due to extreme temperatures	3	4	12
RSK-PDB-12	PDB inadequate alert or warning system	2	3	6
Transmitter				
RSK-TX-01	Transmitter signal interference due to nearby electronic devices	3	4	12
RSK-TX-02	Transmitter range limitations	2	3	6
RSK-TX-03	Transmitter power failure or low battery	2	4	8
RSK-TX-04	Transmitter signal loss or weak signal strength	3	4	12
RSK-TX-05	Transmitter firmware or software compatibility issues	2	3	6
Receiver				
RSK-RX-01	Receiver sensitivity issues resulting in poor signal reception	2	3	6
RSK-RX-02	Receiver signal interference due to nearby electronic devices	3	4	12
RSK-RX-03	Receiver power failure or low battery	2	4	8
RSK-RX-04	Receiver signal loss or weak signal strength	3	4	12
RSK-RX-05	Receiver firmware or software compatibility issues	2	3	6
Hawkeye micro control board				
RSK-HWKB-01	Micro control board fails to display or provides inaccurate information	2	3	6
RSK-HWKB-02	Micro control board hardware failure or malfunction	2	4	8
RSK-HWKB-03	Compatibility issues with other onboard components	2	3	6
RSK-HWKB-04	Micro control board power failure or low voltage	2	3	6
RSK-HWKB-05	Micro control board overheating or thermal issues	2	3	6
Raspberry Pi				
RSK-RASP-01	Raspberry Pi overheating	2	4	8
RSK-RASP-02	Raspberry Pi hardware failure or malfunction	2	4	8
RSK-RASP-03	Incompatibility with required software or libraries	2	3	6
RSK-RASP-04	Power supply issues leading to Raspberry Pi shutdown or reset	2	3	6
RSK-RASP-05	SD card corruption or data loss	2	3	6

Continued on next page

Table 15.1 – continued from previous page

ID	Risk	Likelihood	Impact	Risk Score
RSK-RASP-06	Raspberry pi unavailable on the market	4	2	8
Telemetry				
RSK-TEL-01	Telemetry signal loss or weak signal strength	3	4	12
RSK-TEL-02	Interference with other electronic devices or frequencies	3	4	12
RSK-TEL-03	Telemetry data corruption	2	3	6
RSK-TEL-04	Telemetry module malfunction or hardware failure	2	4	8
RSK-TEL-05	Communication issues with flight controller or ground station	2	3	6
LiDAR				
RSK-LID-01	LiDAR misreads distances or fails to detect obstacles accurately	2	4	8
RSK-LID-02	Interference with other LiDAR devices or environmental factors	2	3	6
RSK-LID-03	LiDAR hardware failure or malfunction	2	4	8
RSK-LID-04	Incompatibility with onboard systems or software	2	3	6
RSK-LID-05	Limited range of view or field of view	2	3	6
Sonar				
RSK-SON-01	Sonar accuracy affected by plumes of smoke or dust	3	4	12
RSK-SON-02	Interference with sonar signals due to environmental factors	2	3	6
RSK-SON-03	Sonar misreads or fails to detect obstacles accurately	2	4	8
RSK-SON-04	Sonar hardware failure or malfunction	2	4	8
RSK-SON-05	Incompatibility with onboard systems or software	2	3	6
RSK-SON-06	Limited range or field of view	2	3	6
RSK-SON-07	Sonar signal degradation due to smoke density	3	4	12
GPS				
RSK-GPS-01	GPS signal loss or weak signal strength	3	4	12
RSK-GPS-02	Inaccurate or unreliable GPS positioning	2	3	6
RSK-GPS-03	Interference with other electronic devices or frequencies	3	4	12
RSK-GPS-04	GPS module failure or malfunction	2	4	8
RSK-GPS-05	Compatibility issues with flight controller or software systems	2	3	6
Camera				
RSK-CAM-01	Camera malfunctions or hardware failure	2	4	8
RSK-CAM-02	Poor image quality or resolution	2	3	6
RSK-CAM-03	Camera lens damage or scratches	2	3	6

Continued on next page

Table 15.1 – continued from previous page

ID	Risk	Likelihood	Impact	Risk Score
RSK-CAM-04	Compatibility issues with other equipment or software	2	3	6
RSK-CAM-05	Insufficient battery life or power supply	3	3	9
RSK-CAM-06	Camera falls of when being installed	2	4	8
RSK-CAM-07	Camera malfunction due to high temperatures	3	4	12
RSK-CAM-08	Impaired visibility due to smoke plume	3	4	12
Thermal Camera				
RSK-THC-01	Thermal camera malfunctions or hardware failure	2	4	8
RSK-THC-02	Poor image quality or resolution in thermal imaging	2	3	6
RSK-THC-03	Compatibility issues with other equipment or software	2	3	6
RSK-THC-04	Insufficient battery life or power supply for extended operation	3	3	9
RSK-THC-05	Thermal camera lens damage or scratches	2	3	6
RSK-THC-06	Thermal camera malfunction due to high temperatures	1	4	4
RSK-THC-07	Inaccurate temperature readings or calibration issues	2	4	8
RSK-THC-08	Limited range or field of view in thermal imaging	2	3	6
Wiring				
RSK-WIR-01	Loose or poor connections	2	4	8
RSK-WIR-02	Incorrect wiring and connections	2	4	8
RSK-WIR-03	Wiring damage due to vibration or physical stress	2	3	6
RSK-WIR-04	Inadequate wire gauge for current requirements	2	3	6
RSK-WIR-05	Wiring short circuit or electrical faults	2	4	8
RSK-WIR-06	Wiring interference with other components or signals	2	3	6
RSK-WIR-07	Inaccessible or hard-to-reach wiring locations	2	3	6
Waterpump				
RSK-WTP-01	Malfunction or failure of pressure sensor	2	4	8
RSK-WTP-02	Malfunction or failure of pressure valve	2	4	8
RSK-WTP-03	Inaccurate pressure measurement	2	3	6
RSK-WTP-04	Insufficient water pressure	3	4	12
RSK-WTP-05	Excessive water pressure	2	4	8
RSK-WTP-06	Pump malfunction or failure	3	5	15
RSK-WTP-07	Leakage or damage to water tank	2	4	8
RSK-WTP-08	Power supply failure to pump	2	3	6
Market Analysis				
RSK-MKT-01	The battery is too expensive	3	2	6
RSK-MKT-02	The cameras and sensors are too expensive	3	2	6
RSK-MKT-03	The unit price will exceed € 25,000	3	2	6

Continued on next page

Table 15.1 – continued from previous page

ID	Risk	Likelihood	Impact	Risk Score
RSK-MKT-04	Competitors come up with better and cheaper ideas	2	3	6
Safety				
RSK-SAF-01	Battery catches fire during flight	2	5	10
RSK-SAF-02	Battery catches fire during ground operation	1	4	4
RSK-SAF-03	Someone cuts themselves with a propeller	1	2	2
RSK-SAF-04	Drone gets hacked	2	4	8
RSK-SAF-05	After the signal is lost, the drone fails to return	2	3	6
RSK-SAF-07	Collision with a person	1	4	4
RSK-SAF-08	Explosion of the pump	1	5	5
RSK-SAF-09	Extinguishing material has a reaction with surrounding materials inside the building	2	4	8
Sustainability				
RSK-SUS-01	The drone is not recyclable for 30%	2	1	2
RSK-SUS-02	Extinguishing material is non-degradable	2	2	4
Organisational				
RSK-ORG-01	Communication error between two firefighters during the mission	2	3	6
RSK-ORG-02	Communication error between firefighters and designers/engineers	3	2	6
RSK-ORG-03	Insufficient training of firefighters to control the drone	2	2	4
RSK-ORG-04	Distraction during control	3	4	12
RSK-ORG-05	Tiredness caused by excessive working hours	2	3	6

15.2. Risk Maps

In this section, the risk maps are shown in Figure 15.1 and Figure 15.2a to Figure 15.2r. The likelihood of the risks is plotted on the x-axis, while the impact of each risk is plotted on the y-axis. The lower left corner, or the green zone, indicates a less severe risk. The risks in the upper right corner, or the red zone, can be categorised as a more catastrophic risk. During the design, manufacturing and mission of the drone, all the risks, but especially the more severe ones, should be taken into account at all times and some may be analysed in more depth.

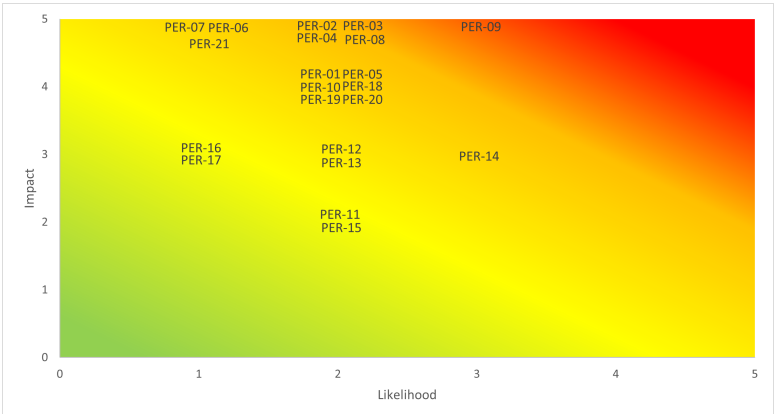

Figure 15.1: *Risk assessment: performance*

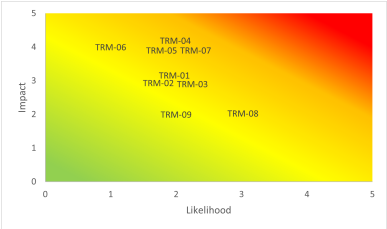

(a) *Technical risk management*

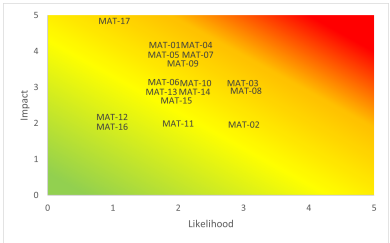

(b) *Materials*

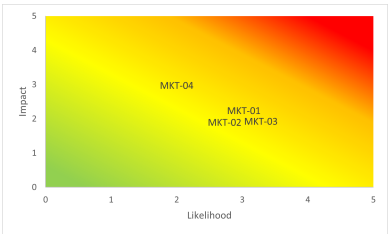

(c) *Market analysis*

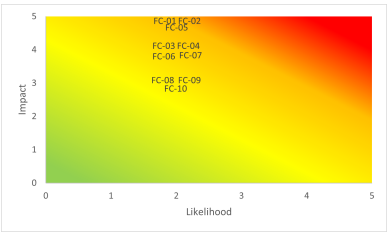

(d) *Flight Controller*

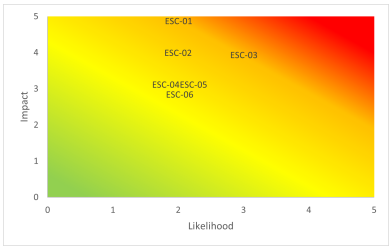

(e) *Electronic Speed Controller*

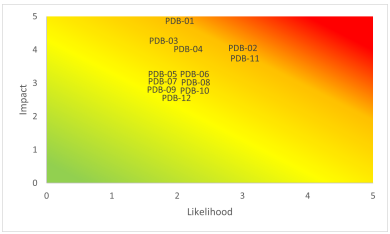

(f) *Power Distribution Board*

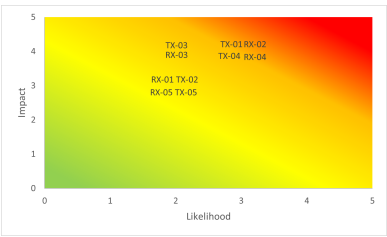

(g) *Transmitter and receiver*

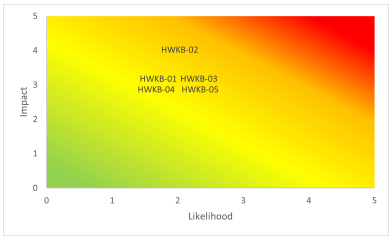

(h) *Hawkeye Micro Control Board*

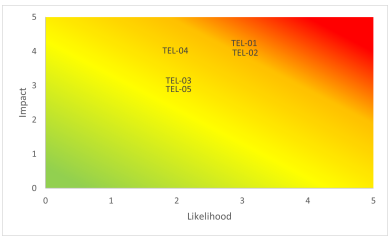

(i) *Telemetry*

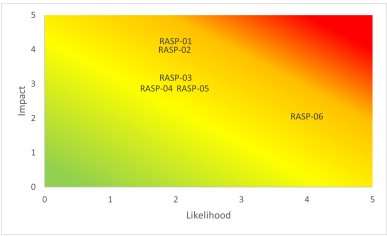

(j) *Raspberry Pi*

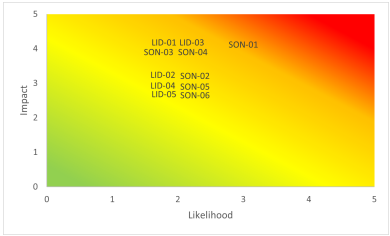

(k) *LiDAR and Sonar*

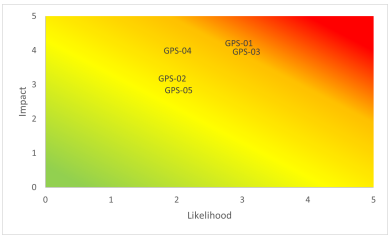

(l) *GPS*

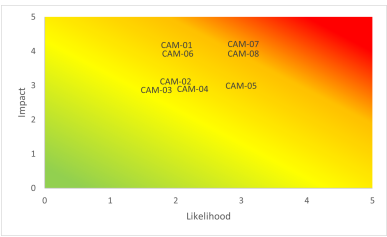

(m) *Camera*

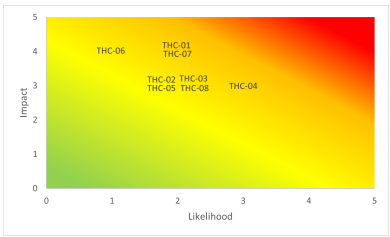

(n) *Thermal Camera*

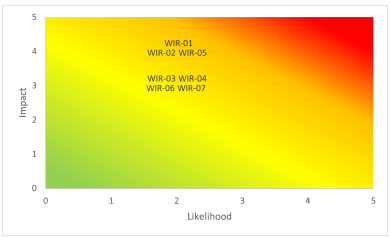

(o) *Wiring*

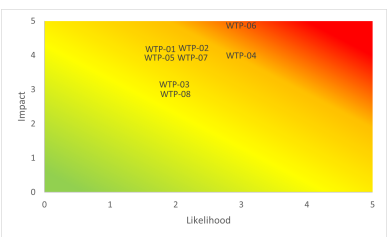

(p) *Water pump*

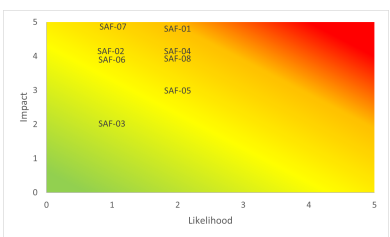

(q) *Safety*

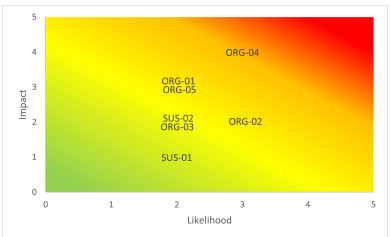

(r) *Sustainability and organisation*

Figure 15.2: *Risk assessment*

15.3. Mitigation Plan

A mitigation plan primarily focuses on diminishing the likelihood or impact of a risk occurrence. Its objective is to proactively implement measures, strategies, or actions that minimise the possibility of risks materialising. By identifying vulnerabilities and addressing them, a mitigation plan aims to lower the probability of risk events. Emphasising risk prevention, preparedness, and enhancing overall system resilience are central components of a mitigation plan.

All risks given in Table 15.1 with a risk score equal to or higher than ten, can be categorised as catastrophic. For these risks, a mitigation plan is worked out. For each of the risks, a mitigation action is established, shown in Table 15.2. The action is meant to lower the likelihood of occurrence of the risk. The new likelihood and new risk scores are also presented in the table. It is assumed that the impact of the risk remains the same.

Table 15.2: *Risk mitigation assessment*

ID	Mitigating action	New likeli-hood	New risk score
Performance			
RSK-PER-02	Implement a Collision Avoidance System.	1	5
RSK-PER-03	Regular tests of the hardware under different circumstances.	1	5
RSK-PER-04	Have a back up battery / check battery before take-off.	1	5
RSK-PER-08	Analyse the design and perform tests under different circumstances.	1	5
RSK-PER-09	Have a proper aim system and perform regular tests.	2	10
Flight Controller			
RSK-FC-01	Implement rigorous software testing and backup systems, Regularly update and test the flight control software to ensure its stability and reliability.	1	5
RSK-FC-02	Implement redundant hardware components or backup systems.	1	5
RSK-FC-05	Implement redundant flight computers or backup control mechanisms.	2	10
Electronic Speed Controller			
RSK-ESC-01	Implement redundant hardware components or backup systems.	1	5
RSK-ESC-03	Improve cooling mechanisms and optimise power distribution.	2	8
Power Distribution Board			
RSK-PDB-01	Implement redundant PDBs or backup power distribution mechanisms.	2	10
RSK-PDB-02	Ensure proper sizing and distribution of power channels.	2	8
RSK-PDB-11	Use battery monitor systems rated for high-temperature environments.	2	8
Transmitter			
RSK-TX-01	Perform frequency analysis and select less crowded transmission bands.	2	8
RSK-TX-04	Use higher-quality transmitters and optimise antenna placement.	2	8
Receiver			
RSK-RX-02	Perform frequency analysis and select less crowded frequency bands.	2	8

Continued on next page

Table 15.2 – continued from previous page

ID	Mitigating action	New likelihood	New risk score
RSK-RX-04	Use higher-quality receivers and optimise antenna placement.	2	8
Telemetry			
RSK-TEL-01	Use high-quality telemetry systems and optimise antenna placement	2	8
RSK-TEL-02	Perform frequency analysis and select less crowded	2	8
Sonar			
RSK-SON-01	Implement alternative or supplementary sensors for reliable altitude sensing, such as LiDAR or visual odometry systems	2	8
GPS			
RSK-GPS-01	Use high-quality GPS systems and ensure proper antenna placement	2	8
RSK-GPS-03	Perform frequency analysis and select less crowded frequency bands	2	8
Camera			
RSK-CAM-07	Use cameras rated for high-temperature environments and monitor heat	2	8
RSK-CAM-08	Utilise cameras with suitable filters or thermal cameras for visibility enhancement	2	8
Waterpump			
RSK-WTP-04	Check water supply and pump functionality	1	4
RSK-WTP-06	Regular pump maintenance and backup pump system	2	10
Safety			
RSK-SAF-01	Establish designated areas with proper ventilation and fire suppression systems for battery charging and maintenance.	1	5
Organisational			
RSK-ORG-4	Establish and enforce protocols that minimise distractions, such as designated control areas, clear guidelines on focus, and avoiding multitasking.	1	4

15.4. Mitigation Risk Maps

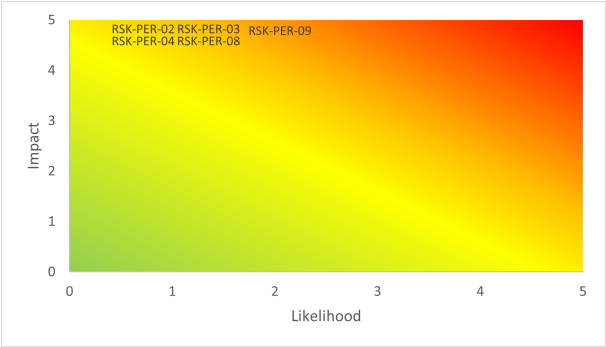

(a) *Performance*

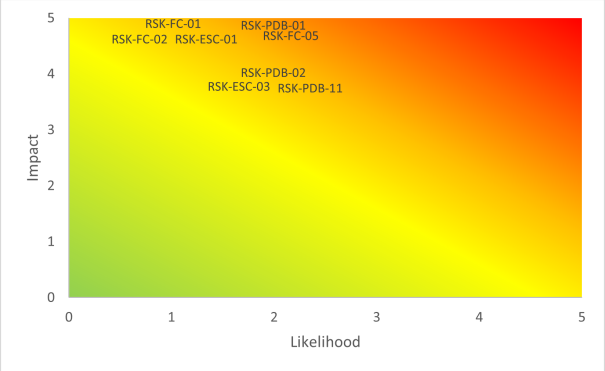

(b) *Flight Controller, Electronic Speed Controller and Power Distribution Board*

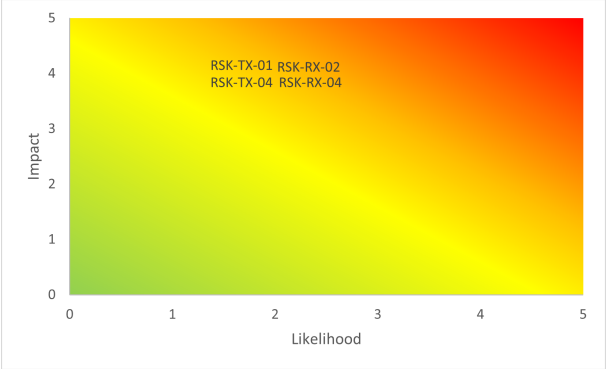

(c) *Transmitter and receiver*

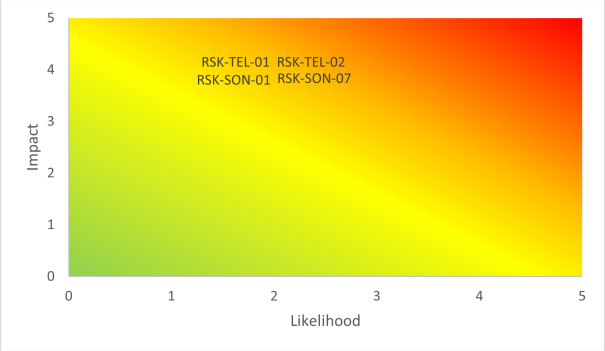

(d) *Telemetry and Sonar*

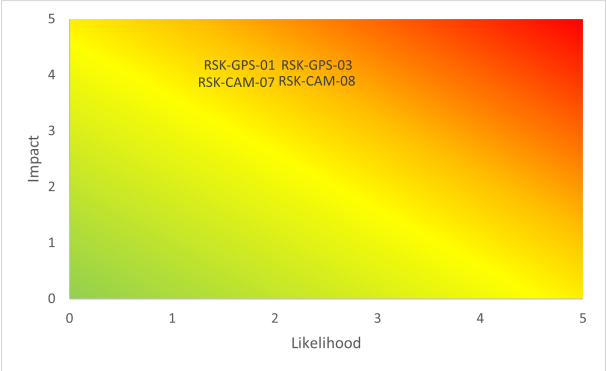

(e) *Camera and GPS*

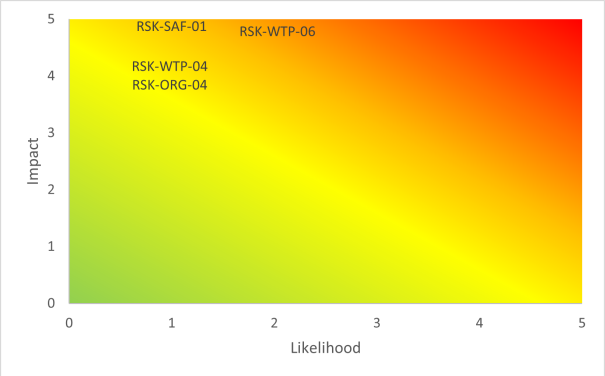

(f) *Water pump, safety and organisation*

Figure 15.3: *Mitigation assessment*

15.5. Contingency Plan

In this section, the contingency plan will be presented. The risks that were previously categorised as catastrophic necessitate the formulation of a contingency plan due to their elevated potential severity. It is important to highlight the distinction between a contingency plan and a mitigation plan.

A mitigation plan was previously described in Section 15.3. A contingency plan, on the other hand, outlines the specific actions that need to be executed if a risk event materialises. It serves as a comprehensive road map for effectively managing and responding to risk incidents that have transpired despite mitigation efforts. The purpose of a contingency plan is to provide guidance, procedures, and protocols that mitigate the consequences of a risk event, thereby facilitating a prompt and efficient response.

Table 15.3: *Contingency plan*

ID	Contingency
Performance	
RSK-PER-02	Restart the software. Check for any recent updates or patches that may have caused the issue and revert to a stable version. Contact the software provider for technical support and guidance.
RSK-PER-03	Implement obstacle detection and avoidance systems to mitigate the risk. Establish clear flight paths and avoid flying in areas with significant obstructions.
RSK-PER-04	Identify the faulty hardware component and replace it with a backup if available. Conduct regular maintenance and inspections to identify and address potential hardware issues proactively.
RSK-PER-08	Confirm the payload attachment and connection. Perform a functional check before the flight to ensure the payload mechanism is working correctly.
RSK-PER-09	Enhance GPS accuracy and navigation systems to improve payload delivery precision.
Flight Controller	
RSK-FC-01	Restart the Flight Controller software. Check for any recent updates or patches that may have caused the issue and revert to a stable version. Contact the FC software provider for technical support and guidance.
RSK-FC-02	Identify the faulty Flight Controller hardware component and replace it with a backup if available. Conduct regular maintenance and inspections to identify and address potential FC hardware issues proactively.
RSK-FC-05	Reboot the Flight Controller and re-calibrate the sensors. Check for any loose connections or damaged components. Update the FC firmware to the latest stable version. If the issue persists, consult the FC manufacturer or technical support for further assistance.
Electronic Speed Controller	
RSK-ESC-01	Identify the faulty ESC hardware component and replace it with a backup if available. Ensure proper ESC calibration and check for any loose connections. Regularly inspect ESCs for signs of damage or overheating.
RSK-ESC-03	Implement proper heat dissipation mechanisms such as cooling fans or heat sinks for critical components. Monitor temperature levels during operation and ensure adequate ventilation. Reduce excessive power usage or workload if necessary.
Power Distribution Board	
RSK-PDB-01	Identify the faulty Power Distribution Board component and replace it with a backup if available. Conduct regular inspections and maintenance of the PDB to prevent malfunctions. Ensure proper wiring connections and check for any signs of damage or loose connections.
RSK-PDB-02	Optimise power distribution by redistributing power sources or upgrading the PDB to handle higher loads. Ensure proper power management and use components with appropriate power ratings. Regularly monitor power consumption and identify any potential issues.
RSK-PDB-11	Implement temperature monitoring and protection mechanisms for the battery system. Use battery systems with built-in temperature sensors or external temperature monitoring devices. Ensure proper battery maintenance and storage to prevent exposure to extreme temperatures.
Transmitter	

Continued on next page

Table 15.3 – continued from previous page

ID	Contingency
RSK-TX-01	Identify and mitigate potential sources of interference such as electronic devices, power lines, or radio frequency signals. Use frequency-hopping or spread spectrum technology for improved
RSK-TX-04	Check transmitter batteries and replace if necessary. Relocate the pilot or ground station to a position with better line-of-sight to the aircraft. Use signal amplifiers or range extenders.
Receiver	
RSK-RX-02	Identify and mitigate potential sources of interference such as electronic devices, power lines, or radio frequency signals. Relocate or shield the receiver from interfering devices. Use frequency-hopping or spread spectrum technology for improved signal resilience.
RSK-RX-04	Verify receiver connections and antenna positioning. Replace the receiver or antenna if damaged. Use signal amplifiers or range extenders.
Telemetry	
RSK-TEL-01	Check telemetry system connections and antenna positioning. Replace damaged components if necessary. Use signal amplifiers or range extenders.
RSK-TEL-02	Conduct a thorough electromagnetic interference analysis and identify the sources of interference. Implement shielding or isolation measures for sensitive electronic devices. Adjust frequencies or use filters to avoid interference.
Sonar	
RSK-SON-01	Deploy sonar systems with higher penetration capability or advanced algorithms to compensate for signal degradation in smoky conditions. Implement redundant or backup sensors for critical operations.
GPS	
RSK-GPS-01	Relocate the GPS antenna to a position with better line-of-sight to the satellites. Verify GPS connections and antenna integrity. Use external GPS antennas or signal amplifiers. Implement alternative navigation systems (e.g., inertial navigation systems) as backup.
RSK-GPS-03	Conduct a thorough electromagnetic interference analysis and identify the sources of interference. Implement shielding or isolation measures for sensitive electronic devices. Adjust frequencies or use filters to avoid interference.
Camera	
RSK-CAM-07	Ensure proper camera ventilation and cooling mechanisms. Use cameras with higher temperature ratings. Implement thermal insulation or shielding to protect the camera from excessive heat.
RSK-CAM-08	Use alternative vision systems such as infrared or thermal cameras for enhanced visibility in smoky conditions. Deploy additional lighting systems or radar for improved situational awareness. Consider delaying or rescheduling the flight until visibility improves.
Waterpump	
RSK-WTP-04	Verify water supply connections and pressure settings. Adjust the water pump settings or use alternative water sources if available.
RSK-WTP-06	Regularly inspect and maintain water pumps. Carry backup water pumps and replace the faulty pump if necessary. Implement redundancy in water pumping systems for critical operations.
Safety	

Continued on next page

Table 15.3 – continued from previous page

ID	Contingency
RSK-SAF-01	Establish strict battery safety protocols, including proper storage, handling, and charging procedures. Use fire-resistant battery containers or bags. Install thermal monitoring systems for early detection of overheating. Have fire extinguishing equipment readily available. Train personnel on fire response procedures and emergency battery shutdown protocols. Implement redundant battery systems with built-in fire suppression mechanisms.
Organisational	
RSK-ORG-04	Implement a “sterile cockpit” concept, where non-essential conversations and distractions are minimised during critical phases of flight. Emphasise crew focus and attention to control inputs and flight parameters. Use checklists and procedures to ensure a systematic and focused approach to control inputs. Provide appropriate training to pilots on effective workload management and mitigating distractions. Establish clear communication protocols and roles within the flight crew. Use automation systems to assist with workload and minimise distractions.

16
RAMS Characteristics

The Reliability, Availability, Maintainability and Safety (RAMS) of the drone are important factors to take into account when designing. It ensures that the drone works consistently, is available when needed, requires minimal maintenance, and prioritises the safety of its users and surroundings. The RAMS analysis provides insight into these factors to ensure the viability of the drone. The results can aid in decreasing downtime and the possibility of failures. It reduces maintenance costs and can lead to an increase in the drone's lifetime. A higher-quality product gets designed as a result, improving both reputation and value.

In Section 16.1 multiple methods to improve the reliability will be given. An assessment of the availability will be done in Section 16.2. Next, in Section 16.3, the maintainability of the drone will be investigated, including the scheduled and the unscheduled maintenance. Lastly, the safety of the drone itself and its environment will be analysed in Section 16.4.

16.1. Reliability

The reliability of the drone is defined as the probability of failure. To ensure effective operations, it is important to minimise this likelihood. Therefore, the drone has to be designed, operated and maintained in a way that maximises its reliability.

The possible ways the drone, and more specifically its mission, are visualised in the fault tree shown in Figure 16.1 and Figure 16.2.

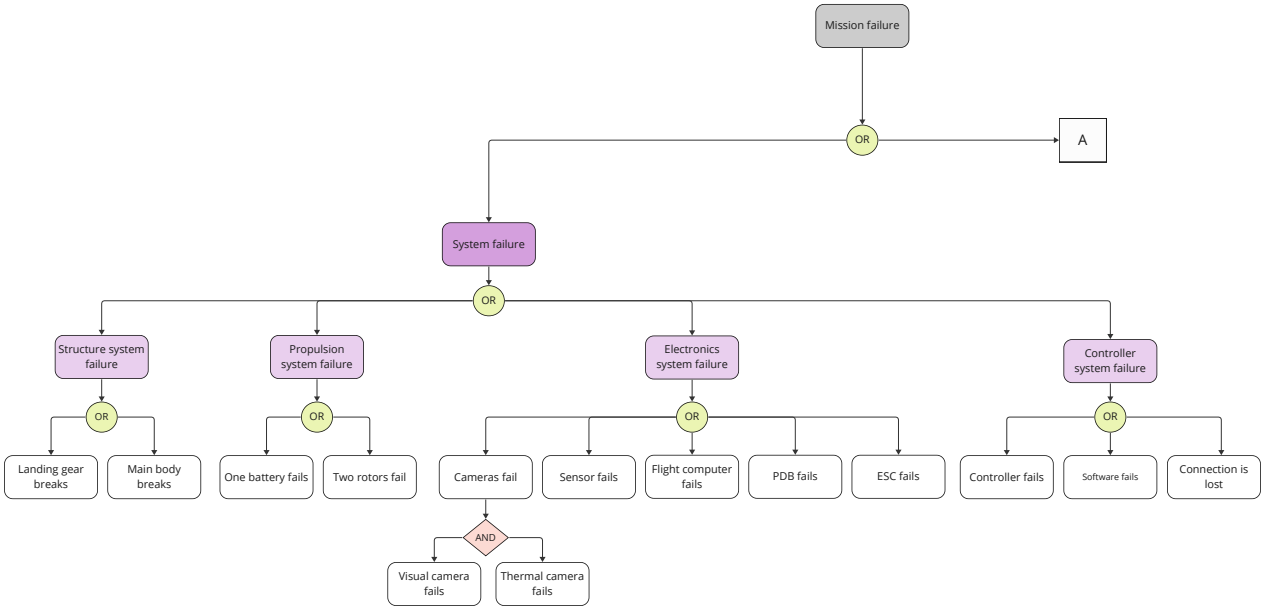

Figure 16.1: *Fault tree*

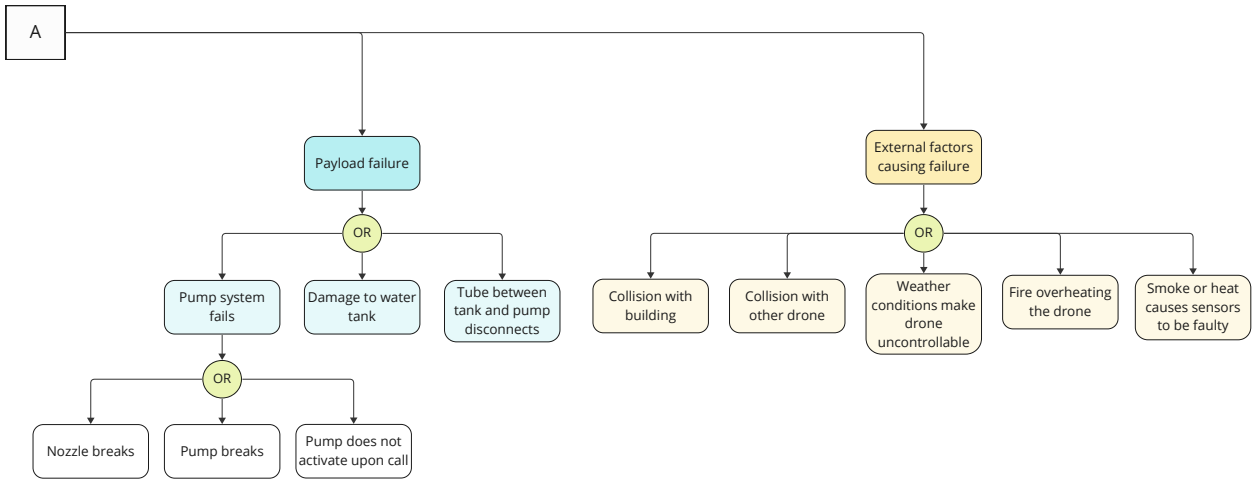

Figure 16.2: *Fault tree (contd.)*

As can be seen, the mission can fail in three different ways. The first way is if the drone breaks down itself due to system failure. Secondly, payload failure leads to an unsuccessful mission. The drone might still be able to fly but if the payload is not deployed correctly, the mission is considered to be unsuccessful. Lastly, the mission can fail due to external factors that may affect the drone, such as collision or heat.

To improve reliability, redundancy can be applied to several systems in order to decrease the probability of failure. The six-rotor configuration has redundancy built into it, as the drone is still able to fly when one rotor stops working. In this situation, the drone will not be able to fly as normal, however, it is more likely to recover the drone safely in case something goes wrong. In addition, several components have a backup, such as the frontal LiDAR. The drone is equipped with two sonar sensors as the LiDAR is not as effective in case there is a great amount of smoke. In case one of the sonars fail, the other one is sufficient to continue the mission. Adding the sonars is an easy solution as they are inexpensive and do not add much weight. However, simply duplicating components is not the solution for every system as it increases cost, weight, and complexity. Implementing redundancy for a system like the batteries has a greater amount of consequences, as the batteries are heavy and cost more than €3000. Therefore, this method is not feasible for the whole design.

Some mitigation measurements are also taken to increase reliability and reduce the risks that are shown in the fault tree. These are further discussed in Section 16.4.

16.2. Availability

The availability is a measure of what percentage of its operational lifetime the drone is actually available to be used. This is dependent on the reliability and maintainability of the drone. It is desired to maximise the operational time and it is therefore essential to identify the critical components which, due to long maintenance time or high failure rates, lead to the drone being unavailable. For this mission the components that will most likely have the highest failure rates are the batteries, the motors, the rotors, the landing gear and the ESCs.

During the mission, the Turn Around Time (TAT) is of significance. The drone has to deliver water to floors in high rise buildings, and when the tank is empty, the drone must safely land, reload and take off again within 300 seconds. The same amount of time is attributed to changing the batteries. As delivering as much water as possible is of utmost importance, TAT needs to be carefully planned out. The drone is designed in such a way that the water tank can be easily refilled by removing the lid from the tank. Furthermore, with the three-layer design of the main body, the battery can be quickly replaced. This ensures high availability during the mission.

16.3. Maintainability

Throughout its lifetime, the drone will require occasional maintenance to ensure safe and reliable operations. This section will examine the planned and unforeseen maintenance tasks that must be taken into account to

maintain optimal performance. To ensure maintenance has been carried out, the maintenance tasks performed on the drone should be logged.

16.3.1. Scheduled Maintenance

Scheduled maintenance will be done at regular intervals to reduce downtime of the drone and the chance of failure of (sub-)systems. By preventing failure, the lifetime of the drone and its components is increased. Planning maintenance reduces maintenance costs as time is used more efficiently and expensive breakdowns are prevented.

Clean components of drone

After each mission, dirt and debris should be removed from the drone to prevent build-up. This is especially essential for moving parts, such as the propellers, motors and gimbal. Small particles entering moving parts of the drone can accelerate mechanical erosion, which should be prevented [57]. Depending on the component, cleaning can be done with a damp or dry cloth or using compressed air.

Inspect drone components for damage

The chassis, propellers, landing gear, motors and batteries are crucial components and it is therefore important to discover damage to these parts as soon as possible. It should be checked whether the parts do not contain any cracks and deformations to prevent malfunction during the next flight. Additionally, the batteries of the drone (and the controller) should be checked for swelling and leaking. After turning off the power, one should check whether the propellers are able to freely rotate without any obstructions. The wiring should be examined to make sure no cables are loose or worn. The mounting of the drone's antenna should be secure and they should still be correctly positioned. These checks should be run after each operation.

Inspect and clean water tank

The water tank should be inspected for signs of leaks or other damage that could affect its structural integrity. Furthermore, the tank should be regularly cleaned to remove any debris, dirt or contaminants that may build up over time. The lids and fittings should be checked for wear or deterioration.

Maintenance and testing of water pump

The water pump may require regular maintenance, such as lubrication, seal replacement, or cleaning. The valves and the hose connecting the tank and the pump should be checked for any leaks, cracks, or wear. The recommendations provided by the manufacturer for the maintenance should be followed. In addition, the pump should regularly be tested to ensure the pressure and flow rate meet the required specifications.

Clean sensors and cameras

The sensors and cameras of the drone should be cleaned to remove dirt and contaminants after every flight. To prevent damage to the sensitive components, cleaning materials and methods as recommended by the manufacturer should be used.

Check for software updates

To ensure effective functioning, the drone and its controllers should regularly be checked for software updates. Moreover, it reduces security risks.

Manage battery discharge

After every 30 battery cycles, the battery should be fully discharged. This is done to reset the battery's digital memory. If not properly done, this can decrease the accuracy of the battery [23].

Calibrate sensors

To ensure optimal performance, safety, and reliability during the mission, the sensors should be calibrated to ensure high accuracy.

Check fastenings

After roughly ten operations, the connections of the drone components should be checked. The fastenings should not be loose, however, they should not be too tight, as this will induce internal stresses.

16.3.2. Unscheduled Maintenance

Unscheduled maintenance is hard to plan for as it is caused by unexpected failure arising during operations. To minimise the drone's downtime, it is essential to anticipate these unforeseen maintenance occurrences and have critical resources readily available.

Unforeseen breakdowns can for instance occur due to collisions or extreme weather conditions. Critical components might have to be replaced or repaired on site and therefore the necessary resources should be readily available. Calibration of the sensors may be necessary when inaccuracies or inconsistencies occur in the trajectory or payload deployment. Unexpected battery failure or sudden battery depletion may occur, which can be solved by battery replacement. The drone might experience communication issues, requiring the root of the problem to be identified so the problem can be resolved.

By preparing for these scenarios, the necessary resources can be arranged to quickly resolve issues when they arise. This minimises the downtime of the drone, as it can provide consistent support to the firefighting team.

16.4. Safety

It is of utmost importance that the drone shall operate safely. It is crucial that the drone causes no threat to its surroundings at all times. The potential risks have to be determined so that mitigation actions can be taken.

The biggest risks that have to be prevented are the ones harming humans and damaging equipment. The consequences of an accident are high as it may result in serious injury. The drone can collide with a person or the rotors can cause harm to someone. Furthermore, if the drone is damaged, the mission will be slowed down which results in the fire spreading further causing more harm to the building and its residents. The drone can collide with the building or other surroundings, and unfavourable weather conditions might cause a loss of control over the drone.

In order to prevent these events, the safety-critical functions, shown below, can be determined. These are the functions that are essential for the drone, i.e. damage to these leads to an inoperable drone.

- Rotors
- Batteries
- Motors
- Wiring
- Communication components
- Frame
- Flight computer

Mitigation measurements are set up to reduce the likelihood of the aforementioned risks. For these safety-critical functions, the following mitigation measurements have been identified:

- The drone pilot is highly qualified and has sufficient experience. The training should have covered operational procedures, safety guidelines and emergency response protocols. Additional training is required specific to the firefighting operation.
- A minimum distance should be kept between the drone and humans or buildings at all times to avoid a collision.
- Regular maintenance should be carried out to reduce the risks of components failing during flight.
- A pre-flight checklist should be followed to ensure that no critical steps are forgotten.
- For safe and legal operations, the drone has to comply with regulations as specified by the government of the Netherlands and the European Union.
- A safe location for take-off and landing has to be determined to prevent damage to the drone and hurting any humans.
- An eye has to be kept on the weather, to ensure the conditions are still within the operating limits of the drone.
- Obstructions have to be detected, either by the drone or the operator.

17
Sustainable Development Strategy

HYDRONE aims to contribute to the Sustainable Development Goals of the United Nations. In Section 17.1, it will be explained to which specific goals it aims to contribute. In previous reports, a Sustainable Development strategy for the design of the UAV was constructed. This strategy will first be revised in Section 17.2. It will then be explained how this strategy was implemented for the design of the subsystems. For each subsystem then, it will be explained how the design contributes to the Sustainable Development goals of the United Nations. In Section 17.3, the EOL strategy of the UAV will be explained. Lastly, certain contributions of the UAV to sustainability will be discussed in Section 17.4.

17.1. Sustainable Development Goals

In 2015, all the member states of the United Nations (UN) adopted the 2030 agenda for sustainable development. Seventeen main goals were set up, which are urgent for all member states to follow. In Figure 17.1, the 17 Sustainable Development Goals (SDG) can be found.

Figure 17.1: *The 17 sustainable development goals from the United Nations [179]*

HYDRONE aims to contribute to the SDG by specifically tackling goals 3 and 13. Goal 3 aims to improve the health of people by tackling causes of death and diseases [83]. Goal 13 aims to fight climate change by decreasing greenhouse emissions [36]. In the following sections, it will be explained in more detail how these goals are implemented for different subsystems.

17.2. Sustainable Design Strategy

The strategy for sustainable design has been constructed in previous reports [56]. A flow diagram of the new strategy can be found in Figure 17.2.

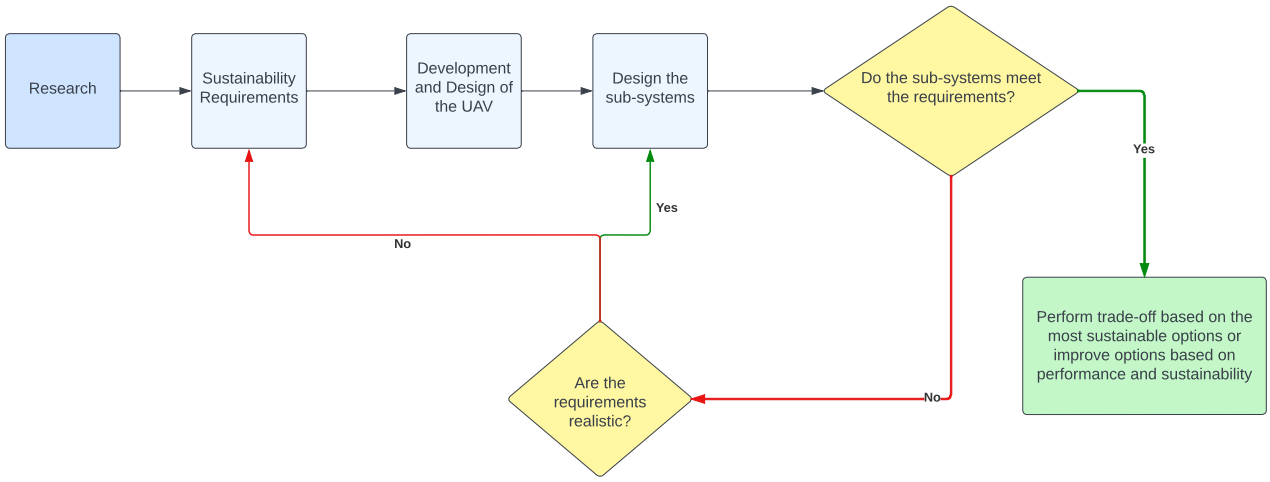

Figure 17.2: *Flow diagram of the development process of the final design*

The strategy starts with analysing the sustainability requirements, which can be found in Section 3.5. The requirements state that the UAV shall use a clean energy source and non-toxic and biodegradable extinguishing agents. The environmental impact will be evaluated in the EOL procedure and should be minimised. The next step is to look at how the sustainability requirements have been implemented in the trade-off of the subsystems. The Power, Payload, Propulsion, Electronics and Structure subsystems all had a trade-off or a selection where sustainability was taken into account.

Payload

REQ-SUS-2 and REQ-SUS-3 are sustainability requirements that are of importance for the payload subsystem. In Subsection 5.2.2, the final trade-off for the subsystem was done. The water tank with a pressure pump came out to be the best option. By using water as the extinguishing agent, REQ-SUS-2 and REQ-SUS-3 are both met. Even though this may seem minor, meeting these requirements allows the drone to be used in all emergency situations, without questioning the environmental impact that the extinguishing agent will have on humans and nearby flora and fauna. The water tank that is used for the payload will also be reusable.

Power

The trade-off for the power subsystem has already been executed in the previous report [56]. REQ-SUS-1 is an important requirement with respect to the power subsystem. As mentioned in Chapter 8, the batteries are lithium-polymer batteries. Using electrical power for the drone aligns with the previously mentioned UN Sustainability Goal 13 [36]. As the UN is aiming to drop global CO_2 emissions by 45% by 2030 and reach net zero by 2050, it is crucial that this drone is tailored to support these goals. Using electrical energy ensures the longevity of the design in future societies as it can be recharged using sustainable/renewable energy sources.

Propulsion

The trade-off for the final configuration was done in the midterm report [56]. A crucial factor for the trade-off was ‘transportability’. The aim was to fit the drone within the smaller fire transport vans rather than the large firetrucks to minimise the CO_2 emissions when transporting the UAV to each emergency scene. Due to this factor, this criterion was awarded a weight factor of 15% and had a significant impact on the design/configuration of the drone.

Electronics

With the selection of the electrical components, sustainability was taken into account in other parameters. The weight, cost and power usage were preferably low combined with a performance as high as possible. With lower

weight and power usage, the UAV will be more energy efficient, which contributes to the goal of sustainability.

Some sensors and cameras are sensitive to heat radiation. The heat might affect the lifetime and performance of the sensors. This is why insulation is used on the sensors and cameras. Polyurethane foam is used for the sensors. For the cameras, glass and silica aerogel is used. Adding this insulation ensures a longer lifetime of the fault-prone components, requiring less replacement of components and less allocation of resources for the operation of HYDRONE.

Structure

The sandwich panels of the main body and the rods that connect the rotors to the main body are both made of carbon fibre. The landing gear will consist of carbon fibre tubes. All the rotors of the UAV are made of carbon fibre epoxy finished with a glossy finish.

Therefore, it can be said that the UAV structure is mainly made of carbon fibre. This material is lighter than metal, which decreases fuel usage. Carbon fibre does not corrode, degrade, rust or fatigue. Its lifetime is longer than that of metal [98].

17.3. End-of-Life Strategy

The payload subsystem uses a custom water tank. The tank can be refilled without removing it and can be used multiple times. If one of the sensors or cameras needs to be changed, it can be accessed by removing only the upper panel. To access the batteries, the lower panel, attached to the payload mechanism, needs to be removed. All of the components are thus accessible by removing one panel. This means that the components can possibly be reused at the end of the UAV's lifetime. For a more detailed analysis of the recyclability of specific components, can be referred to Subsection 11.7.3.

17.4. Contribution to Sustainability

There are several ways in which the UAV can contribute to sustainability for future generations. One of the most important ones is that it can improve the efficiency of firefighting. The UAV uses visual light and thermal cameras, which can be used to quickly evaluate the situation and locate the fire. This can help the firefighters respond more adequately and instantly fighting the fire with the payload. With a reduced response time, the UAV can prevent the fire from spreading further, reducing property damage and environmental impact. Less property damage also means that more costly reconstructions can be prevented. This makes the UAV contribute to SDG 3 and 13 [83, 36].

The UAV will also have a large contribution to the safety of the firefighters. With the UAV, the risks of human life are drastically reduced. The UAV can locate dangerous areas accurately, which makes it possible for firefighters to work around those areas. It will thus contribute to Goal 3.

The 'traditional' firefighting methods were such that large amounts of water would be wasted. The newly designed UAV will spray water more precisely, which contributes to less water wastage. Fires in high-rise buildings can possibly release toxic gasses, which are harmful to the environment. By precisely and efficiently fighting the fire, the harmful pollutants can be reduced. The ecological balance will then be preserved, and there will be less impact on the environment and on human health. It contributes thus to SDG 3 and 13 [83, 36].

18
Feasibility Analysis

In this chapter, an analysis will be conducted to evaluate if the final design is feasible. First, the requirements compliance matrix will be set up in Section 18.1. With the matrix, it will be evaluated whether the requirements are met. The verification process for the requirements is outlined, and if requirements are not met, an explanation is given. Next, a sensitivity analysis will be done in Section 18.2, to assess the robustness of the design and the sensibility to change.

18.1. Requirements Compliance Matrix

The requirements compliance matrix assesses whether the requirements established at the beginning of the design phase have been met. It is presented in Table 18.1. It provides a clear overview of the compliance of the design with the requirements. Reviewing all requirements at this stage of the design ensures a successful outcome. A rationale is provided for how the requirement is verified. For requirements that are not met, a justification is given below.

Table 18.1: *Requirement compliance matrix*

ID	Requirement	Compliance	Verification/Rationale
USER REQUIREMENTS			
PERFORMANCE			
REQ-USER-P-1	The UAV shall be able to carry a minimum payload of 10 kg	Yes	The UAV will carry a payload of 18.6 kg
REQ-USER-P-2	The UAV shall have an average operational time of 20 min	Yes	The UAV has an average operational time of about 23 minutes
REQ-USER-P-3	The UAV shall be able to fit inside a fire brigade transport vehicle	Yes	The dimensions of the UAV can be seen in Figure 10.1a
REQ-USER-P-4	The UAV shall be equipped with a thermal camera	Yes	The UAV is equipped with the FLIR Lepton 3.5
REQ-USER-P-5	The UAV shall be equipped with a visual light camera	Yes	The UAV is equipped with the Hawkeye Camera
SAFETY			
REQ-USER-S-1	The UAV shall be controllable up to a minimum wind speed of 6 Bft	Yes	This is analysed in Section 11.5
REQ-USER-S-2	The UAV shall be equipped with a visual warning system	Yes	The UAV is equipped with LEDs to alert people on the ground
REQ-USER-S-3	The UAV shall be able to safely land in case of loss of signal	Yes	The UAV can be configured such that a failsafe will be triggered in case of signal loss
COST			

Continued on next page

Table 18.1 – continued from previous page

ID	Requirement	Compliance	Verification/Rationale
REQ-USER-C-1	The cost of the single unit shall not exceed € 25.000	Yes	The predicted cost of the UAV is € 24,777
REQ-USER-C-2	The UAV shall have a modular payload	No	The UAV is equipped solely with a water tank
REQ-USER-C-3	The UAV shall consist of at least 20% recyclable components.	Yes	Most components of the UAV at EOL can be recycled as discussed in Subsection 11.7.3
STAKEHOLDER REQUIREMENTS			
REQ-STAKE-1	The UAV shall perform the mission without causing additional damage	Yes	Sensors mounted on the UAV will prevent collisions and the pilot is a certified drone pilot, ensuring professional operations
REQ-STAKE-2	The UAV shall comply with EU regulations for unmanned vehicles	Yes	The UAV will be certified by EASA
REQ-STAKE-3	The UAV shall have minimum operating costs in comparison to competitors	UND	This requirement cannot be verified, as discussed in **Operational cost** (Section 18.1)
REQ-STAKE-4	The UAV shall be easily visible in unclear conditions	Yes	The UAV is equipped with multiple bright LEDs
REQ-STAKE-5	The UAV shall be operable in unfavourable weather conditions	Yes	This is analysed in Section 11.5
REQ-STAKE-6	The UAV shall not cause damage to the environment	Yes	The UAV is equipped with multiple sensors to ensure no collisions will occur during flight. Moreover, the UAV does not pollute the environment during its lifetime and at EOL
REQ-STAKE-7	The UAV shall be recoverable upon failure of one of its subsystems	Yes	The UAV's FC can trigger a failsafe upon detection of a system failure
REQ-STAKE-8	The UAV shall be easily deployable with minimum personnel	Yes	Two people are needed to lift the drone out of the car, one pilot is needed to fly the drone
REQ-STAKE-9	The UAV shall be monitorable at any point during the mission	Yes	The UAV is equipped with a visual camera and a GPS, which will transmit information to the controller
SYSTEM REQUIREMENTS			
REQ-SYS-1	The UAV shall have a minimum operational time of 20 min at an average T/W of 1.4	No	The UAV has an operational time of 16.5 minutes, a rationale is given in **Operational time** (Section 18.1)

Continued on next page

Table 18.1 – continued from previous page

ID	Requirement	Compliance	Verification/Rationale
REQ-SYS-2	The UAV shall have a vertical hovering accuracy of ±0.1 m in nominal conditions	TBD	This will be determined during testing, as discussed in Subsection 19.1.1
REQ-SYS-3	The UAV shall have a horizontal hovering accuracy of ±0.1m in nominal conditions	TBD	This will be determined during testing, as discussed in Subsection 19.1.1
REQ-SYS-4	The UAV shall be able to achieve a flight altitude of 250 m	Yes	The change in air density at this altitude will be negligible, hence this will not affect the performance. Additionally, the receiver has a range of 20 km and will thus not limit the UAV at an altitude of 250 m [27]
REQ-SYS-5	The UAV shall achieve a climb rate of 7 m/s	Yes	Figure 11.2 shows that with the minimum payload of 10 kg, the UAV will be able to achieve climb rates higher than 7 m/s
REQ-SYS-6	The UAV shall have the option to be controlled remotely.	Yes	The transmitter and receiver are discussed in Subsection 7.2.2
REQ-SYS-7	The UAV shall be able to operate in a 55°C environment for at least 120 seconds	Yes	The chosen components are able to operate at high temperatures and are where necessary protected by insulation
REQ-SYS-8	The UAV shall have a minimum MTBF of 100 operating hours	TBD	This will be determined during testing, but preliminary analysis is done in Section 16.1
REQ-SYS-9	The UAV shall have a maximum deployment time of 120 seconds	No	The deployment time will be 480 seconds in order to comply with the pre-flight safety checklist
REQ-SYS-10	The UAV shall have a maximum T/W ratio of at least 2.5	No	A rationale is given in **Thrust-to-Weight ratio** (Section 18.1)
REQ-SYS-11	The UAV shall be able to yaw at a rate of 90 deg/s	TBD	This will be determined during testing, as discussed in
REQ-SYS-12	The UAV shall have a Turn Around Time (TAT) between flights of at most 300 seconds	Yes/No	The TAT is 300 seconds only if no batteries are changed, this is discussed in more detail in **Operational efficiency** (Section 18.1)
REQ-SYS-13	The UAV shall be able to deliver the payload from a horizontal distance of at least 4 m	Yes	The minimum range of 4 meters will be met, as discussed in Subsection 5.3.3
REQ-SYS-14	The UAV and its payload shall be water resistant	Yes	The UAV is designed to be water resistant, as discussed in Section 10.1

Continued on next page

Table 18.1 – continued from previous page

ID	Requirement	Compliance	Verification/Rationale
REQ-SYS-15	The UAV shall not exceed an empty mass of 50 kg	Yes	The empty mass of the UAV is roughly 37.8 kg, as discussed in Section 10.1
SUBSYSTEM REQUIREMENTS			
PROPULSION			
REQ-SYS-PROP-1	The propulsion system at max throttle shall be able to achieve a T/W of 2	Yes	This is established in Section 11.4
REQ-SYS-PROP-2	The propulsion system shall be fully compatible with the power system	Yes	A discussion on the propulsion system can be found in the Midterm Report [56]
POWER			
REQ-SYS-POW-1	The power system shall be able to withstand temperatures up to 55°C for 120 seconds	Yes	The power system will be able to operate at temperatures above 55 ° C [17]
REQ-SYS-POW-2	The power system shall be replaceable within 120 seconds	No	Due to safety procedures, the battery replacement procedure will take 180 seconds
ELECTRONICS			
REQ-SYS-ELEC-1	The UAV shall have an on-board flight controller	Yes	The UAV uses the CubePilot Cube Orange flight controller, as discussed in Subsection 7.2.1
REQ-SYS-ELEC-2	The UAV shall be operable from ground control stations	Yes	The UAV is equipped with a telemetry system
REQ-SYS-ELEC-3	The UAV shall have a recovery system in case of loss of connection	Yes	The UAV can be configured such that a failsafe will be triggered in case of a loss of connection
REQ-SYS-ELEC-4	The UAV shall have a communication range of at least 300 m	Yes	The communication range is 20 km, as discussed in Subsection 7.2.2
REQ-SYS-ELEC-5	The UAV electronics shall integrate all the sensors	Yes	The integration of the sensors is shown in Section 7.4
PAYLOAD			
REQ-SYS-PAY-1	The thermal camera shall have a thermal sensitivity of at least 1 °C	Yes	The FLIR Lepton 3.5 has a thermal sensitivity of 0.050°C [149]
REQ-SYS-PAY-2	The light camera shall have a minimum frame rate of 30 fps	Yes	The Hawkeye Firefly 4K Nakedcam has a frame rate of 60 fps [52]
REQ-SYS-PAY-3	The cameras shall have active stabilisation measures	Yes	The cameras will be mounted on a gimbal to provide stabilisation

Continued on next page

Table 18.1 – continued from previous page

ID	Requirement	Compliance	Verification/Rationale
REQ-SYS-PAY-4	The cameras shall be able to operate in an environment of 55 ° C for 120 seconds	Yes	The thermal camera has an optimum operating temperature of up to 80°C [149], the visual camera will be protected by insulation material
REQ-SYS-PAY-5	The UAV shall be equipped with sensors for measuring altitude	Yes	A LiDAR will be used to measure altitude
STRUCTURE			
REQ-SYS-STR-1	The UAV structure shall be able to support a payload of at least 10 kg	Yes	An analysis of the forces and stresses in the UAV is done in Section 8.4
REQ-SYS-STR-2	The UAV structure shall be able to withstand the ultimate load factor of 3	TBD	This will be determined during testing, as discussed in **Awaiting verification** (Section 18.1)
REQ-SYS-STR-3	The UAV structure shall be able to support all the other subsystems	Yes	This is shown in Section 10.3
REQ-SYS-STR-4	The UAV structure shall allow for disassembly	Yes	It is possible to disassemble the UAV as discussed in Section 10.3
SUSTAINABILITY REQUIREMENTS			
REQ-SUS-1	The UAV shall use a clean energy source	Yes	The UAV is powered by two LiPo batteries
REQ-SUS-2	The UAV shall only use non-toxic extinguishing agents	Yes	The UAV will use water to extinguish fire
REQ-SUS-3	The UAV shall use biodegradable extinguishing agents	Yes	The UAV will use water to extinguish fire
REQ-SUS-4	An End-of-Life (EOL) strategy shall be implemented to improve sustainability	Yes	An EOL strategy is applied, as discussed in Section 17.3

Modular payload After analysing the possible trade-off options (Chapter 5), it was concluded that a water tank with a pressure pump was the most optimal payload design. This means REQ-USER-C-2 is not met. However, the current payload configuration outperforms the other options and is refillable.

Operational cost Requirement REQ-STAKE-3 on the operational cost cannot be assessed, as no information is available on the operating cost of competitors.

Operational time The operational time of the UAV at a T/W of 1.4 is lower than required for REQ-SYS-1. However, during the design process of the UAV, it was decided to put more emphasis on how to perform the mission as optimally as possible. The final payload mechanism design is made for much larger quantities of water, as the water pump used is high pressure with a flow rate of 26.495 LPM. It is more valuable to maximise the payload delivered per minute, by increasing the amount of water delivered, rather than having a longer flight time for the mission. That being said, the average flight time achieved is 22 minutes, and the mission is designed to have a fast refuelling time and maximise the amount of runs, so as to deliver large quantities of water to the high-rise floors.

Operational efficiency Due to safety procedures, replacing the battery will take 180 seconds. This poses a possible issue for REQ-SYS-12 and a definitive issue for REQ-SYS-9 and REQ-SYS-POW-2. REQ-SYS-12 can be met in case no battery replacement takes place, as the TAT will then be 300 seconds, complying with the requirement. Replacing the batteries will introduce an additional 180 seconds, as discussed in Section 11.4.

Thrust-to-Weight ratio For the preliminary design stage, in which many weight parameters are still unknown, it is important to choose motors and propellers capable of performing at a much higher level than necessary. This is because as the design gets more detailed, more unknown weight is added, and in order to avoid having a design that cannot handle these weight additions, an exaggerated T/W was chosen. However, at this stage, the exact weights of all components are known, and the weight estimation is realistic. For this mission, a T/W ratio of a minimum of 2 is required. This value was taken into account in the payload optimisation in Section 11.4, in order to maximise the payload delivered to the high-rise building, rather than an over-designed T/W ratio. However, at a lower payload weight, this requirement can be met.

Awaiting verification Some requirements cannot be verified yet in this stage of the design. This applies to REQ-SYS-2, REQ-SYS-3, REQ-SYS-8, REQ-SYS-11, and REQ-SYS-STR-2. It will be shortly discussed how these requirements will be verified at a later stage.

It is challenging to evaluate the drone's hovering accuracy during the design process. As a result, this will be examined during the wind tunnel test in the testing phase and therefore compliance with REQ-SYS-2 and REQ-SYS-3 cannot be confirmed yet. Given that the drone has a GPS and a flight computer with two barometric pressure sensors, three accelerometers, three gyroscopes, and a compass, it is certain to have the ability to hover.

The yaw rate will be obtained through a test flight of the UAV. Data can be obtained through the IMU and/or through visual inspection. Hence, compliance with REQ-SYS-11 can not be determined yet. Likewise, the Mean Time Between Failure (MTBF) will be determined through testing, resulting in verifying REQ-SYS-8 at a later stage. REQ-SYS-STR-2 related to the ultimate load factor can be verified through simulating load conditions. Using Finite Elements Methods the stress distribution can be analysed under different loading conditions leading to the ultimate load factor.

18.2. Sensitivity Analysis

In this section, the sensitivity analysis of the drone will be presented. The purpose is to discover the margin of values possible in which the drone still meets the system requirements when major parameters are changed. The major system parameters are the motor, battery capacity and payload weight. Firstly, an analysis of the minimum motor thrust which will meet the requirements will be made, as well as an analysis of the maximum take-off weight and T/W ratio with respect to the payload. Then, a sensitivity analysis on battery capacity and battery amount will be performed.

18.2.1. Motor Thrust and Payload

The final weight estimation which will be used for this analysis can be found in Table 10.1. The maximum take-off weight which will be used is 56.235 kg. This is a "dry" mass (no payload) of 37.739 kg, with an 18.6 kg payload. This was decided in Section 11.4, where an optimisation for the maximum amount of payload delivered per minute by the drone was calculated. The maximum thrust achieved by the motor [159] with the propeller and ESC combination chosen is 18.8 kg per motor. The payload was maximised for the amount of thrust available so that the drone reaches the minimum T/W ratio requirement of 2.0, which it reaches exactly with 18.6 kg of payload. This means there is little margin for change in this part of the design. The initial payload designed for is 10 kg. With this, the drone can achieve a maximum T/W ratio of 2.4, and an average flight time of 26.7 minutes. The full analysis and trade-off of motor combinations and T/W can be found in the Midterm Report [56]. In case the specific motor chosen is no longer available, there is an extensive analysis of six other motors which are potential candidates for the mission.

18.2.2. Battery

Changing the battery has a huge effect on the performance of the drone. Based on battery capacity and the number of batteries, the performance can change drastically. In the Midterm Report [56], a full optimisation of these battery characteristics was made, until the ideal capacity, battery weight and battery amount were found. This was two batteries of 12 S, 46 Ah, at 9,5 kg, with a maximum discharge rate of 287 A [17]. This combination can provide the drone with 19.45 minutes of flight time at a T/W ratio of 1.4, and a maximum T/W ratio of 2. This is essentially just meeting the requirements. Several changes can be made to test out the sensitivity of the drone design to the battery.

If one more battery is added, to make three total on board, the endurance requirement is met at 22 minutes of flight time at T/W of 1.4, but the maximum T/W drops to 1.7. This means adding a battery of the same type will affect the drone negatively.

If the battery capacity is halved, to 22 Ah, such that the weight is also decreased to 5050 g [20], the T/W ratio increases by 15%, to 2.3. However, the flight time reduces to 12.25 minutes, decreasing by 36% from the initial design. The performance does not improve with lighter batteries.

If the battery capacity is halved again to 11Ah, and it weighs 2.53 kg [22], more batteries must be added to achieve similar performance, as two will not be sufficient for meeting requirements. Comparable performance to the other two batteries is when the drone is powered by six batteries of this type. The flight time at 1.4 T/W reaches 15.6 minutes, and the maximum T/W is 2.2. This is a good result, but not as good as the original choice. Adding batteries adds complexity, so it is now obvious that higher capacity is better.

Raising the capacity to 62 Ah is the last change to look at. This battery weighs 13.3 kg [18], and powering the drone with two of those has the following results. The flight time at a T/W of 1.4 increases by 9%, at 21.1 minutes. The maximum T/W ratio can only reach 1.8 however. This does not meet the requirements.

It is concluded that while changing battery amount and capacity can affect the drone, in this case, the optimal solution has been chosen, as it is the only one where both requirements of flight time and T/W are met. The full process of battery selection can be examined in detail in the Midterm Report [56].

18.2.3. Conclusion

This design has been extensively analysed for the best option possible when looking at motors, batteries and the amount of payload. The aim of the sensitivity analysis is to find the maximum values of each parameter at which the drone still meets the requirements. Looking at the sensitivity analysis results, the current motor, battery and payload parameters are at their maximum best performance limit. This makes the current drone the best possible robust solution for the mission. On the other hand, the drone is sensitive to changes, as decreasing the performance of any parameters would lead to requirements not being met, such as the T/W ratio.

19
Project Design and Development Logic

The challenging activities to produce a new and innovative product do not stop after the completion of this report. The research done during these ten weeks is the starting point of a more extensive, longer development process for the drone. With the hopes of one day being used in fire departments around the world to be deployed in fires in high-rise buildings and saving lives. In this chapter the activities planned post-DSE will be presented. First, a flow chart denoting all the activities will be shown in Section 19.1. Next, a timeline of the activities will be shown in Section 19.2. Lastly, possible rotor material for further research and rotor optimisation will be presented in Section 19.3 and Section 19.4, respectively.

19.1. Post-DSE Flow Chart

The post-DSE activities have been broken down into three stages and are shown as a flow chart in Figure 19.2. The first part is the finalising of the design stage. Any last iterations which will be made through the guidance of the tutors and external TU Delft faculty will be implemented, to ensure the design is ready to manufacture. Next, there is the development stage. This is when the drone will be manufactured, all the components and wiring will be completed, and the software and control system will be developed. A prototype will first be produced before production on a larger scale starts. The manufacturing of the drone is discussed in more detail in Chapter 13. Furthermore, during this stage, the testing of the powertrain, control system, payload system and all other components will take place. Afterwards, the drone will be certified for flight by European Union Aviation Safety Agency (EASA). Testing and certifying will be discussed in more detail below. Besides that, documentation will be prepared during this stage, including among others test reports, specifications and a user manual. This stage is critical for the success of the project. Finally, a service and maintenance program will be set up for the drone to ensure optimal durability and optimal functioning of the drone. Additionally, during the commercial stage, the drone will be sold and perform its mission for the Dutch fire brigade, and hopefully, revolutionise fire fighting around the world.

A Gantt chart has been created to show all activities on a time scale and their respective dependencies. It can be found in Figure 19.1. The activities are discussed in more detail in the flow chart.

19.1.1. Testing

To evaluate the performance of the drone during all circumstances, testing will be performed. The structural performance of the design will be assessed to determine the load-bearing capacity, overall strength, and durability. Additionally, the safety of the design will be examined, by making sure there are no sharp edges and no fingers can get trapped when changing the payload or batteries. The drone will then be tested in a wind tunnel, where wind will be applied from multiple directions at a slowly increasing speed. Through this, the maximum wind resistance of the drone can be obtained, as well as its hovering accuracy and reactivity to return to the original hovering position [99]. Moreover, the efficiency of the motor-propeller combination over a range of different throttle settings and velocities can be analysed [120]. However, testing in a wind tunnel might be difficult due to the large size of the drone, and additionally comes at a high-risk. If a part comes loose during testing, this could result in great damage to the wind tunnel, resulting in high costs. The field lab Unmanned Valley in Katwijk aan Zee offers extensive indoor and outdoor testing and might therefore be a more preferable option [137].

Furthermore, the drone will be exposed to the environmental conditions which it will experience during its lifetime, such as high temperatures and rough weather conditions. The electrical components, payload mechanism, and datalink performance will be examined. During this stage, the signal obscuration and multipath effects dur-

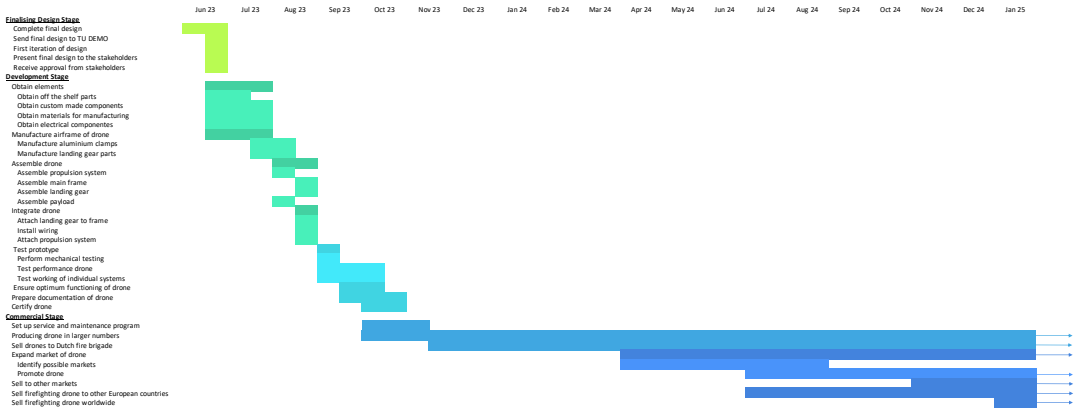

Figure 19.1: *Gantt chart of post-DSE activities*

ing operation will be tested as well as how the UAV will operate in urban environments. The final test phase is the flight tests, through which performance parameters can be determined, such as the drag polar [120].

Based on the result obtained during the testing phase, slight improvements might have to be made to the design to obtain the optimum performance.

19.1.2. Certifying

The drone will be operated in the, as by EASA defined, “specific” category [67]. When operating in this category, the competent authority of registration has to provide an operational authorisation [66]. The risks on the ground and in the air have to be analysed within the specific assurance and integrity level (SAIL). Based on the SAIL, operational safety objectives (OSOs) can be identified, which have to be met with a certain level of robustness. High Specific Assurance and Integrity Level (SAIL)s require design verification by EASA. When applying for the design verification, data has to be provided to EASA, including among others a detailed design description and a risk assessment. Upon approval, the EASA provides a design verification report, including limitations and conditions for its validity [66].

19.2. Post-DSE Timeline

Figure 19.3 shows the timeline of the central post-DSE activities that are presented in the post-DSE flow chart, discussed in Section 19.1. The timeline displays the different tasks and their duration as well as the estimated dates at which they will take place. Since the exact progress of the project is unpredictable, the dates are roughly estimated and may take less or more time, depending on several factors.

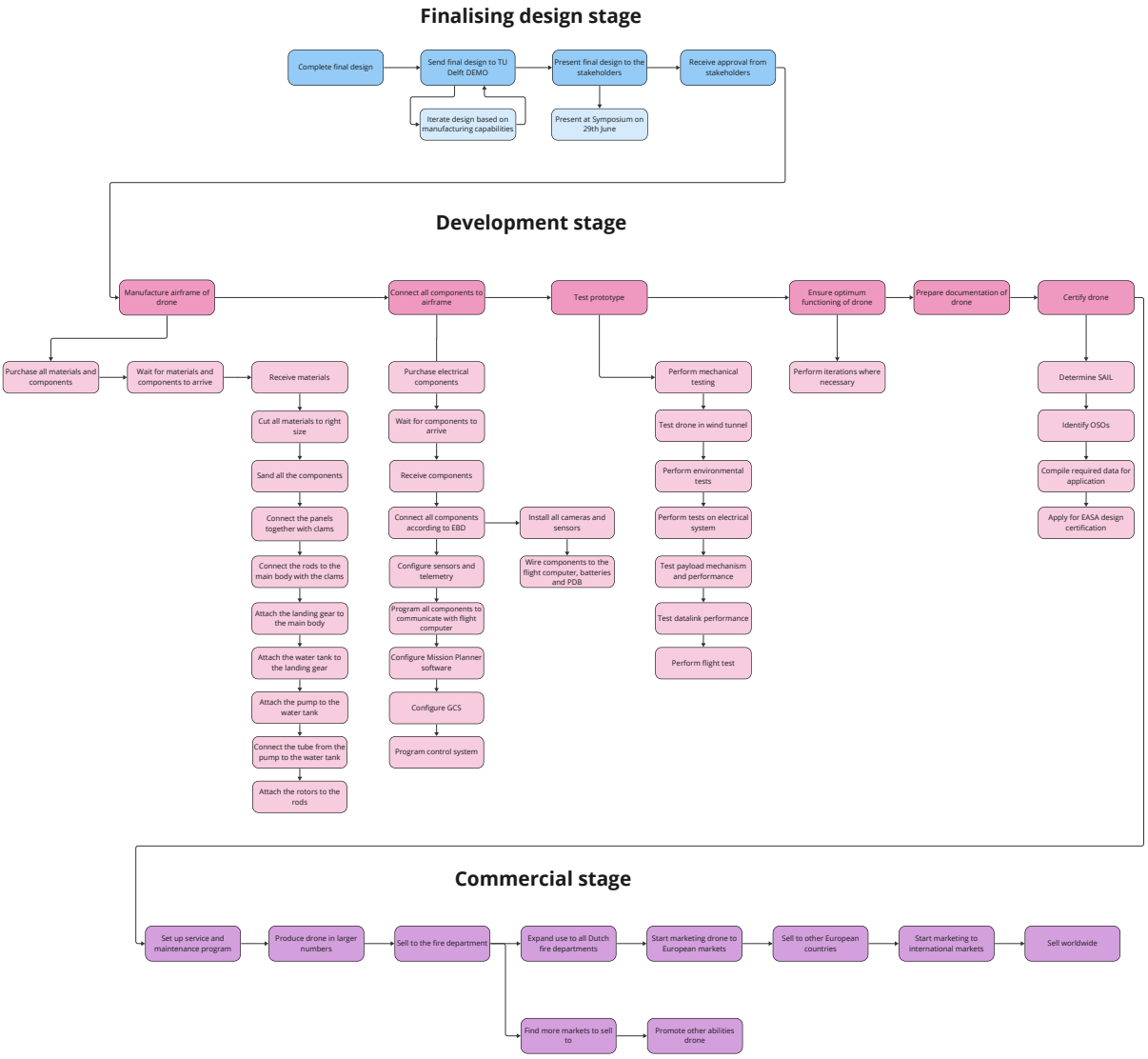

Figure 19.2: *Flow chart of post-DSE activities*

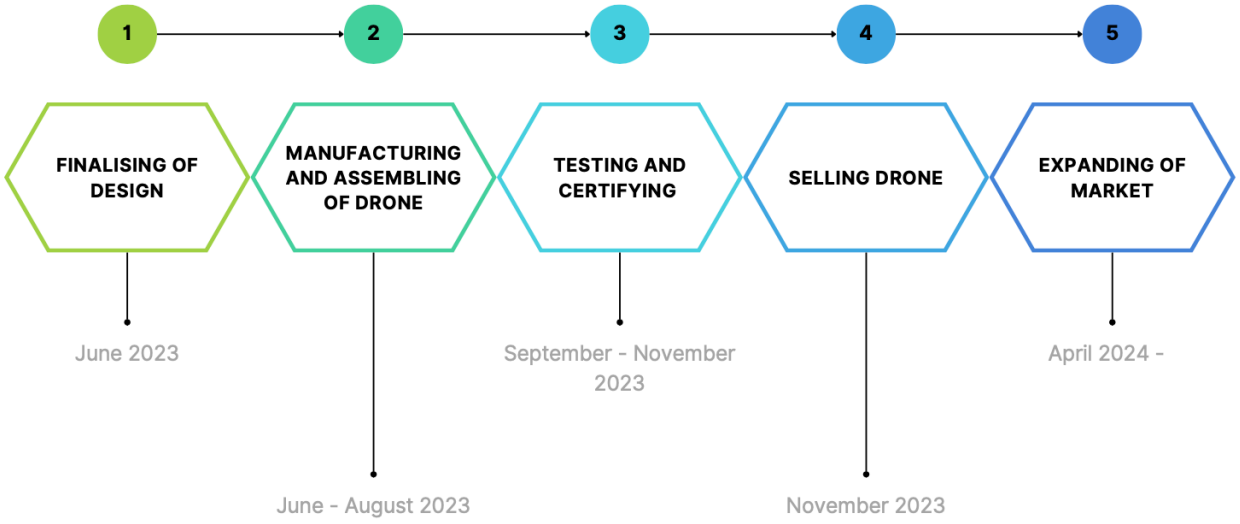

Figure 19.3: *Timeline of post-DSE activities*

19.3. Rotor Material

During the design phase of the UAV, it was decided to use off-the-shelf rotors. However, in the future, there might be an opportunity to design and manufacture the rotors to improve the performance of the drone even further. Therefore, this section will analyse various possible materials and examine the characteristics of the rotor in order to perform rotor optimisation.

The three most commonly used materials for rotors in drones are carbon fibre, fibreglass, and aluminium. These materials offer a balance of strength, stiffness, and vibration-damping properties making them ideal for rotor construction. These materials will be further discussed below. Furthermore, the use of magnesium-based materials will be looked into.

Carbon Fibre

Carbon fibre is a lightweight and high-strength material, widely utilised in the aerospace industry. It is composed of thin, intertwined carbon strings bonded together with a polymer matrix. Carbon fibre offers exceptional stiffness, allowing it to resist deformation and maintain stability during rotor operation. The high strength-to-weight ratio of carbon fibre enables the creation of rotor blades that are both lightweight and robust, enhancing the manoeuvrability and efficiency of the drone.

The vibration-damping properties of carbon fibre are particularly advantageous. The composite nature of carbon fibre helps absorb and disperse vibrations, reducing the impact of oscillations on the drone's performance. Furthermore, carbon fibre possesses a high fatigue resistance, ensuring durability and long-term reliability of the rotor system [177].

Fibreglass

Fibreglass is a widely used material known for its versatility and cost-effectiveness. It is composed of fine glass fibres embedded in a resin matrix. Although fibreglass may not offer the same level of strength and stiffness as carbon fibre, it still provides sufficient rigidity for rotor applications. Fibreglass rotors are lightweight and can effectively dampen vibrations, contributing to improved flight stability and control.

Fibreglass also boasts excellent corrosion resistance, making it suitable for operation in various environmental conditions. Additionally, its affordability compared to carbon fibre makes it an attractive option for drone manufacturers aiming for cost-effective solutions without compromising performance [175].

Aluminium

Aluminium is a lightweight metal that offers favourable mechanical properties for rotor construction. It possesses good strength and stiffness, making it suitable for rotor blades that require both stability and durability.

Although aluminium may not have the same vibration-damping characteristics as composite materials like carbon fibre and fibreglass, it can still effectively mitigate vibrations when designed properly [142].

Magnesium-based

In recent years, there has been growing interest in exploring the potential of novel magnesium-based materials for drone rotor construction. These materials offer unique characteristics that make them appealing options for rotor design, including their low density, high strength-to-weight ratio, and vibration-damping properties [89].

Magnesium possesses a remarkably low density, making it an ideal choice for producing lightweight rotors. This characteristic allows for faster response times when changing the RPM since less force is needed to speed up the RPM which gives improved manoeuvrability [89]. By reducing the weight of the rotor, drones can carry heavier payloads or extend their flight time without compromising performance.

Furthermore, magnesium alloys exhibit a high strength-to-weight ratio, ensuring the structural integrity and durability of the rotor. The use of these materials can significantly reduce the risk of damage or failure during operation, increasing the overall reliability of the drone.

While magnesium-based materials offer significant advantages, it is important to address certain challenges. Magnesium is prone to corrosion, particularly in the presence of moisture or harsh environmental conditions. To mitigate this issue, proper surface treatments and protective coatings must be applied to ensure the longevity of magnesium-based drone rotors.

Discussion

As discussed in the Midterm Report, the rotor for the drone will be purchased off-the-shelf, and it will be made out of carbon fibre [56]. Given that the data and specifications are based on this particular material, it is not feasible to select a different material for the rotor at this time. However, in the future, if there is an opportunity to manufacture the rotor independently and conduct tests with various materials, alternative options can be considered.

For now, it is essential to adhere to the current plan of using a carbon fibre rotor. Carbon fibre has been chosen based on its known properties and suitability for rotor applications. Its lightweight nature, high strength-to-weight ratio, and excellent vibration-damping properties make it an ideal choice for ensuring optimal performance, stability, and efficiency of the drone.

While it is acknowledged that there may be other materials that could potentially offer different advantages, the decision to utilise carbon fibre for the rotor is based on the existing data and the availability of off-the-shelf options. It is important to follow the established plan to ensure the successful operation of the drone. If circumstances permit in the future, further exploration and experimentation with different materials and other factors such as pitch angle, the diameter of the rotor, and RPM be pursued to potentially enhance the rotor's performance and capabilities.

19.4. Future Aerodynamic Analysis

Before the process began, a literature study was conducted. The primary aim of this literature study was to ascertain the viable ranges of propeller diameters and pitch angles and determine which factors play an important role in getting a propeller with the best performance. These parameters are crucial when calculating thrust and torque requirements for the propellers. The literature study revealed three significant aerodynamic effects of the propellers that needed consideration: the vortex ring state, wake interaction and the propellers' airflow stalling.

The propeller material choice determines the Rotations Per Minute (RPM). Handling capability is of great importance as exceeding the RPM limits can cause propeller breakage and ejection at high velocities, potentially damaging the hexacopter. The important propeller parameters are the diameter, pitch, blade count, aspect ratio, and the maximum RPM.

With the assistance of the general parameters and information about the propeller, the propeller modelling process can begin. Equations from "Introduction to multicopter design and control" encompass the modelling

equations for Thrust, Torque, Thrust coefficient, Torque coefficient, and Drag coefficient[129]. Combining the formulas results in the thrust.

With this, the Thrust to Weight ratio (T/W) can be calculated and compared to different types of rotors. It is important that the manufacturers provide information about the rotors. When the thrust is known, the efficiency of the propeller can be calculated using Equation 19.1.

$$\eta_{\text{prop}} = \frac{T}{M \cdot N} \cdot 100 \tag{19.1}$$

Rotor Aerodynamics

There are five main aerodynamic effects that act on a rotor [152]. The ground effect, T_{IGE}, refers to the phenomenon where aerodynamic objects increase their lift force by reducing aerodynamic drag when in close proximity to the ground. It occurs when any solid body is in motion through a fluid medium. During landing, the ground effect can make the aircraft feel as if it is "floating".

H represents the hub force, which is the horizontal component acting on each rotor blade element. The roll moment, RM, is the moment of force caused by the sprung mass of the vehicle, specifically the portion of its weight supported by the tires. For example, the roll moment occurs when an aircraft leans toward the outside of a turn. Roll moments are typically caused by wind gusts, control surfaces (such as ailerons), or flying at an angle of sideslip. Q represents the drag force that opposes the forward motion of the aircraft, creating resistance.

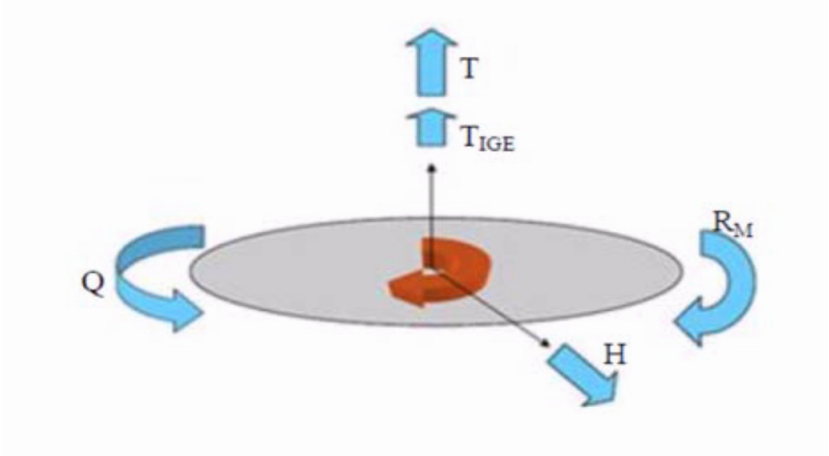

Figure 19.4: *Aerodynamic forces [152]*

The rotation of the blades on a multi-rotor drone generates turbulence known as wake interaction due to the airflow across the blades. Compared to fixed-wing drone systems, multi-rotor drones produce more wake interaction. This turbulence can lead to uncontrollable movements, ultimately affecting the overall drone performance [152]. The wake flows in a downward funnel shape from the rotor blades, causing prop wash that moves radially away from the propeller [43]. In their study, they maintained a distance of 1 inch between the propeller tips to prevent interference.

The selection of a rotor system platform for drone development is determined by the arrangement of rotors and the method of drone control. Controlling a rotorcraft involves manipulating control inputs during flight to achieve controlled aerodynamic movement. These control inputs are transferred to the rotor system, which generates aerodynamic effects on the rotor blades, enabling effective drone control [152]. The drone must also achieve control over heave, pitch, yaw, and roll. Pitch and roll control inputs affect the longitudinal and lateral motion of the drone [93]. Yaw control inputs cause the drone to rotate angularly around its vertical axis, while heave control inputs control vertical movement along the axis.

The Vortex Ring State (VRS), also known as settling with power, is an aerodynamic phenomenon in which the propellers become surrounded by a torus-shaped vortex [123]. This vortex ring is formed when a moving fluid

is introduced into a stationary fluid, causing friction between the two masses. This friction leads to the rotation of the outer core of the torus inwards, initially decelerating the fluid. However, the continuous injection of moving fluid results in its acceleration.

The stalling of the flow at the propeller blade is another aerodynamic effect that must be taken into consideration. A propeller functions as an airfoil, and when the angle of attack becomes excessively large, the airfoil will stall. A higher propeller pitch increases the likelihood of stalling at low speeds, but if the pitch is too low, it will result in reduced thrust at high speeds [182]. Therefore, it is crucial to select a propeller with a balanced pitch, avoiding both excessively high and low pitches.

The propeller pitch refers to the theoretical distance a propeller would move forward during a single revolution. It plays a significant role in determining the amount of thrust that can be generated [29]. The number of blades used combined with the pitch angle has an impact on the T/W. As the designer has a certain range for the T/W those two can be used to influence that. As can be seen in Figure 19.5, for different pitch angles and numbers of blades, different T/W ratios can be determined.

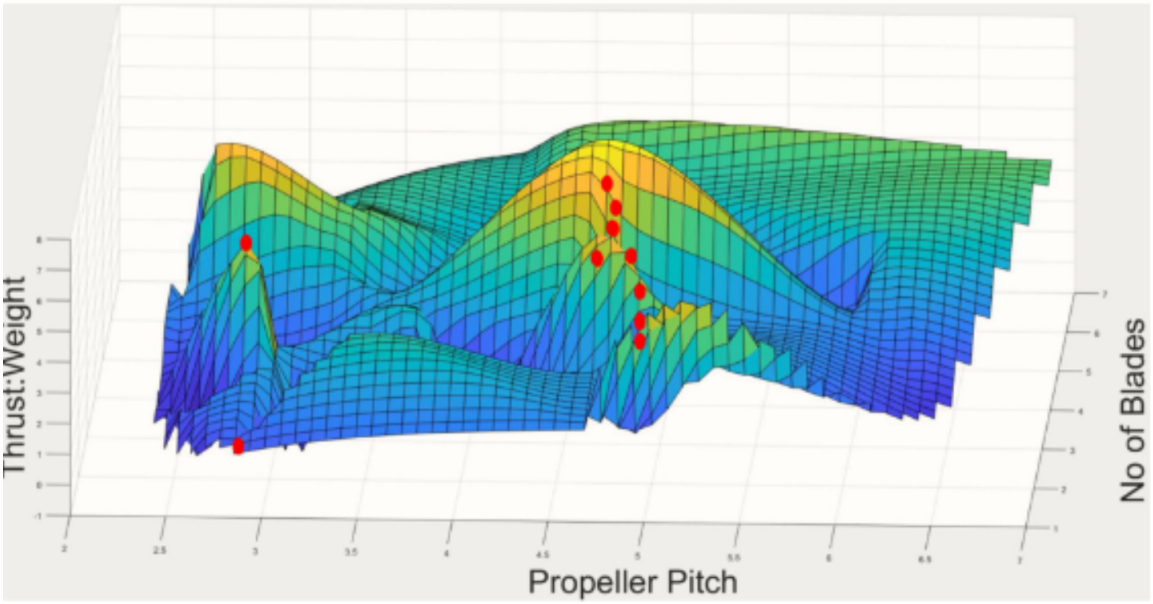

Figure 19.5: *The T/W ratio graph by using different pitch angles and number of blades [113]*

20

Conclusion and Recommendations

The goal of this project was to aid firefighters in combating fires in high-rise buildings by providing quick extinguishing capabilities for top-level floors. This report aimed to summarise the steps taken up to the final stage of the project and to provide a detailed description of how the design was developed. For every step taken, a detailed description was given and the result of each step was discussed. Future steps were given in a general overview.

First, the correct power source was searched, for which multiple options were considered, such as chemical, electrochemical and electrical sources. After considering the different sources, it was decided that lithium polymer (Li-Po) was the best option currently available. The other power sources were not as suitable in terms of performance and/or availability. Next, for the propulsion system, a large variety of design options were presented and discussed. Before determining the best configuration, thorough research was performed to identify market-leading LiPo batteries, motors and their corresponding rotors. With all these different combinations, a trade-off was performed. From this, it was found that the optimal configuration was a hexa-rotor with 32-inch propellers and two Li-Po batteries.

Next, the different possibilities for the payload mechanism were considered. Every option was analysed and a trade-off was conducted. The water tank with a pressurised pump came out as the final decision. The tank will have a volume of 20 L and the pump will have a flow rate of 26.5 LPM. Next, the required electrical components were investigated and selected based on their performance and compatibility. The drone is equipped with sonar sensors and LiDARs for optimal distance and altitude measurements. In addition, a thermal camera and visual light camera allow for situational awareness during the mission.

After the electronics were decided on, a decision was made to place the six rotors in an X-frame. The rotors are connected to the main airframe via carbon fibre rods. The main body consists of three similar carbon fibre sandwich panels, cut as hexagons, placed on top of each other. The batteries are placed within the layers, while the electrical components are placed on top of the upper layer, protected by a cover. The water tank and pump are attached to the landing gear of the drone, which in its turn are attached to the bottom of the drone.

After the general design of the drone was done, a control and stability analysis was performed. From this, the rotation configuration of the rotors was decided on. To ensure sufficient controllability, three rotors will have a clockwise rotation and three rotors will have a counter-clockwise rotation. This configuration was also chosen for redundancy in case of single rotor failure.

The analysis of the mission profile concluded that the mission can be divided into six consecutive steps. The operational time of the entire mission depends on both the payload and the height the drone has to achieve during the mission. After thorough analysis and calculations, it was concluded that a payload of 2.2 kg per minute can be delivered with full batteries. During the entire mission, it is possible to deliver a total of 140 kg payload. The total cost to produce one UAV is estimated to be €25,000.

To ensure a sustainable design, three aspects were looked into. These are the extinguishing agents and the energy sources used, and the End-of-Life (EOL) of the UAV. Since water was chosen as the extinguisher agent, it can be said that the extinguishing agent is non-toxic and biodegradable. To charge the batteries, clean sources such as wind energy or solar energy will be used. Above all, the drone is modular, which means that components can be individually replaced. Lastly, the main material used is carbon fibre. The characteristics of this material ensure a long lifetime. It can also be concluded that the drone contributes to SDG 3 and 13. The UAV can prevent the

deaths of both firefighters and victims and by fighting the fire more effectively and faster, greenhouse emissions will decrease.

To conclude, the proposed design was found to be feasible and promising. The drone will be capable to aid the Dutch fire brigade in missions, specifically for high-rise buildings. To ensure a feasible design, advice was sought from multiple external sources to gain a more in-depth understanding of various topics

Recommendations

Apart from testing and more in-depth rotor and aerodynamic analysis, other research can still be done. These subjects are less urgent, however, are still valuable to look into.

Firstly, the nozzle can be easily changed and has a large influence on the firefighting capabilities. By changing the nozzle, the droplet size and jet angle of the water stream can be influenced [181]. This has an effect on the fire fighting capabilities since smaller droplets will evaporate quicker, dampening fires more effectively. However, smaller droplets will also decrease the range and reduce the amount of water actually reaching the target as more water will be lost along the firing trajectory. Hence, analysing the most effective droplet size and finding the corresponding nozzle can increase the effectiveness of the drone.

Secondly, the current design is only capable of using water. Although this will be effective for most high-rise building fires, having other suppressant agents available will improve deployment ability. Hence researching pumps that can resist more aggressive fluids or foams is valuable. Furthermore, the pressurised tank design can be further analysed. However, this would require extensive research into safety and certifications and therefore be less effective.

Finally, off-the-shelf products were chosen. In future research, custom design and manufacturing of components can be looked at to improve the performance of the drone. One of these is the rotors for example. The rotors can be optimised by considering various possible materials and examining the characteristics of the rotor.

References

[1] Abhiskhek Ghosh. *Aerogel or Frozen Smoke or Blue Smoke*. https://thecustomizewindows.com/2012/08/aerogel-or-frozen-smoke-or-blue-smoke/. Sept. 2012.

[2] Advanced Power Drives. *PDB500*. https://powerdrives.net/pdb500.

[3] European Union Aviation Safety Agency. *Guidelines on Noise Measurement of Unmanned Aircraft Systems Lighter than 600 kg Operating in the Specific Category (Low and Medium Risk)*. TE.RPRO.00034-011. European Union, Oct. 2022.

[4] Betsy Chesnutt Alireza Farvard. *Small-Angle Approximation: Formulas, Proofs & Applications*. Feb. 2022.

[5] Product Marketing Alliance. "How to Calculate the Perfect Product Selling Price". In: *Product Marketing Alliance* (July 2021).

[6] Amazon. *Clear Vinyl Tubing*. https://www.amazon.com/Tubing-Flexible-Hybrid-Lightweight-10-Feet/dp/B07HF4SYWY/ref=sr_1_3?keywords=1%2F2+Tube&qid=1686643032&sr=8-3.

[7] Amazon. *Radiolink R12DS 2.4GHz DSSS Receiver*. https://www.amazon.com/Radiolink-R12DS-2-4GHz-DSSS-Receiver/dp/B07G32VQCL.

[8] ArduPilot. *APM Copter Programming: Attitude Control*. https://ardupilot.org/dev/docs/apmcopter-programming-attitude-control-2.html.

[9] ArduPilot. *Ardu Pilot Extended Kalman Filter*. https://ardupilot.org/dev/docs/extended-kalman-filter.html.

[10] ArduPilot. *Ardu Pilot Software Architecture*. https://ardupilot.org/dev/docs/apmcopter-code-overview.html.

[11] ArduPilot. *Battery Failsafe*. https://ardupilot.org/copter/docs/failsafe-battery.html. 2023.

[12] ArduPilot. *CUAV V5 Plus Overview*. https://ardupilot.org/copter/docs/common-cuav-v5plus-overview.html. 2023.

[13] ArduPilot. *SiK Telemetry Radio*. https://ardupilot.org/copter/docs/common-sik-telemetry-radio.html.

[14] Ashish Kumar Srivastav. *Rate of Return on Investment (ROI)*. https://www.wallstreetmojo.com/rate-of-return-on-investment/.

[15] Avy. *Drones for firefighters*. https://avy.eu/stories/drones-for-firefighters/#:~:text=Firefighting%20drones%20in%20the%20EU&text=The%20implementation%20of%20drones%20by,by%20providing%20real%2Dtime%20data..

[16] Vivekananthan Balakrishnan et al. "Thermal Flow Sensors for Harsh Environments". In: *Sensors* 17.9 (2017), p. 2061. DOI: 10.3390/s17092061.

[17] Maxamps Lithium Battery. https://maxamps.com/products/lipo-46000-12s-44-4v-battery-pack.

[18] Maxamps Lithium Battery. https://maxamps.com/collections/12s-lipo-battery-44-4v/products/lipo-62000-12s-44-4v-battery-pack.

[19] Maxamps Lithium Battery. https://maxamps.com/products/lipo-34000-12s-44-4v-battery-pack.

[20] Maxamps Lithium Battery. https://maxamps.com/products/lipo-22000-44-4v-12s-battery-pack.

[21] Maxamps Lithium Battery. https://www.adorama.com/fralta12ssb.html.

[22] Maxamps Lithium Battery. https://maxamps.com/products/lipo-11000-12s-44-4v-battery-pack.

[23] Northeast Battery. *Battery 101: How to Prolong the Life of Your Lithium Battery*. https://northeastbattery.com/prolong-lithium-battery-life/. Feb. 2021.

[24] Ofodike A. Ezekoye Ben Trettel. "Theoretical range and trajectory of a water jet". In: *5 International Mechanical Engineering Congress and Exposition* (2015).

[25] Archy de Berker. *Understand Your Aluminum Emissions*. https://www.carbonchain.com/blog/understand-your-aluminum-emissions.

[26] Bilgepompen.nl. *Membraanpomp*. https://bilgepompen.nl/membraanpomp-drinkwaterpomp-24v-189-lmin-38-bar/92043813-p-43813.html. 2023.

[27] Team BlackSheep. *Crossfire Nano RX*. https://www.team-blacksheep.com/products/prod:crossfire_nano_rx.

[28] Team BlackSheep. *Crossfire Nano RX - Quickstart guide*. https://www.team-blacksheep.com/media/files/tbs-crossfire-nano-quickstart.pdf. Apr. 2021.

[29] BoatUS. *How to Choose the Right Prop for Your Boat*. https://www.boatus.com/expertadvice/expertadvicearchive/2012/july/howtochoosetherightpropforyourboat. July 2012.

[30] Brandweer Informatie. *Brandweerkazernes Nederland*. https://brandweer-informatie.nl/brandweerkazernes-nederland/.

[31] Brouav. *UAV Fire Fighting System*. https://brouav.com/uav-fire-fighting-p.html.

[32] Hibbeler R. C. and Yap K. B. *Mechanics of materials*. Harlow, England: Pearson Education, 2018.

[33] Carbon Fiber Gear. *How Durable Is Carbon Fiber?* https://carbonfibergear.com/blogs/carbonfiber/carbon-fiber-durability.

[34] Carbonwebshop. *Carbonwebshop*. https://www.carbonwebshop.com/.

[35] Roger's Hobby Center. *A Guide to Understanding LiPo Batteries*. https://www.rogershobbycenter.com/lipoguide/.

[36] *Climate Action*. United Nations Development Programme (UNDP). URL: https://www.undp.org/sustainable-development-goals/climate-action.

[37] European Commission. *Pressure Equipment Directive*. https://single-market-economy.ec.europa.eu/sectors/pressure-equipment-and-gas-appliances/pressure-equipment-sector/pressure-equipment-directive_en. May 2021.

[38] RS Components. *CRC White Polyurethane Foam, 500 ml Aerosol*. https://nl.rs-online.com/web/p/expanding-foams/9082818.

[39] Comprenew. *Why Refurbished Electronics Are the Key to Sustainable Technology*. https://comprenew.org/refurbished-electronics-the-key-to-sustainable-technology/. Apr. 2022.

[40] Custom Gimbals. *2 Axis Hawkeye Firefly 4K Nano Camera Stabilizer*. https://customgimbals.com/en/2-axis-hawkeye-firefly-4k-nano-gimbal.

[41] Dave A. and, Sonia M. *Firefighting Drone Market by Product Type, Application, and Industry Vertical: Global Opportunity Analysis and Industry Forecast, 2021–2028*. https://www.alliedmarketresearch.com/firefighting-drone-market-A06280. Oct. 2022.

[42] Richard Demirjian. "Embracing a New Alternative to Wind Tunnel Testing". In: *OEM Off-Highway* (May 2021).

[43] Antonio DiCesare, Kyle Gustafson, and Paul Lindenfelzer. "Design optimization of a quad-rotor capable of autonomous flight". In: *Final Year Thesis, Worchester Polytechnic Institute, Worcester, MA* (2008).

[44] Digital Eagle UAV. *YM-8160 Security Drone*. https://www.digitaleagle-uav.com/ym-8160-security-drone.html.

[45] KDE Direct. *KDE10218XF-105*. https://www.kdedirect.com/collections/uas-multi-rotor-brushless-motors/products/kde10218xf-105.

[46] DJI. *DJI Osmo Action 3 - Specifications*. https://www.dji.com/nl/osmo-action-3/specs.

[47] Sky-Drones Online Documentation. *Installation*. https://docs.sky-drones.com/avionics/smartap-pdb/installation. Nov. 2022.

[48] DragonPlate. *Modular Connectors*. https://dragonplate.com/angularly-adjustable-tube-to-tube-connectors.

[49] Drone Engr Store. *Heavy Load Drone with 40kgs Payload & 20 Minutes Endurance*. https://www.droneassemble.com/product/heavy-load-drone-with-40kgs-payload-20-minutes-endurance/.

[50] Drone Engr Store. *Hercules FDT100 Heavy Lift Drone with Max 70kg Payload*. https://www.droneassemble.com/product/hercules-fdt100-heavy-lift-drone-with-max-70kg-payload/.

[51] Droneland. *Verzekering - Droneland*. https://droneland.nl/verzekering?___store=nl.

[52] Droneshop.nl. *Hawkeye 4K Split NakedCam*. https://droneshop.nl/hawkeye-4k-split-nakedcam.

[53] Dronevolt. *DJI Zenmuse X5S*. https://dronevolt.nl/Product/dji-zenmuse-x5s-camera-haarscherpe-beelden-en-52k-video/.

[54] Dronewatch. *EU Drone Regels*. https://www.dronewatch.nl/2020/01/17/eu-droneregels-in-welke-subcategorie-kom-je-op-1-juli-2020-terecht/.

[55] Dronewatch. *NLR opleiding*. https://www.dronewatch.nl/2020/05/06/nlr-start-opleiding-voor-vliegen-met-drones-boven-de-25-kg/.

[56] DSE Group 29. *Unmanned fire-fighting multi-vehicle Midterm Report*. 2023.

[57] James P Duffy et al. "Location, location, location: considerations when using lightweight drones in challenging environments". In: *Remote Sensing in Ecology and Conservation* 4.1 (2018), pp. 7–19.

[58] Massimo Durante et al. "Investigation on the Mechanical Recycling of Carbon Fiber-Reinforced Polymers by Peripheral Down-Milling". In: *Polymers* 15.4 (Feb. 2023), p. 854. ISSN: 2073-4360. DOI: 10.3390/polym15040854.

[59] Dutch Drone Academy. *Specific Category - Dutch Drone Academy*. https://www.dutchdroneacademy.com/specific-category/.

[60] DutchNews.nl. *Rotterdam's Zalmhaven Tower is the Netherlands' Highest Building*. https://www.dutchnews.nl/2021/10/rotterdams-zalmhaven-tower-is-the-netherlands-highest-building/. Oct. 2021.

[61] Catherine Early. *How geothermal lithium could revolutionise green energy*. https://www.bbc.com/future/article/20201124-how-geothermal-lithium-could-revolutionise-green-energy. Nov. 2022.

[62] Economic Research Institute (ERI). *UAV Test Engineer Salary in Netherlands*. https://www.erieri.com/salary/job/uav-test-engineer/netherlands. June 2023.

[63] EHang. *EHang 216F (Firefighting Model)*. https://www.ehang.com/ehang216f/.

[64] ElProCus. *What is a PID Controller : Working & Its Applications*. https://www.elprocus.com/the-working-of-a-pid-controller/.

[65] Attollo Engineering. *WASP-200 LRF*. https://attolloengineering.com/product/wasp-200-lrf/.

[66] European Union Aviation Safety Agency. *Guidelines on Design verification of UAS operated in the 'specific' category and classified in SAIL III and IV*. Mar. 2021.

[67] European Union Aviation Safety Agency. *Specific Category - Civil Drones*. https://www.easa.europa.eu/en/domains/civil-drones-rpas/specific-category-civil-drones.

[68] Exel Composites. *Gluing of Carbon Fiber Composite to Aluminum - Exel Composites*. https://exelcomposites.com/guide-to-composites/gluing-of-carbon-fiber-composite-to-aluminum/.

[69] Fact.MR. *Autonomous Firefighting Drones Market Outlook (2023-2033)*. https://www.factmr.com/report/autonomous-firefighting-drones-market. Nov. 2022.

[70] Farnell. *Aluminium Spacers*. https://nl.farnell.com/c/fasteners-mechanical/fasteners-fixings/spacers-feet/spacers?spacer-material=aluminium. 2023.

[71] Firefighternation. *Nozzle Knowledge Is More Than Just Smooth Bore or Fog*. https://www.firefighternation.com/training/nozzle-knowledge-is-more-than-just-smooth-bore-or-fog/#gref. Feb. 2020.

[72] Firefly Cameras. *Hawkeye 4K Split NakedCam V 4.0 with Gyroflow*. https://fireflycameras.com/products/hawkeye-4k-split-nakedcam-v-4-0-with-gyroflow.

[73] Fly Dragon Drone Tech. *FD-1600 Fire-fighting Drone*. http://www.dronefromchina.com/product/FD-1600-Fire-fighting-drone.html.

[74] FlytNow. *How Firefighters Can Better Manage Emergency Situations Using Drones*. https://www.flytbase.com/blog/drone-fire-fighting. Apr. 2023.

[75] Foxeer. *Foxeer Mini Night Cat 3 1200TVL 0.00001Lux IR Sensitive Night Vision Camera 850nm IR Light*. https://www.foxeer.com/foxeer-mini-night-cat-3-1200tvl-0-00001lux-ir-sensitive-night-vision-camera-850nm-ir-light-g-347.

[76] FPVFrenzy. *Spektrum Vs FrSky Taranis: Which is better for multirotors?* URL: https://fpvfrenzy.com/spektrum-vs-frsky-taranis.

[77] Henry Xue Frank M. White. *Fluid Mechanics*. McGraw Hill, 2021.

[78] FrSky. *Taranis X9D Plus*. https://www.frsky-rc.com/product/taranis-x9d-plus-2/.

[79] Jian Gao and Yufan Zhao. *LQR and Linearization: A Tutorial*. https://arxiv.org/pdf/2009.13175.pdf. 2020. arXiv: 2009.13175 [math.OC].

[80] GetFPV. *HereLink HD Air Unit v1.1*. https://www.getfpv.com/herelink-hd-air-unit-v1-1.html.

[81] GetPFV. *HEX Here3 CAN GNSS GPS*. https://www.getfpv.com/hex-here3-can-gnss-gps-module-w-istand.html.

[82] GlobeNewswire. *Firefighting Drone Market Size to Garner $2.4 Billion by 2031: Allied Market Research*. https://www.globenewswire.com/en/news-release/2022/11/08/2550530/0/en/Firefighting-Drone-Market-Size-to-Garner-2-4-Billion-by-2031-Allied-Market-Research.html. Nov. 2022.

[83] *Good Health and Well-Being*. United Nations Development Programme (UNDP). 2023. URL: https://www.undp.org/sustainable-development-goals/good-health.

[84] GoPro. *HERO11 Black Mini*. https://gopro.com/en/us/shop/cameras/hero11-black-mini/CHDHF-111-master.html.

[85] Quan Quan GuangXun Du. "Controllability Analysis for Multirotor Helicopter Rotor Degradation and Failure". In: *Journal of Guidance, Control, and Dynamics* 38.5 (2015). DOI: 10.2514/1.G000731.

[86] Hans Eric Melin. "Analysis of the climate impact of lithium-ion batteries and how to measure it". In: *Circular Energy Storage-Research and Consulting* (July 2019).

[87] Hawkeye. *Hawkeye Firefly 4K 50FPS Split Cam Instructions*. https://manuals.plus/hawkeye/firefly-4k-50fps-split-cam-manual. Feb. 2022.

[88] Herelink. *Herelink User Manual*. Tech. rep.

[89] Daniel Höche et al. "Novel Magnesium Based Materials: Are They Reliable Drone Construction Materials? A Mini Review". In: *Frontiers in Materials* 8 (2021), p. 575530. DOI: 10.3389/fmats.2021.575530.

[90] Holybro. *DroneCAN H-RTK F9P Helica*. https://holybro.com/collections/gps-rtk-systems/products/dronecan-h-rtk-f9p-helical.

[91] Holybro. *Holybro Pixhawk 6X*. https://docs.holybro.com/autopilot/pixhawk-6x/technical-specification. 2023.

[92] University of Illinois Urbana-Champaign. *ECE486: Control Systems - Lecture 6C Routh–Hurwitz stability criterion*. https://courses.engr.illinois.edu/ece486/fa2021/documentation/lectures/slides/Lecture6C_RouthHurwitzCriterion.pdf.

[93] A. Imam and R. Bicker. "Design and Construction of a Small-scale Rotorcraft UAV System". In: *International Journal of Engineering Science and Innovative Technology (IJESIT)* 3.1 (2014).

[94] Grenfell Tower Inquiry. *Grenfell Tower Inquiry*. https://www.grenfelltowerinquiry.org.uk/. 2021.

[95] Inside Unmanned Systems. "Autonomous Firefighting Drone Market Set for Growth". In: *Inside Unmanned Systems* (Dec. 2022).

[96] Inspectie Leefomgeving en Transport. *Vliegen buiten de Uniforme Daglicht Periode*. https://www.ilent.nl/onderwerpen/drones/categorie-specifiek/ontheffingen/vliegen-buiten-de-uniforme-daglicht-periode-udp. Feb. 2023.

[97] Jantine van den Hoven. "Toen in Delft: Bouwkunde verwoest door brand". In: *indebuurt* (May 2016).

[98] Robert Jennings. *Is Carbon Fiber Better for the Environment Than Steel?* https://recyclenation.com/2015/10/is-carbon-fiber-better-for-environment-than-steel/. Oct. 2015.

[99] Won Ho Jeong, Dea-Nyeon Kim, and Do Hun Kim. "A Study On The Evaluation Techniques Of Wind Resistance For Uav-Based Bridge Inspection". In: *International Journal of Electrical, Electronics and Data Communication* 8 (Mar. 2020). ISSN: 2320-2084.

[100] Gordon Kelly and Stefan Hallström. *Bearing strength of carbon fibre/epoxy laminates: effects of bolt-hole clearance*. https://www.sciencedirect.com/science/article/pii/S1359836803001380. 2004.

[101] Georgette Kilgore. *Carbon Footprint of Lithium-ion Battery Production*. https://8billiontrees.com/carbon-offsets-credits/carbon-footprint-of-lithium-ion-battery-production/. Apr. 2023.

[102] Alex Kim. *Lithium: Not as Clean as We Thought*. https://climate360news.lmu.edu/lithium-not-as-clean-as-we-thought/. Jan. 2022.

[103] Level Five Supplies. *Blickfeld Cube Range 1 - Extra Long Range High Accuracy LiDAR*. https://levelfivesupplies.com/product/blickfeld-cube-range-1-extra-long-range-high-accuracy-lidar/.

[104] Shuo Li et al. *Visual Model-predictive Localization for Computationally Efficient Autonomous Racing of a 72-gram Drone*. May 2019.

[105] Oscar Liang. *Flight Controller Explained*. https://oscarliang.com/flight-controller-explained/. Feb. 2023.

[106] LightWare Lidar. *SF20 - LiDAR Manual - Rev 12*. https://www.documents.lightware.co.za/SF20%20-%20LiDAR%20Manual%20-%20Rev%2012.pdf. 2019.

[107] LightWare Optoelectronics. *SF000 - LiDAR Product Guide - Rev 5*. https://www.documents.lightware.co.za/SF000%20-%20LiDAR%20Product%20guide%20-%20Rev%205.pdf. Sept. 2021.

[108] LightWare Optoelectronics. *SF30 - Laser Altimeter Manual - Rev 9*. https://www.documents.lightware.co.za/SF30%20-%20Laser%20Altimeter%20Manual%20-%20Rev%209.pdf. Dec. 2018.

[109] Market Business News. *Market Volume - Definition and Example*. https://marketbusinessnews.com/financial-glossary/market-volume-definition-example/.

[110] Mauch Electronic. *030: 2x 200A PDB with 400A main switch*. https://www.mauch-electronic.com/apps/webstore/products/show/7863063.

[111] MaxBotix. *MB1222 - I2CXL-MaxSonar-EZ2*. https://maxbotix.com/products/mb1222.

[112] Mazrouei-Sebdani et al. "A review on silica aerogel-based materials for acoustic applications". In: *Journal of Non-Crystalline Solids* 562 (2021), p. 17. DOI: 10.1016/j.jnoncrysol.2021.120770.

[113] Tony Oliver Mogorosi et al. "Thrust-to-Weight Ratio Optimization for Multi-Rotor Drones Using Neural Network with Six Input Parameters". In: *2021 International Conference on Unmanned Aircraft Systems (ICUAS)*. IEEE. 2021, pp. 1194–1199. DOI: 10.1109/IC3T50837.2021.9476744.

[114] MRT Castings. *Sand Casting Process*. https://www.mrt-castings.co.uk/sand_casting_process.html.

[115] SR Naqvi et al. "A critical review on recycling of end-of-life carbon fibre/glass fibre reinforced composites waste using pyrolysis towards a circular economy". In: *Resources, conservation and recycling* 136 (2018), pp. 118–129.

[116] Nationaal Informatiecentrum voor de Praktijk van de Overheid (NIPO). *Kerncijfers Kazernes*. URL: https://kerncijfers.nipv.nl/mosaic/kerncijfers-veiligheidsregio-s/kerncijfers-kazernes.

[117] National Aeronautics and Space Administration. *Stardust Aerogel*. https://solarsystem.nasa.gov/stardust/photo/aerogel.html.

[118] NOS. "Brandweer waarschuwt voor veiligheid nieuwe hoogbouw". In: (Aug. 2019).

[119] Dave Olsen. *Investment Casting (Lost Wax Casting)*. https://www.metaltek.com/blog/what-is-investment-casting-and-how-does-it-work/. Nov. 2020.

[120] Jon N Ostler et al. "Performance flight testing of small, electric powered unmanned aerial vehicles". In: *International Journal of Micro Air Vehicles* 1.3 (2009), pp. 155–171.

[121] Permabond. *How to Bond Carbon Fiber - Permabond*. https://www.permabond.com/materials_bonded/how-to-bond-carbon-fiber-2/.

[122] Joanna Pietrzak. "Development of high-rise buildings in Europe in the 20th and 21st centuries". In: *Challenges of Modern Technology* 5.4 (2014), pp. 31–38.

[123] Pilot Institute. *Vortex Ring State – What Drone Pilots Need to Know*. https://pilotinstitute.com/vortex-ring-state/. July 2021.

[124] Rotterdam Plastics. *12 Liter Watertank Horizontaal*. https://rotterdamplastics.nl/nl/12-liter-watertank-plat.

[125] Rotterdam Plastics. *Watertank op maat*. https://rotterdamplastics.nl/nl/watertank-op-maat.

[126] Praxis. *Slangpilaar 1|2" x 19mm*. https://www.praxis.nl/tuin-buitenleven/vijver/vijverslang-koppelingen/slangpilaar-1-2-x-19mm/2491869?channable=02490e69640032343931383639a3&gclid=CjwKCAjwp6CkBhB_EiwAlQVyxbmMDOSJMEsniryKEpS3UdlNdHT0ucYfOu64wGruEOBbzwPVt0Rq8RoC7RcQAvD_BwE.

[127] PX4. *CubePilot Cube Orange Flight Controller*. https://docs.px4.io/main/en/flight_controller/cubepilot_cube_orange.html. Apr. 2023.

[128] PX4. *mRo Pixhawk Flight Controller*. https://docs.px4.io/v1.9.0/en/flight_controller/mro_pixhawk.html. Oct. 2020.

[129] Quan Quan. *Introduction to multicopter design and control*. Springer, 2017.

[130] Quan Quan. *rfly-openha/OpenHA*. https://github.com/rfly-openha/OpenHA.

[131] RadioLink. *AT10II 2.4Ghz 12CH Remote Control System*. https://www.radiolink.com/at10ii.

[132] Daniele Ragni. *Project Guide Design Synthesis Exercise: UNMANNED FIRE-FIGHTING MULTI-VEHICLE*. PDF. 2023.

[133] Randstad. *Gemiddeld Salaris van een Assemblagemedewerker*. https://www.randstad.nl/functies/assemblagemedewerker#gemiddeld-salaris-van-een-assemblagemedewerker.

[134] Raspberry Pi. *Raspberry Pi 4 Model B - Specifications*. https://www.raspberrypi.com/products/raspberry-pi-4-model-b/specifications/.

[135] Cognitive Market Research. "Firefighting Drone Market to Reach $2.76 Billion by 2030: Cognitive Market Research". In: *PR Newswire* (Jan. 2021).

[136] RFly OpenHA. *ACAI Tutorials*. https://rfly-openha.github.io/documents/2_tutorial/examples/tutorial.html.

[137] Rijksvastgoedbedrijf. *Unmanned Valley en testen drones*. https://www.rijksvastgoedbedrijf.nl/vastgoed/projecten-in-uitvoering/katwijk-marinevliegkamp-valkenburg/unmanned-valley-en-testen-drones.

[138] Robots for Roboticists. *Perception in Smoke, Dust, or Fog*. https://www.robotsforroboticists.com/perception-in-smoke-dust-or-fog/. Dec. 2021.

[139] John Rossiter. *State space analysis 5 - controllability worked examples*. https://www.youtube.com/watch?v=3tjfOKmDVSA&ab_channel=JohnRossiter. Feb. 2016.

[140] John Rossiter. *State space analysis 7 – observability continued*. https://www.youtube.com/watch?v=O6fw_G_9iek&ab_channel=JohnRossiter. Feb. 2016.

[141] RTL Nieuws. "Brandweer: Veiligheid hoogbouw moet beter na lessen Grenfell Tower". In: (Aug. 2019).

[142] H. Sai Teja et al. "Design and analysis of drone propeller by using aluminium and nylon materials". In: *E3S Web Conf.* (2023), p. 15. DOI: 10.1051/e3sconf/202339101032.

[143] R Thamizh Selvan et al. "Recycling technology of epoxy glass fiber and epoxy carbon fiber composites used in aerospace vehicles". In: *Journal of Composite Materials* 55.23 (2021), pp. 3281–3292. DOI: 10.1177/00219983211011532. eprint: https://doi.org/10.1177/00219983211011532.

[144] Dongjie Shi. "A Practical Performance Evaluation Method for Electric Multicopters". In: 22.3 (2017), pp. 1337–1348. DOI: 10.1109/TMECH.2017.2675913.

[145] M. Shioya and T. Kikutani. "Chapter 7 - Synthetic Textile Fibres: Non-polymer Fibres". In: *Textiles and Fashion*. Ed. by Rose Sinclair. Woodhead Publishing Series in Textiles. Woodhead Publishing, 2015, pp. 139–155. ISBN: 978-1-84569-931-4. DOI: https://doi.org/10.1016/B978-1-84569-931-4.00007-6.

[146] Ansu Man Singh. *Successive Loop Closure Based Controller Design for an Autonomous Quadrotor Vehicle*. https://ieeexplore.ieee.org/stamp/stamp.jsp?tp=&arnumber=7866879. 2013. DOI: 10.4028/www.scientific.net/AMM.483.361.

[147] Sky-Drones. *SmartAP Power Distribution Board (PDB)*. https://sky-drones.com/power/smartap-pdb.html.

[148] Sky-Drones. *SmartLink*. https://sky-drones.com/smartlink.

[149] *Specifications*. FLIRGTC-SBA-001. Teledyne FLIR. Meer, Belgium, Nov. 2021.

[150] Spektrum. *AR8010T DSMX 8-Channel Air Integrated Telemetry Receiver*. https://www.spektrumrc.com/product/ar8010t-dsmx-8-channel-air-integrated-telemetry-receiver/SPMAR8010T.html.

[151] Spektrum. *DX8 8-Channel Transmitter with AR8000, TM1000 - No Servos*. https://www.spektrumrc.com/product/dx8-8ch-transmitter-with-ar8000-tm1000-no-servos/SPM8800.html.

[152] Colleen Spiegel. *Analysis of Applied Mathematics Journal of The International Journal of Applied Mathematics for Secondary School Students*. Analysis of Applied Mathematics, 2017.

[153] StackExchange. *How are Hall effect gimbals different than standard gimbals?* https://drones.stackexchange.com/questions/715/how-are-hall-effect-gimbals-different-than-standard-gimbals. Apr. 2022.

[154] T-MOTOR. *ALPHA 120A 12S*. https://store.tmotor.com/goods.php?id=909.

[155] T-MOTOR. *ALPHA 80A 12S*. https://store.tmotor.com/goods.php?id=584.

[156] T-MOTOR. *FLAME 80A 12S V20*. https://store.tmotor.com/goods-830-FLAME+80A+12S+V20.html.

[157] T-MOTOR. *G32*11 Prop-2PCS/PAIR*. https://store.tmotor.com/goods-412-G32%2A11+Prop-2PCSPAIR.html.

[158] T-motor. *AntiG MN8017 KV12*. https://uav-en.tmotor.com/html/2021/Antigravity_0119/668.html.

[159] T-motor. *MN1010 KV135*. https://store.tmotor.com/goods.php?id=1088.

[160] T-motor. *MN805-S KV150*. https://uav-en.tmotor.com/html/2018/navigato_0402/46.html.

[161] T-motor. *U12II KV120*. https://uav-en.tmotor.com/html/2018/u_1021/174.html.

[162] Zaid Tahir, Waleed Tahir, and Saad Ali Liaqat. "State space system modelling of a quad copter UAV". In: *arXiv preprint arXiv:1908.07401* (2019).

[163] Texo Precision Castings. *Investment Casting vs Sand Casting: A Comparison*. https://www.texmoprecisioncastings.com/advice/comparisons/investment-casting-vs-sand-casting/.

[164] C. Theobald. "The Effect of Nozzle Design on the Stability and Performance of Turbulent Water Jets". In: *Fire Safety Journal* (1980), pp. 1–13.

[165] M. Trabia and F. Ferri. "Application of LQR and LQG techniques for autonomous satellite formation flying control". In: *2016 IEEE 15th International Conference on Environment and Electrical Engineering (EEEIC)*. Florence, Italy, 2016, pp. 1–6. DOI: 10.1109/EEEIC.2016.7555676.

[166] Michael Trettel. "Theoretical Range and Trajectory of a Water Jet". In: *Journal of Hydraulic Engineering* 141.6 (2015), pp. 1–9.

[167] TS2 SPACE. *DJI Matrice 210 V2 Drone*. https://ts2.shop/en/drones/11096-dji-matrice-210-v2-drone-6958265186738.html.

[168] TS2 Space. *How does a drone's radio frequency system work?* https://ts2.space/en/how-does-a-drones-radio-frequency-system-work/. Feb. 2023.

[169] TurboSquid. *3D Model - Mercedes-Benz Sprinter Fire Brigade*. https://www.turbosquid.com/3d-models/3d-model-mercedes-benz-sprinter-fire-brigade-1402952.

[170] European Union. *Directive 2014/29/EU of the European Parliament and of the Council of 26 February 2014 on the harmonisation of the laws of the Member States relating to the making available on the market of simple pressure vessels*. https://eur-lex.europa.eu/legal-content/EN/TXT/?uri=celex:32014L0029. May 2014.

[171] Juan Carlos Vergara. *Handbook of Simulation: Principles, Methodology, Advances, Applications, and Practice*. Pages 335-393. 1998.

[172] VERTICAL Hobby. *Walkera Zhun 1800 Firefighting Drone - 30x Optical Zoom Lidar*. https://www.verticalhobby.com/kauppa/en/walkera-zhun-1800-firefighting-drone-30xoptical-zoom-lidar-p-7189.html.

[173] VEVOR. *VEVOR Washdown Dekpompset Waterpomp 12V 7 GPM 60 PSI 10 Voet Zelfaanzuigende Kop*. https://www.vevor.nl/diafragma-pomp-c_11958/vevor-washdown-dekpompset-waterpomp-12v-7-gpm-60-psi-10-voet-zelfaanzuigende-kop-p_010846289808.

[174] VIFLY. *VIFLY Strobe - FAA Drone Strobe Light*. https://viflydrone.com/products/vifly-drone-strobe-light?variant=44184027037992.

[175] Giuseppe Virone et al. "Effect of Conductive Propellers on VHF UAV-based Antenna Measurements: Experimental Results". In: *2021 IEEE Conference on Antenna Measurements & Applications (CAMA)*. IEEE. Antibes Juan-les-Pins, France: IEEE, Nov. 2021, pp. 1–4. DOI: 10.1109/CAMA49227.2021.9703392.

[176] Chau V. Vo et al. "Advances in Thermal Insulation of Extruded Polystyrene Foams". In: *Journal of XYZ* (2011), pp. 1–20. DOI: 10.1177/026248931103000303.

[177] Yu Wang et al. “Rotor Stress Analysis of High-Speed Permanent Magnet Machines With Segmented Magnets Retained by Carbon-Fibre Sleeve”. In: *IEEE Transactions on Energy Conversion* 36.2 (2020), pp. 971–983. DOI: 10.1109/TEC.2020.3022475.

[178] Wellbots. *Walkera WK1900 Firefighting Drones*. https://www.wellbots.com/products/walkera-wk1900-firefighting-drones.

[179] *What are the Sustainable Development Goals?* United Nations Development Programme (UNDP). 2023. URL: https://www.undp.org/sustainable-development-goals.

[180] Seeed Studio Wiki. *Grove - SPDT Relay (30A)*. https://wiki.seeedstudio.com/Grove-SPDT_Relay_30A/.

[181] Wildkamp. *Vyr nozzle voor sproeier, type 60, 70 en 33 AF, 4,8 mm*. https://www.wildkamp.nl/product/vyr-nozzle-voor-sproeier-type-60-70-en-33-af-4-8-mm/780218.

[182] Andrew Wood. “Aircraft Propeller Theory”. In: Sept. 2022. Chap. Engine and Propeller Combination.

A

Appendix A

At the beginning of the design project, a Gantt Chart was set up. A Gantt Chart shows all tasks that need to be completed, their duration, and the team member(s) assigned to work on them. As it breaks the project down into smaller, more manageable steps, it is a useful tool to gain a comprehensive view of all tasks that need to be completed and their deadline. The Gantt Chart was a living document that was updated frequently. It was reviewed and updated during the final meeting of the day, resulting in a clear overview of the progress made that day and the remaining work. The final project Gantt Chart is shown on the next two pages.